

Western University

Scholarship@Western

---

Digitized Theses

Digitized Special Collections

---

2006

## Subband Adaptive Modeling of Digital Hearing Aids

Michael Roy Wirtzfeld

Follow this and additional works at: <https://ir.lib.uwo.ca/digitizedtheses>

---

### Recommended Citation

Wirtzfeld, Michael Roy, "Subband Adaptive Modeling of Digital Hearing Aids" (2006). *Digitized Theses*. 3220.

<https://ir.lib.uwo.ca/digitizedtheses/3220>

This Thesis is brought to you for free and open access by the Digitized Special Collections at Scholarship@Western. It has been accepted for inclusion in Digitized Theses by an authorized administrator of Scholarship@Western. For more information, please contact [wlsadmin@uwo.ca](mailto:wlsadmin@uwo.ca).

**Subband Adaptive Modeling of Digital Hearing Aids**

(Spine title: Subband Adaptive Modeling of Digital Hearing Aids)  
(Thesis format: Monograph)

by

Michael Roy Wirtzfeld

Faculty of Engineering  
Department of Electrical and Computer Engineering

Submitted in partial fulfillment  
of the requirements for the degree of  
Master of Engineering Science

Faculty of Graduate Studies  
The University of Western Ontario  
London, Ontario, Canada

18<sup>th</sup> April, 2006

© Michael Roy Wirtzfeld, 2006

## Abstract

In this thesis, the application of a subband adaptive model to characterize compression behaviour of five digital hearing aids is investigated. Using a signal-to-error ratio metric, modeling performance is determined by varying the number of analysis bands in the subband structure as well as consideration of three adaptive algorithms. The normalized least mean-squares (NLMS), the affine projection algorithm (APA), and the recursive least-squares (RLS) algorithms are employed using a range of parameters to determine the impact on modeling performance. Using the subband adaptive model to estimate the time-varying frequency response of each hearing aid allows the Perceptual Evaluation of Speech Quality (PESQ) mean-opinion score (MOS) to be computed. The PESQ MOS facilitates an estimation of a subjective assessment of speech quality using an objective score. Initial results suggest the PESQ MOS score is able to differentiate speech processed by hearing aids allowing them to be ranked accordingly. Further work is required to obtain subjective assessments of the processed speech signals and determine if possible correlations exist.

**Key words:** hearing aid, modeling, subband, fullband, adaptive algorithm, NLMS, APA, RLS

## For my father... Walter

"Young Man Dies" by David Wilcox (Album: Underneath)

*There's a young man dying as he stands beside the sea.*

*You can see him smiling, unbelievably free:*

*wind in his hair, light in his eyes.*

*He looks a lot like you, and you look so surprised  
that he would send you on your way with no good-byes.*

*But he can't go, and you can't stay,  
'cause in the years it takes to make one man wise, the young man dies.*

*Meanwhile you're sailing,  
as you wave good-bye to shore.*

*You're anticipating what these new days will hold in store.*

*It's the mystery of the ocean,  
but now he's in over his head.*

*This is no place for the young man,  
he's got to send you on instead.*

*And still you're looking so surprised  
that this change has come as prophesied  
but the years won't compromise,*

*'cause in the years it takes to make one man wise, the young man dies.*

*The young man: He was such a lonely boy.*

*Yeah, but he could dream, all right.*

*He could picture you a perfect sunrise  
in the middle of your darkest night.*

*And he could take a sip from someday,  
like he had a secret well.*

*He could listen to the voices calling  
from a distant time will tell.*

*It's you in that picture where you're looking far away  
like you hear a whisper of the things  
you'll know someday.*

*But back then your heart was hungry  
for something hard to find; you were  
just holding out for someday,  
but you've left that pain behind*

*'cause he walked you through those mountains,  
for as long as he could bear.*

*He never reached the fountain,  
but he could take you there.*

*The young man's dying  
'cause in the years it takes to make one man wise,  
the young man dies.*



## Acknowledgments

Thank you to my father, mother, sister, and nephew for their love and endless encouragement.

Thank you to my wife, Lauren, for putting up with me over the course of this adventure. Her love, understanding, and guidance to keep me on track during this work, and in our life together, is immeasurable.

To Oscar, your easygoing disposition and caring purr helped ease the challenging moments. I love rough-housing with you.

My deepest gratitude to Vijay for offering me the opportunity to return to full-time academic studies after a prolonged absence and work towards this degree; a transition difficult to put into words. It has been a rewarding experience. Thank you.

My sincere gratitude to Sheila Moodie for her guidance and direction on the "next step."

To fine colleagues, Dr. Susan Scollie, Marlene Bagatto, Dr. Mary Beth Jennings, and Lucy Kieffer for their openness and willingness to answer my questions.

I am grateful to Mark Neukom for making time in his schedule to help gather data for my work.

To Steve Beaulac, I am indebted for on-going assistance in answering my software development and hardware questions. Thanks also to David Grainger.

I would like to gratefully acknowledge funding support from the Oticon Foundation of Denmark, Western Graduate Research Scholarship, and the Ontario Rehabilitation Technology Consortium.

# Contents

<b>Certificate of Examination</b>	<b>ii</b>
<b>Abstract</b>	<b>iii</b>
<b>Acknowledgements</b>	<b>v</b>
<b>List of Tables</b>	<b>x</b>
<b>List of Figures</b>	<b>xii</b>
<b>List of Acronyms &amp; Abbreviations</b>	<b>xvi</b>
<b>1 Introduction</b>	<b>1</b>
1.1 Hearing . . . . .	1
1.1.1 The Physiological Process of Hearing . . . . .	1
1.1.2 Hearing Sensitivity and its Measurement . . . . .	7
1.1.3 Normal Hearing . . . . .	10
1.1.4 Hearing Loss . . . . .	10
1.2 Digital Hearing Aids . . . . .	15
1.2.1 General Structure . . . . .	15
1.2.2 Bands and Channels . . . . .	17
1.3 Compression . . . . .	18
1.3.1 Compression . . . . .	19
1.3.2 Compression Characteristics . . . . .	20
1.3.3 Application and Efficacy of Compression . . . . .	21
1.4 Hearing Aid Performance Verification . . . . .	23
1.5 Objective Speech Quality Measures . . . . .	24
1.5.1 Speech Intelligibility Index . . . . .	24
1.5.2 Coherence Measures . . . . .	25
1.5.3 PESQ Mean Opinion Score . . . . .	25
1.6 System Identification . . . . .	30
1.7 Motivation and Objectives . . . . .	30

1.8	Thesis Contents . . . . .	31
<b>2</b>	<b>Subband Adaptive Modeling</b>	<b>33</b>
2.1	Introduction . . . . .	33
2.2	Adaptive Modeling of Hearing Aids . . . . .	34
2.2.1	System Modeling . . . . .	34
2.2.2	Full Band Modeling . . . . .	36
2.3	Subband Adaptive Filters . . . . .	38
2.3.1	Introduction and Motivation . . . . .	38
2.3.2	General Structure . . . . .	40
2.3.3	Uniform and Non-uniform Filter Banks . . . . .	43
2.3.4	Quadrature Mirror Filters . . . . .	44
2.4	Adaptive Algorithms . . . . .	48
2.4.1	Normalized Least-Mean-Squares ( $\epsilon$ -NLMS) . . . . .	49
2.4.2	Affine Projection Algorithm ( $\epsilon$ -APA) . . . . .	51
2.4.3	Recursive Least Squares . . . . .	54
2.4.4	QRD Recursive Least-Squares (QRD-RLS) . . . . .	56
2.5	Tracking Behaviour of Adaptive Algorithms . . . . .	56
2.5.1	Tracking Model . . . . .	57
2.5.2	Bias and Variance . . . . .	58
2.5.3	Simulation Results . . . . .	59
2.5.4	Final Comments on Tracking Performance . . . . .	64
2.6	Summary of Chapter 2 . . . . .	66
<b>3</b>	<b>Simulations</b>	<b>68</b>
3.1	Introduction . . . . .	68
3.1.1	Overview of Hearing Aid Model . . . . .	68
3.1.2	Gain Compensation . . . . .	70
3.1.3	Uniform Filter Bank . . . . .	71
3.1.4	Amplitude Compression . . . . .	73
3.1.5	Model Justification . . . . .	73
3.2	Channel Offset Modeling . . . . .	74
3.3	Bias Tone with Broadband Excitation . . . . .	77
3.3.1	Introduction . . . . .	77
3.3.2	Procedure . . . . .	79
3.3.3	Experimental Results . . . . .	81
3.3.4	Discussion . . . . .	83
3.4	Summary of Chapter 3 . . . . .	84
<b>4</b>	<b>Methodology</b>	<b>86</b>
4.1	Digital Hearing Aids . . . . .	86
4.1.1	Bernafon Symbio XT BTE 110 . . . . .	87

4.1.2	Oticon Syncro V2 . . . . .	89
4.1.3	Phonak Perseo 311 dAZ Forte . . . . .	89
4.1.4	Siemens Triano S . . . . .	92
4.1.5	Sonic Innovations Natura 2 SE . . . . .	94
4.2	Hearing Aid Summary . . . . .	94
4.3	Hearing Aid Test System . . . . .	94
4.3.1	Overview . . . . .	95
4.3.2	Calibration . . . . .	97
4.4	Hearing Aid Programming . . . . .	98
4.5	Response Measurement . . . . .	99
4.6	Modeling . . . . .	100
4.6.1	Subband Adaptive Modeling . . . . .	100
4.7	Summary . . . . .	103
<b>5</b>	<b>Modeling Results</b>	<b>105</b>
5.1	General Modeling Performance of the Oticon Syncro V2 . . . . .	106
5.1.1	NLMS Results . . . . .	107
5.1.2	APA Results . . . . .	112
5.1.3	QRD RLS Results . . . . .	117
5.2	Modeling Summary of the Oticon Syncro V2 . . . . .	120
5.2.1	Audiogram "F" . . . . .	120
5.2.2	Audiogram "I" . . . . .	122
5.3	Fullband and Subband Model Summary . . . . .	123
5.3.1	Subband Model . . . . .	124
5.3.2	Fullband Model . . . . .	127
5.4	Summary . . . . .	129
<b>6</b>	<b>Discussion, Conclusions, and Future Work</b>	<b>131</b>
6.1	Discussion . . . . .	131
6.1.1	Subband Model Versus Fullband Model . . . . .	132
6.1.2	Deviations on Subband Modeling Performance . . . . .	132
6.1.3	PESQ Mean Opinion Score . . . . .	136
6.1.4	General Comments on Algorithm Performance . . . . .	145
6.2	Conclusions . . . . .	148
6.3	Future Work . . . . .	149
<b>A</b>	<b>Hearing Aid Specifications</b>	<b>158</b>
A.1	Bernafon Symbio XT 110 . . . . .	159
A.2	Oticon Syncro V2 . . . . .	161
A.3	Phonak Perseo 311 dAZ Forte . . . . .	163
A.4	Siemens Triano S . . . . .	167
A.5	Sonic Innovations Natura 2 SE . . . . .	171

<b>B Hearing Aid ANSI Measurements</b>	<b>173</b>
B.1 Bernafon Symbio XT 110 . . . . .	174
B.2 Oticon Syncro V2 . . . . .	177
B.3 Phonak Perseo 311 dAZ Forte . . . . .	180
B.4 Siemens Triano S . . . . .	183
B.5 Sonic Innovations Natura 2 SE . . . . .	186
<b>C Modeling Results</b>	<b>189</b>
C.1 Normalized Least Mean Squares (NLMS) . . . . .	190
C.2 Affine Projection Algorithm (APA) . . . . .	196
C.3 QRD Recursive Least Squares (QRD RLS) . . . . .	212
<b>Vita</b>	<b>218</b>
1.1 Introduction	219
1.2 Overview of the Hearing Aid	220
1.3 Hearing Aid Types	221
1.4 Hearing Aid Components	222
1.5 Hearing Aid Performance	223
1.6 Hearing Aid Evaluation	224
1.7 Hearing Aid Design	225
1.8 Hearing Aid Testing	226
1.9 Hearing Aid Modeling	227
1.10 Hearing Aid Simulation	228
1.11 Hearing Aid Implementation	229
1.12 Hearing Aid Optimization	230
1.13 Hearing Aid Adaptation	231
1.14 Hearing Aid Control	232
1.15 Hearing Aid Monitoring	233
1.16 Hearing Aid Maintenance	234
1.17 Hearing Aid Troubleshooting	235
1.18 Hearing Aid Safety	236
1.19 Hearing Aid Security	237
1.20 Hearing Aid Privacy	238
1.21 Hearing Aid Accessibility	239
1.22 Hearing Aid Usability	240
1.23 Hearing Aid Reliability	241
1.24 Hearing Aid Durability	242
1.25 Hearing Aid Portability	243
1.26 Hearing Aid Interoperability	244
1.27 Hearing Aid Compatibility	245
1.28 Hearing Aid Interference	246
1.29 Hearing Aid EMI/RFI	247
1.30 Hearing Aid EMC	248
1.31 Hearing Aid ESD	249
1.32 Hearing Aid EFT	250
1.33 Hearing Aid ESD/ESD	251
1.34 Hearing Aid ESD/ESD	252
1.35 Hearing Aid ESD/ESD	253
1.36 Hearing Aid ESD/ESD	254
1.37 Hearing Aid ESD/ESD	255
1.38 Hearing Aid ESD/ESD	256
1.39 Hearing Aid ESD/ESD	257
1.40 Hearing Aid ESD/ESD	258
1.41 Hearing Aid ESD/ESD	259
1.42 Hearing Aid ESD/ESD	260
1.43 Hearing Aid ESD/ESD	261
1.44 Hearing Aid ESD/ESD	262
1.45 Hearing Aid ESD/ESD	263
1.46 Hearing Aid ESD/ESD	264
1.47 Hearing Aid ESD/ESD	265
1.48 Hearing Aid ESD/ESD	266
1.49 Hearing Aid ESD/ESD	267
1.50 Hearing Aid ESD/ESD	268
1.51 Hearing Aid ESD/ESD	269
1.52 Hearing Aid ESD/ESD	270
1.53 Hearing Aid ESD/ESD	271
1.54 Hearing Aid ESD/ESD	272
1.55 Hearing Aid ESD/ESD	273
1.56 Hearing Aid ESD/ESD	274
1.57 Hearing Aid ESD/ESD	275
1.58 Hearing Aid ESD/ESD	276
1.59 Hearing Aid ESD/ESD	277
1.60 Hearing Aid ESD/ESD	278
1.61 Hearing Aid ESD/ESD	279
1.62 Hearing Aid ESD/ESD	280
1.63 Hearing Aid ESD/ESD	281
1.64 Hearing Aid ESD/ESD	282
1.65 Hearing Aid ESD/ESD	283
1.66 Hearing Aid ESD/ESD	284
1.67 Hearing Aid ESD/ESD	285
1.68 Hearing Aid ESD/ESD	286
1.69 Hearing Aid ESD/ESD	287
1.70 Hearing Aid ESD/ESD	288
1.71 Hearing Aid ESD/ESD	289
1.72 Hearing Aid ESD/ESD	290
1.73 Hearing Aid ESD/ESD	291
1.74 Hearing Aid ESD/ESD	292
1.75 Hearing Aid ESD/ESD	293
1.76 Hearing Aid ESD/ESD	294
1.77 Hearing Aid ESD/ESD	295
1.78 Hearing Aid ESD/ESD	296
1.79 Hearing Aid ESD/ESD	297
1.80 Hearing Aid ESD/ESD	298
1.81 Hearing Aid ESD/ESD	299
1.82 Hearing Aid ESD/ESD	300
1.83 Hearing Aid ESD/ESD	301
1.84 Hearing Aid ESD/ESD	302
1.85 Hearing Aid ESD/ESD	303
1.86 Hearing Aid ESD/ESD	304
1.87 Hearing Aid ESD/ESD	305
1.88 Hearing Aid ESD/ESD	306
1.89 Hearing Aid ESD/ESD	307
1.90 Hearing Aid ESD/ESD	308
1.91 Hearing Aid ESD/ESD	309
1.92 Hearing Aid ESD/ESD	310
1.93 Hearing Aid ESD/ESD	311
1.94 Hearing Aid ESD/ESD	312
1.95 Hearing Aid ESD/ESD	313
1.96 Hearing Aid ESD/ESD	314
1.97 Hearing Aid ESD/ESD	315
1.98 Hearing Aid ESD/ESD	316
1.99 Hearing Aid ESD/ESD	317
1.100 Hearing Aid ESD/ESD	318

## List of Tables

3.1	Steeply Sloping, Moderate-to-Severe Audiogram Thresholds . . . . .	70
3.2	Compression Settings for Simulated Hearing Aid . . . . .	73
4.1	Oticon Syncro V2 Identities with Respective Attack and Release Times	89
4.2	Hearing Aid Structure Summary . . . . .	94
4.3	Theoretical Audiograms . . . . .	98
4.4	Adaptive Algorithm Parameters . . . . .	101
4.5	Hearing Aid Structure Summary . . . . .	103
5.1	Best Modeling Parameters . . . . .	107
5.2	Syncro V2 "Best" MOS Results Summary for 64 Taps, Audiogram "F"	122
5.3	Syncro V2 "Best" MOS Results Summary for 128 Taps, Audiogram "F"	122
5.4	Syncro V2 "Best" MOS Results Summary for 256 Taps, Audiogram "F"	123
5.5	Syncro V2 "Best" MOS Results Summary for 64 Taps, Audiogram "I"	123
5.6	Syncro V2 "Best" MOS Results Summary for 128 Taps, Audiogram "I"	124
5.7	Syncro V2 "Best" MOS Results Summary for 256 Taps, Audiogram "I"	124
5.8	Modeling Comparison of all Instruments using 20 Band Subband Model SER Metric, Audiogram "F" . . . . .	125
5.9	Modeling Comparison of all Instruments using 20 Band Subband Model MOS Metric, Audiogram "F" . . . . .	126
5.10	Modeling Comparison of all Instruments using 20 Band Subband Model SER Metric, Audiogram "I" . . . . .	126
5.11	Modeling Comparison of all Instruments using 20 Band Subband Model MOS Metric, Audiogram "I" . . . . .	127
5.12	Modeling Comparison of all Instruments using Fullband Model SER Metric, Audiogram "F" . . . . .	128
5.13	Modeling Comparison of all Instruments using Fullband Model MOS Metric, Audiogram "F" . . . . .	128
5.14	Modeling Comparison of all Instruments using Fullband Model SER Metric, Audiogram "I" . . . . .	129

5.15	Modeling Comparison of all Instruments using Fullband Model MOS Metric, Audiogram "I" . . . . .	130
6.1	Modeling Comparison of all Instruments using 20 Band Subband Model SER Metric, Audiogram "F" . . . . .	134
6.2	Modeling Comparison of all Instruments using 20 Band Subband Model SER Metric, Audiogram "I" . . . . .	134
6.3	Results of Tukey's Honestly Significant Difference Criterion . . . . .	144

1.1	Introduction	1
1.2	Objectives	2
1.3	Scope	3
1.4	Organization	4
2.1	Background	5
2.2	Background	6
2.3	Background	7
2.4	Background	8
2.5	Background	9
2.6	Background	10
2.7	Background	11
2.8	Background	12
2.9	Background	13
2.10	Background	14
2.11	Background	15
2.12	Background	16
2.13	Background	17
2.14	Background	18
2.15	Background	19
2.16	Background	20
2.17	Background	21
2.18	Background	22
2.19	Background	23
2.20	Background	24
2.21	Background	25
2.22	Background	26
2.23	Background	27
2.24	Background	28
2.25	Background	29
2.26	Background	30
2.27	Background	31
2.28	Background	32
2.29	Background	33
2.30	Background	34
2.31	Background	35
2.32	Background	36
2.33	Background	37
2.34	Background	38
2.35	Background	39
2.36	Background	40
2.37	Background	41
2.38	Background	42
2.39	Background	43
2.40	Background	44
2.41	Background	45
2.42	Background	46
2.43	Background	47
2.44	Background	48
2.45	Background	49
2.46	Background	50
2.47	Background	51
2.48	Background	52
2.49	Background	53
2.50	Background	54
2.51	Background	55
2.52	Background	56
2.53	Background	57
2.54	Background	58
2.55	Background	59
2.56	Background	60
2.57	Background	61
2.58	Background	62
2.59	Background	63
2.60	Background	64
2.61	Background	65
2.62	Background	66
2.63	Background	67
2.64	Background	68
2.65	Background	69
2.66	Background	70
2.67	Background	71
2.68	Background	72
2.69	Background	73
2.70	Background	74
2.71	Background	75
2.72	Background	76
2.73	Background	77
2.74	Background	78
2.75	Background	79
2.76	Background	80
2.77	Background	81
2.78	Background	82
2.79	Background	83
2.80	Background	84
2.81	Background	85
2.82	Background	86
2.83	Background	87
2.84	Background	88
2.85	Background	89
2.86	Background	90
2.87	Background	91
2.88	Background	92
2.89	Background	93
2.90	Background	94
2.91	Background	95
2.92	Background	96
2.93	Background	97
2.94	Background	98
2.95	Background	99
2.96	Background	100

# List of Figures

1.1	Anatomy of the Human Ear . . . . .	2
1.2	Middle Ear Ossicles of Chinchilla . . . . .	3
1.3	Parts of the Cochlea . . . . .	4
1.4	Parts of the Cochlea . . . . .	5
1.5	Equal Loudness Contours or Fletcher-Munson Curves . . . . .	8
1.6	Typical Audiogram - Normal Hearing . . . . .	9
1.7	Typical Audiogram - Sensorineural Hearing Loss . . . . .	11
1.8	Typical Audiogram - Conductive Hearing Loss . . . . .	12
1.9	Typical Audiogram - Mixed Hearing Loss . . . . .	13
1.10	Normal and Damaged Inner and Outer Hair Cells ( <i>Top and bottom three rows in each image, respectively. From "The Biology of Hearing and Deafness", (pg. 21), by R. Harrison, 1998</i> ) . . . . .	13
1.11	Loudness Growth Curves . . . . .	14
1.12	Generic block diagram of digital signal processing hearing aid . . . . .	16
1.13	Relationship between Bands and Channels . . . . .	18
1.14	A Simple Static Input-Output Curve, and Associated Gain Curve . . . . .	19
1.15	Objective Measures Analysis . . . . .	26
1.16	PESQ Overview . . . . .	29
2.1	System Identification Block Diagram (1) . . . . .	34
2.2	A Direct-form FIR Adaptive Filter . . . . .	36
2.3	Subband Adaptive Filter Structure . . . . .	40
2.4	DFT Analysis Filter Bank . . . . .	41
2.5	DFT Synthesis Filter Bank . . . . .	42
2.6	$I^{th}$ Band of M-Channel Analysis/Synthesis Filter Bank . . . . .	44
2.7	(a) Quadrature Mirror Filter Bank, and (b) Frequency Magnitude Responses . . . . .	44
2.8	Kaiser-based Lowpass Prototype Filter ( $12\Delta\omega = 0.07$ radians/sample, $A_s = 100$ dB) . . . . .	46
2.9	4 Band Uniform Filter Bank Fullband Distortions . . . . .	46
2.10	Memory Characteristic of the RLS Algorithm . . . . .	55
2.11	Tracking Model . . . . .	57



2.12	Adaptive Filter Implementation for Tracking Analysis . . . . .	59
2.13	NLMS Tracking Performance . . . . .	60
2.14	NLMS Tracking Performance, Attack Region . . . . .	61
2.15	NLMS Tracking Performance, Release Region . . . . .	61
2.16	APA Tracking Performance . . . . .	62
2.17	APA Tracking Performance, Release Region . . . . .	63
2.18	APA Tracking Performance, Release Region . . . . .	63
2.19	RLS Tracking Performance - Attack Region . . . . .	64
2.20	RLS Tracking Performance - Release Region . . . . .	65
3.1	Simulated Hearing Aid . . . . .	69
3.2	Steeply Sloping Moderate-to-moderately Severe Audiogram . . . . .	69
3.3	16 <sup>th</sup> Order FIR Fit with Desired Frequency Magnitude Response . . . . .	72
3.4	RMS Error Versus FIR Order . . . . .	72
3.5	Subband Adaptive Model . . . . .	74
3.6	Four Channel Model . . . . .	76
3.7	Model of Simulated Hearing Aid Output . . . . .	77
3.8	System Identification Patterns . . . . .	79
3.9	Paired Filter Adaptive System . . . . .	80
3.10	Experimental and Ideal System Identification Patterns . . . . .	82
4.1	CASI Block Diagram . . . . .	88
4.2	Critical Bands, Relationship to Cochlea . . . . .	90
4.3	Critical Band Structure of the Human Ear . . . . .	91
4.4	Critical Band Shape Versus Excitation Level . . . . .	91
4.5	Overall Excitation Pattern . . . . .	92
4.6	Hearing Aid Testing System (HATS) . . . . .	95
4.7	Subband Adaptive Filter Structure . . . . .	101
5.1	NLMS Averaged SER and MOS, Audiogram F . . . . .	108
5.2	NLMS Averaged SER and MOS, Audiogram I . . . . .	109
5.3	NLMS SER Mean with Error Bar, Audiogram F . . . . .	110
5.4	NLMS SER Mean with Error Bar, Audiogram I . . . . .	111
5.5	NLMS MOS Mean with Error Bar, Audiogram F . . . . .	111
5.6	NLMS MOS Mean with Error Bar, Audiogram I . . . . .	112
5.7	APA Averaged SER and MOS, Audiogram F . . . . .	113
5.8	APA Averaged SER and MOS, Audiogram I . . . . .	114
5.9	APA SER Mean with Error Bar, Audiogram F . . . . .	114
5.10	APA SER Mean with Error Bar, Audiogram I . . . . .	115
5.11	APA MOS Mean with Error Bar, Audiogram F . . . . .	116
5.12	APA MOS Mean with Error Bar, Audiogram I . . . . .	116
5.13	QRD RLS Averaged SER and MOS, Audiogram F . . . . .	117
5.14	QRD RLS Averaged SER and MOS, Audiogram I . . . . .	118

5.15	QRD RLS SER Mean with Error Bar, Audiogram F . . . . .	119
5.16	QRD RLS SER Mean with Error Bar, Audiogram I . . . . .	119
5.17	QRD RLS MOS Mean with Error Bar, Audiogram F . . . . .	120
5.18	QRD RLS MOS Mean with Error Bar, Audiogram I . . . . .	121
6.1	Bark Spectrograms . . . . .	133
6.2	APA MOS Mean with Error Bar, Audiogram "F" . . . . .	138
6.3	NLMS One-Way ANOVA (20 Bands, 256 Taps, Step-size of 1.0) . . . . .	140
6.4	APA One-Way ANOVA (20 Bands, 256 Taps, Step-size of 1.0, Projection-order of 15) . . . . .	141
6.5	QRD RLS One-Way ANOVA (20 Bands, 256 Taps, Forgetting-factor of 0.95) . . . . .	142
6.6	QRD RLS One-Way ANOVA (20 Bands, 256 Taps, Forgetting-factor of 0.5) . . . . .	143
B.1	ANSI S3.22 (2003) Test Results for Bernafon Symbio 110 XT SE (Audiogram "F") . . . . .	175
B.2	ANSI S3.22 (2003) Test Results for Bernafon Symbio 110 XT SE (Audiogram "I") . . . . .	176
B.3	ANSI S3.22 (2003) Test Results for Oticon Syncro V2 (Audiogram "F")	178
B.4	ANSI S3.22 (2003) Test Results for Oticon Syncro V2 (Audiogram "I")	179
B.5	ANSI S3.22 (2003) Test Results for Phonak Perseo 311 dAZ Forte (Audiogram "F") . . . . .	181
B.6	ANSI S3.22 (2003) Test Results for Phonak Perseo 311 dAZ Forte (Audiogram "I") . . . . .	182
B.7	ANSI S3.22 (2003) Test Results for Siemens Triano S (Audiogram "F")	184
B.8	ANSI S3.22 (2003) Test Results for Siemens Triano S (Audiogram "I")	185
B.9	ANSI S3.22 (2003) Test Results for Sonic Innovations Natura 2 SE (Audiogram "F") . . . . .	187
B.10	ANSI S3.22 (2003) Test Results for Sonic Innovations Natura 2 SE (Audiogram "I") . . . . .	188
C.1	NLMS Model, SER-MOS, Bernafon Symbio 110 XT SE . . . . .	191
C.2	NLMS Model, SER-MOS, Oticon Syncro V2 . . . . .	192
C.3	NLMS Model, SER-MOS, Phonak Perseo 311 dAZ Forte . . . . .	193
C.4	NLMS Model, SER-MOS, Siemens Triano S . . . . .	194
C.5	NLMS Model, SER-MOS, Sonic Innovations Natura 2 SE . . . . .	195
C.6	APA Model, SER-MOS, PO 5, Bernafon Symbio 110 XT SE . . . . .	197
C.7	APA Model, SER-MOS, PO 10, Bernafon Symbio 110 XT SE . . . . .	198
C.8	APA Model, SER-MOS, PO 15, Bernafon Symbio 110 XT SE . . . . .	199
C.9	APA Model, SER-MOS, PO 5, Oticon Syncro V2 . . . . .	200
C.10	APA Model, SER-MOS, PO 10, Oticon Syncro V2 . . . . .	201
C.11	APA Model, SER-MOS, PO 15, Oticon Syncro V2 . . . . .	202

C.12 APA Model, SER-MOS, PO 5, Phonak Perseo 311 dAZ Forte . . . .	203
C.13 APA Model, SER-MOS, PO 10, Phonak Perseo 311 dAZ Forte . . . .	204
C.14 APA Model, SER-MOS, PO 15, Phonak Perseo 311 dAZ Forte . . . .	205
C.15 APA Model, SER-MOS, PO 5, Siemens Triano S . . . . .	206
C.16 APA Model, SER-MOS, PO 10, Siemens Triano S . . . . .	207
C.17 APA Model, SER-MOS, PO 15, Siemens Triano S . . . . .	208
C.18 APA Model, SER-MOS, PO 5, Sonic Innovations Natura 2 SE . . . .	209
C.19 APA Model, SER-MOS, PO 10, Sonic Innovations Natura 2 SE . . . .	210
C.20 APA Model, SER-MOS, PO 15, Sonic Innovations Natura 2 SE . . . .	211
C.21 QRDRLS Model, SER-MOS, Bernafon Symbio 110 XT SE . . . . .	213
C.22 QRDRLS Model, SER-MOS, Oticon Syncro V2 . . . . .	214
C.23 QRDRLS Model, SER-MOS, Phonak Perseo 311 dAZ Forte . . . . .	215
C.24 QRDRLS Model, SER-MOS, Siemens Triano S . . . . .	216
C.25 QRDRLS Model, SER-MOS, Sonic Innovations Natura 2 SE . . . . .	217

# List of Acronyms & Abbreviations

APA	Affine Projection Algorithm
AT	Attack Time
AVC	Automatic Volume Control
CL	Compression Limiting
CR	Compression Ratio
CT	Compression Threshold
dB HL	dB Hearing Level
dB SPL	dB Sound Pressure Level
DSP	Digital Signal Processing
FIR	Finite Impulse Response
IHC	Inner Hair Cell
MMSE	Minimum Mean Squared Error
MNB	Measuring Normalizing Blocks
MOS	Mean Opinion Score
NLMS	Normalized Least Mean Squares
OHC	Outer Hair Cell
PESQ	Perceptual Evaluation of Speech Quality
QMF	Quadrature Mirror Filters
QRD-RLS	QR-Decomposition Recursive Least Squares
RLS	Recursive Least Squares
RT	Release Time

SER	Signal-to-Error Ratio
WDRC	Wide Dynamic Range Compression

## Chapter 3

### Introduction

#### 3.1 Hearing

Understanding of the way in which the human ear processes sound is essential for the development of hearing aids. This chapter discusses the basic principles of hearing and the way in which the ear processes sound.

#### 3.1.1 The Physiology of Hearing

The human ear is a complex organ that is capable of detecting and processing a wide range of sounds. The ear is divided into three main parts: the outer ear, the middle ear, and the inner ear. The outer ear is responsible for collecting sound waves and directing them into the ear canal. The middle ear contains three small bones (the ossicles) that amplify the sound waves and transmit them to the inner ear. The inner ear is responsible for converting the sound waves into electrical signals that can be processed by the brain.

The ear is also capable of detecting the frequency and intensity of sounds. The frequency of a sound is determined by the number of cycles per second (Hertz) of the sound wave. The intensity of a sound is determined by the amplitude of the sound wave. The ear is able to detect sounds with frequencies ranging from 20 Hz to 20,000 Hz and with intensities ranging from 0 dB to 140 dB.

# Chapter 1

## Introduction

### 1.1 Hearing

Understanding of key areas of the sensation of hearing is critical to its assessment and development of techniques to overcome its loss. This chapter highlights several of these areas.

#### 1.1.1 The Physiological Process of Hearing

The physiological process of hearing is complex, involving several mechanisms that facilitate the conversion of acoustical sound energy into nerve impulses the brain uses for the perception of hearing. Each aspect of this highly developed process is in and of itself highly specialized. Figure 1.1 illustrates the anatomy of the human ear (2).

The anatomy of the human ear can be segmented into three regions, each with its own unique contribution to the overall process of hearing. The outer ear, the middle ear, and the cochlea are these three regions. A brief description of the anatomy of each region and how it contributes to the sense of hearing is described in the following sections.

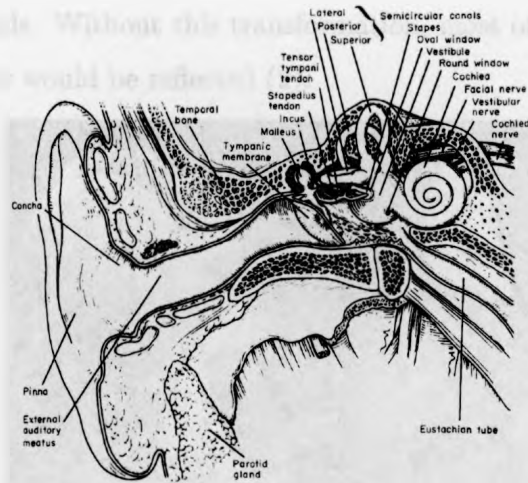


Fig. 1.1: Anatomy of the Human Ear (*From Tissues and Organs: A Text-Atlas of Scanning Electron Microscopy, by R.G. Kessel and R.H. Kardon. W.H. Freeman and Company. Copyright 1979*)

#### 1.1.1.1 Outer Ear

The outer ear consists of a partially cartilaginous flange called the pinna, which includes a resonant cavity called the concha, and together with the ear canal, or external auditory meatus, lead to the eardrum or the tympanic membrane (2). It has two noteworthy characteristics. First, the overall resonant properties of the outer ear alter the sound pressure at the tympanic membrane. And second, the anatomy of the outer ear aids in sound localization.

#### 1.1.1.2 Middle Ear

The middle ear consists of a set of three small, interconnected bones collectively referred to as the ossicles. The malleus, incus, and stapes facilitate the coupling of sound energy from the auditory canal to the cochlea. Figure 1.2 shows the malleus, incus, and stapes bones of a chinchilla.

The unique shape and relative placement of the malleus, incus, and stapes aid in matching the low acoustical impedance of the auditory canal with the higher im-

pedance cochlear fluids. Without this transformation, most of the acoustical energy entering the outer ear would be reflected (2).



Fig. 1.2: Middle Ear Ossicles of Chinchilla (From Auditory Science Lab - Sick Kids, The Hospital for Sick Children, Toronto, Ontario, Canada)

#### 1.1.1.3 Inner Ear

The inner ear, or cochlea, is one of the most developed and highly specialized organs in the human body. It is an extremely small, spiral-shaped structure within the temporal bone of the skull, about the size of the nail on the little finger (3). The cochlea converts acoustical energy entering the outer ear, conducted through the middle ear ossicles, into auditory nerve impulses that are transmitted to the brain.

Figure 1.3.A illustrates the internal structure of the cochlea using a cross-sectional view. The cochlea is bored out of the temporal bone and is divided into three distinct regions: the Scala Vestibuli (sv), the Scala Media (sm), and the Scala Tympani (st). Figure 1.3.B provides a more detailed view of the relationship between these three regions.

Figure 1.4.A elaborates on the cross-sectional views of Figures 1.3.A and B by showing a simplified cross-sectional view of the cochlea unfolded. The stapes bone



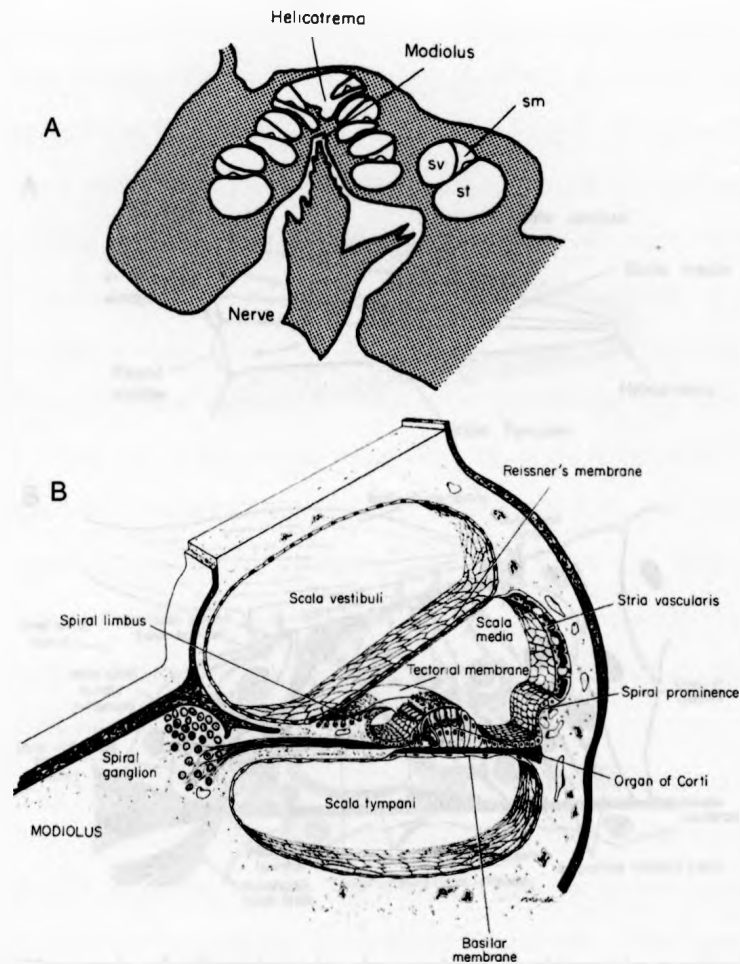


Fig. 1.3: (A) In a transverse section of the whole cochlea, the cochlear duct is cut across several times as it coils round and round. Abbreviations: sv - scala vestibuli; sm - scala media; st - scala tympani. (B) The three scalae and associated structures are shown in a magnified view of a cross-section of the cochlear duct. From Fawcett (1986, Fig. 35.11).

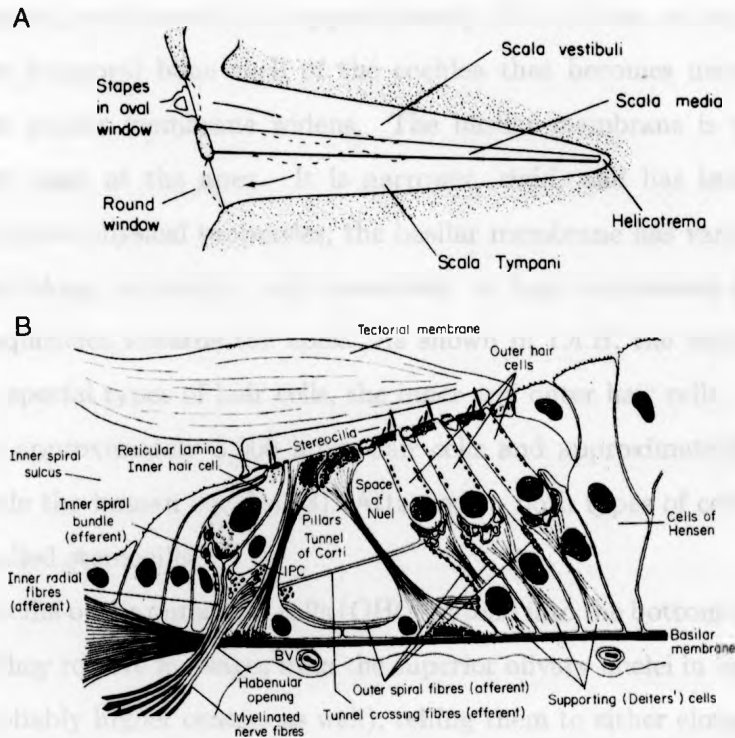


Fig. 1.4: (A) The path of vibrations in the cochlea is shown in a schematic diagram in which the cochlear duct is depicted as unrolled. (B) Detailed cross-section of the organ of Corti. From Ryan and Dallos (1984, Fig. 22-4, slightly modified).

meets the cochlea at the oval window. The scala vestibuli and scala tympani form one continuous space, connected to each other at the helicotrema. The scala media divides this volume along the complete length of the cochlea. Cochlear fluids fill these compartments.

The basilar membrane forms the boundary between the scala tympani and the scala media, as depicted in Figure 1.3.B. It runs the length of the cochlea, from base to apex. Unfolded, end-to-end, it is approximately 24 to 35 mm in length (2).

Unlike the temporal bone shell of the cochlea that becomes narrower towards the apex, the basilar membrane widens. The basilar membrane is wider, flaccid, and has more mass at the apex. It is narrower, rigid, and has less mass at the base. Due to these physical properties, the basilar membrane has varying resonance characteristics along its length, with sensitivity to high frequencies near the base and lower frequencies towards the apex. As shown in 1.4.B, the basilar membrane supports two special types of hair cells, the inner and outer hair cells.

There are approximately 3,000 inner hair cells and approximately 12,000 outer hair cells inside the human cochlea (3). Attached to both types of cells are hair-like projections called stereocilia.

The stereocilia of the outer hair cells (OHC) extend into the bottom of the tectorial membrane. They receive messages from the superior olivary nuclei in the lower brain-stem (and probably higher centres as well), telling them to either elongate or shrink. This mechanical action changes the mechanical properties of the basilar membrane at specific spots (3).

The stereocilia of the inner hair cells (IHC) do not touch the tectorial membrane and are mostly afferent, sending information to the brain. As noted by (3), a person with IHC damage may have difficulty understanding speech in quiet environments and especially with background noise (4).

#### **1.1.1.4 Hearing Dynamics**

Sound energy entering the outer ear, and conducted through the middle ear, is coupled to the cochlea through the stapes at the oval window. Excitation of the oval window transfers energy to the cochlear fluid common to the scala vestibuli and the scala media. As the hard surface of the temporal bone forms the outer surface of the cochlea, fluid motion is restricted. Some fluid motion is possible because of the round window, a membranous window located at the base in the scala tympani. This restricted motion results in a standing wave being created in the scala media. The displacement of the scala media by a traveling wave peak bends regions of the scala media, stimulating a particular location. Low frequency sounds are heard when stimulation occurs at the apex of the cochlea, while high frequency sounds are associated with regions near the base of the cochlea.

OHC have two critical functions in this complex process. For soft sounds, less than 40 to 60 dB hearing level, the OHC pull the tectorial membrane closer to the IHC, allowing them to sense the shearing action of the tectorial membrane caused by the standing wave. OHC also "sharpen" the peak of the traveling wave to improve frequency sensitivity of the IHC along the entire length of the basilar membrane. For more intense sounds, the OHC elongate to protect the IHC from damage.

Damage to the outer hair cells can result in a moderate hearing loss (5). Severe hearing loss is usually attributable to damage of the inner hair cells in addition to the outer hair cells.

#### **1.1.2 Hearing Sensitivity and its Measurement**

As the two previous sections detail, the physiological process of hearing involves intricate associations between the outer ear, middle ear, and cochlea. As a result, hearing sensitivity varies with frequency and accurate assessment of hearing ability is critical to determine the underlying problems and the proper remedial action.

Presbycusis, the loss of hearing sensitivity at higher frequencies due to aging, is the most common type of hearing loss. This is attributable to damage or loss of outer hair cells in the cochlea.

Hearing sensitivity is a function of frequency, mid-range frequencies being most easily heard. This phenomenon is graphically depicted by a set of curves referred to as the Fletcher-Munson curves. The vertical axis represents the sound pressure intensity measured at the tympanic membrane in units of dB sound pressure level (SPL, referenced to  $20 \mu\text{Pa}$ ). Figure 1.5 illustrates these curves.

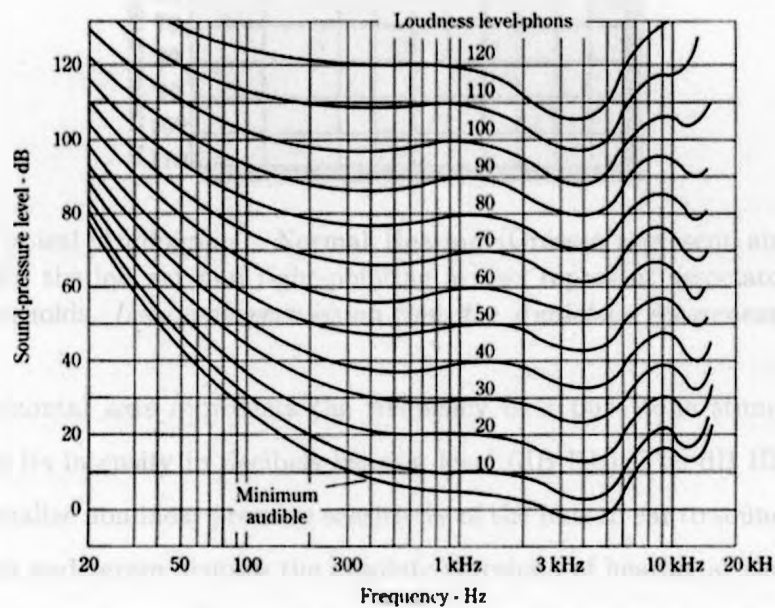


Fig. 1.5: Equal Loudness Contours or Fletcher-Munson Curves (6)

The Fletcher-Munson curves are equal-loudness contours for the human ear. They represent measures of sound pressure, over the frequency spectrum, for which a listener perceives a constant loudness.

Pure tone audiometry is a standardized test procedure used to measure hearing sensitivity using pure tone test frequencies. The results of this test are shown visually in a graph known as an audiogram. It captures a person's ability to hear the softest

sounds possible as a function of frequency. Figure 1.6 shows a typical audiogram characterizing normal, left ear hearing thresholds.

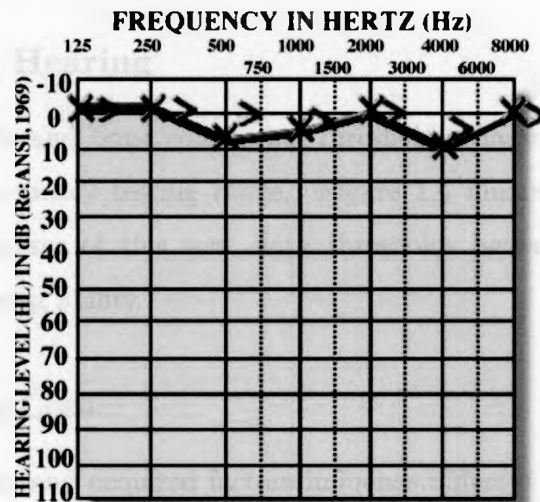


Fig. 1.6: Typical Audiogram - Normal Hearing (Crosses represent air conduction thresholds for the left ear and right-pointing arrows represent associated bone conduction thresholds. *Used with permission from the Audiology Awareness Campaign.*)

The horizontal axis represents the frequency of a pure tone stimulus and the vertical axis its intensity in decibels hearing level (dB HL). The dB HL measure is used to normalize nonlinear pressure sensitivity of the human ear to sound pressure. 0 dB HL on an audiogram denotes the absolute threshold of hearing at that frequency.

Air conduction is tested by using earphone-inserts in each ear that are attached to an audiometer, a calibrated device that creates pure tones with the correct intensity. As tones are presented, the patient is asked to indicate when they are heard. The minimum intensity required demarcates the respective threshold. With a bone oscillator, placed against the mastoid bone behind each ear, bone conduction behaviour can be measured. This test helps distinguish hearing loss contributions from either one or both conductive and sensorineural factors.

As shown in Figure 1.6, blue crosses and right-pointing arrows mark air and bone conduction thresholds for the left ear, respectively. Red circles and left-pointing

arrows mark air and bone conduction thresholds for the right ear, respectively. These are usually shown on the same audiogram.

### 1.1.3 Normal Hearing

Relatively flat air and bone conduction thresholds characterize normal hearing across the entire frequency testing range. Figure 1.6 illustrates a typical normal audiogram. Audiograms of this sort, with thresholds between 0 and 20 dB HL, indicate normal hearing ability.

### 1.1.4 Hearing Loss

Several congenital and acquired factors influence different portions of ear physiology, resulting in hearing loss. Where and how these factors influence the hearing process is reflected in the air and bone conduction thresholds discussed previously. Of primary relevance to this thesis is hearing loss attributable to damage or loss of cochlea hair cells. The resulting mild-to-moderate and moderate-to-severe hearing losses are characterized by reduced dynamic range and increased loudness growth.

Congenital hearing loss factors include, but are not limited to,

- *Aplasia* - An irregularity of or complete absence of the cochlea.
- *Chromosomal Syndromes* - Inherited genetic defects (no concise data supporting this factor presently exists).
- *Cholesteatoma* - A tumour-like mass usually occurring in the middle ear or mastoid region.

Acquired hearing loss factors include, but like congenital factors, are not limited to,

- *Presbycusis* - An age related hearing loss starting in the higher frequency range (typically in the 4 to 8 kHz region of the normal 20 to 20 kHz range) and progressing to lower frequencies.
- *Noise Induced* - Prolonged exposure to loud noise resulting in hearing loss, typically mid-to-high frequencies.
- *Ototoxicity* - This factor is closely associated with commonly occurring drugs that damage cochlea hair cells due to their extreme sensitivity to oxygen deprivation. Examples include salicylates found in aspirin and amino glycosides found in broad-spectrum antibiotics, like streptomycin.

A sensorineural hearing loss is indicated when air conduction and bone conduction thresholds are at the same relative, elevated level, as shown in Figure 1.7.

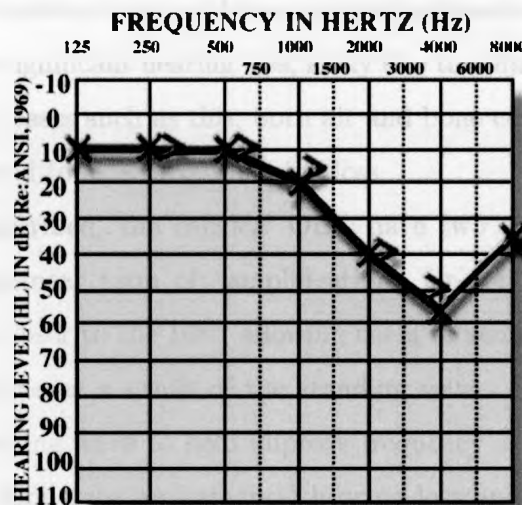


Fig. 1.7: Typical Audiogram - Sensorineural Hearing Loss (*Used with permission from the Audiology Awareness Campaign.*)

A conductive hearing loss is indicated when air conduction thresholds show a hearing loss, but the bone conduction thresholds are normal as shown in Figure 1.8. In this case, a middle ear condition, such as Cholesteatoma, exists.



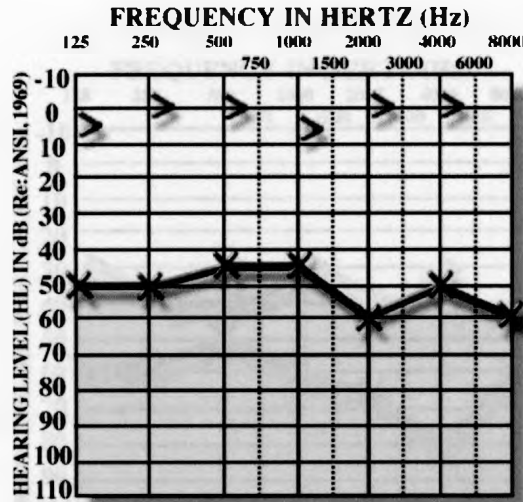


Fig. 1.8: Typical Audiogram - Conductive Hearing Loss (*Used with permission from the Audiology Awareness Campaign.*)

A complex combination of air and bone conduction thresholds, as shown in Figure 1.9, suggests a more significant hearing loss, likely due to ailments in both the middle ear and cochlea. For cases such as this, both air and bone conduction thresholds are higher. This is referred to as a mixed hearing loss.

As previously described, the cochlea's OHC have two critical functions. First, they facilitate a nonlinear form of "amplification" for soft sounds by pulling the tectorial membrane closer to the IHC, allowing them to sense the shearing action of the tectorial membrane as a result of the standing wave. Second, they "sharpen" the peak of the traveling wave to help improve frequency selectivity. OHC damage results in a mild-to-moderate sensorineural hearing loss and further damage to the IHC results in moderate-to-severe sensorineural hearing losses. Figure 1.10 illustrates both normal and damaged human IHC and OHC.

The dynamic range of normal hearing is defined as the region bound by the threshold of hearing and the uncomfortable listening level (UCL), the point at which discomfort or pain is experienced. On average, a 100 dB difference separates these

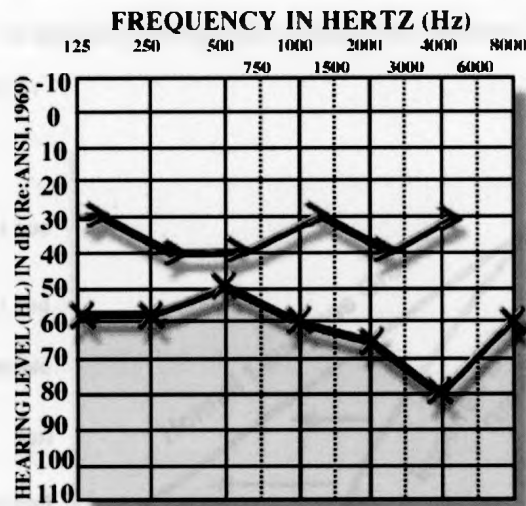
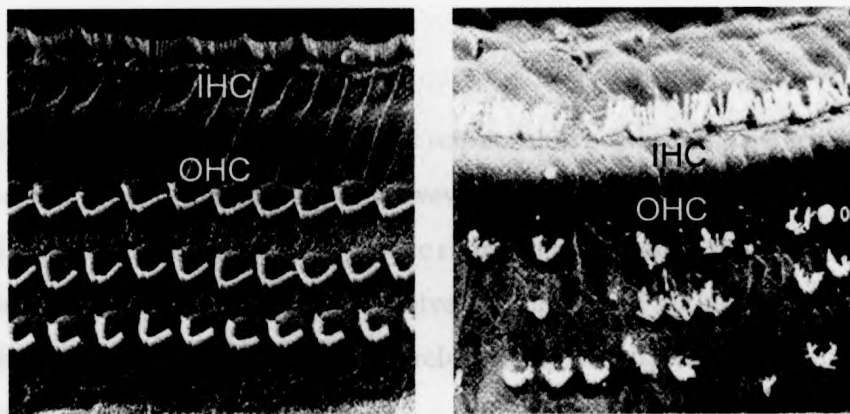


Fig. 1.9: Typical Audiogram - Mixed Hearing Loss (*Used with permission from the Audiology Awareness Campaign.*)



(a) Healthy Hair Cells

(b) Damaged Hair Cells

Fig. 1.10: Normal and Damaged Inner and Outer Hair Cells (*Top and bottom three rows in each image, respectively. From "The Biology of Hearing and Deafness", (pg. 21), by R. Harrison, 1998)*

boundaries across the nominal frequency range of hearing. This arrangement facilitates what is known as normal perception of loudness growth. Figure 1.11 graphically illustrates this concept.

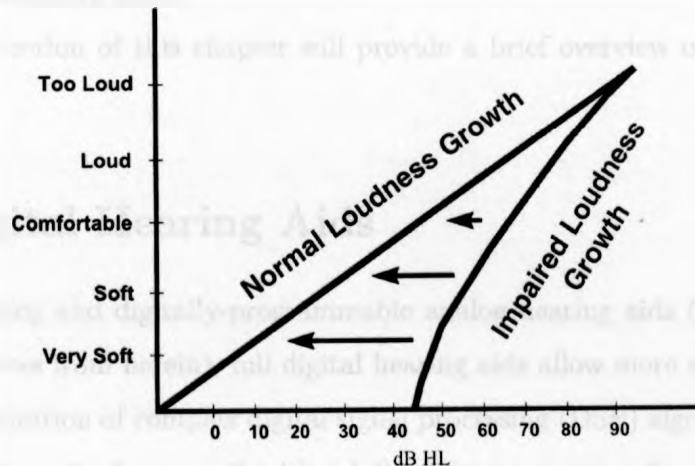


Fig. 1.11: Loudness Growth Curves (3) *Length of arrows indicate level amplification required to restore normal loudness perception.*

With normal loudness growth, a linear relationship between the perceived loudness and the actual sound intensity exists. However, a sensorineural hearing loss attributed to loss of OHC reduces the overall dynamic range, typically at higher frequencies. This alters the relationship between the perceived loudness and actual sound intensity as shown in Figure 1.11. The nonlinear relationship results from a psycho-acoustic phenomenon known as recruitment.

The most common form of intervention for hearing losses are hearing aids. They attempt to restore normal loudness growth using gain and amplitude compression in several sections or channels across the frequency range of importance. The arrows shown in Figure 1.11 indicate the amplification required to restore normal loudness growth.

Modern multichannel, nonlinear hearing aids use complex digital signal processing algorithms to provide the features needed to restore normal loudness growth. Because of algorithm complexity, and the need to keep hearing aids compact in size, digital circuitry is commonly used.

The next section of this chapter will provide a brief overview of digital hearing aids.

## 1.2 Digital Hearing Aids

Unlike analog and digitally-programmable analog hearing aids (both referred to as analog devices from herein), full digital hearing aids allow more effective and efficient implementation of complex digital signal processing (DSP) algorithms yet allow hearing aid size to be kept small with minimal power consumption (7). DSP-based hearing aids readily scale traditional methods of analog signal processing, including amplification, frequency response shaping, compression in two or three bands, and output limiting. Many of today's digital hearing aids are referred to as "intelligent" devices, independently managing the processing features of the hearing aid.

### 1.2.1 General Structure

Figure 1.12 shows a generic block diagram of a digital hearing aid.

As noted by (7), the processing path through the hearing aid extends from the microphone to the receiver, while the upper three blocks, *Clock*, *Logic*, and *Memory* items are auxiliary control functions. For completeness, a brief description of each functional block shown in Figure 1.12 follows.

**Microphone** - Converts acoustical sound energy into an analog electrical signal.

**Preamplifier** - In order to improve the working signal-to-noise ratio, amplification is applied. Ranging anywhere from 10 to 30 dB, amplification is used to offset

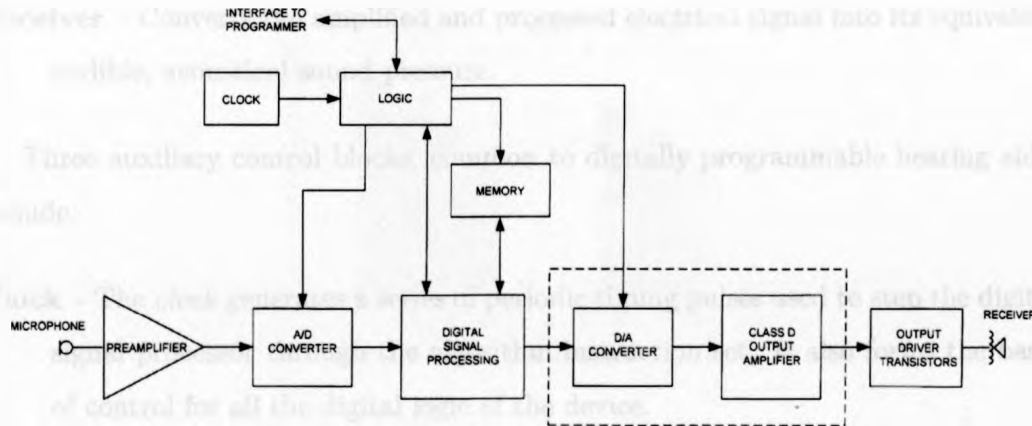


Fig. 1.12: Generic block diagram of digital signal processing hearing aid (7)

the perception of internally generated noise from the hearing aid. Compression may also be applied to control transient inputs and saturation.

**A/D Converter** - Of all the functional blocks, this one is the most critical. The analog-to-digital converter is responsible for converting the amplified analog signal from the microphone into an equivalent digital representation. The most common type of converter is the sigma-delta converter.

**Digital Signal Processor** - This block implements the complex speech processing algorithms. These include: filtering, gain, compression, and noise reduction.

**D/A Converter** - The final digital representation of the processed signal is converted back into an equivalent analog form. The D/A converter and Class D output amplifier, as denoted by the outlined box, can be removed allowing the processed signal to enter directly into the output driver transistors. This is done to minimize the introduction of additional noise components associated with these elements.

**Output Driver Transistors** - This is the final stage that drives the receiver with the processed, analog electrical signal.

**Receiver** - Converts the amplified and processed electrical signal into its equivalent audible, acoustical sound pressure.

Three auxiliary control blocks, common to digitally programmable hearing aids, include,

**Clock** - The *clock* generates a series of periodic timing pulses used to step the digital signal processor through the algorithm instruction set. It also forms the basis of control for all the digital logic of the device.

**Logic** - It performs a set of functions controlling sequences of operations within the hearing aid that facilitate necessary function (i.e. communicate with the programmer, route data into and out of the process and memory, etc.).

**Memory** - Provides storage of the processing algorithm and other instructions that instruct the digital signal processing block how to process the incoming signal. There are typically two types of RAM, volatile memory and non-volatile memory. Temporary processing data is stored in volatile memory. The speech processing algorithms and other critical data is stored in non-volatile memory.

## 1.2.2 Bands and Channels

Two processing concepts important for the restoration of normal loudness growth due to a sensorineural hearing loss are bands and channels. Figure 1.13 shows the relationship between these two elements.

A band refers to a frequency range in which a gain adjustment can be made. Splitting the working frequency range into several independent processing regions allows more precise gain adjustments to be made. Implementation of these frequency bands depends on a manufacturer's rationale and the bands may be uniform, one-third octave, or some other variation.

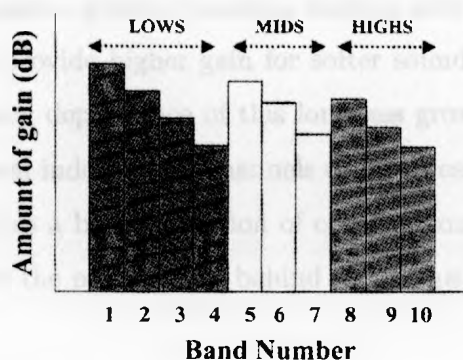


Fig. 1.13: Relationship between Bands and Channels *Frequency increases from left to right.* (7)

A channel refers to a collection of consecutive frequency bands to which the same type of signal processing is applied. The number of channels can be equal to or less than the number of frequency bands. As shown in Figure 1.13, for the ten bands, there are three processing channels. Bands 1, 2, 3, and 4 are associated with a “low-frequency” processing channel; bands 5, 6, and 7 with a “mid-frequency” channel; and bands 8, 9, and 10 are associated with a “high-frequency” channel.

As already noted, how the working frequency range is divided into bands and how these resulting bands are grouped into channels depends on a given manufacturer’s philosophy. Regardless of the final working arrangement between these structures, they serve to attempt to restore normal loudness growth to individuals with mild-to-moderate sensorineural hearing losses.

### 1.3 Compression

As discussed by (8) and (9), a common observation of individuals with sensorineural hearing losses is the recruitment phenomenon or the occurrence of a steeper-than-normal loudness growth function across frequency, together with an elevated absolute upper threshold known as the upper comfort level (UCL). In an attempt

to restore a normal loudness growth function, hearing aids use nonlinear compressor circuits. Compressors provide higher gain for softer sounds than for louder sounds. Because of the frequency dependence of this loudness growth, as noted earlier, it is necessary to have several independent channels of compression.

This chapter provides a basic definition of compression, its working parameters, and a brief summary of the philosophies behind its various forms of implementation.

### 1.3.1 Compression

Amplitude compression, in essence, is a nonlinear transfer function used to reduce the dynamic range of a signal. Unlike a linear transfer function, which applies a constant amount of gain regardless of input level, compression provides varying amounts of gain that is dependent on the input level of the applied signal. Figure 1.14.A illustrates a basic input-output (I/O) curve illustrating this concept.

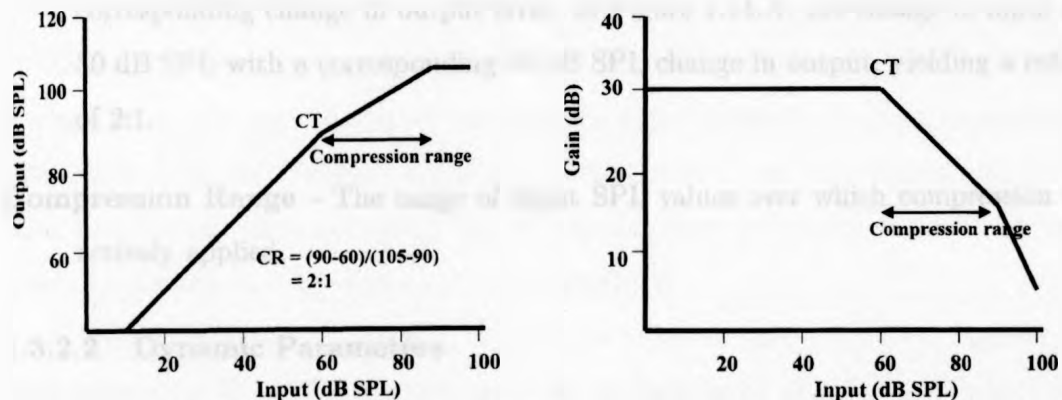


Fig. 1.14: A.) A Simple Static Input-Output Curve, B.) Associated Gain Curve (10)

Figure 1.14.A shows three distinct linear regions; each region has a different level of gain. The degree of gain as a function of input level can also be graphed as shown in Figure 1.14.B. For input levels up to 60 dB SPL, 30 dB of gain is applied. Once the input level is above 60 dB SPL, the amount of gain decreases with input, which



is a fundamental property of compression. Further input level increases beyond 90 dB SPL result in a further decrease in gain.

### **1.3.2 Compression Characteristics**

Compression characteristics can be controlled by parameters that can be classified into two broad categories: static parameters and dynamic parameters.

#### **1.3.2.1 Static Parameters**

**Compression Threshold (CT)** - Represents the lowest input sound pressure at which the hearing aid begins to reduce its gain. In Figure 1.14.A this value is 60 dB SPL. The compression threshold is also referred to as the compression knee-point (TK).

**Compression Ratio (CR)** - Represents the ratio of change in input level to the corresponding change in output level. In Figure 1.14.A, the change in input is 30 dB SPL with a corresponding 15 dB SPL change in output, yielding a ratio of 2:1.

**Compression Range** - The range of input SPL values over which compression is actively applied.

#### **1.3.2.2 Dynamic Parameters**

Compression circuits operate through the use of feedback loops and, as a result, time constants determine the effective rate of application of gain reduction and gain reduction removal. The two important values here are the attack time and the release time.

**Attack Time (AT)** - As defined by the ANSI S3.22 (2003) standard, attack time is the time required for hearing aid compression to change from linear gain to

within 3 dB of the final, compressed steady state after applying a calibrated signal.

**Release Time (RT)** - As defined by the ANSI S3.22 (2003) standard, release time is the time required for hearing aid compression to change from the compressed steady-state to within 4 dB of the linear steady-state after the application of a calibrated signal.

### **1.3.3 Application and Efficacy of Compression**

Choosing the working parameters to achieve different results can alter compression behaviour. In this section three key applications will be briefly discussed, relative to the characteristics of linear gain. One or two brief notes on respective efficacy will be made where appropriate.

#### **1.3.3.1 Linear Gain**

As noted earlier, linear gain refers to the application of the same amount of gain across a range of inputs. Applying gain in this manner preserves the relative intensity differences of the input signal, retaining important speech cues for patients with more than a moderate degree of hearing loss (11)(12). In order to control the level of gain, a volume control on the hearing aid can be adjusted.

A critical problem associated with the use of linear gain occurs for high-input level sounds ( $> 70$  dB SPL). With moderate to high levels of gain, sounds may be uncomfortably loud. This is often addressed by peak clipping the resulting sound. This affects speech sound quality and intelligibility because of high distortion levels.

#### **1.3.3.2 Compression Limiting**

Compression limiting (CL) is an approach used to limit hearing aid output without creating distortion such as peak clipping. CL is characterized by a moderately high

compression threshold ( $> 70$  dB SPL), a high compression ratio ( $> 8:1$ ), and a short attack time ( $< 10$  ms).

A linear hearing aid with CL provides the same fixed gain up to a relative high level beyond which gain is drastically reduced due to the high compression ratio. This action prevents loud sounds from becoming too loud and saturation of the hearing aid. As noted by (8), compression limiting is preferable over peak clipping and is likely because distortion is minimized, with the temporal and spectral integrity of the signal being maintained most of the time (13).

#### **1.3.3.3 Wide Dynamic Range Compression (WDRC)**

Wide dynamic range compression (WDRC) is used to ensure audibility and comfort without the continual need for volume control adjustment. WDRC is characterized by a low compression threshold ( $< 60$  dB SPL), a low compression ratio ( $< 4:1$ ), and a short attack ( $< 10$  ms) and release time ( $< 50$  ms).

Hearing aids implementing WDRC typically provide more gain than linear hearing aids for soft sounds, ensuring soft sounds are heard. With a lower threshold (less than 60 dB SPL) and a low compression ratio (less than 4:1), risk of saturation is minimized, but still possible. As noted by (10), the choice of attack time and release time on a WDRC hearing aid is critical. Physiological data of the outer hair cell functions and basilar membrane suggest a very fast, active compression mechanism in the healthy cochlea (14).

Dillon's literature survey (15) concluded that WDRC improved speech recognition in quiet conditions over a linear hearing aid at a low input level and when subjects were not allowed to adjust the volume control on the hearing aids.

#### **1.3.3.4 Automatic Volume Control (AVC)**

Automatic volume control is characterized by moderate compression thresholds (between 65 and 75 dB SPL), low to moderate compression ratios (4-6:1), long attack

(> 20 ms.) and release (> 1 second) times. The working parameters for AVC are very similar to those of WDRC. The primary difference is the longer attack and release times.

Providing more gain to soft sounds and less gain to loud sounds with longer time constants results in reduction of intensity contrasts in the speech signal. These contrasts are referred to as smearing artefacts.

## 1.4 Hearing Aid Performance Verification

Verification of hearing aid performance can be done at one of several different levels. From the manufacturers who design and fabricate hearing aids, to the audiologists and hearing-aid practitioners who select and fit them, the need to assess and ensure correct operation is important to each of these groups of professionals for different reasons. The ultimate goal is to determine whether the device is of benefit to the patient in terms of speech intelligibility and quality.

The current document (16) on hearing aid verification techniques is the American National Standards Institute (ANSI) standard, "*Specification of Hearing Aid Characteristics*," commonly referred to by its abbreviation, ANSI S3.22 (2003)(17). This standard is used as a tool for assessing hearing instrument functionality and consists of a number of well defined tests, promoting the following,

- A common set of definitions and tests allowing comparisons throughout the hearing aid industry, thereby providing a standard for performance measurement.
- Policing of manufacturer's products to ensure specifications are met, thereby regulating the hearing aid manufacturing industry.

The last point helps create an initial understanding of how ANSI S3.22 (17) aids the professional groups mentioned earlier. To further clarify the standard's intended

scope, two noteworthy limitations are,

- The primary test signals are pure tones and broadband noise. As noted by (16), these are not representative of what hearing aids are expected to amplify.
- A growing disparity between what the standard is able to properly characterize and continued introduction of new processing technologies.

The ANSI S3.22 standard provides very little information on how hearing aid processing affects the intelligibility and quality of more important complex acoustical signals like speech. Researchers are beginning to examine the potential for evaluating hearing aids using more complex stimuli in predicting benefits to speech intelligibility and quality.

## **1.5 Objective Speech Quality Measures**

Beyond ANSI S3.22 (2003), several objective quality measures hold significant potential to aid further understanding and support verification procedures in predicting how complex signal processing affects intelligibility and quality of speech. These measures include,

- Speech Intelligibility Index
- Coherence Measures
- Perceptual Evaluation of Speech Quality

### **1.5.1 Speech Intelligibility Index**

The Speech Intelligibility Index (SII) (ANSI S3.5, 1997) defines a method for computing a physical measure that is highly correlated with the intelligibility of speech as evaluated by subjective speech perception tests.

### 1.5.2 Coherence Measures

Several coherence measures (18)(19)(20)(21) are frequency-domain measures of the degree to which the output of a system is linearly related to its input.

### 1.5.3 PESQ Mean Opinion Score

The Perceptual Evaluation of Speech Quality (PESQ) (22) is an objective method for assessing end-to-end speech quality of narrow-band telephone networks and speech Coders-Decoders (CODECS).

The field of telecommunications has made several significant contributions to the topic of objective speech quality measures. These measures have been traditionally applied to communication systems assessment and, under certain conditions, they exhibit good correlation with respective assessments of subjective speech quality (23). Due to innumerable types of distortion and the psycho-acoustic complexities of the hearing process, no one objective measure is all encompassing in its ability to predict subjective speech quality. Despite limitations, objective measures may hold promise in assessing speech quality of hearing aids (24). One approach, which has had significant consideration in our research group, is the Perceptual Evaluation of Speech Quality (PESQ) (22).

As noted by (23), research was undertaken in order find objective fidelity measures which were both highly correlated with subjective measures over all possible distortions and compactly computable. This was accomplished by following the flowchart shown in 1.15.

(23) summarizes the critical relationship between the hearing process and types of distortion that make determination of a single, all encompassing objective measure difficult to find,

Although the speech perception process is poorly understood, it is apparent that the human listener is an active perceiver, responding to pragmatic, semantic, prosodic, syntactic, and talker related information as

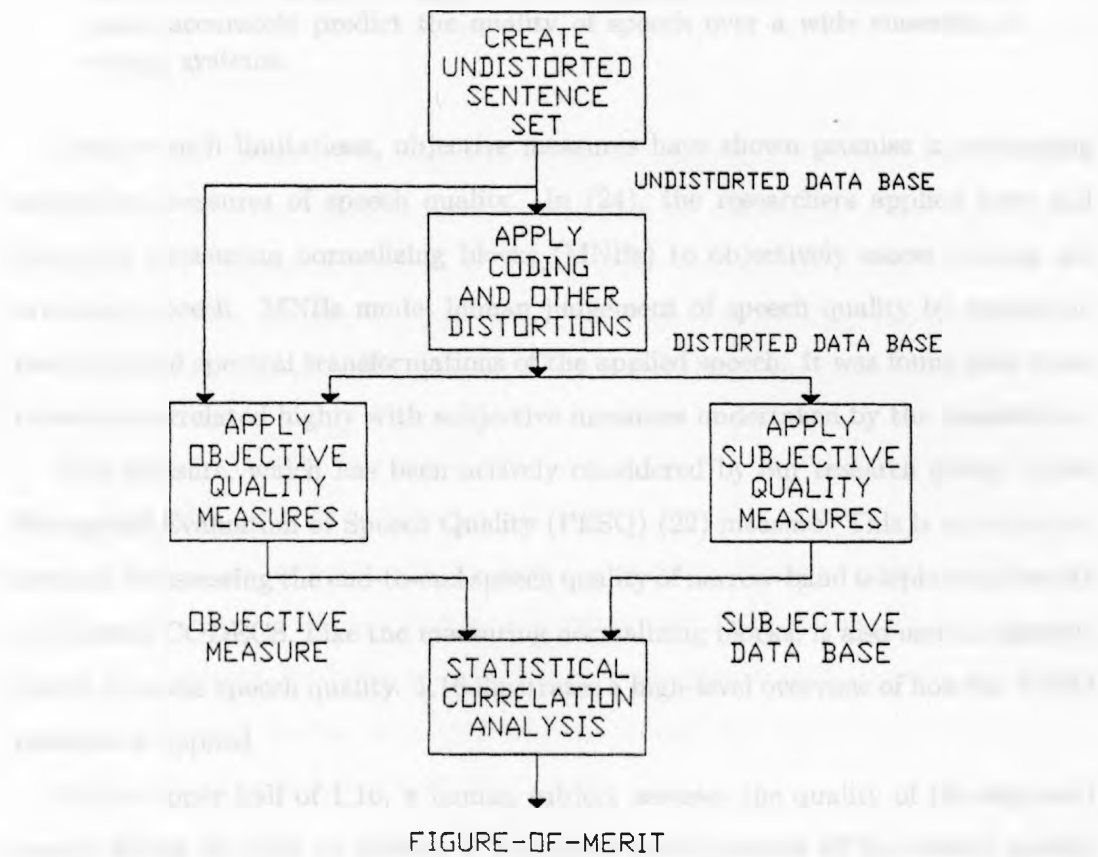


Fig. 1.15: Objective Measures Analysis (23)

well as to phonemic content. In short, he uses his vast knowledge of the language in the speech perception process. The acoustic correlates of the various hierarchically structured elements of the language in the speech signal are simultaneously overlapping and redundant. This means that certain very small distortions or the semantic content could cause complete loss of intelligibility, while other more extensive distortions might hardly be perceivable. Hence, it can be argued that objective fidelity measures that do not use high level or language related information could never accurately predict the quality of speech over a wide ensemble of coding systems.

Despite such limitations, objective measures have shown promise in estimating subjective measures of speech quality. In (24), the researchers applied time and frequency measuring normalizing blocks (MNBs) to objectively assess hearing aid processed speech. MNBs model human judgement of speech quality by employing temporal and spectral transformations of the applied speech. It was found that these measures correlated highly with subjective measures undertaken by the researchers.

One measure, which has been actively considered by our research group, is the Perceptual Evaluation of Speech Quality (PESQ) (22) measure. This is an objective method for assessing the end-to-end speech quality of narrow-band telephone networks and speech CODECS. Like the measuring normalizing blocks, it also uses a cognitive model to assess speech quality. 1.16 illustrates a high-level overview of how the PESQ measure is applied.

In the upper half of 1.16, a human subject assesses the quality of the degraded speech signal in order to provide a subjective interpretation of the overall quality of the processed speech signal. A computer model of the subject, consisting of a perceptual and a cognitive model, is used to compare the degraded output of the device under test with its respective input. These two assessments are compared to render a degree of correlation between the estimates.

The lower half of 1.16 provides additional high-level implementation details of the model. The three functional blocks provide the following functionality,



- *Perceptual Model* - As noted in (22), this involves a transformation of both the original and degraded signals to an internal representation that is analogous to the psychophysical representation of audio signals in the human auditory system, taking into account perceptual frequency (Bark) and loudness (Sone).
- *Time Alignment* - The perceptual model is susceptible to time offsets between the original and degraded signals. Time alignment is used to mitigate these negative impacts.
- *Cognitive Model* - The cognitive model is responsible for assigning an appropriate objective measure based on the internal differences of the original and degraded signals. It does so by considering several factors, which include: loudness scaling, internal cognitive noise, asymmetry processing, and silent interval processing (the reader is referred to (25) for further details on this topic).

The output of PESQ is a prediction of the perceived quality that would be given to the degraded signal by subjects in a subjective listening test.

Advances in technology, with respect to processing techniques and smaller form-factors, will introduce greater levels of distortion and noise in hearing aid processed speech; reducing intelligibility and quality of the resulting amplified speech. Objective measures of sound quality are of primary importance due to the negative impact of distortion on speech quality [KaKo94, Kuk96].

Objective measures like these are helping to further the understanding of how hearing aids alter the intelligibility and quality of speech. Like the ANSI S3.22 standard, however, they have limitations.

In order to apply the aforementioned objective measures, hearing aid behaviour must be modeled using a system identification approach. This allows hearing aids to be tested using real-world signals such as speech and music, and direct comparisons between hearing aids based on the respective objective measure (24), (26).

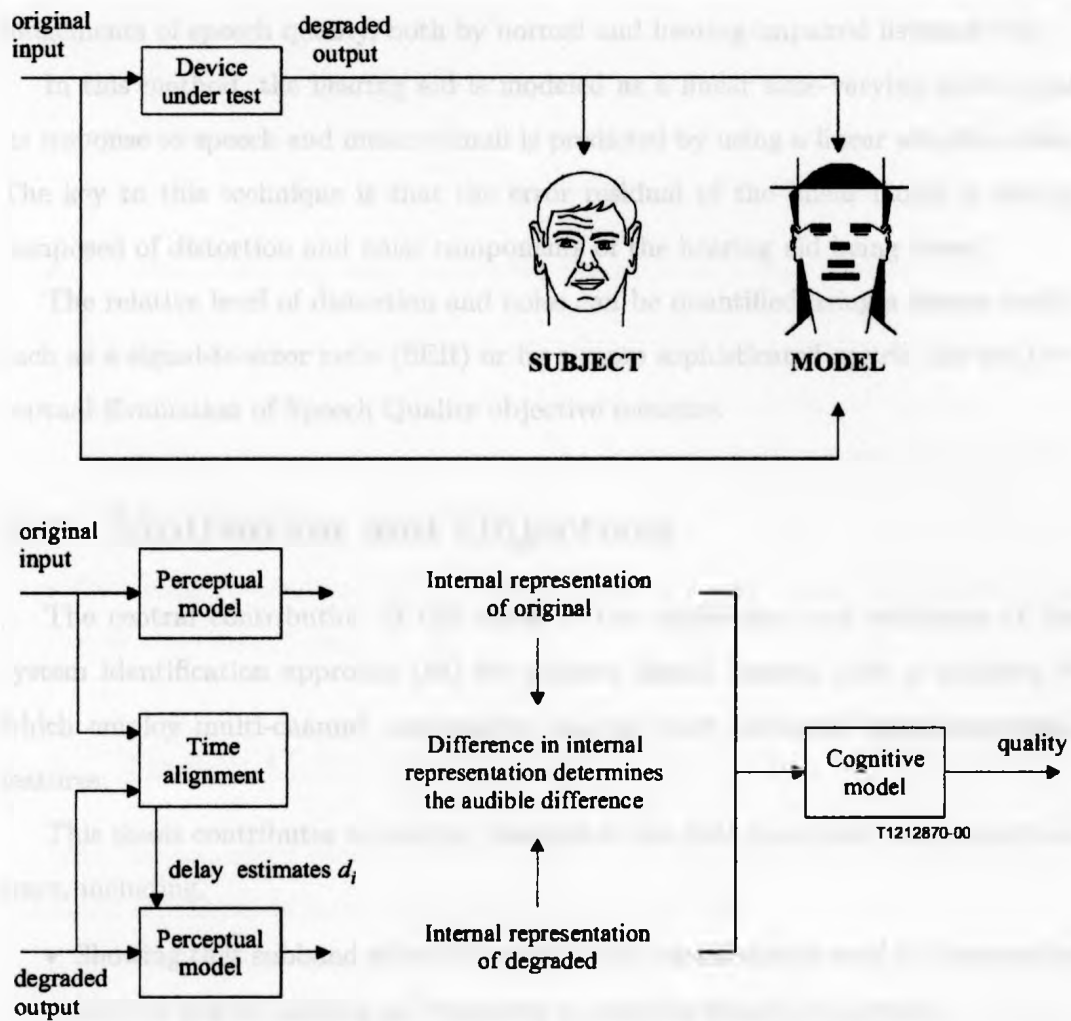


Fig. 1.16: PESQ Overview (22)

## 1.6 System Identification

Previous studies with analog hearing aids have shown that the speech quality metrics derived using a system identification approach correlated well with perceptual judgements of speech quality, both by normal and hearing-impaired listeners (24).

In this method, the hearing aid is modeled as a linear time-varying system and its response to speech and music stimuli is predicted by using a linear adaptive filter. The key to this technique is that the error residual of the linear model is mainly composed of distortion and noise components of the hearing aid being tested.

The relative level of distortion and noise can be quantified using a simple metric such as a signal-to-error ratio (SER) or by a more sophisticated metric like the Perceptual Evaluation of Speech Quality objective measure.

## 1.7 Motivation and Objectives

The central contribution of this thesis is the application and validation of the system identification approach (24) for modern digital hearing aids, a majority of which employ multi-channel compression among other advanced signal processing features.

This thesis contributes to existing research in this field in several other important ways, including,

- Showing that subband adaptive modeling can be effectively used to characterize modern digital hearing aid responses to complex stimuli like speech.
- Validating the need to have the working number of analysis filter bank bands equal to or larger than the number of compression channels in the hearing aid being testing.
- Further investigation of adaptive filtering to model nonlinear hearing aid behaviour.

- Ensure stochastic-gradient and least-squares based algorithms, which are used to update adaptive filter coefficients, perform adequately in learning and tracking the statistical nature of the processed speech signals.
- Application of the Perceptual Evaluation of Speech Quality (PESQ) mean-opinion score to validate modeling performance. This serves to help address a critical lack of objective hearing aid testing procedures that use natural acoustical stimuli to capture the processing abilities of current digital hearing aids.
- Selection of hearing aid pre-screening based on individual hearing loss.
- Holding potential to develop test procedures that use complex acoustical stimuli found in everyday hearing situations to supplement the set of standardized (ANSI S3.22) testing procedure used for quality control and hearing aid performance verification.
- Extending the existing testing methods used to extract the processing architecture of a hearing aid.

## 1.8 Thesis Contents

With the necessary background, motivation, and objectives of this research outlined, the remainder of this thesis is structured as follows.

Chapter 2 contains an introduction and detailed discussion of the subband adaptive model. This includes the rationale supporting a subband approach as well as details on the adaptive algorithms considered. This chapter concludes with an analysis of the tracking behaviour of these algorithms.

Chapter 3 presents details of the simulated hearing aid used to investigate the potential application of a subband model to characterize modern digital hearing aids. Modeling results for simulated hearing aids with four and eight channels of active

compression are presented. This chapter concludes with a description and initial results of an experimental procedure developed by (27) to determine the hearing aid processing architecture.

Chapter 4 describes the test methodology. This chapter describes the procedure used to program the digital hearing aids and how hearing aid responses to speech stimuli are captured and modeled. Also, the quality measures used to characterize modeling performance are described.

Chapter 5 contains modeling results for five digital hearing aids considered in this research. Results of modeling performance are presented with a discussion of the limitations associated with the three adaptive algorithms.

This thesis concludes with Chapter 6 with comments on the subband modeling approach and a discussion of its limitations. Items for future consideration and possible development are noted.

## Chapter 2

# Subband Adaptive Modeling

### 2.1 Introduction

System modeling or identification is one of several key applications of adaptive filter theory. With their richer theoretical treatment, linear models have been predominately used in this area (28), but other, relatively newer historically, approaches are also relevant. The underlying problem of system modeling is one of choosing that particular model structure that provides an adequate description of the system for the intended purpose without being excessively complicated. This latter property is referred to as the principle of parsimony.

As noted by Niedźwiecki (29), modeling is based on process identification and the form of the resulting model is, to a certain degree, arbitrary and its coefficients are determined experimentally using statistical procedures similar to curve fitting. These models are not phenomenologically justified and therefore their coefficients have no physical significance. However, this approach has several practical advantages. They are easy to build and update without the need for physical insights and, more importantly, due to their relative simplicity they allow mathematically tractable formulations and solutions for many important problems.

The focus of this research is on validating the application of linear adaptive filter-

ing applied in subband architectures to model compression characteristics associated with today's current market digital hearing aids. In addition, it is desirable to confirm the postulate that the subband adaptive model must have an equal or greater number of analysis bands than the number of channels in which compression is applied in the hearing aid.

With these goals firmly in mind, the following sections will cover the concepts of system modeling or identification, a full band model, and an extension of the full band model to a subband model. In addition, the adaptive algorithms used to update the tap weights or coefficients will be presented in detail.

## 2.2 Adaptive Modeling of Hearing Aids

### 2.2.1 System Modeling

Fig. 2.1 illustrates how linear adaptive filter theory is applied to model or identify a complex process or system.

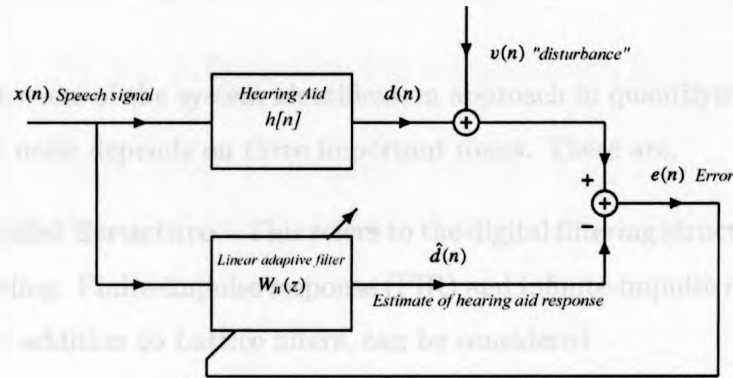


Fig. 2.1: System Identification Block Diagram (1)

For this case, an input sequence,  $x(n)$ , is fed into the “unknown” system or hearing aid,  $h[n]$ , to be identified or modeled, and the adaptive filter,  $W_n(z)$ . The adaptive filter produces an estimate,  $\hat{d}[n]$ , of the hearing aid response,  $d[n]$ , or the desired

sequence in the presence of a disturbance,  $v(n)$ . This estimate is subtracted from the desired response of the hearing aid to determine the error in the estimate,  $e[n]$ . An appropriate adaptive filtering algorithm updates the coefficients of the adaptive filter,  $W_n(z)$ .

Adaptive filters typically use stochastic or non-deterministic input and desired sequences. Since no *a-priori* knowledge is assumed regarding these sequences, the adaptive filter uses estimates of their statistical properties to minimize a cost or performance function, typically the power of the error residual signal as this is a mathematically tractable function and has a single local minimum. The minimization will occur when the adaptive filter characterizes the “unknown” system to the best of its abilities.

Modeling the non-linear compression behavior of a digital hearing aid by the application of a linear, time-varying adaptive filter allows the degree of distortion and noise inherent in the aid’s processing to be quantitatively measured. This is the fundamental postulate of the modeling approach (30): that the model’s residual error is composed primarily of distortion and noise components of the hearing aid under test.

The effectiveness of the system identification approach in quantifying hearing aid distortion and noise depends on three important items. These are,

**Adaptive Model Structure** - This refers to the digital filtering structure employed for modeling. Finite-impulse response (FIR) and infinite-impulse response (IIR) filters, in addition to Lattice filters, can be considered.

**Parameter Estimation Algorithm** - This refers to one of several, standard algorithms used to update the tap-weights or coefficients of the model structure.

**Quality Metric** - This refers to a measure that quantifies the amount of hearing aid distortion and noise. There are several well-known measures, for example, the Perceptual Evaluation of Speech Quality (PESQ) mean-opinion score. See



(23) for a comprehensive treatment.

The next section describes a full band model based on the finite-impulse response (FIR) structure.

### 2.2.2 Full Band Modeling

Finite-impulse response, or non-recursive, filters are routinely used in adaptive modeling applications. Fig. 2.2 shows a direct-form finite-impulse response (FIR) adaptive filter.

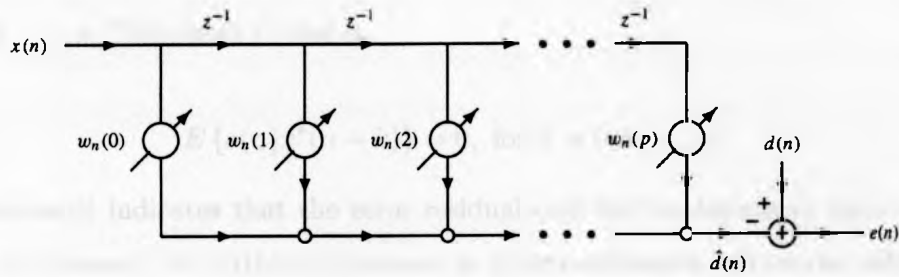


Fig. 2.2: A Direct-form FIR Adaptive Filter (31)

The filter's estimate,  $\hat{d}(n)$ , of the desired sequence,  $d(n)$ , from an input signal,  $x(n)$ , is a weighted sum of delayed samples from the input signal. This can be written as,

$$\hat{d}(n) = \sum_{k=0}^p w_n(k)x(n-k) = \mathbf{w}_n^T \mathbf{x}(n) \quad (2.1)$$

where  $p$  is the number of weights or filter length.

As indicated earlier,  $x(n)$  and  $d(n)$  are not deterministic, having time-varying statistical properties.

The objective is to find the coefficient vector,  $\mathbf{w}_n$ , at time index  $n$ , which minimizes the variance of the mean-square error of the error residual,  $e(n)$ . This can be expressed using the statistical expectation operator in the following way,

$$\xi(n) = E \{ |e(n)|^2 \} \quad (2.2)$$

where the error residual is,

$$e(n) = d(n) - \hat{d}(n) = d(n) - \mathbf{w}_n^T \mathbf{x}(n) \quad (2.3)$$

As noted by (31), the solution to this minimization problem is found by setting the derivative of the mean-square error variance with respect to  $w_n^*$  equal to zero for  $k = 0, 1, \dots, p$ . The result of this is,

$$E \{ e(n) x^*(n - k) \} = 0, \text{ for } k = 0, 1, \dots, p. \quad (2.4)$$

This result indicates that the error residual and the tap-inputs at time index  $n$  are not correlated. No further adjustment to filter coefficients will extract additional information from the input sequence,  $x(n)$ , in the estimate of the desired sequence,  $d(n)$ .

Further rearrangement of the above equation results in a set of  $p + 1$  unknowns. This can be expressed as,

$$\sum_{l=0}^p w_n(l) E \{ x(n - l) x^*(n - k) \} = E \{ d(n) x^*(n - k) \}, \text{ for } k = 0, 1, \dots, p. \quad (2.5)$$

This may also be expressed in vector form,

$$\mathbf{R}_x(n) \mathbf{w}_n = \mathbf{r}_{dx}(n) \quad (2.6)$$

where  $\mathbf{R}_x$  is the auto-correlation matrix and  $\mathbf{r}_{dx}$  is the cross-correlation vector of the tap-input vector,  $x(n - k)$ , and the desired sequence,  $d(n)$ .

If the input,  $x(n)$ , and desired,  $d(n)$ , sequences are jointly wide-sense stationary, a solution of  $\mathbf{w} = \mathbf{w}_o$  would exist, representing the optimal linear solution. This solution is independent of the time index and is commonly referred to as the Wiener-Hopf solution.

In cases where the input and desired sequences are not jointly wide-sense stationary, with statistical properties that vary with  $n$ , iterative approaches based on the Method of Steepest-Descent, Newton's Method, and least-squares can be employed to estimate the filter's coefficients. The adaptive algorithms used to estimate the filter's coefficients will be discussed later in this chapter.

Dividing the working frequency range into smaller regions or bands can optimize this full band modeling approach further. The benefits of this approach include shorter computational time and lower modeling residual for a dynamic system over the full band approach. This method is described in the next section.

## 2.3 Subband Adaptive Filters

### 2.3.1 Introduction and Motivation

There are several benefits of using a full band modeling approach based on the finite-impulse response (FIR) adaptive filter. First, ensuring the full band model's coefficients are bounded easily controls stability. Second, there are several efficient algorithms for the update of the coefficients. Third, the performance of these algorithms, based on the mean-squared error cost or performance function, is well understood in terms of convergence and stability properties (31). However, attempts to apply this technique to complex systems requiring a large order model is plagued by slow convergence and large numbers of numerical computations. These limitations could be addressed using adaptive infinite-impulse response (IIR) structures. But unlike the FIR-based adaptive filters, IIR approaches have several local minima rather

than one global minimum for the solution of the filter coefficients.

Subband adaptive filters use FIR-based filtering structures to facilitate faster convergence, reduced computational complexity, and stability. Furukawa (1984) and Kellermann (1984) introduced the concept of subband adaptive filtering, applying the technique in acoustic echo cancellation systems.

The premise behind subband adaptive filtering is the decomposition of the working frequency spectrum of the input and desired sequences into several segments, commonly referred to as subbands (1). This is accomplished by applying the input and desired sequences to a designed filter bank. The resulting sets of sequences may be decimated to reduce the number of working samples, expanding each band's filtered sequence across the full working spectrum. Standard adaptive filtering can then be applied in each subband before the final, full band output is reconstructed. If decimation operations are performed, a synthesis filter bank must be used on the adapted data to prevent aliasing. This approach facilitates parallel computation using smaller amounts of data. In addition, the number of coefficients for each adaptive filter can be smaller and processing data using a subband approach reduces the overall computation time. There are, however, limitations associated with this processing technique.

In general, the analysis and synthesis filters must satisfy certain conditions in order that the reconstructed full band signals have no, or at least insignificant distortion (11). In order to realize a reconstructed full band output signal with no distortion using subband adaptive filtering, the combined responses of the analysis and synthesis filters should be that of a *strictly complementary* (SC) filter bank (11). In essence, this implies that, if a sequence is split into several subband signals using SC analysis filters, the filter outputs can be added to get the original sequence with no distortion, just a delay (11). However, the use of analysis and synthesis filter banks not meeting the SC condition may also be used. In these cases, knowledge as to what distortions will occur due to aliasing should be kept in mind.

The use of static filter structures for decomposition does not take into consideration the time-varying dispersion of the spectral content of the sequences. For sequences with critical spectral characteristics, static and adaptive non-uniform filter structures have been investigated and applied by several researchers (32; 33; 34; 35).

### 2.3.2 General Structure

The general structure of the subband adaptive filter is shown in Fig. 2.3.

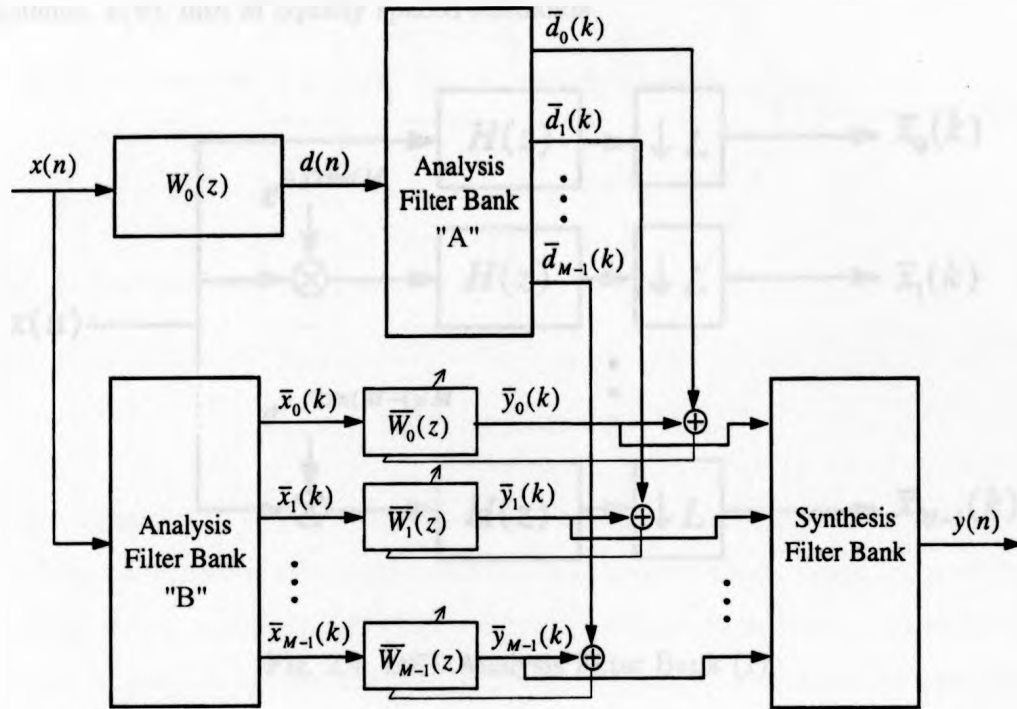


Fig. 2.3: Subband Adaptive Filter Structure (1)

The excitation sequence,  $x(n)$ , is applied to the system to be modeled or identified,  $W_o(z)$ , and one of two analysis filter banks. The outputs of analysis filter bank "B" form the set of reference sequences,  $\bar{x}_0(k) \rightarrow \bar{x}_{M-1}(k)$ , for respective adaptive filters,  $\bar{W}_0(z) \rightarrow \bar{W}_{M-1}(z)$ . The output of the system,  $d(n)$ , is applied to analysis filter bank

"A". The resulting set of sequences,  $\bar{d}_0(k) \rightarrow \bar{d}_{M-1}(k)$  form the desired sequences for the adaptive filters. The output of each adaptive filter,  $\bar{y}_0 \rightarrow \bar{y}_{M-1}(k)$ , is applied to the synthesis filter bank that adds the resulting filtered sequences into the final, full band output,  $y(n)$ .

Several approaches exist for the design of the analysis and synthesis filter banks (11; 1). For the sake of completeness of this work, the computationally efficient, over-sampled Discrete Fourier Transform (DFT) filter bank is described next.

As detailed by (1), Fig. 2.4 illustrates the steps required to partition the input sequence,  $x(n)$ , into  $M$  equally spaced subbands.

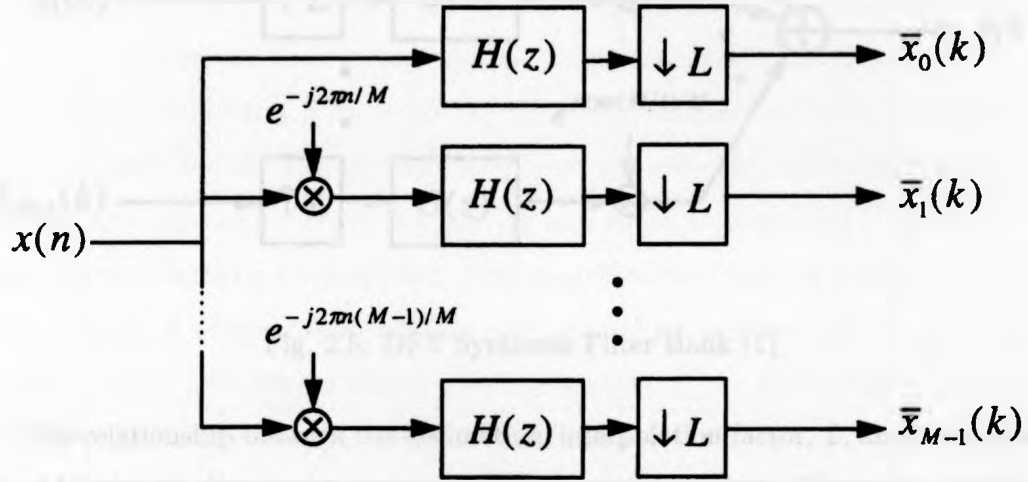


Fig. 2.4: DFT Analysis Filter Bank (1)

A prototype low pass filter,  $H(z)$ , applied to the input sequence,  $x(n)$ , extracts the low frequency region of its spectrum. To extract other spectral segments of  $x(n)$ , the desired spectral segment is shifted into the base-band region (centered around  $w = 0$ ) by multiplying  $x(n)$  by a complex sinusoid. The low pass filter can then be applied to extract the desired portion of the spectrum. The number of bands,  $M$ , is arbitrary, determined by the application at hand. The resulting set of sequences can

is no longer carried out. This case is called an over sampled system. The latter system is used in this research.

It should be noted that in the preceding discussion the assumption is made that the analysis and synthesis filter banks are uniform in nature, dividing the full band spectrum into  $M$  linearly spaced regions on a linear frequency axis. Also, the prototype low pass filters,  $H(z)$  and  $G(z)$ , are complementary, yielding a delayed output with no distortion.

### 2.3.3 Uniform and Non-uniform Filter Banks

Filter banks are a key element of subband adaptive filter structures, which can be classified into the two broad categories of uniform and non-uniform implementations. Their primary objective is to divide the working spectrum into several separate regions or bands, ideally with no overlap between non-adjacent, and more importantly, between adjacent bands. Significant overlap may result in distortions to the processed signals due to aliasing artefacts and other contributions. Various design approaches offer a range of filtering specifications with associated implementation and computational costs. Quadrature Mirror Filters were one of the first filtering structures offering near ideal performance, but was limited to only two bands. More generalized approaches followed to facilitate several uniform bands, allowing more flexibility in their application. Less stringent design approaches followed, such as cosine-modulated filter banks, yet still offered acceptable performance within the frameworks of certain application.

The fundamental premise of filter banks is to divide a working spectrum into several separate bands. In doing so, the resulting sequences may be decimated and processed at a lower effective sampling frequency before interpolating and filtering to obtain the final signal. Fig. 2.6 illustrates this concept.

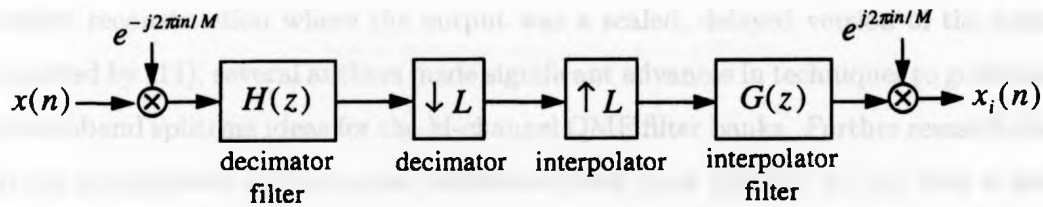


Fig. 2.6:  $I^{th}$  Band of M-Channel Analysis/Synthesis Filter Bank (1)

### 2.3.4 Quadrature Mirror Filters

Quadrature Mirror Filters (QMF's), introduced in the mid-70s, were one of the first implementations of this general approach. This structure allowed a full band signal to be divided into two overlapping half-band signals. The properties of QMF filters allowed these two half-band signals to be decimated by a factor of two and still be reconstructed correctly later. This found significant use in speech coding applications (37). Fig. 2.7 illustrates a quadrature mirror filter bank and the frequency magnitude responses of the analysis filters.

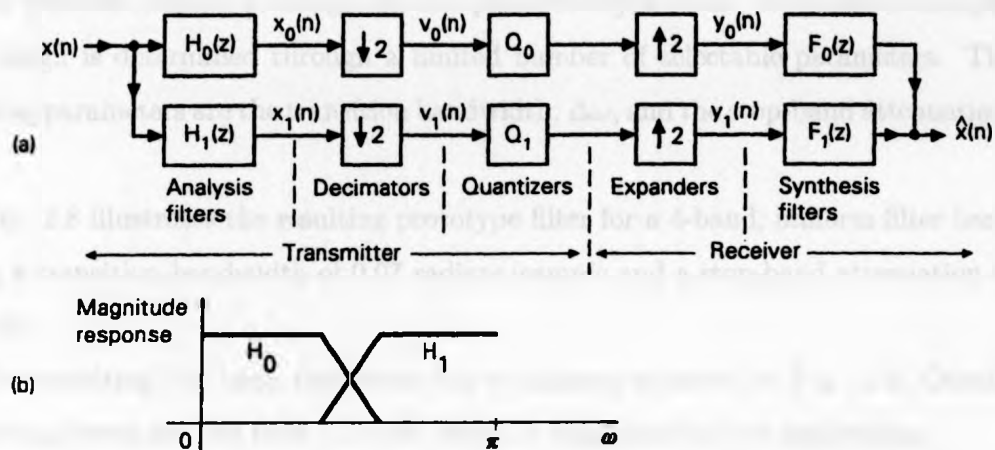


Fig. 2.7: (a) Quadrature Mirror Filter Bank, and (b) Frequency Magnitude Responses (11)

Careful consideration and design of the four filters, as shown by (38), allowed



perfect reconstruction where the output was a scaled, delayed version of the input. As noted by (11), several authors made significant advances in techniques to generalize the subband splitting ideas for the M-channel QMF filter banks. Further research lead to the development of the cosine modulated filter bank (39; 40; 41; 42) that is used in this research.

Cosine modulated filter banks are a class of QMF banks in which all filters are derived from cosine-modulated versions of a single low-pass filter prototype. As noted by (11), the primary benefits of cosine modulated filter banks are,

- The computational cost of the analysis bank is equal to that of the low pass prototype filter design and modulation. Consequently, the synthesis filters have the same cost.
- Only the filter coefficients for the low pass prototype filter need to be optimized.

The design approach developed by (43) was used in our research in order to minimize the complexity of the design of the filter banks. This approach uses a Kaiser window method to design the low pass prototype filter. With this technique, the design is determined through a limited number of selectable parameters. The working parameters are the transition bandwidth,  $\Delta\omega$ , and the stop-band attenuation,  $A_s$ .

Fig. 2.8 illustrates the resulting prototype filter for a 4-band, uniform filter bank using a transition bandwidth of 0.07 radians/sample and a stop-band attenuation of 100 dB.

The resulting full band distortion due to aliasing is shown in Fig. 2.9. Overall distortion levels are less than -110 dB, which is negligible for this application.

The application of the uniform cosine-modulated filter bank structure in our research had several benefits. First, as previously noted in this section, this approach greatly simplifies the design of the analysis filter bank. This approach requires that the number of bands, degree of stop-band attenuation, and the transition bandwidth

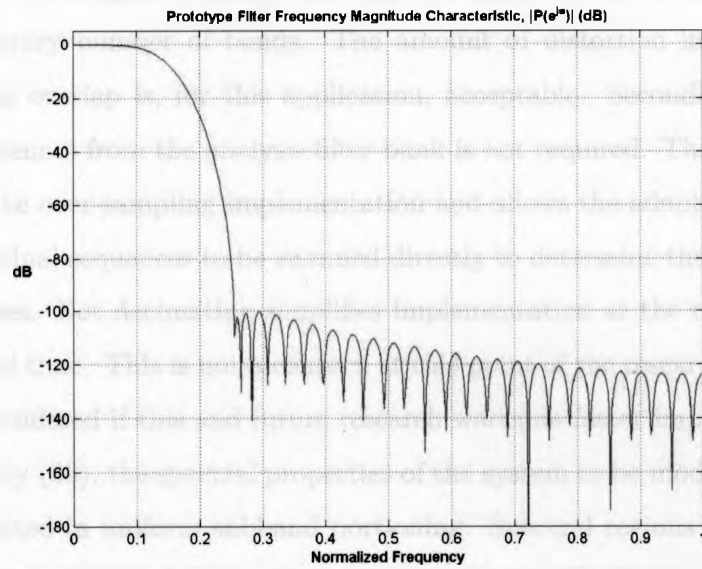


Fig. 2.8: Kaiser-based Lowpass Prototype Filter ( $\Delta\omega = 0.07$  radians/sample,  $A_s = 100$  dB)

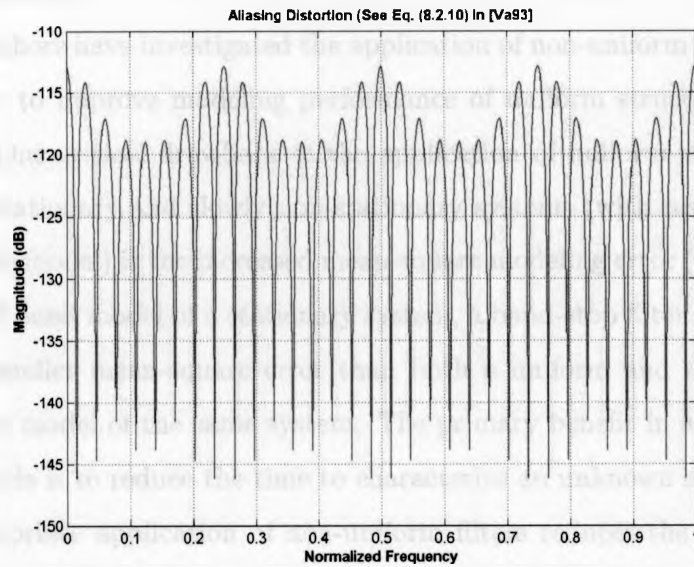


Fig. 2.9: 4 Band Uniform Filter Bank Fullband Distortions

be chosen by the designer, readily allowing fast implementation of filter structures with an arbitrary number of bands. The amount of distortion introduced due to adjacent band overlap is, for this application, acceptable. Secondly, decimation of resulting sequences from the analysis filter bank is not required. This approach is referred to as the over-sampling implementation and allows the adaptive filter outputs and error residual sequences to be summed directly to determine the full band equivalent sequences. Not decimating simplifies implementation at the cost of additional computational time. This is not a concern at this point of the research, but obviously should be considered if this and future research warrants faster implementation.

As noted by (33), the spectral properties of the system to be modeled or identified are not exploited in uniform subband portioning. Spectral regions of the system to be modeled or identified, which may be stationary or slowly time varying, with small variation, will often be split over one or, very possibly, several bands. Regions with significant spectral variation would be better modeled with multiple filters acting on smaller bandwidths.

Several authors have investigated the application of non-uniform filter bank structures in order to improve modeling performance of uniform structures (32; 35; 34; 33; 44; 45). One critical drawback of the application of uniform subband adaptive modeling to stationary and slowly non-stationary systems (with respect to the time constant of the model) is the increased mean-square modeling error (33). As noted by (34; 33), a full band model of a stationary system, a band-stop filter in this particular case, has a smaller mean-square error than both a uniform and non-uniform subband adaptive model of the same system. The primary benefit in applying subband adaptive models is to reduce the time to characterize an unknown system.

The appropriate application of non-uniform filters reduces the modeling mean-square error compared to the uniform case, however, it does not reduce it to full band levels. This behaviour is attributable to the whitening of the adaptive filter input (1). As noted by (33), equalizing energy across a given subband decreases

the eigenvalue spread of the input covariance matrix, which in turn, decreases the effective mean-square error for the respective band.

With the concept of non-uniform filter banks in mind and the desire to model hearing aid performance, potential questions about the application of non-uniform filter banks that take into account the critical bands of the cochlea should be addressed. Two important, interrelated considerations need to be discussed in order to provide insight on this topic. First, hearing aid manufacturers choose to design and manufacture different filter bank structures. The Phonak Perseo 311 dAZ Forte, for example, uses a critical band structure while the Triano S has a uniform band structure. The Syncro V2 has a non-uniform band structure, however, it is not based on the critical bands of the cochlea. Because of this disparity, modeling with uniform bands that are easily adjusted to approximate the non-uniform structures appears to be the best approach. Second, characteristics of filter banks based on critical bands have significant overlap between non-adjacent bands in addition to adjacent bands (45). It is difficult to say at this point what potential impacts this would have on the modeling performance of the subband adaptive filter.

## 2.4 Adaptive Algorithms

In this section the adaptive algorithms used to update the filter tap-weights, or coefficients, of each finite-impulse response filter of the subband adaptive model are described in detail. The use of Hearing in Noise Test, or HINT, speech sequences (House Ear Institute of Los Angeles, CA, USA) to elicit a hearing aid response for the purpose of modeling captures the true nature of the function a hearing aid is designed to accomplish. However, complete knowledge of the underlying signal statistics of speech is difficult to model, let alone truly characterize. As a result, adaptive algorithms that learn and track the time-varying or stochastic properties of speech sequences must be applied.

The adaptive algorithms considered in this research include the *Normalized Least-Mean-Squares (NLMS)* algorithm, the *Affine Projection (APA)* algorithm, and the *Recursive Least-Squares (RLS)* algorithm. Each algorithm has a unique approach to estimating the instantaneous statistical measures required to compute an optimal linear least-mean squares estimate of the filter coefficients. As a result, each approach has an associated level of computational complexity. Several good references indicating each algorithm's degree of computational complexity exist (46; 1; 47).

These algorithms exhibit two critical behaviours that allow them to be applied to this application. As noted by (1), a *learning mechanism* allows each method the ability to estimate the necessary signal statistics of the applied sequences and a *tracking mechanism* to track these statistics with time.

#### 2.4.1 Normalized Least-Mean-Squares ( $\varepsilon$ -NLMS)

The normalized least-mean-squares algorithm considered in this thesis is an extension of a regularized form of the steepest-descent approach called Newton's recursion (46). With reference to Fig.2.2, the direct-form FIR adaptive filter described previously in this chapter, with constant regularization and step-size terms, Newton's recursion may be expressed in the following form,

$$w_i = w_{i-1} + \mu [\varepsilon \mathbf{I} + \mathbf{R}_x]^{-1} [\mathbf{r}_{dx} - \mathbf{R}_x w_{i-1}] \quad (2.7)$$

where  $w_i$  is the tap-weight vector at time index  $i$ ,  $w_{i-1}$  is the tap-weight vector at time index  $i - 1$ ,  $\mu$  is the step-size parameter,  $\varepsilon$  is the regularization factor,  $\mathbf{R}_x$  is the auto-correlation matrix of the tap-input vector, and  $\mathbf{r}_{dx}$  is the cross-correlation vector between the tap-input vector,  $x(n - k)$ , and the desired sequence,  $d(n)$ .

Instantaneous approximations for the  $(\varepsilon \mathbf{I} + \mathbf{R}_x)$  and  $(\mathbf{r}_{dx} - \mathbf{R}_x w_{i-1})$  terms may be substituted,

$$\begin{aligned}\varepsilon \mathbf{I} + \mathbf{R}_x &\rightarrow \varepsilon \mathbf{I} + x_i^* x_i \\ \mathbf{r}_{dx} - \mathbf{R}_x w_{i-1} &\rightarrow x_i^* [d(i) - x_i w_{i-1}]\end{aligned}\quad (2.8)$$

With the resulting equation being,

$$w_i = w_{i-1} + \mu [\varepsilon \mathbf{I} + x_i^* x_i]^{-1} x_i^* [d(i) - x_i w_{i-1}] \quad (2.9)$$

This recursive equation is an indexed update for the tap-weight vector using instantaneous approximations for the auto-covariance matrix of the filter input sequence and cross-covariance between the filter input and the desired sequence (46).

In this form, the inversion of the matrix  $(\varepsilon \mathbf{I} + x_i^* x_i)$ , is to be computed at every single iteration. The length of the finite-impulse response filter-input vector,  $x_i$ , also referred to as the regressor vector due to the least mean-square basis, determines the order of the matrix. It follows that using a higher order filter results in a larger matrix to be inverted which is more computationally expensive. The necessary inversion can be simplified by taking advantage of the fact that  $\varepsilon \mathbf{I} + x_i^* x_i$  is a rank-one modification of a multiple of the identity matrix.

Applying the *matrix inverse lemma* (47) we arrive at,

$$[\varepsilon \mathbf{I} + x_i^* x_i]^{-1} = \varepsilon^{-1} \mathbf{I} - \frac{\varepsilon^{-2}}{1 + \varepsilon^{-1} \|x_i\|^2} x_i^* x_i \quad (2.10)$$

Multiplying this equation by  $x_i^*$  from the right we have,

$$\begin{aligned}[\varepsilon \mathbf{I} + x_i^* x_i]^{-1} x_i^* &= \varepsilon^{-1} \mathbf{I} x_i^* - \frac{\varepsilon^{-2}}{1 + \varepsilon^{-1} \|x_i\|^2} x_i^* x_i x_i^* \\ &= \varepsilon^{-1} \mathbf{I} x_i^* - \frac{\varepsilon^{-2}}{1 + \varepsilon^{-1} \|x_i\|^2} x_i^* \|x_i\|^2 \\ &= \varepsilon^{-1} x_i^* \left[ 1 - \frac{\|x_i\|^2}{\varepsilon + \|x_i\|^2} \right] \\ &= \frac{x_i^*}{\varepsilon + \|x_i\|^2}\end{aligned}\quad (2.11)$$

Substituting this result into Eq. 2.9 above finalizes the derivation of the regularized, normalized least-mean squares recursion formula,

$$w_i = w_{i-1} + \frac{\mu}{\varepsilon + \|x_i\|^2} x_i^* [d(i) - x_i w_{i-1}] \text{ with } i \geq 0 \quad (2.12)$$

Due to the use of regularization, the above equation will be referred to as the regularized, normalized least-mean square( $\varepsilon$ -NLMS) algorithm.

The primary working parameter for this algorithm is the step-size,  $\mu$ , which is selected from the range  $0 < \mu < 2$  (46; 47; 31). The regularization parameter,  $\varepsilon$ , is a small, positive constant and was set to 0.001.

An inherent attribute of speech sequences is the significant variation in signal level that occurs over time. As a result, the use of any adaptive algorithm that uses an estimate of the power in the updating of the tap-weights or coefficients is susceptible to gradient noise. The Least-Mean-Square (LMS) algorithm is a first order approximation using an instantaneous statistical estimate and is prone to this limitation. NLMS solves this problem by normalizing the step-size parameter by the power of the instantaneous input vector as shown in Eq. 2.12.

#### 2.4.2 Affine Projection Algorithm ( $\varepsilon$ -APA)

The affine projection algorithm is a generalization of the normalized least-mean squares (NLMS) algorithm (46; 48). Like the NLMS algorithm, the affine projection algorithm uses an instantaneous estimate for both the covariance matrix,  $\mathbf{R}_x$ , and the cross-covariance vector,  $\mathbf{r}_{dx}$ . However, the affine projection algorithm uses an estimate of greater complexity, which is more computationally expensive.

Like the NLMS algorithm, the affine projection algorithm can be derived from the steepest-descent, Newton's recursion equation (46). This will be the starting point for the derivation presented here and will follow the steps as outlined in (46).

Newton's recursion equation, with a fixed step-size,  $\mu$ , and regularization constant,

$\varepsilon$ , is expressed as,

$$w_i = w_{i-1} + \mu [\varepsilon' \mathbf{I} + \mathbf{R}_x]^{-1} [\mathbf{r}_{dx} - \mathbf{R}_x w_{i-1}] \quad (2.13)$$

A positive integer,  $K$ , is selected that is less than or equal to the number of tap-weights or filter coefficients,  $M$ , and the estimates for the covariance matrix and cross-covariance vector are replaced with the following instantaneous approximations,

$$\hat{\mathbf{R}}_x = \frac{1}{K} \left( \sum_{j=i-K+1}^i x_j^* x_j \right) \quad (2.14)$$

$$\hat{\mathbf{r}}_{dx} = \frac{1}{K} \left( \sum_{j=i-K+1}^i d(j) x_j^* \right) \quad (2.15)$$

These equations indicate that at each iteration,  $i$ , the  $K$  most recent regressors or set of tap-inputs and the  $K$  most recent desired values or observations,

$$\{x_i, x_{i-1}, \dots, x_{i-K+1}\}, \{d(i), d(i-1), \dots, d(i-K+1)\} \quad (2.16)$$

are used to determine the estimates for the auto-covariance matrix,  $\mathbf{R}_x$ , and the cross-covariance vector,  $\mathbf{r}_{dx}$ .

Vector notation can be used to reduce the complexity of the above summations. Letting  $\varepsilon = \varepsilon'/K$ , the  $K \times M$  block data matrix may be introduced,

$$\mathbf{X}_i = \begin{bmatrix} x_i \\ x_{i-1} \\ \vdots \\ x_{i-K+1} \end{bmatrix} \quad (K \times M)$$

and the  $K \times 1$  data vector,

$$\mathbf{d}_i = \begin{bmatrix} d(i) \\ d(i-1) \\ \vdots \\ d(i-K+1) \end{bmatrix} \quad (K \times 1)$$



yielding the following compact forms for each respective estimate,

$$\hat{\mathbf{R}}_x = \frac{1}{K} X_i^* X_i \quad (2.17)$$

$$\hat{\mathbf{r}}_{dx} = \frac{1}{K} X_i^* d_i \quad (2.18)$$

With these compact forms, Newton's recursion takes the following form,

$$w_i = w_{i-1} + \mu (\epsilon \mathbf{I} + X_i^* X_i)^{-1} X_i^* [d_i - X_i w_{i-1}] \quad (2.19)$$

At this point, not unlike with the derivation of the  $\epsilon$ -NLMS algorithm, the affine projection algorithm necessitates the inversion of a  $M \times M$  matrix,  $(\epsilon \mathbf{I} + X_i^* X_i)$  at each iteration.

As noted by (46), the matrix inversion lemma may be applied in the following manner,

$$(\epsilon \mathbf{I} + X_i^* X_i)^{-1} X_i^* = X_i^* (\epsilon \mathbf{I} + X_i X_i^*)^{-1} \quad (2.20)$$

and the resulting equation becomes,

$$w_i = w_{i-1} + \mu X_i^* (\epsilon \mathbf{I} + X_i X_i^*)^{-1} [d_i - X_i w_{i-1}] \quad (2.21)$$

This is the affine projection algorithm and, in this form, requires the inversion of the usually smaller  $K \times K$  matrix at each iteration.

Like the  $\epsilon$ -NLMS algorithm, the affine projection algorithm depends on the step-size parameter in addition to the projection order,  $K$ . The step-size is typically selected from the working range of  $0 < \mu \leq 1$ , while the projection order is less than the order of the filter (i.e.  $K \leq M$ ). The offset for the input-signal covariance matrix,  $\epsilon$ , was set to 0.0001.

### 2.4.3 Recursive Least Squares

The third adaptive algorithm considered is the recursive least-squares algorithm. Like the affine projection and normalized least-mean-squares algorithms, the recursive least-squares algorithm is derived from the steepest-descent, Newton's recursion equation (46). This will be the starting point for the derivation presented here and will follow the steps as outlined in (46).

The regularized form of Newton's recursion is as follows,

$$w_i = w_{i-1} + \mu(i) [\varepsilon(i)\mathbf{I} + \mathbf{R}_x]^{-1} [\mathbf{r}_{dx} - \mathbf{R}_x w_{i-1}] \quad (2.22)$$

with the last term being replaced by its equivalent instantaneous approximation,

$$w_i = w_{i-1} + \mu(i) [\varepsilon(i)\mathbf{I} + \mathbf{R}_x]^{-1} x_i^* [d_i - x_i w_{i-1}] \quad (2.23)$$

The next step is to replace the estimate of the auto-covariance matrix of the filter input or reference signal by the exponentially weighted sample average,

$$\hat{\mathbf{R}}_x = \frac{1}{i+1} \sum_{j=0}^i \lambda^{i-j} x_j^* x_j, \text{ where } 0 < \lambda \leq 1 \quad (2.24)$$

$\lambda$  is called the forgetting-factor. When  $\lambda$  is set to unity, the above equation computes the average outer-product of all tap-input vectors up to time index,  $i$ . Selecting a value for  $\lambda$  that is less than unity introduces a finite *memory* behaviour into this estimation. This relationship is depicted in Fig. 2.10.

As illustrated in Fig. 2.10, small forgetting-factor values places more emphasis on recent regressor values than on past values. It is intuitive to suggest that use of a small forgetting-factor is better for non-stationary sequences like speech.

Continuing further with the derivation, the step-size is chosen from,

$$\mu(i) = \frac{1}{i+1} \quad (2.25)$$

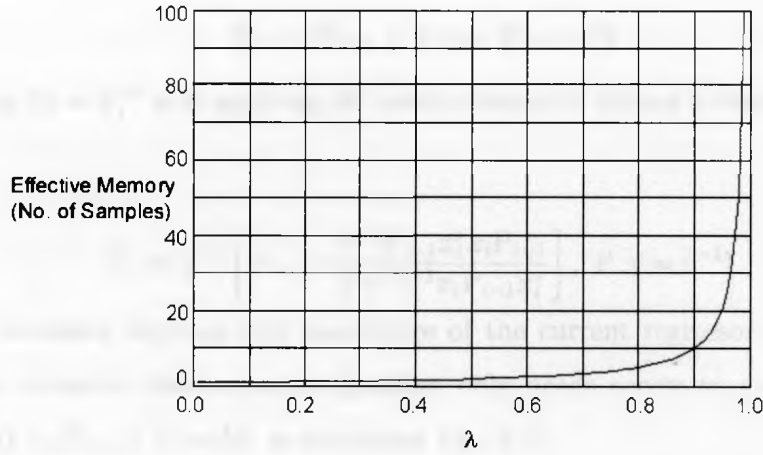


Fig. 2.10: Memory Characteristic of the RLS Algorithm

and the regularization factor is chosen as,

$$\varepsilon(i) = \lambda^{i+1} \frac{\varepsilon}{i+1}, i \geq 0 \quad (2.26)$$

From Eq. 2.26, it is clear that the regularization factor disappears as time,  $i$ , progresses.

With the above modifications and approximations, the regularized Newton's recursion equation becomes,

$$w_i = w_{i-1} + \left[ \lambda^{i+1} \varepsilon \mathbf{I} + \sum_{j=0}^i \lambda^{i-j} x_i^* x_i \right]^{-1} x_i^* [d(i) - x_i w_{i-1}] \quad (2.27)$$

As noted by (46), this recursion is not convenient because it requires all previous and present data be combined in the matrix form,

$$\Phi_i = \left( \lambda^{i+1} \varepsilon \mathbf{I} + \sum_{j=0}^i \lambda^{i-j} x_i^* x_i \right) \quad (2.28)$$

and then inverted. However, the above definition of  $\Phi_i$  satisfies the general recursion,

$$\Phi_i = \lambda \Phi_{i-1} + x_i^* x_i, \quad \Phi_{-1} = \varepsilon \mathbf{I} \quad (2.29)$$

Letting  $P_i = \Phi_i^{-1}$  and applying the matrix inversion lemma to the above equation yields,

$$P_i = \lambda^{-1} \left[ P_{i-1} - \frac{\lambda^{-1} P_{i-1} x_i^* x_i P_{i-1}}{1 + \lambda^{-1} x_i P_{i-1} x_i^*} \right], \quad P_{-1} = \varepsilon^{-1} \mathbf{I} \quad (2.30)$$

This recursion requires only knowledge of the current regressor vector. In this form, the recursive least-squares algorithm only needs access to a subset of data,  $\{w_{i-1}, d(i), x_i, P_{i-1}\}$ , in order to determine  $\{w_i, P_i\}$ .

The working parameter for the recursive least-squares algorithm is the forgetting-factor, which is taken from the range  $0 \ll \lambda \leq 1$ .

#### 2.4.4 QRD Recursive Least-Squares (QRD-RLS)

Unlike the standard RLS algorithm, the QR decomposition-based RLS algorithm works directly with the incoming data matrix via a QR decomposition rather than a time-average correlation matrix of the input data (47).

Despite this different computational approach, the QR-RLS algorithm retains the key traits of the standard RLS algorithm as noted in (47),

... all three QR-RLS algorithms preserve the desirable convergence properties of the standard RLS algorithm, namely, a fast rate of convergence and insensitivity in the eigenvalue spread of the correlation matrix of incoming data.

The reader is referred to (47) for the details of this algorithm.

## 2.5 Tracking Behaviour of Adaptive Algorithms

The ability of an adaptive filter to follow the statistical variations of an unknown system is characterized by its tracking behaviour. Most of the current literature on

this topic (46; 29; 1; 47) derives theoretical results for restricted cases using several assumptions to guide the derivations. Our work on this topic will follow the same approach. The model we used for tracking analysis will consider a stationary, broadband stepped-input signal that will be compressed by a single full band compressor with short attack and release time constants. Completed simulations suggest the algorithms considered in this research are capable of tracking the dynamic behaviour of the applied compression algorithm with attack and release time constants (based on the respective definitions found in the ANSI S3.22 (2003) standard) on the order of those found in today's digital hearing aids. An attack time of 1 msec. and release time of 50 msec. are used (49).

### 2.5.1 Tracking Model

In order to examine the tracking behaviour of the adaptive algorithms considered in this research, we used the system illustrated in Fig. 2.11.

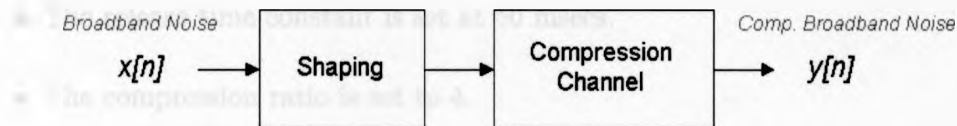


Fig. 2.11: Tracking Model

A stationary, broadband excitation sequence,  $x[n]$ , is applied to a shaping function that applies a step-wise amplitude to this sequence. The resulting sequence is then applied to a compression channel with an appropriate set of parameters, producing the final compressed sequence,  $y[n]$ .  $x[n]$  and  $y[n]$  are the reference and desired sequences, respectively, of a five-tap adaptive filter. One of the three adaptive algorithms updates these tap values.

In order to put this model into the appropriate context, Section 6.15.2, *Dynamic AGC Characteristics*, of the ANSI S3.22 (2003) standard was consulted in order to

define the conditions of the step-wise shaped noise and the compression channel. These conditions are as follows,

- The step-wise shaped, broadband noise should have levels relative to the 55 to 90 to 55 dB SPL levels associated with the pure tone signals used by the ANSI S3.22 (2003) standard.
- The attack time is defined as the time between the abrupt increase from 55 to 90 dB SPL and the point where the level has stabilized to within 3 dB of the steady value for the 90 dB input SPL.
- The release time is defined as the interval between the abrupt drop from 90 to 55 dB SPL and the point where the signal has stabilized to within 4 dB of the steady-state value for the 55 dB input SPL.
- The attack time constant is set at 1 msec.
- The release time constant is set at 50 msec.
- The compression ratio is set to 4.

Under these conditions, several simulations were completed in order to visually characterize the tracking behaviour of the normalized least-mean squares, the affine projection, and the recursive least-squares algorithms.

### **2.5.2 Bias and Variance**

The adaptive algorithms discussed in this research are referred to as finite memory estimators, due to the characteristic feature that they gradually 'forget' information from the remote past as new data is considered. Despite this apparent limitation, finite memory parameter tracking algorithms are able to compromise between estimation accuracy (variance) and awareness (bias) of parameter changes (29).

One or two comments that characterize the properties of variance and bias will be made along the way as the simulation results are presented and discussed in the following section.

### 2.5.3 Simulation Results

The step-wise shaped broadband noise sequence,  $s[n]$ , and the compressed realization of this sequence,  $y[n]$ , are applied to a transversal adaptive filter as shown in Fig. 2.12.

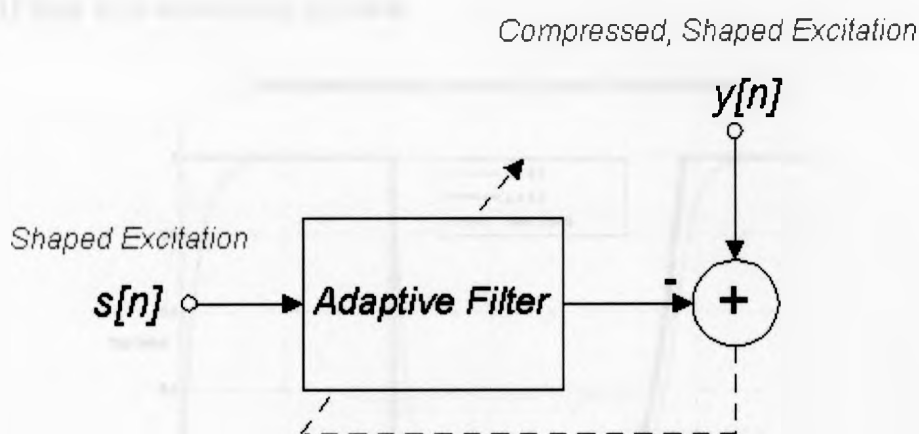


Fig. 2.12: Adaptive Filter Implementation for Tracking Analysis

An ensemble average of the tracking behaviour was established using 100 experiments for each of the three adaptive algorithms. For each algorithm, an appropriate set of parameters was selected and used in the simulation to determine a working set for modeling. Simulation results for each algorithm are outlined in the following sections of this chapter.

It should be noted at this point that the selection of the working parameters for each respective adaptive algorithm is highly dependent on the statistical properties of the applied signals. As a result, the values obtained based on this simulated tracking analysis will not provide the optimal estimates for these parameters for

hearing aid modeling. However, they can be treated as initial estimates from which more appropriate values can be selected through empirical measures.

### 2.5.3.1 Normalized Least-Mean Squares

The theoretical range for the NLMS step-size parameter is  $0 < \mu < 2$ . From this range, step-sizes of 0.1 and 1.0 were used in conjunction with a filter order of 20 for tracking performance simulations. Fig. 2.13 shows the average tracking performance of the NLMS algorithm for the considered step-sizes along with the gain envelop (ideal trend) that it is attempting to track.

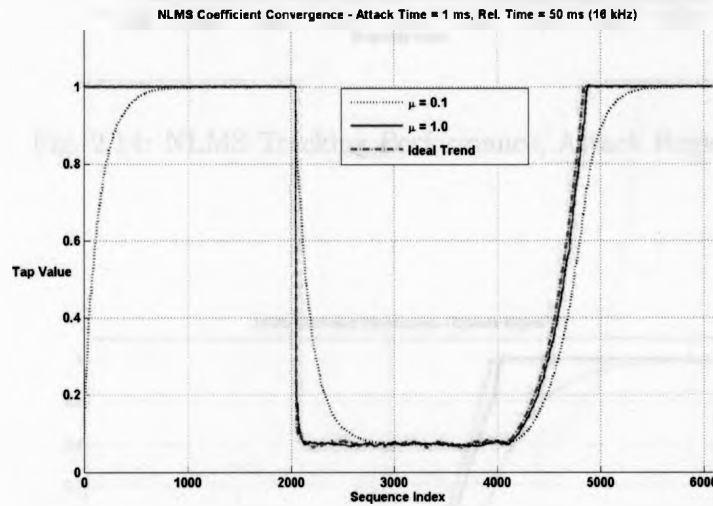


Fig. 2.13: NLMS Tracking Performance

Fig. 2.14 and Fig. 2.15 illustrate the attack and release regions, respectively, in greater detail.

It can be seen in Fig. 2.14 that the NLMS algorithm is better able to track the gain envelope with larger step-sizes. At a step-size value of 0.1, there is a readily observable significant bias; there is less awareness by the algorithm to changes in the parameter it is attempting to track. With this in mind, there is more accuracy in its



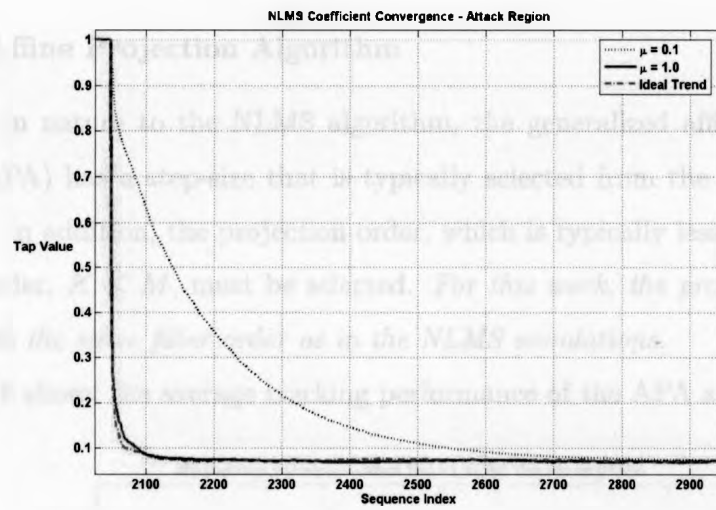


Fig. 2.14: NLMS Tracking Performance, Attack Region

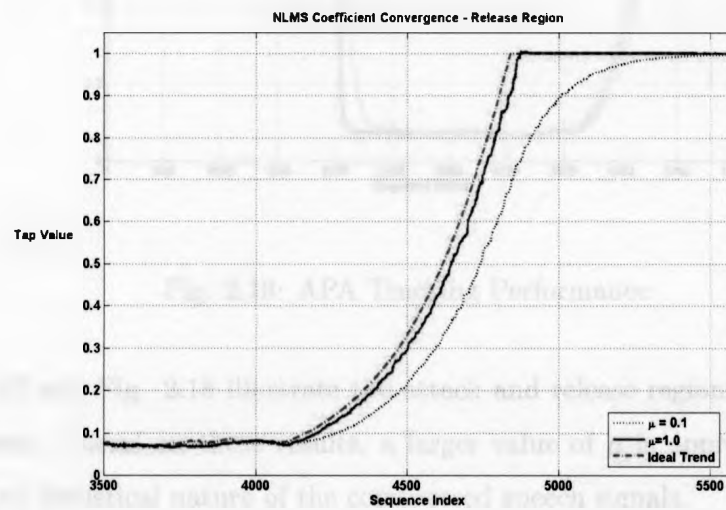


Fig. 2.15: NLMS Tracking Performance, Release Region

estimate in steady-state regions.

### 2.5.3.2 Affine Projection Algorithm

Similar in nature to the NLMS algorithm, the generalized affine projection algorithm (APA) has a step-size that is typically selected from the working range of  $0 < \mu \leq 1$ . In addition, the projection order, which is typically less than or equal to the filter order,  $K \leq M$ , must be selected. *For this work, the projection-order was set at 5 with the same filter order as in the NLMS simulations.*

Fig. 2.16 shows the average tracking performance of the APA algorithm.

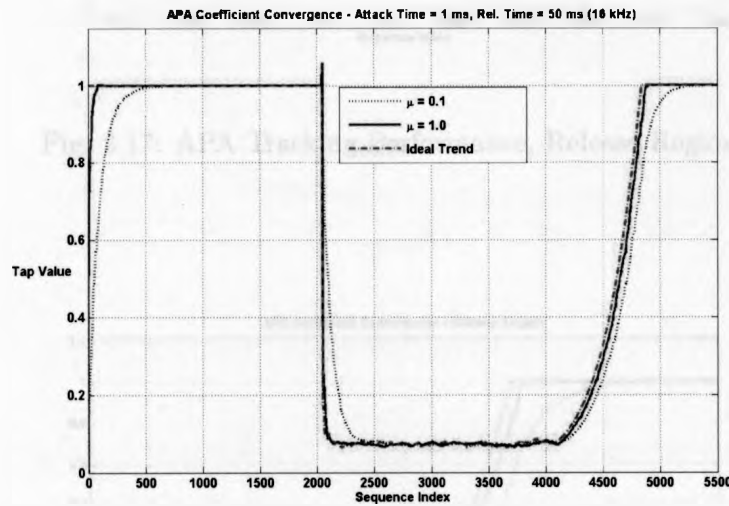


Fig. 2.16: APA Tracking Performance

Fig. 2.17 and Fig. 2.18 illustrate the attack and release regions, respectively, in greater detail. Based on these results, a larger value of  $\mu$  is appropriate given the time-varying statistical nature of the compressed speech signals.

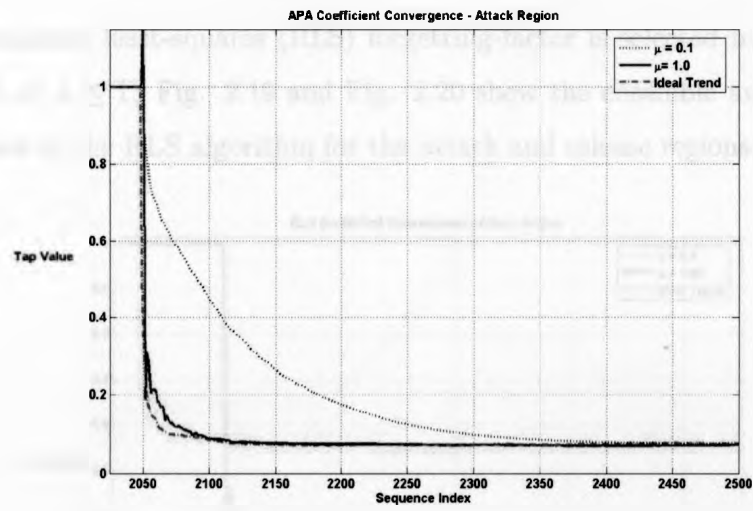


Fig. 2.17: APA Tracking Performance, Release Region

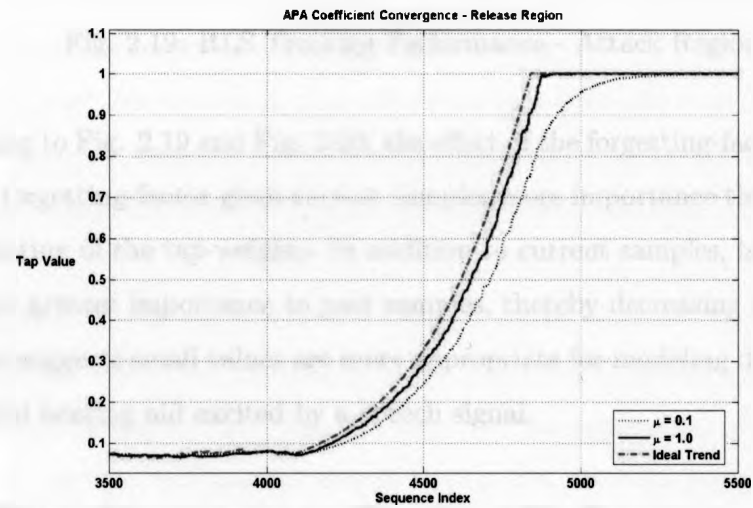


Fig. 2.18: APA Tracking Performance, Release Region

### 2.5.3.3 Recursive Least Squares

The recursive least-squares (RLS) forgetting-factor is selected from the working range of  $0 \ll \lambda \leq 1$ . Fig. 2.19 and Fig. 2.20 show the ensemble averaged tracking performance of the RLS algorithm for the attack and release regions respectively.

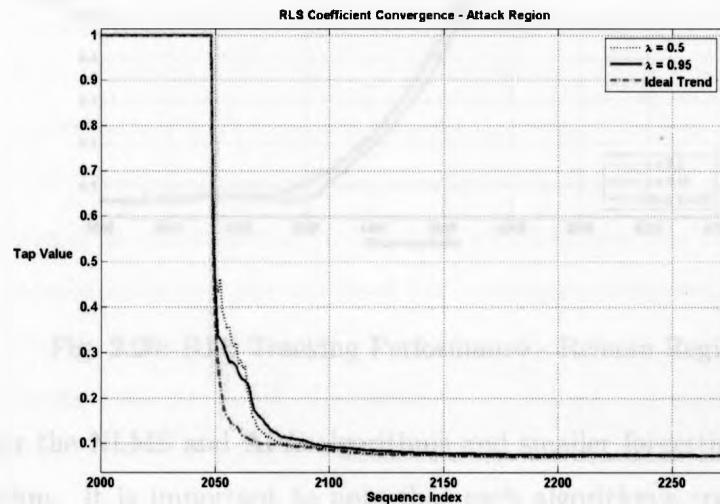


Fig. 2.19: RLS Tracking Performance - Attack Region

Referring to Fig. 2.19 and Fig. 2.20, the effect of the forgetting-factor can be seen. A smaller forgetting-factor gives current samples more importance than past samples in the updating of the tap-weights. In addition to current samples, larger forgetting-factors give greater importance to past samples, thereby decreasing tracking ability. This result suggests small values are more appropriate for modeling dynamic systems like a digital hearing aid excited by a speech signal.

### 2.5.4 Final Comments on Tracking Performance

Based on these tracking results, each of the three adaptive algorithms are likely to perform appropriately for the intended subband modeling application using larger

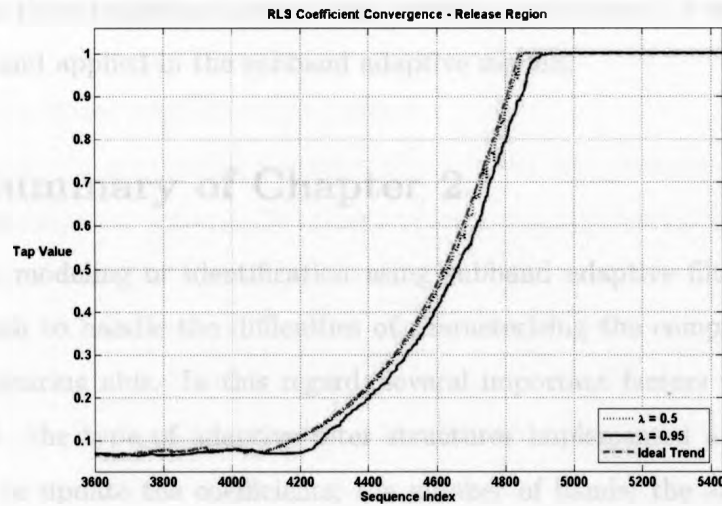


Fig. 2.20: RLS Tracking Performance - Release Region

step-sizes for the NLMS and APA algorithms and smaller forgetting-factors for the RLS algorithm. It is important to note that each algorithm's tracking behaviour, like that of its respective steady-state convergence properties, is dependent on the statistical nature of the system they attempt identify.

The intent of this section is to suggest that an extensive tracking performance analysis of complex systems is a substantial undertaking and, in a suitable fashion, attempt to justify the applicability of the adaptive algorithms considered in this thesis.

Several factors make a complete tracking analysis difficult: the non-stationary statistical properties of the Hearing in Noise Test (HINT) speech sequences used to excite the hearing instruments; the dependence of the application of compression on the intensity level of the applied speech signal; the resulting compression channel parameters determined from the applied fitting method.

Simulation results of the model considered suggest that the adaptive algorithms are capable of tracking the time-varying compression characteristics of digital hearing

aids. From these empirical observations, working parameters for the algorithms can be chosen and applied in the subband adaptive models.

## 2.6 Summary of Chapter 2

System modeling or identification using subband adaptive filtering is a practical approach to handle the difficulties of characterizing the compression behaviour of digital hearing aids. In this regard, several important factors must be carefully considered: the type of adaptive filter structures implemented and the respective algorithm to update the coefficients; the number of bands; the application of decimation/interpolation governing the need for a corresponding synthesis filter bank; whether the bands will be uniform or non-uniform in nature.

Finite-impulse response (FIR) digital filters are commonly used for the adaptive filter structures because they are inherently stable and readily facilitate the development of mathematically tractable performance equations having a single optimal performance point. The associated tap-weights may be updated using one of several algorithms that estimate the tap-input covariance matrix and the cross-covariance vector associated with the desired sequence and the tap-input vector. The normalized least-mean squares algorithm, the affine projection algorithm, and the recursive least-squares algorithm are three possible adaptive algorithms. Because of their properties, they possess the two important behaviours of learning and tracking the underlying statistics of the applied sequences.

Employing numerous bands in a subband adaptive model allows the full band spectral characteristics of the system being modeled to be separated into several independent adaptive filters of smaller order. Decimation lowers the effective sampling frequency of each band, decreasing the number of samples to be processed. This allows complex, large order systems to be modeled adequately and in a timely manner. When the decimation factor is equal to the number of bands, the subband adaptive model

is said to be critically decimated. The other extreme where no decimation is applied is called over-sampled. Interpolation is required when decimation occurs and the synthesis minimizes possible aliasing effects.

Several design approaches are available to select the parameters of the analysis and synthesis filter structures. The choice of structure depends on the application and computational time required for implementation. We used an over-sampled uniform subband adaptive filter model based on a cosine-modulated filter bank structure (43).

Standard adaptive algorithms may be used in each band's adaptive filter to update the tap-weights of the filter structure. The NLMS, APA, and RLS (along with the QRD RLS implementation) algorithms have varying degrees of computational complexity. The NLMS algorithm makes use of a normalized instantaneous estimate for updates to filter tap-weights, while the APA and RLS algorithms use past data for improved estimates. Overall performance of each algorithm has significant dependence on the statistical nature of the applied signals.

Results of the last section of this chapter show the difficulty of completing a comprehensive tracking analysis for complex systems. References on the subject (46; 47) typically use a simplified model in order to facilitate a rigorous treatment. In this thesis we considered a simplified model based on ANSI S3.22 (2003) and concluded that the NLMS, APA, and RLS algorithms exhibit adequate tracking behaviour in this context with suitable parameters.

## Chapter 3

# Simulations

### 3.1 Introduction

Using controlled simulations we hope to confirm two key postulates of this research,

1. The applicability of the subband adaptive model investigated by (24) to today's digital hearing aids.
2. The number of bands in the subband adaptive model must be at least equal to the number of hearing aid compression channels to ensure adequate modeling performance.

In addition, we reviewed a bias-tone with broadband excitation method developed by (27) as a possible approach to determine the number of compression channels employed in a hearing aid.

#### 3.1.1 Overview of Hearing Aid Model

A software-based simulated hearing aid was implemented to investigate the effect of channel-mismatch on modeling performance. The term channel-mismatch indicates



that the number of bands used in the model may be different than the actual number of hearing aid channels.

A block-form representation of this model is shown in Fig. 3.1.

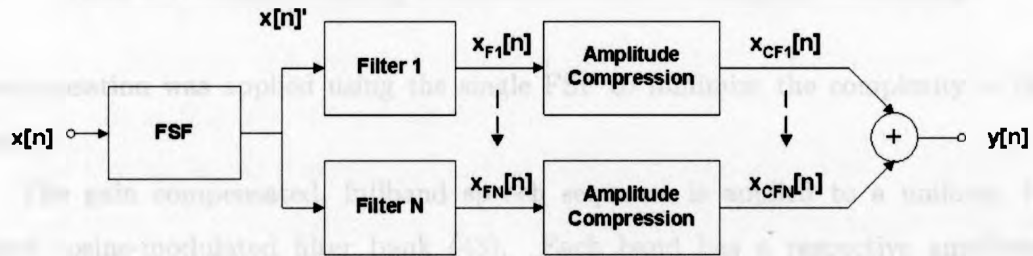


Fig. 3.1: Simulated Hearing Aid

A Hearing In Noise Test (HINT - House Ear Institute of Los Angeles, CA, USA) speech sequence,  $x[n]$ , is applied to a frequency shaping filter (FSF). This filter provides gain compensation for a steeply sloping, moderate-to-moderately severe hearing loss (50). Fig. 3.2 shows an audiogram typical of this type of hearing loss.

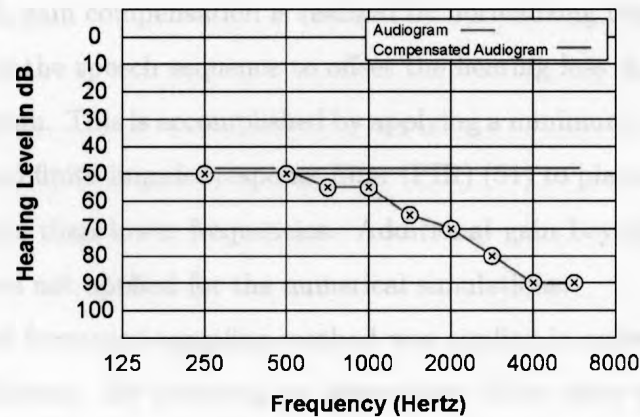


Fig. 3.2: Steeply Sloping Moderate-to-moderately Severe Audiogram

In actual hearing aids, gain compensation is applied on a per band basis (i.e. at the filter level with respect to Fig. 3.1) rather than in one processing block. Gain

Frequency (Hz)	250	500	750	1000	1500	2000	3000	4000	6000	8000
dB (HL)	50	50	55	55	65	70	80	90	90	90

Table 3.1: Steeply Sloping, Moderate-to-Severe Audiogram Thresholds

compensation was applied using the single FSF to minimize the complexity of the model.

The gain compensated, fullband speech sequence is applied to a uniform, N-band cosine-modulated filter bank (43). Each band has a respective amplitude compression channel with independently set compression parameters. The resulting fullband, compressed sequence,  $y[n]$ , is the sum of the individual branch sequences,  $x_{CF1}[n] \rightarrow x_{CFN}[n]$ .

Aside from compression, no other signal dependent processing features were included (e.g. adaptive time constants, noise reduction, and so forth).

### 3.1.2 Gain Compensation

In our model, gain compensation is realized by normalizing the frequency magnitude spectrum of the speech sequence to offset the hearing loss characterized by the specified audiogram. This is accomplished by applying a minimum, mean-square-error (MMSE) designed finite-impulse response filter (FIR) (51) to place more emphasis on higher frequencies than lower frequencies. Additional gain beyond the initial spectrum shaping was not applied for the numerical simulations.

The standard frequency-sampling method was applied in order to determine the FIR filter coefficients. By selecting an appropriate filter order and providing the normalized frequency values with the respective normalized magnitude values, this function produces the desired filter coefficients. The data required for this calculation is available from the considered audiogram and presented in Table 3.1.

In order to obtain the normalized magnitude values, threshold values in dB were

converted to a linear scale and normalized by the largest value of the resulting set. To obtain the normalized frequency values, each frequency in Table 3.1 is divided by the considered Nyquist frequency. In our work a sampling frequency of 16 kHz is used, providing a Nyquist frequency of 8 kHz. An additional column was added to Table 3.1 with a frequency of 8 kHz and threshold value of 90 dB HL. These values must exist for the application of the FIR2 function.

The Matlab Signal Processing Toolbox function, FIR2, allows an arbitrary FIR filter of order,  $N$ , to be designed using a set of sampled frequency-magnitude values. In addition to this data, the FIR2 function allows the filter order to be specified. The output of the FIR2 function is a set of filter coefficients providing an approximate fit to the given data.

At each filter order, the corresponding frequency magnitude characteristic is determined from the filter coefficients and plotted against the desired response to provide a visual indication of how well the designed filter matches the required response. Fig. 3.3 shows the fit of a 16<sup>th</sup> order FIR filter and the required response acquired from the audiogram. This result allows a root-mean-square (RMS) difference or error to be calculated in order to select and set an acceptable filter order.

Figure 3.4 shows the relationship between the RMS error and the FIR filter order. With increasing filter order, the fitting error decreases indicating a better overall fit with respect to the given normalized magnitude values. The asymptotic characteristic suggests a practical working order for the filter of 16. This is the filter order we used for the FSF filter in the hearing aid model. The frequency-phase characteristic is linear.

### 3.1.3 Uniform Filter Bank

A Kaiser-window based, cosine-modulated design technique was used to implement the uniform filter bank (43). The stop band attenuation is 100 dB and the transition bandwidth is 0.07 radians per sample. This technique allows uniform filter

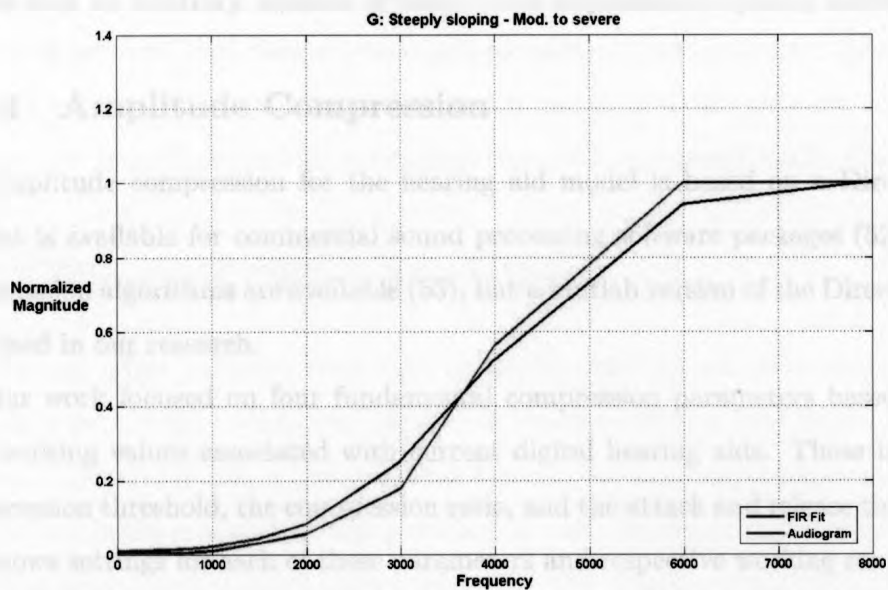


Fig. 3.3: 16<sup>th</sup> Order FIR Fit with Desired Frequency Magnitude Response

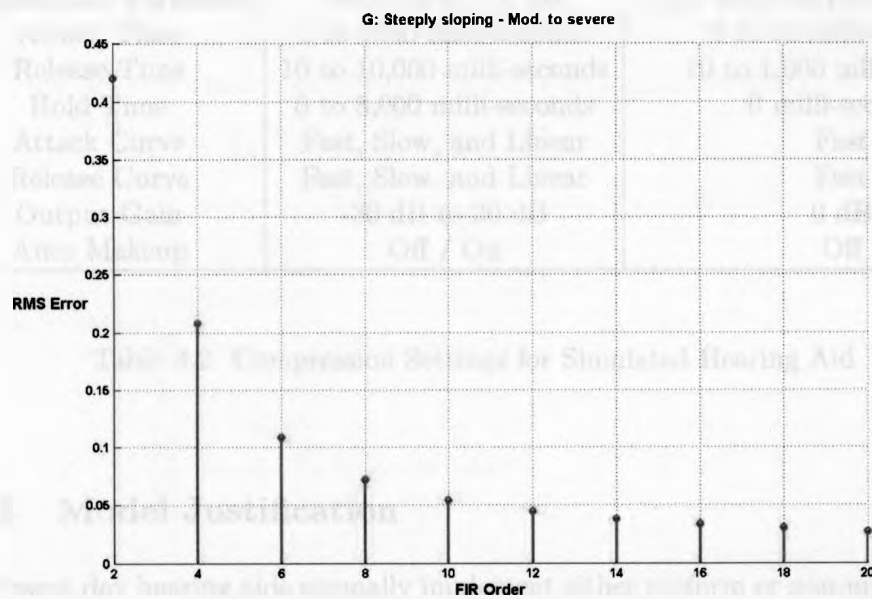


Fig. 3.4: RMS Error Versus FIR Order

banks with an arbitrary number of bands to be implemented quickly and efficiently.

### 3.1.4 Amplitude Compression

Amplitude compression for the hearing aid model is based on a DirectX plug-in that is available for commercial sound processing software packages (52). Several compression algorithms are available (53), but a Matlab version of the DirectX plug-in was used in our research.

Our work focused on four fundamental compression parameters based on nominal working values associated with current digital hearing aids. These include the compression threshold, the compression ratio, and the attack and release times. Table 3.2 shows settings for each of these parameters and respective working ranges for the implemented compression algorithm.

Feature	Range	Settings Used
Compression Ratio	1:1 to 20:1	1:1 to 4:1
Compression Threshold	-96.0 dB to 0.0 dB	<See Text for Further Details>
Attack Time	0 to 1000 milli-seconds	5 to 10 milli-seconds
Release Time	10 to 10,000 milli-seconds	10 to 1,000 milli-seconds
Hold Time	0 to 5,000 milli-seconds	0 milli-seconds
Attack Curve	Fast, Slow, and Linear	Fast
Release Curve	Fast, Slow, and Linear	Fast
Output Gain	-30 dB to 30 dB	0 dB
Auto Makeup	Off / On	Off

Table 3.2: Compression Settings for Simulated Hearing Aid

### 3.1.5 Model Justification

Present day hearing aids normally implement either uniform or non-uniform filter banks for gain compensation, with groups of adjacent bands applied to one of several discrete compression channels. In addition to this fundamental structure, manufac-

turers offer a broad range of proprietary digital signal processing features and options that their research indicates are beneficial to users of their products. Given the proprietary nature of these processing features, it would be a difficult task to accurately incorporate these features into a comprehensive software-based research model.

## 3.2 Channel Offset Modeling

Channel offset modeling was used to validate the impact on subband adaptive modeling performance when the number of bands of the analysis filter bank in the subband adaptive model is different than the number of compression channels in the hearing aid being modeled. A key postulate of this research is that optimal subband adaptive model performance occurs only when the number of bands in the analysis filter bank is equal to or greater than the actual number of compression channels.

The channel-offset modeling approach is based on the subband adaptive model structure, which is illustrated in Fig. 3.5.

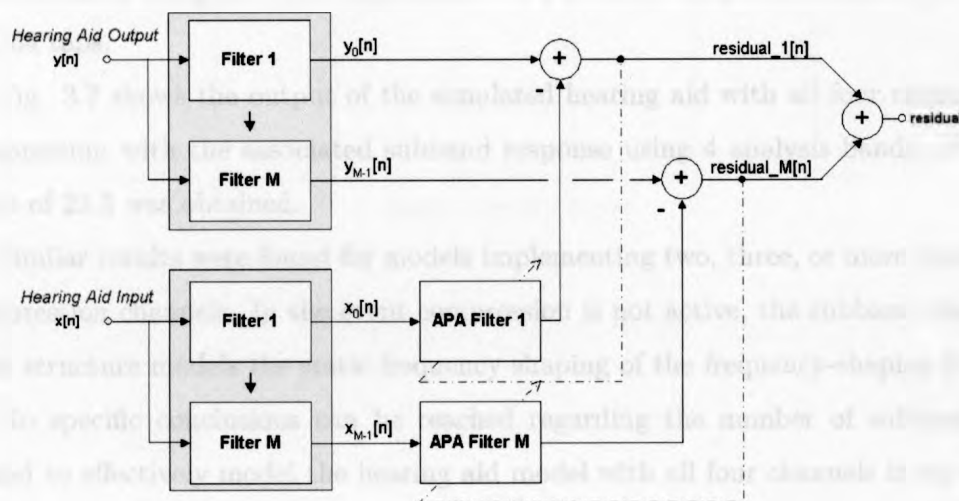


Fig. 3.5: Subband Adaptive Model

Rather than using a fixed number of analysis filters,  $M$ , the channel-offset modeling

approach implements varying numbers of analysis filters ranging over a number of bands that spans the number of hearing aid model channels ( $M = 1 \rightarrow M \gg \text{number of channels}$ ). At each discrete configuration, a signal-to-error ratio (SER) is calculated from the ratio of the covariance of the filtered hearing aid model response,  $y[n]$ , to the covariance of the associated error residual,  $\text{residual}[n]$ , for each respective band as noted by Equation 4.1.

$$10\log_{10} \left( \frac{\text{cov}(\text{Net Model Output})}{\text{cov}(\text{Net Model Error})} \right) \quad (3.1)$$

Plotting SER against the number of analysis bands offers a visual determination of the optimal number of discrete sub-bands required to effectively model the hearing aid model's compression characteristics.

Fig. 3.6 illustrates this result for our hearing aid model with all four channels in compression (indicated by the vertical red bar). SER metric values increase asymptotically with additional increments to the number of analysis bands. These results were obtained using the APA algorithm with a step-size of 1, projection-order of 15, and 64 taps.

Fig. 3.7 shows the output of the simulated hearing aid with all four channels in compression with the associated subband response using 4 analysis bands. A SER value of 23.5 was obtained.

Similar results were found for models implementing two, three, or more than four compression channels. In the event compression is not active, the subband adaptive filter structure models the static frequency shaping of the frequency-shaping filter.

No specific conclusions can be reached regarding the number of subbands required to effectively model the hearing aid model with all four channels in an active compression state. However, the performance of the model improves as the number of subbands increases. As noted in Chapter 2, in the section on uniform and non-uniform filter banks, additional bands improve the whitening of the spectral regions, which in turn reduces the eigenvalue spread of the input covariance matrix resulting

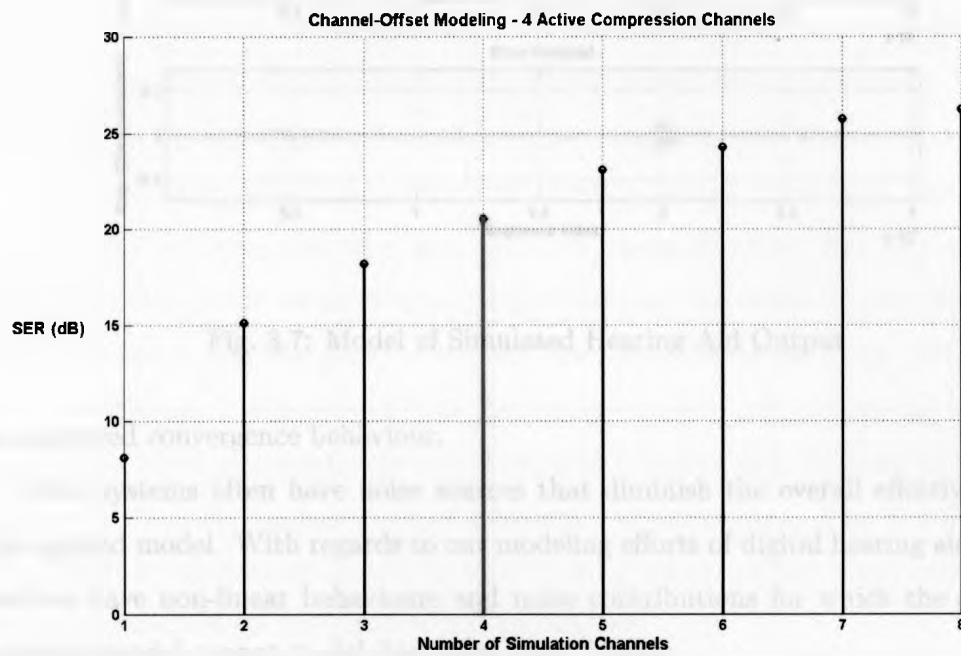


Fig. 3.6: Four Channel Model



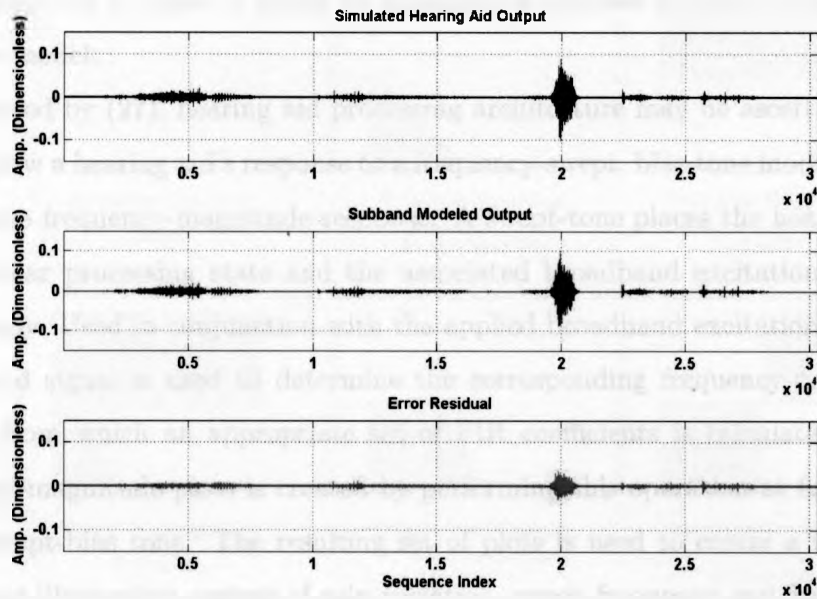


Fig. 3.7: Model of Simulated Hearing Aid Output

in improved convergence behaviour.

Real systems often have noise sources that diminish the overall effectiveness of the applied model. With regards to our modeling efforts of digital hearing aids, these devices have non-linear behaviours and noise contributions for which the subband adaptive model cannot model due to its linear nature.

### 3.3 Bias Tone with Broadband Excitation

#### 3.3.1 Introduction

The bias-tone with broadband excitation procedure developed by (27) facilitates determination of a hearing aid's underlying processing structure. Despite limited practical application of this technique, which appears to be only theoretical at the time of this writing, we concluded it may be effectively used prior to modeling of

the hearing aid in order to select an appropriate number of bands in the subband adaptive model.

As noted by (27), hearing aid processing architecture may be ascertained by observing how a hearing aid's response to a frequency-swept, bias-tone modifies a broadband noise frequency-magnitude response. A swept-tone places the hearing aid into a non-linear processing state and the associated broadband excitation is modified accordingly. Used in conjunction with the applied broadband excitation, the altered broadband signal is used to determine the corresponding frequency-magnitude response, from which an appropriate set of FIR coefficients is calculated. A set of frequency-magnitude plots is created by performing this operation at fixed intervals of the swept-bias tone. The resulting set of plots is used to create a three dimensional plot illustrating regions of gain variation, sweep-frequency and frequency form the x-axis and y-axis, respectively, and gain forming the z-axis. A two-level, gain-threshold conversion is applied to convert this three-dimensional gain profile into a two-dimensional plane representation that retains the sweep-frequency and frequency axes. This two-dimensional representation of the hearing aids response is then correlated or "scored" against a set of standard representations. Fig. 3.8 illustrates identification patterns for several types of hearing aid processing. Dark regions indicate gain reduction or the presence of compression.

Even within its theoretical context, (27) successfully applied this processing type test in hearing aid simulations to detect several common processing architectures. As shown in Fig. 3.8, these include,

**Linear** - Due to the linear basis of this test approach, the resulting patterns will not show gain alterations.

**Automatic Signal Processing (ASP)** - Monitors a characteristic of the incoming signal and alters device performance in real-time. In this pattern, as the swept frequency increases, the cut-off frequency of the high-pass filter decreases

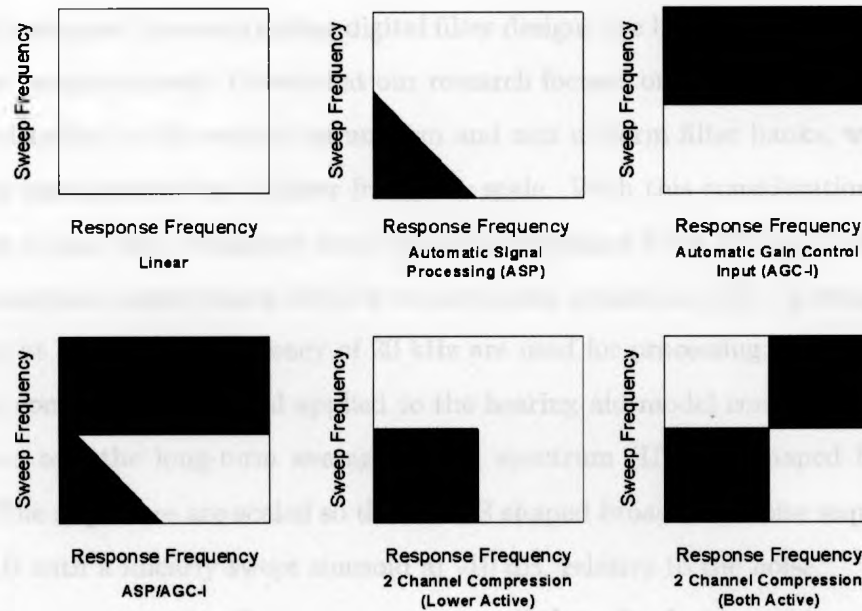


Fig. 3.8: System Identification Patterns

resulting in equal gain across the spectrum.

**Automatic Gain Control Input (AGC-I)** - Like ASP, this approach monitors the input level and activates gain reduction, or clipping, once the input level is larger than a set threshold.

**ASP/AGC-I** - This is a combination of the automatic signal processing and automatic gain control processing approaches.

**Compression** - The lower two patterns illustrate those associated with a device having one or two channels in active compression, respectively.

### 3.3.2 Procedure

In (27), the author makes the assumption that multi-band hearing aids employing analog filter designs typically employ bands uniformly spaced on a logarithmic fre-

quency scale and those employing digital filter designs use bands uniformly spaced on a linear frequency scale. Given that our research focuses on digital hearing aids, and as noted earlier in the section on uniform and non uniform filter banks, we consider uniform bands spaced on a linear frequency scale. With this consideration in mind, changes in gain and frequency response are determined from 222 to 9,500 Hz; 222 Hz is one-third octave below 315 Hz as noted and applied in (27). A total of 53248 samples at a sampling frequency of 20 kHz are used for processing.

The composite test signal applied to the hearing aid model consists of the swept bias-tone and the long-term average speech spectrum (LTASS) shaped broadband noise. The sequences are scaled so the LTASS shaped broadband noise sequence is at a -30 dB with a linearly swept sinusoid at -10 dB, relative to the noise.

The resulting composite sequence was applied to the hearing aid model, using nominal compression parameters, and stored. In addition, model responses to the swept-tone and broadband noise alone were capture and stored. This set of three sequences were applied to a paired-filter adaptive noise cancellation system, shown in Fig. 3.9, in order to estimate changes in the hearing aid's frequency response.

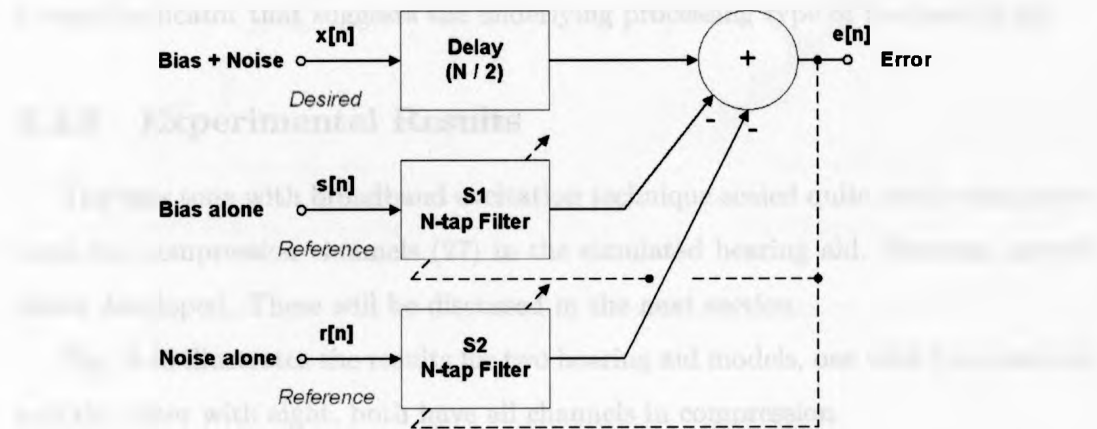


Fig. 3.9: Paired Filter Adaptive System

The bias-and-noise response,  $x[n]$ , is applied to an  $N/2$  delay block, forming the

desired sequence for both of the adaptive algorithms,  $S1$  and  $S2$ . The bias response,  $s[n]$ , is applied to an  $N$ -tap adaptive filter,  $S1$ , which removes the bias-tone component from the desired response. The noise response,  $r[n]$ , is applied to the paired adaptive filter,  $S2$ , which removes the noise component.

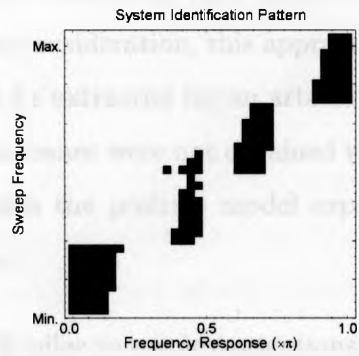
Extracting the tap-weights of  $S2$  at periodic intervals allows the frequency-magnitude characteristic of the hearing aid to be determined. This set of magnitude responses captures a time-varying response that models the underlying linear response of the hearing aid (54). The residual error is attributed to non-linear distortions introduced by compression (30; 24; 55). No portion of this error is due to inherent noise that exists in actual hearing aids, since no noise was included in our model.

A threshold is applied to the resulting set of frequency-magnitude characteristics to generalize the data presentation to a two-level representation. Magnitude values larger than an applied threshold represent frequency regions where gain is present, indicating the absence of compression. Magnitudes below the threshold represent frequency regions where gain has been reduced, indicating the presence of compression. Plotting this transformed set of responses, as documented in the introduction, offers a visual indicator that suggests the underlying processing type of the hearing aid.

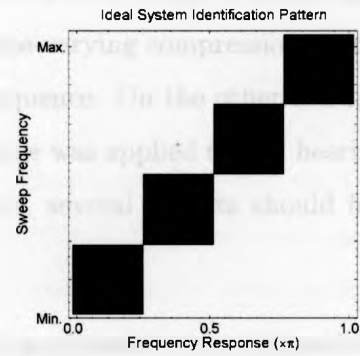
### 3.3.3 Experimental Results

The bias tone with broadband excitation technique scaled quite easily using more than two compression channels (27) in the simulated hearing aid. However, several issues developed. These will be discussed in the next section.

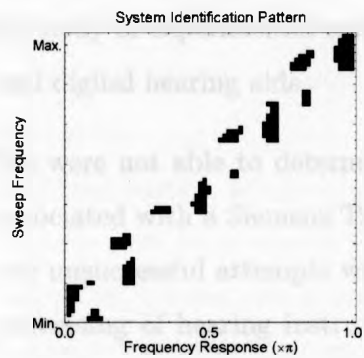
Fig. 3.10 illustrates the results for two hearing aid models, one with four channels and the other with eight, both have all channels in compression.



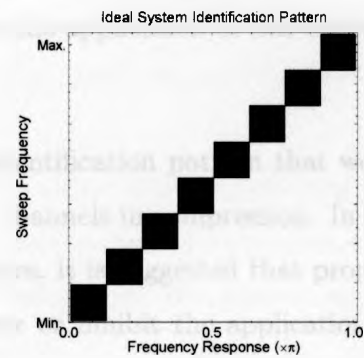
(a) 4 Channel, Experimental



(b) 4 Channel, Ideal



(c) 8 Channel, Experimental



(d) 8 Channel, Ideal

Fig. 3.10: Experimental and Ideal System Identification Patterns

### 3.3.4 Discussion

From our preliminary results, which were applied to hearing aid models different than the one implemented in (27) and in a controlled environment, the bias-tone with broadband excitation method may have benefit in providing an estimation of the number of bands for the subband adaptive model to ensure adequate modeling. With further consideration, this approach may allow time-varying compression characteristics to be extracted for an arbitrary excitation sequence. On the other hand, results of significance were not obtained when the technique was applied to real hearing aids.

Given the positive model experimental results, several caveats should be highlighted,

- Similar to our investigations, Kate's original application was restricted to models of linear and compression based hearing aids under controlled conditions. No body of experimental evidence exists on the application of this approach to real digital hearing aids.
- We were not able to determine a system identification pattern that would be associated with a Siemens Triano S with 4 channels in compression. In light of our unsuccessful attempts with actual devices, it is suggested that proprietary processing of hearing instruments may skew or inhibit the application of the processing-type test. For example, long-term application of excitation sequence may be required in order to place the hearing aid in the desired state prior to measurement. Determination of the necessary excitation signal to overcome this issue may be very difficult or impossible.
- Due to the linear nature of the underlying adaptive filtering processing, hearing aids using a linear processing strategy will not demonstrate changes to their frequency magnitude characteristic (27).
- Significant work is required to optimize this technique. One particular item is

the determination and setting of the required threshold used in the application of the two-level threshold transformation of the frequency-magnitude set. In our work, this was done visually to provide adequate results. Again, prior knowledge of the model configuration may influence this selection. A more objective, optimized approach is very much needed.

### 3.4 Summary of Chapter 3

A hearing aid model was developed in order to investigate two techniques used to determine the most beneficial number of bands to effectively model real hearing aids using the subband adaptive model with uniform band structure. Our model implemented gain compensation using a single frequency-shaping filter with a uniform filter bank, each band having a respective compression channel. Channel-offset modeling and the bias-tone with broadband excitation techniques were applied to this model. Both approaches provide estimates for the number of bands required for the subband adaptive model.

Unlike real hearing aids, our model employed a single frequency-shaping filter to normalize the gain for a typical steeply sloping hearing loss. Suitable gain compensation in actual hearing aids is applied on a per band basis. We chose to apply gain in this manner to reduce the complexity of the model.

Band structures in real hearing aids typically employ either a uniform or a non-uniform distribution. Adjacent groups of bands are then grouped and applied to one of several compression channels. Our model had a one-to-one ratio of bands to compression channels.

Channel-offset modeling employs the actual structure used by the subband adaptive model. By using a number of bands that spans the possible number of active compression channels in the hearing aid, modeling effectiveness can be determined and reported as a signal-to-error (SER) ratio. Given the asymptotic behaviour of SER



versus the number of analysis bands, it is not obvious how many bands should be selected to realize effective modeling. The application of objective measures, as done with our actual hearing aid measurements and discussed in the next chapter, could provide a suitable indicator for estimating this number. Selecting a large number of bands would offer more effective modeling, but it may not be required and result in lengthened modeling times.

The bias-tone with broadband excitation technique developed by Kates (27) did facilitate the determination of the number of bands required within the confines of our modeling and a controlled simulation environment. Given the vast nature of possible process features offered by today's digital hearing aids that are proprietary in nature, and the lack of experimental evidence with real hearing aids, of which our own testing proved inconclusive, it not possible to judge the effectiveness of the technique at this time.

## 8.1 Digital Hearing Aids

The hearing aid is a device that is used to assist in the hearing process. It is a device that is used to assist in the hearing process. It is a device that is used to assist in the hearing process.

The hearing aid is a device that is used to assist in the hearing process. It is a device that is used to assist in the hearing process. It is a device that is used to assist in the hearing process.

## Chapter 4

# Methodology

This chapter provides details of the five digital hearing aids used in this research; an overview of the experimental system and measurement procedure; and the modeling results for these hearing aids.

Modeling results obtained for each of the three considered adaptive algorithms are presented in their own section with associated comments. Chapter 5 will note comparative conclusions between all three sections of results.

### 4.1 Digital Hearing Aids

Five current market digital hearing aids were selected for this study in order to determine the applicability of a uniform subband adaptive model to the characterization of the compression behaviour of these instruments.

Due to noteworthy differences in the nature of each instrument's band structure, the number of these bands, and the number of compression channels, efforts were made to obtain detailed data on each hearing aid. However, due to the proprietary nature of this information and disparity in the hearing aid industry in terms of how the concepts of band and channel are used, it was not possible to present comprehensive information in a standardized fashion across all of the hearing aids considered. As

a result, information on each instrument was compiled using corporate web-sites in addition to contacting representatives from each company directly. This information is presented here.

All hearing aids used in this research are behind-the-ear (BTE) devices. In alphabetical order of manufacturer the set includes,

- **Bernafon, Symbio XT 110 BTE**
- **Oticon, Syncro V2**
- **Phonak, Perseo 311 dAZ Forte**
- **Siemens, Triano S**
- **Sonic Innovations, Natura 2 SE**

The subsequent sub-sections describe each hearing aid.

The Bernafon Symbio XT BTE 110 is the first channel-free hearing instrument. The stated working frequency range extends from 100 to 5,900 Hertz (ANSI S3.22 2003).

Bernafon's approach with this device is to handle sounds as a whole rather than processing them using a frequency-domain approach based on frequency bands and compression channels. It is Bernafon's reasoning that this approach results in clear, natural sound, offering optimal speech quality.

Bernafon's on-line literature suggests signals processed using multi-channel strategies may present an apparent high quality signal at the output of an electro-acoustic amplification system, but an impaired cochlea has less ability to use this signal than does a healthy cochlea.

#### **4.1.1 Bernafon Symbio XT BTE 110**

As noted by O'Brien (56), the following aspects support a channel-free processing approach,

- In addition to loss of sensitivity to less intense or soft sounds, sensorineural hearing loss also results in the broadening of critical auditory filters, with the perceptual consequence of reduced frequency selectivity (57).
- Internal representation of acoustic signals for hearing impaired listeners for acoustic signals has a lower signal-to-noise ratio than for normal hearing individuals (58). Multi-channel compression will effectively bombard the cochlea with sound having less spectral contrast; spectral contrast is important for speech understanding (59).
- Impaired cochlear frequency resolution means spectral cues may still not be useful to the listener despite audibility (60).

The ChannelFree<sup>TM</sup> technology analyzes and makes gain adjustments 16,000 times per second to the whole signal. Bernafon refers to this processing strategy as Continuously Adaptive Speech Integrity (CASI) and is illustrated in Fig. 4.1.

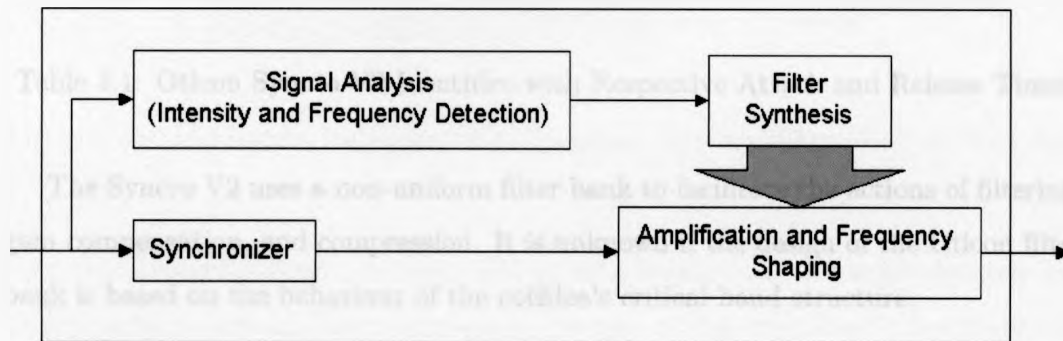


Fig. 4.1: CASI Block Diagram

This processing strategy retains the natural signal structure, facilitating quicker patient adaptation to this instrument than for those that employ multi-channel amplification.

### 4.1.2 Oticon Syncro V2

The Oticon Syncro V2 is an 8-channel programmable digital hearing aid. The stated working frequency range extends from 130 to 6,900 Hertz (ANSI S3.22 2003).

The eight compression channels are independent, but make use of a coupling process to avoid large distortions that may occur because of narrow band signals. Applied attack and release times for each channel depend on which Oticon rationale or "Identity" is used to configure the instrument. Table 4.1 presents the five Oticon Identities and the respective attack and release times. As noted by a Oticon representative, the technique used to measure the attack and release times influences the values obtained.

Identity	Attack Time (milliseconds)	Release Time (milliseconds)
Energetic	5 - 10	80
Dynamic	5 - 10	80 - 320
Active 5	640	640
Gradual	5	1,280
Calm	10 - 20	2,560

Table 4.1: Oticon Syncro V2 Identities with Respective Attack and Release Times

The Syncro V2 uses a non-uniform filter bank to facilitate the actions of filtering, gain compensation, and compression. It is unknown if the design of the Oticon filter bank is based on the behaviour of the cochlea's critical band structure.

### 4.1.3 Phonak Perseo 311 dAZ Forte

The Phonak Perseo 311 dAZ Forte is a 20-channel programmable digital hearing aid. The stated working frequency range extends from 100 to 6,000 Hertz (ANSI S3.22 2003).

The Perseo 311 dAZ Forte employs a processing strategy Phonak refers to as Digital Perception Processing (DPP<sup>2</sup>). This approach attempts to adhere to the way

sounds are perceived by a healthy cochlea by modeling its natural behaviour. A key aspect of this behaviour is how the basilar membrane is stimulated by sound.

Pure tone stimulation of the basilar membrane stimulates not only the locus of the membrane associated with the applied frequency, but also excites a wider surrounding area. As noted in (61), this effect can be described as a band pass filter with a distinct center frequency and variable roll-off, with several of these bands spread along the length of the cochlea's basilar membrane. These bands are commonly referred to as the critical bands. Fig. 4.2 illustrates the relationship between the cochlea and the critical bands of the Forte.

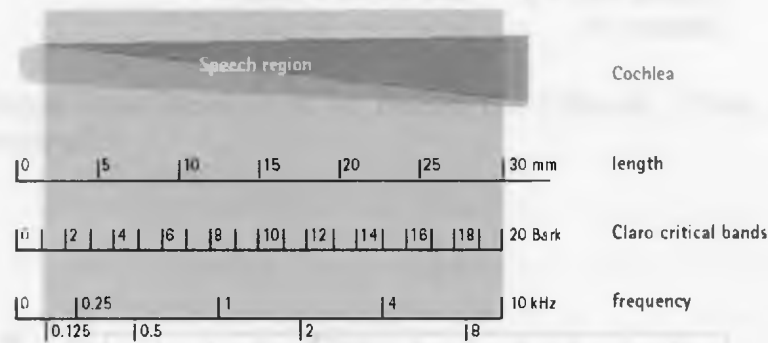


Fig. 4.2: Critical Bands, Relationship to Cochlea (*Phonak, "Claro, Digital Perception Processing"*)

Critical filter bandwidth is dependent on both frequency (being approximately logarithmically scaled) and excitation level. Because of this dependency, bands overlap resulting in interactions and dependencies in the firing patterns of auditory neurons. Fig. 4.3 illustrates the dependency of critical band bandwidth with center frequency and the coupling relationship between critical bands.

Critical band shape also depends on the level of the excitation signal, as illustrated in Fig. 4.4.

Due to these dependencies the overall excitation pattern is related to the maximum excitation occurring from all frequency components of a complex signal. Fig. 4.5

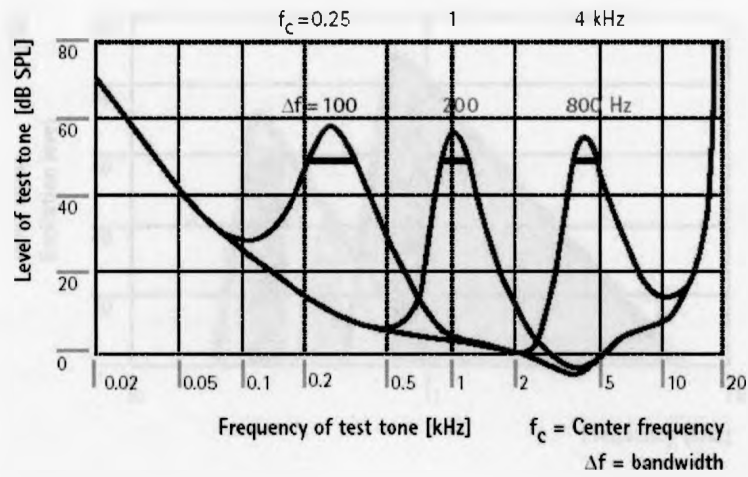


Fig. 4.3: Critical Band Structure of the Human Ear (*Phonak, "Claro, Digital Perception Processing"*)

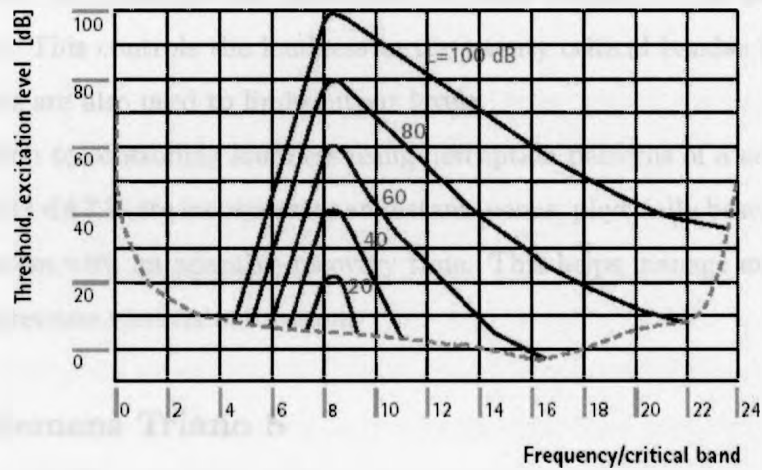


Fig. 4.4: Critical Band Shape Versus Excitation Level (*Phonak, "Claro, Digital Perception Processing"*)

illustrates this behaviour for a simplified three-tone signal.

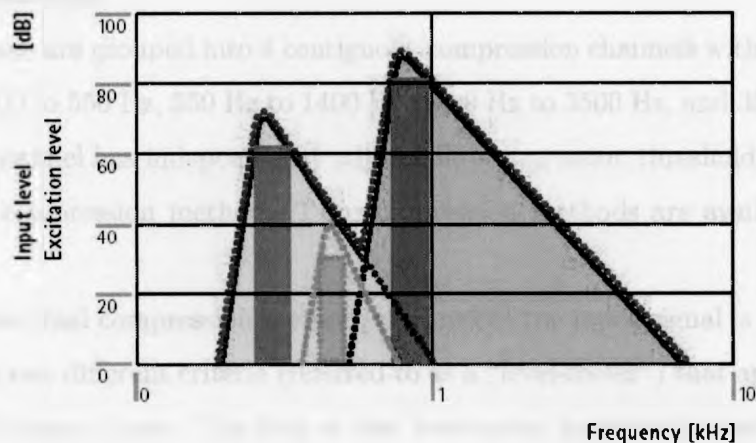


Fig. 4.5: Overall Excitation Pattern (*Phonak, "Claro, Digital Perception Processing"*)

Once normally perceived sounds are established, loudness is controlled using the principle of *loudness summation*. Digital Perception Processing applies a psychoacoustic model to determine the perceptual patterns created by the normal cochlea (62; 63; 64). This controls the loudness in the twenty critical bands. These perception patterns are also used to limit output levels.

In addition to controlling loudness using perception patterns of a normal cochlea, the Perseo 311 dAZ Forte incorporates an instantaneous, physically based compression limiting system with an adaptive recovery time. This helps manage excessive sound levels and prevents receiver saturation.

#### 4.1.4 Siemens Triano S

The Siemens Triano S is a 4-channel programmable digital hearing aid. The stated working frequency range extends from 100 to 5,500 Hertz (ANSI S3.22 2003).

The Triano S has 16 bands (160, 315, 400, 500, 630, 800, 1000, 1250, 1600, 2000, 2500, 3200, 4000, 5000, 6300, and 8000 Hertz) linearly spaced across the working



frequency. Each band has an attenuation of 42 dB per octave for the application of gain compensation.

The bands are grouped into 4 contiguous compression channels with the frequency ranges of 100 to 550 Hz, 550 Hz to 1400 Hz, 1400 Hz to 3500 Hz, and 3500 Hz to 6500 Hz. Each channel has independently adjustable compression thresholds, compression ratio, and compression method. Two compression methods are available: Dual or Syllabic.

With the Dual compression method, the level of the input signal is actively monitored using two different criteria (referred to as a "level-meter") that apply respective attack and release times. The first or fast level-meter provides immediate reduction in gain for high-level, intense sounds with an attack time of 5 ms and an associated release time of 90 ms. The second or slow level-meter monitors the average level of the input signal and applies an attack time of 900 ms and a release time of 1.5 seconds.

The Syllabic compression method adjusts the applied gain to instantaneous fluctuations of the incoming signal using the fast-level meter with an attack time of 9 ms and a release time of 90 ms.

The Triano S utilizes 16 discreet automatic gain control circuits that compress the input signal (AGC-I). With this implementation, there are 16 working compression channels controlled through a set of 4 pseudo controlling channels. In order to obtain the input level for each circuit, which determines the application of compression, the weighted values of immediately adjacent channel levels are added. For the Triano S, as noted by a Siemens representative, the AGC-I input level for channel 2 would be one-quarter of the channel 1 input level added to one-half of the channel 2 input level added to one-quarter of the channel 3 input level. This approach aids in ensuring continuity of the processed signal, which minimizes the introduction of potential harmful auditory artefacts.

This instrument also uses an automatic gain control circuit at the output (AGC-O). The attack time is less than 0.5 ms and a release time of 100 ms.

Hearing Aid	Number of Channels	Number of Bands	ANSI S3.22 Time Constants	
			Attack	Release
Symbio XT 110 BTE	Channel Free <sup>TM</sup>		N/A	N/A
Syncro V2	8	8, <i>Non-uniform</i>	N/A	N/A
Perseo 311 dAZ Forte	20	20, <i>Critical</i>	6 ms	60 ms
Triano S	4	16, <i>Uniform</i>	0.5 ms	100 ms
Natura 2 SE	9	9, <i>Critical</i>	5 ms (2 kHz)	11 ms (2 kHz)

Table 4.2: Hearing Aid Structure Summary

#### 4.1.5 Sonic Innovations Natura 2 SE

Sonic Innovations Natura 2 SE is a 9-channel programmable digital hearing aid. The stated working frequency range extends from 220 to 5,000 Hertz (ANSI S3.22 2003).

As stated in Sonic Innovations on-line literature, the Natura 2 SE uses a 9-band, critical-band structure with 9 independent compression channels. Each compression channel uses a low compression threshold and moderate compression ratio or wide-dynamic range compression (WDRC) approach. No additional information could be found on band or channels for this instrument.

### 4.2 Hearing Aid Summary

Table 4.2 summarizes the compression parameters for each instrument considered in this research. Additional information may be found in the manufacturers data-sheets located in Appendix A.

### 4.3 Hearing Aid Test System

The Hearing Aid Test System (HATS) developed at the National Centre for Audiology was used to record hearing aid responses. A block-diagram of the HATS system is illustrated in Fig. 4.6.



The following sections detail the HATS system in three sections: *Programming*, *Excitation*, and *Recording*.

Each hearing aid was programmed using its respective proprietary software module provided by the manufacturer via the *Hearing Instrument Manufacturers' Software Association (HIMSA) NOAH* software application that executes on the personal computer (PC). A *GN Otometrics HI-PRO Universal Programming Interface* facilitates communication through serial port COM2 of the PC to the hearing instrument using a proprietary programming cable. The programming cable is positioned in the acoustically sealed passage of the anechoic test box.

95

#### 4.3.1.2 Excitation

Each speech sequence was digitally streamed from the PC over a USB 2.0 connection to a Sound Devices USBPre device that converted the digital sequence to an analog signal. The resulting analog signal was applied to a Tucker Davis PA5 Programmable Attenuator and then fed into a Carver PM420 amplifier, energizing the anechoic test box speaker. Attenuation introduced by the programmable attenuator was set by the HATS software to provide the desired average dB SPL presentation level to the hearing aid being tested. A system calibration procedure is required prior to making measurements. Further information on this procedure is presented in Section 4.3.2, *Calibration*.

#### 4.3.1.3 Recording

Each hearing aid was placed in a *Bruel & Kjaer Type 4232 Anechoic Test Box* (serial number 2357535) with the hearing aid microphone located within the measuring plane (as marked by a round piece of blue foam by manufacturer). This location provides constant sound pressure level conditions with low acoustic distortion.

Two *Bruel & Kjaer Type 4192 1/2" Pressure Response Microphones*, with associated *Type 2669 Falcon Range 1/2" Microphone Preamplifiers*, were used to record the acoustic signal presented to the hearing aid (reference signal) and its response. A 2cc coupler was connected to the hearing aid in order to provide a standardized response measure (coupler signal). The *Type 4192 1/2" Pressure Response Microphones* have serial numbers of 2337046 for the reference microphone and 2337047 for the 2cc coupler microphone.

The reference and 2cc coupler recording channels form channel 1 and channel 2 inputs, respectively, of a *Bruel & Kjaer Nexus 2-Channel Microphone Conditioning Amplifier* that is manually adjusted by the operator. The conditioned analog signals were then applied to the *Sound Devices USBPre* device and recorded at a sampling

frequency of 32 kHz at 16-bit resolution.

The HATS software stores each recorded sequence in a single stereo-WAV file and in two separate mono-WAV files, one with the reference signal and the other with the 2cc coupler signal.

#### 4.3.2 Calibration

Prior to using the HATS measurement system, calibration procedures were performed to ensure the system was presenting excitation signals at the desired sound level (in units of dB SPL) to the instrument being tested. This was done by a pure-tone calibration procedure followed by a frequency calibration procedure.

For pure-tone calibration, a Bruel & Kjaer Type 4231 Sound Level Calibrator (serial number 2191799 with a UC 0210 1/2" diameter adaptor), producing a 1 kHz, 94 dB SPL test signal, was attached to the reference microphone. A recording of this test signal was made and used to determine and then set a system-scaling factor based on the root-mean-square value of the recorded digital signal. Subsequent digital signals were scaled appropriately in order to realize the necessary dB SPL presentation level.

For frequency calibration, the frequency response of the reference and coupler recording channels are computed and normalized with respect to each other. A pink-noise signal is delivered through the built-in speaker of the anechoic test box and recordings are made using both the reference and 2cc coupler channels. From each recording, the respective frequency response is determined in  $1/3^{rd}$  octave bands using a 1024-point FFT with Hamming window scaling. Using the coupler and reference microphone frequency responses, an equalization filter is derived to compensate for the differences between them.

The equalization filter is a 512-tap FIR filter designed using a windowing method based on the differences between the coupler and reference microphone spectra. The equalization filter ensures that the transfer function between the coupler and refer-

Frequency (Hz)		125	250	500	750	1k	1.5k	2k	3k	4k	6k	8k
Type	"F"	50	50	50	55	55	65	70	80	90	90	90
	"I"	90	90	90	90	90	90	90	90	90	90	90

Table 4.3: Theoretical Audiograms

ence microphones is flat across the audio bandwidth of 20 Hz to 20,000 Hz. With the equalization filter in place, hearing aid gain characteristics can be computed directly by taking the difference between the coupler and reference microphone spectra (in dB). Frequency compensation also ensures hearing aid responses are accurately obtained when system identification procedures are applied.

## 4.4 Hearing Aid Programming

Due to the proprietary nature of each manufacturer's design and implementation of their instruments, in addition to the inability to separate the control of band gain and channel compression parameters in the programming software, it was necessary to establish a standardized testing framework. Two theoretical audiograms and a standard hearing aid fitting method were chosen to accommodate this need.

Two theoretical audiograms were selected in order to obtain different degrees of hearing aid compression behaviour. As discussed in Chapter 1, these audiograms are typical of commonly occurring sensorineural hearing losses. A *steeply sloping, moderate-to-severe* or Type "F" audiogram and a flat, severe or Type "I" audiogram were considered. The respective audiometric thresholds, in dB HL units, are summarized in Table 4.3 for each audiogram.

The fitting method employed to program each instrument was the Desired Sensation Level Input/Output (DSL [i/o]) method. The procedure used to configure each instrument included,

- Consulting suggested fitting regions to ensure audiograms fit within these areas

of nominal operation.

- Visual inspection to ensure standard set of mechanical components.
- Installation of a new battery.
- A “first fit” configuration of the hearing aid using the desired audiogram and the DSL [i/o] fitting method.
- Disabling processing features not associated with compression.
- Using an omni-directional microphone setting.
- Saving configuration to hearing aid in addition to being saved in the NOAH database for future reference.

Each programmed hearing aid was placed in the anechoic test-box and its response was recorded using the HATS system.

One final comment should be made at this point for the sake of completeness. Despite the fact that several independent fitting methods are provided in each manufacturer’s NOAH programming module, these are not independently verified to ensure the fitting targets specified by the fitting methods are met. It is known that the DSL [i/o] targets are not met by several vendors’ software. While this is an issue for patient fittings, this will not impact the significance of this work; we are trying to establish the modeling potential of a uniform subband adaptive model in characterizing compression behaviour across a range of different hearing aids.

## 4.5 Response Measurement

A sequence of ten concatenated Hearing in Noise Test (HINT) speech sequences (1-1, “A Boy fell From the Window.”; 1-10, “The car is going too fast.”; 10-10, “The truck made it up the hill.”; 11-1, “The neighbours boy has black hair.”; 11-2, “The

*rain came pouring down.*"; 11-3, *"The orange is very sweet."*; 11-4, *"He took the dogs for a walk."*; 11-5, *"Children like strawberries."*; 11-6, *"Her sister stayed for lunch."*; 11-7, *"The train is moving fast."*) was created to excite each hearing aid. This sequence was generated with a 32 kHz sampling frequency and a 16-bit resolution and stored locally on the HATS computer.

Using the HATS software, this sequence was scaled and presented to each hearing aid at 65 dB SPL within the uniform sound field of the desktop, anechoic test box. This level is representative of the average sound pressure level of the long-term average speech spectrum for normal conversational speech in a noise free environment.

Recordings of the reference and 2cc coupler microphone signals were made and stored locally on the computer's hard drive. These sequences were manually parsed off-line and stored individually as stereo WAV files with the 2cc coupler recording in the left-channel and the reference recording in the right-channel.

## 4.6 Modeling

The uniform subband adaptive model was applied to each pair of recorded sequences across an incrementally increasing number of analysis bands (1, 2, 4, 8, 16, and 20) using a fixed-set of parameters for each of the three adaptive algorithms.

A signal-to-error ratio (SER) metric was calculated to monitor modeling performance. In addition to SER, the Perceptual Evaluation of Speech Quality (PESQ) mean-opinion score (MOS) was calculated as a second objective measure of performance.

### 4.6.1 Subband Adaptive Modeling

Figure 4.7 illustrates the subband adaptive model structure used in this research.

Before application to the model, each recorded sequence is decimated by a factor of two to use the full bandwidth of 0 to 8 kHz, approximately. This facilitates an



Algorithm	Parameter		
	Step Size / Forgetting Factor	Projection Order	Number of Taps
APA	0.1, 0.5, 1.0	5, 10, 15	64, 128, 256
NLMS	0.1, 0.5, 1.0	n/a	
RLS	0.5, 0.725, 0.95	n/a	

Table 4.4: Adaptive Algorithm Parameters

effective sampling frequency of 16 kHz. The decimated reference and 2cc coupler sequences are filtered using identical uniform analysis filter banks. The resulting filtered sequences form, respectively, the reference and desired sequences for each adaptive filter in the model.

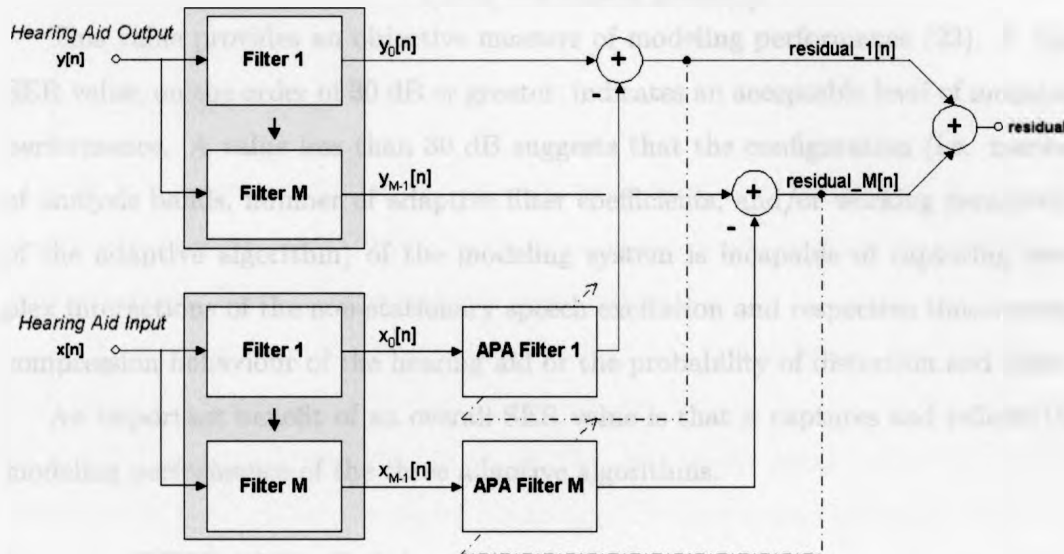


Fig. 4.7: Subband Adaptive Filter Structure

For each number of analysis bands considered the hearing aid's compression behaviour is modeled using the Affine Projection (APA) algorithm, the Normalized Least Mean Squares (NLMS) algorithm, and Recursive Least Squares (RLS) algorithm with a set of parameters, see Table 4.4.

Parameters were selected in order to investigate a broad range of modeling per-

formance and should not be considered optimal in any sense. Further work would be required to extract a general set of optimal parameters for each algorithm.

The overall model output and residual sequences were obtained by adding the respective sequences from each adaptive filter.

#### 4.6.1.1 Signal-to-Error Ratio

An effectual signal-to-error ratio (SER) was calculated using the model's accumulative output and residual sequences and is noted in Eq. 4.1.

$$10\log_{10} \left( \frac{\text{cov}(\text{Net Model Output})}{\text{cov}(\text{Net Model Error})} \right) \quad (4.1)$$

This value provides an objective measure of modeling performance (23). A high SER value, on the order of 30 dB or greater, indicates an acceptable level of modeling performance. A value less than 30 dB suggests that the configuration (i.e. number of analysis bands, number of adaptive filter coefficients, and/or working parameters of the adaptive algorithm) of the modeling system is incapable of capturing complex interactions of the non-stationary speech excitation and respective time-varying compression behaviour of the hearing aid or the probability of distortion and noise.

An important benefit of an overall SER value is that it captures and reflects the modeling performance of the three adaptive algorithms.

#### 4.6.1.2 PESQ Mean Opinion Score

In addition to the standard signal-to-error ratio (SER) performance measure commonly associated with adaptive modeling investigations, the Perceptual Evaluation of Speech Quality (PESQ) Mean Opinion Score (MOS) was also calculated using Version 1.2 (August 2, 2002) of the International Telecommunications Union P.862 software.

The PESQ P.862 standard is an internationally recognized and accepted measure of predicting a subjective interpretation of speech quality that is typically used to

Hearing Aid	Number of Channels	Number of Bands	ANSI S3.22 Time Constants	
			Attack	Release
Symbio XT 110 BTE	Channel Free <sup>TM</sup>		N/A	N/A
Syncro V2	8	8, <i>Non-uniform</i>	N/A	N/A
Persco 311 dAZ Forte	20	20, <i>Critical</i>	6 ms	60 ms
Triano S	4	16, <i>Uniform</i>	0.5 ms	100 ms
Natura 2 SE	9	9, <i>Critical</i>	5 ms (2 kHz)	11 ms (2 kHz)

Table 4.5: Hearing Aid Structure Summary

assess telecommunication systems. Using this measure, along with the SER metric, we hope to determine which linear adaptive algorithm provides the best modeling performance.

## 4.7 Summary

Five programmable digital hearing aids, representative of the current hearing aid market, are described with respect to their respective band, channel, and ANSI S3.22 time constants. Table 4.2 presents this information.

Each of these devices is programmed with the DSL [i/o] fitting method using a first-fit approach using two theoretical audiograms. The response of each instrument to 10 HINT sentences, presented at 65 dB SPL, is recorded using the HATS systems developed at the National Centre for Audiology. Two calibration procedures are completed prior to making measurements to ensure hearing aid responses are accurately obtained when system identification procedures are applied, as it the case for this research.

Recorded sequence sets, consisting of the hearing aid excitation signal and the associated 2cc coupler signal (hearing aid response), are used as the reference and desired sequences of an over-sampled, uniform subband adaptive model. Modeling is completed using six different numbers of analysis bands (1, 2, 4, 8, 16) and three adaptive algorithms. The NLMS, APA, and RLS algorithms were all implemented



## Chapter 5

# Modeling Results

The primary objective of this research is to assess the potential application of a uniform subband linear adaptive filter model to characterize the compression behaviour of five digital programmable hearing aids. With this in mind, a signal-to-error ratio (SER) metric will be used to assess the overall performance of this model based on several factors that include: the number of analysis bands, the adaptive algorithm used to update the coefficients of the tap-delay filter structure, and a corresponding set of parameters. The mean-opinion score (MOS) metric is also computed to investigate the potential success of using a subband model in conjunction with objective measures to estimate subjective assessments of speech quality.

The standard recursive least-squares algorithm from the Mathworks Matlab Filter Design Toolbox was initially used in the modeling process. However, due to numerical instabilities of the input-signal covariance matrix, an orthogonal matrix triangularization, or QR decomposition, implementation based on (65) was used.

Due to the large body of data collected in this research, results for the Oticon Syncro V2 are presented in detail. Results for this instrument are, in general, representative of those obtained for the other four hearing aids. Appendix C, *Modeling Results*, presents graphical results for these instruments.

The contents of this chapter are presented in the following order,

## General Modeling Performance of the Oticon Syncro V2

- NLMS Results
- APA Results
- QRD RLS Results

## Modeling Performance Summary of the Oticon Syncro V2

- Audiogram "F"
- Audiogram "I"

## Fullband and Subband Model Performance Summary - All Hearing Aids

- Audiogram "F"
- Audiogram "I"

# 5.1 General Modeling Performance of the Oticon Syncro V2

In this section modeling results for the Oticon Syncro V2 hearing aid are presented for each of the three adaptive algorithms. This is done using each algorithm's parameters associated with the "best" modeling performance based on a signal-to-error ratio (SER) performance metric. This rationale is consistent with the fundamental research objective of this thesis of applying a subband adaptive model to characterize compression behaviour of digital hearing aids and using this model as a basis for objective speech quality measures such as PESQ. It also helps manages the large body of data developed by this research. Modeling results for the remaining algorithm parameters for the Syncro V2 and complete results for the other four hearing aids are presented in Appendix C, *Modeling Results*.

From an initial review of the modeling results, the parameters for each algorithm giving the best performance are noted in Table 5.1.

Algorithm	Parameters
NLMS	Step-size of 1.0
APA	Step-size of 1.0; projection-order of 15
QRD RLS	Forgetting-factor of 0.5

Table 5.1: Best Modeling Parameters

Modeling results associated with these parameters are presented for each algorithm in three types of graphs,

1. A double y-axis plot with average SER and MOS values
2. SER mean with standard error bar
3. MOS mean with standard error bar

The number of analysis bands is the independent variable for each of these graphs with trends for 64, 128, and 256 filter coefficients shown. Results for both type "F" and "I" audiograms are presented.

### 5.1.1 NLMS Results

The results in this section are for an NLMS step-size of 1.

Fig. 5.1 illustrates the mean SER and mean MOS values obtained by averaging discrete SER and MOS results over the 10 HINT sentences used on a per band basis for audiogram "F", a *steeply sloping, moderate-to-severe* hearing loss.

As the number of analysis bands of the subband adaptive model is increased, both the averaged SER and averaged MOS values increase in an asymptotic manner. At 20 bands, the largest SER value is approximately 21 dB and the largest MOS value is approximately 4.25 on a scale of 1.0 (worst) to 4.5 (best).

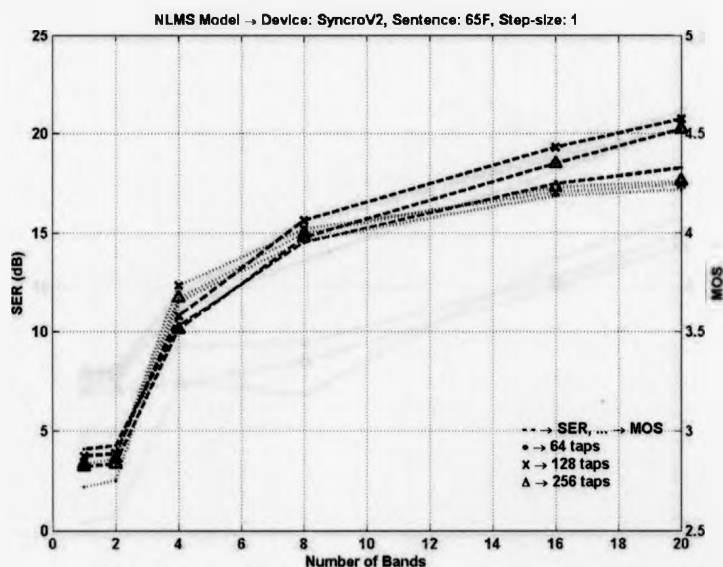


Fig. 5.1: NLMS Averaged SER and MOS, Audiogram F

With respect to the number of taps used in the tap-delay filter, there is a modeling improvement as the number of bands increases. With a larger number of bands, 128 taps provides the highest SER, followed by 256 taps and then 64 taps.

Fig. 5.2 illustrates the mean SER and mean MOS values for audiogram "I", a flat, severe hearing loss. Asymptotic trends are still present, but less pronounced when compared to the type "F" audiogram results. The MOS trends exhibit more variability when a smaller number of analysis bands are used.

At 20 bands, the largest SER value is approximately 16 to 17 dB and the largest MOS value is approximately 4.1.

With respect to the number of taps, with a larger number of bands, 128 taps provides the highest SER, followed by 256 taps and the 64 taps.

Fig. 5.3 illustrates the SER error mean and error bar using one standard deviation for audiogram "F". This was obtained by averaging discrete SER results over the 10 HINT sentences used on a per band basis.



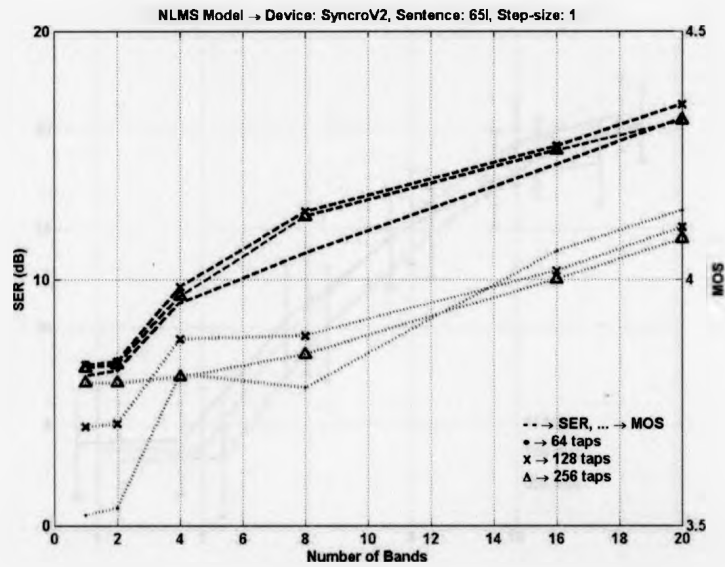


Fig. 5.2: NLMS Averaged SER and MOS, Audiogram I

SER means for 64, 128, and 256 taps increase as the number of analysis bands implemented increases. With a small number of analysis bands, a larger SER mean is associated with fewer filter taps. As the number of analysis bands increases, this relationship deviates. At 16 and 20 bands, the mean SER value decreases with 128, 256, and 64 taps, respectively.

There is a gradual decrease in the level of variability with additional analysis bands, as indicated by the error bars. There is significant overlap of the error bars when comparing model results in which the number of analysis bands is not large. However, a larger difference in the number of analysis bands provides greater separation with no overlap.

Fig. 5.4 illustrates the SER error mean and error bar for audiogram "I". Like audiogram "F" trends, SER means for 64, 128, and 256 taps increase as the number of analysis bands implemented increases. However, the trends are more linear than asymptotic in nature.

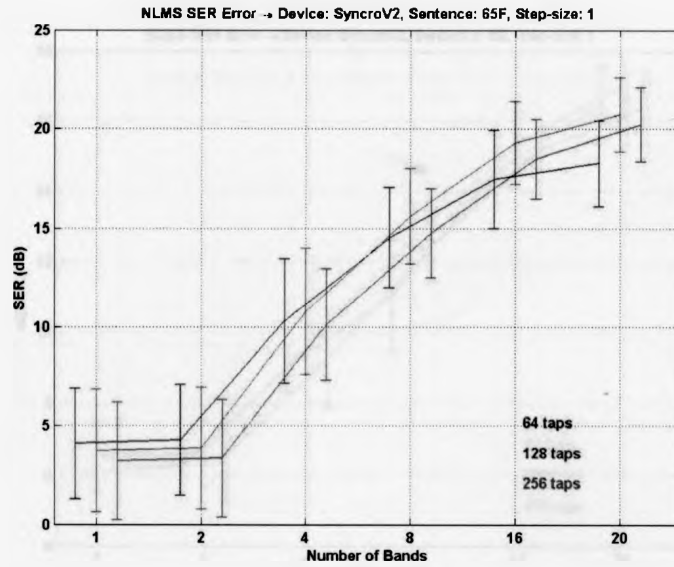


Fig. 5.3: NLMS SER Mean with Error Bar, Audiogram F

Variability does not decrease as the number of analysis bands used increases. This trend occurs for all three taps values considered.

Fig. 5.5 illustrates the MOS error mean and error bar using one standard deviation. This was obtained by averaging discrete MOS values over the 10 HINT sentences used on a per band basis.

The MOS means, for all number of taps, increase as the number of analysis bands increases. Like the SER results, the MOS trends exhibit asymptotic behaviour. However, it is more pronounced.

There is a significant decrease in variability with an associated increase in analysis bands.

Fig. 5.6 illustrates the MOS error mean and error bars for audiogram "I". Like audiogram "F", MOS means increase with the number of analysis bands. However, in a similar fashion to the SER trends, they are more linear than asymptotic in nature.

A general decrease in variability does not exist and there is overlap of the error

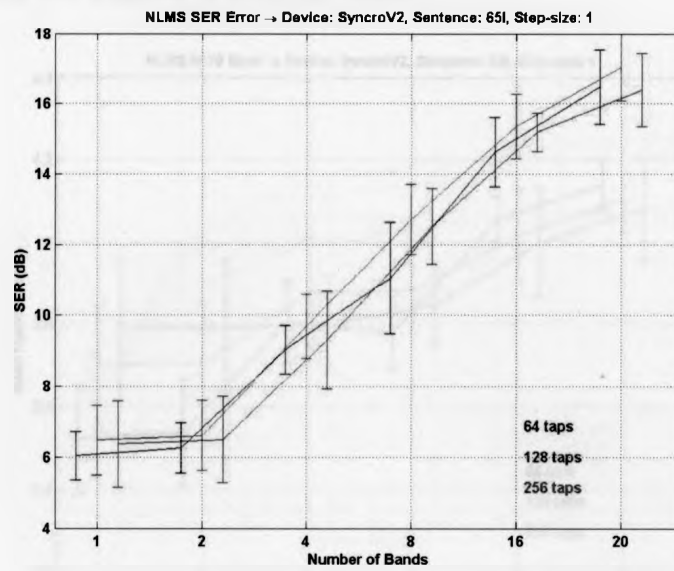


Fig. 5.4: NLMS SER Mean with Error Bar, Audiogram I

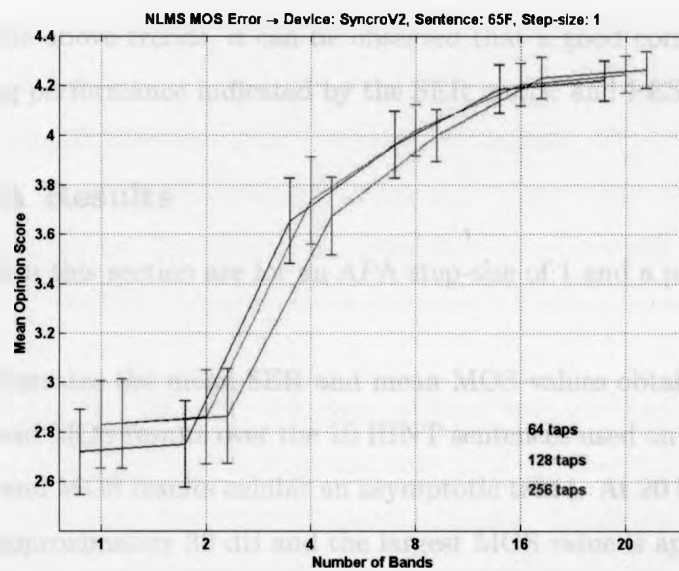


Fig. 5.5: NLMS MOS Mean with Error Bar, Audiogram F

bars right across the number of analysis bands.

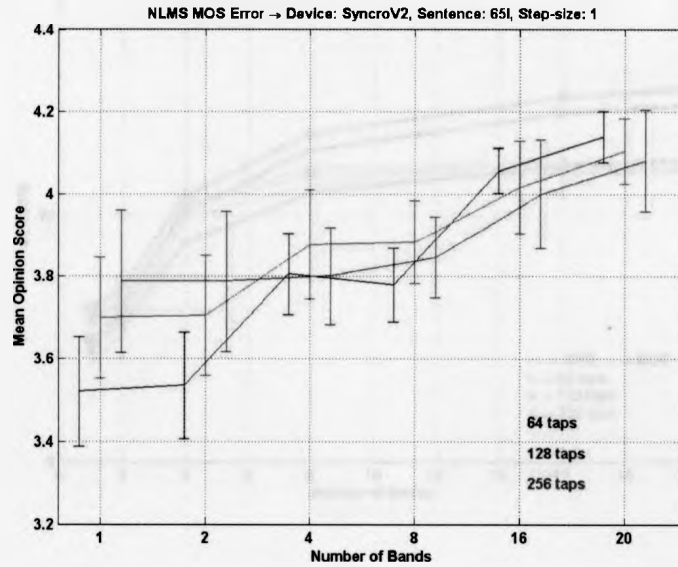


Fig. 5.6: NLMS MOS Mean with Error Bar, Audiogram I

Based on the above trends, it can be observed that a good correlation exists between modeling performance indicated by the SER metric and PESQ quality metric.

### 5.1.2 APA Results

The results in this section are for an APA step-size of 1 and a projection-order of 15.

Fig. 5.7 illustrates the mean SER and mean MOS values obtained by averaging discrete SER and MOS results over the 10 HINT sentences used on a per band basis.

Both SER and MOS results exhibit an asymptotic trend. At 20 bands, the largest SER value is approximately 30 dB and the largest MOS value is approximately 4.4.

With respect to the number of taps used in the tap-delay filter, modeling performance improves in a one-to-one relationship as the number of taps increases. This occurs across the number of analysis bands considered.

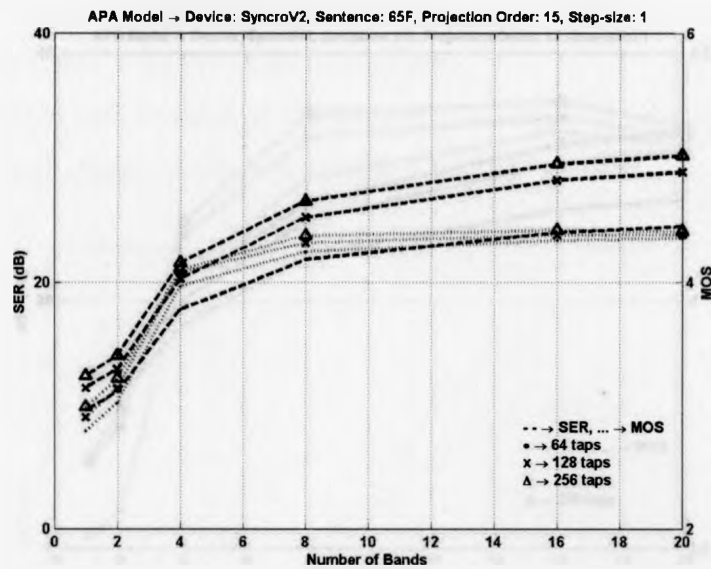


Fig. 5.7: APA Averaged SER and MOS, Audiogram F

Fig. 5.8 illustrates the mean SER and mean MOS values for audiogram “I”. Asymptotic trends are present, but in relation to audiogram “F” trends, MOS mean values drop at 20 bands.

Like the averaged SER and MOS trends for audiogram “F”, With respect to the number of taps, modeling performance improves in a one-to-one relationship as the number of taps increases. This occurs across the number of analysis bands considered.

Fig. 5.9 illustrates the SER error mean and error bar using one standard deviation for audiogram “F”.

SER means for 64, 128, and 256 taps increase with an increase in number of analysis bands. Modeling performance improves in a one-to-one relationship as the number of taps increases. This occurs across the number of analysis bands considered.

There is a gradual decrease in the level of variability with additional analysis bands.

Fig. 5.10 illustrates the SER error mean and error bar for audiogram “I”. Like

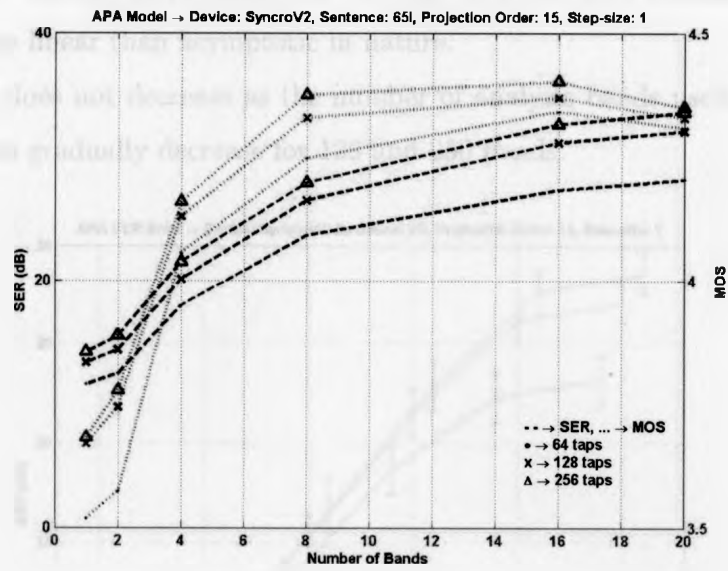


Fig. 5.8: APA Averaged SER and MOS, Audiogram I

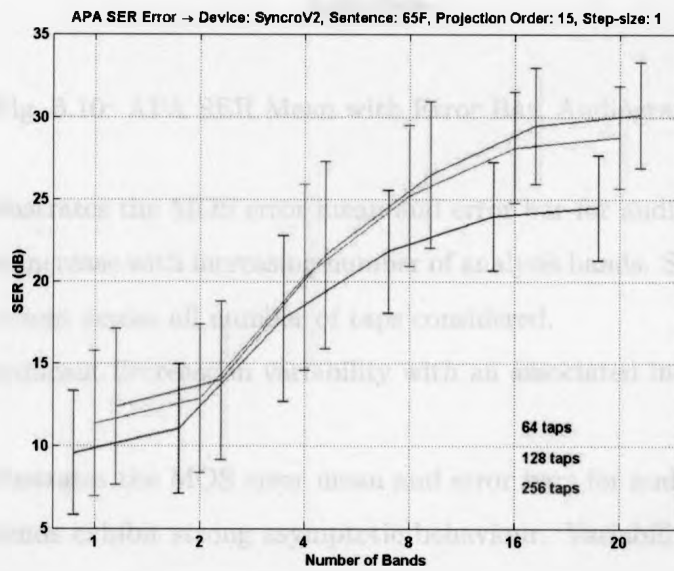


Fig. 5.9: APA SER Mean with Error Bar, Audiogram F

audiogram “F” trends, SER means for 64, 128, and 256 taps increase. However, trends are more linear than asymptotic in nature.

Variability does not decrease as the number of analysis bands used increases for 64 taps. It does gradually decrease for 128 and 256 bands.

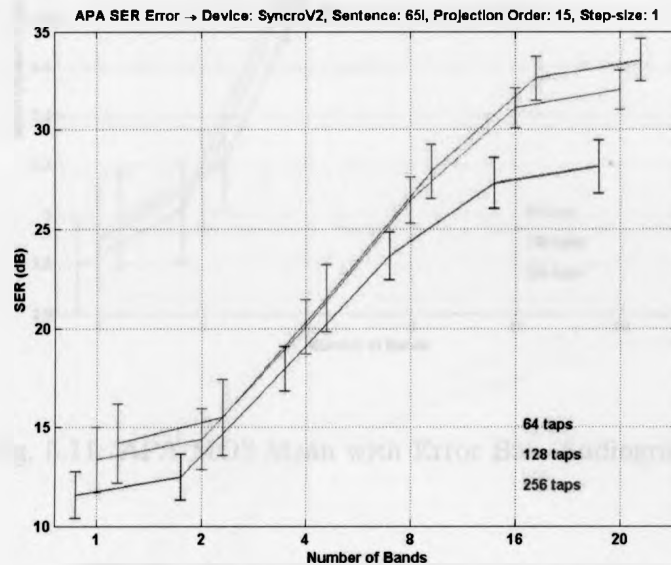


Fig. 5.10: APA SER Mean with Error Bar, Audiogram I

Fig. 5.11 illustrates the MOS error mean and error bar for audiogram “F”.

MOS means increase with increasing number of analysis bands. Strong asymptotic behaviour is present across all number of taps considered.

There is significant decrease in variability with an associated increase in analysis bands.

Fig. 5.12 illustrates the MOS error mean and error bars for audiogram “I”.

All three trends exhibit strong asymptotic behaviour. Variability decreases with increase in the number of analysis bands.

As with the NLMS results, there is an observable correlation between the SER and MOS performances metrics.

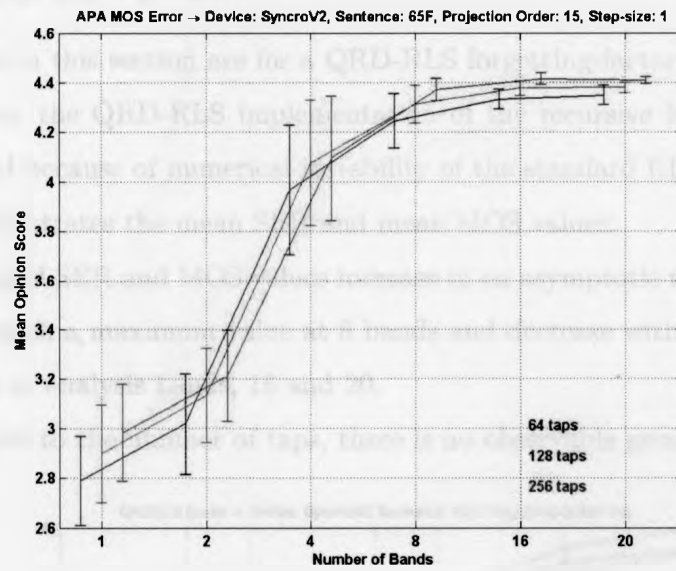


Fig. 5.11: APA MOS Mean with Error Bar, Audiogram F

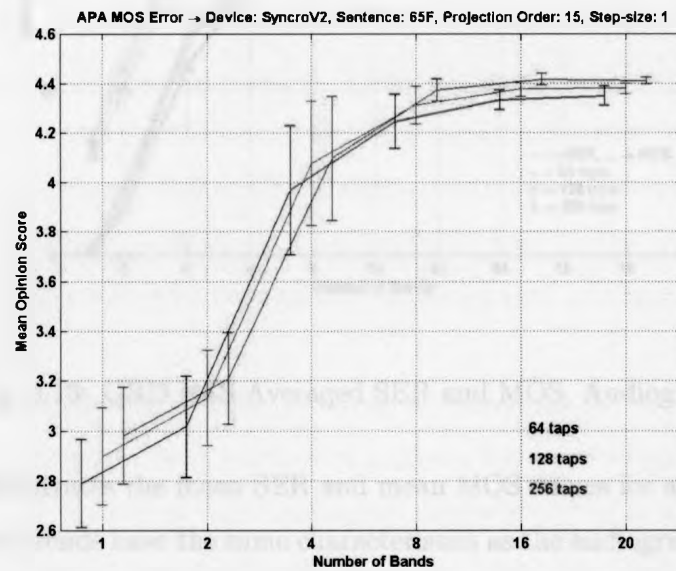


Fig. 5.12: APA MOS Mean with Error Bar, Audiogram I



### 5.1.3 QRD RLS Results

The results in this section are for a QRD-RLS forgetting-factor of 1.

To reiterate, the QRD-RLS implementation of the recursive least-squares algorithm was used because of numerical instability of the standard RLS algorithm.

Fig. 5.13 illustrates the mean SER and mean MOS values.

Both averaged SER and MOS values increase in an asymptotic manner. However, MOS trends reach a maximum value at 8 bands and decrease with further increases in the number of analysis bands, 16 and 20.

With respect to the number of taps, there is no observable general trend.

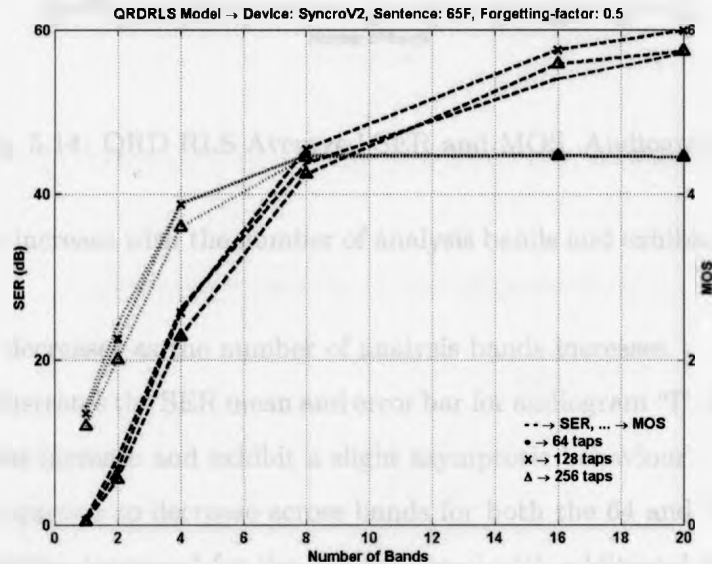


Fig. 5.13: QRD RLS Averaged SER and MOS, Audiogram F

Fig. 5.14 illustrates the mean SER and mean MOS values for audiogram "I".

Both sets of trends have the same characteristics as the audiogram "F" trend sets. Again the MOS trends reach maximum values at 8 bands and decrease at 16 and 20 bands.

Fig. 5.15 illustrates the SER error mean and error bar for audiogram "F".

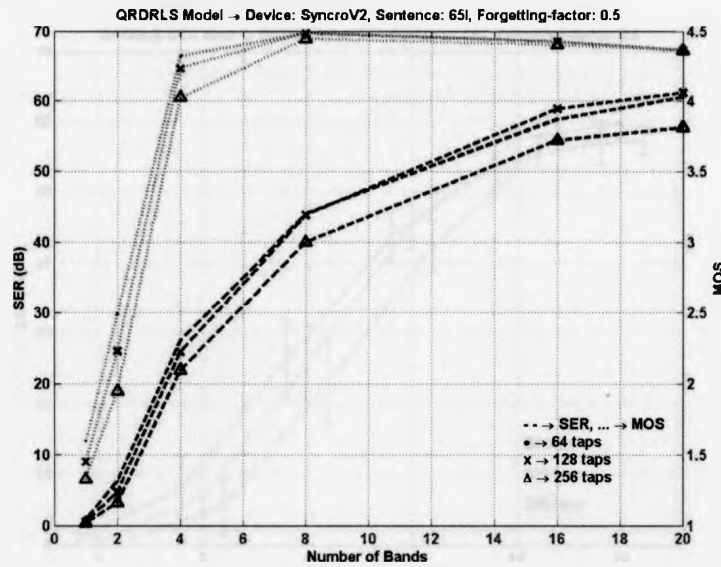


Fig. 5.14: QRD RLS Averaged SER and MOS, Audiogram I

SER means increase with the number of analysis bands and exhibit an asymptotic behaviour.

Variability decreases as the number of analysis bands increases.

Fig. 5.16 illustrates the SER mean and error bar for audiogram “I”. Like audiogram “F”, SER means increase and exhibit a slight asymptotic behaviour.

Variability appears to decrease across bands for both the 64 and 128 tap trends. However, variability increased for the 256 tap trend with additional increases in the number of bands.

Fig. 5.17 illustrates the MOS error mean and error bar for audiogram “F”.

MOS means increase with number of analysis bands. Asymptotic behaviour is present across all number of taps considered. However, there is a more pronounced plateau with higher band numbers. MOS means, for all tap values, converge to the upper limit of the MOS scale, 4.5 (best).

Variability decreases with increase in number of bands. However, for larger band

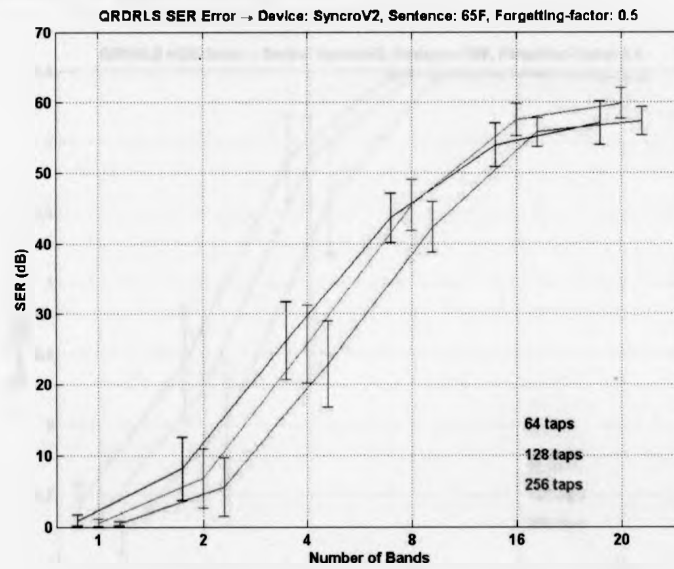


Fig. 5.15: QRD RLS SER Mean with Error Bar, Audiogram F

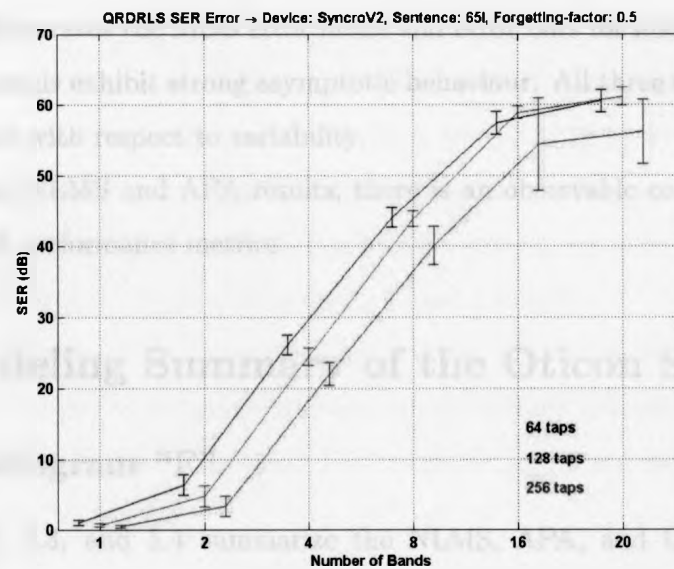


Fig. 5.16: QRD RLS SER Mean with Error Bar, Audiogram I

numbers, variability is significantly small.

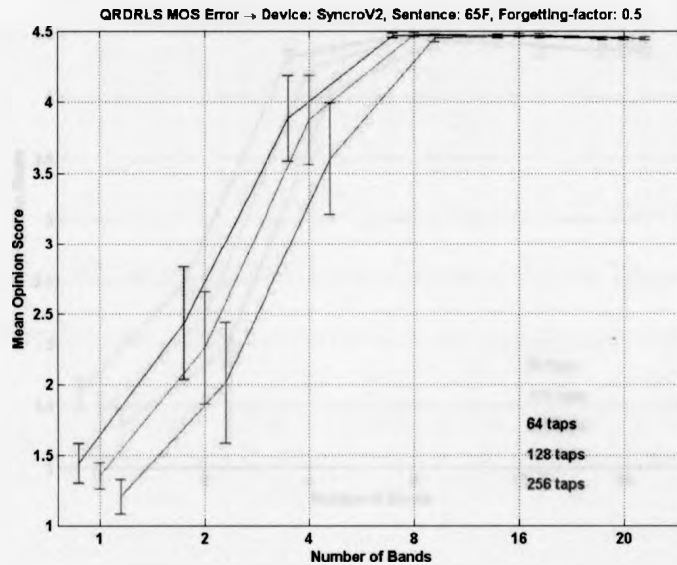


Fig. 5.17: QRD RLS MOS Mean with Error Bar, Audiogram F

Fig. 5.18 illustrates the MOS error mean and error bars for audiogram “I”.

All three trends exhibit strong asymptotic behaviour. All three trends exhibit the same behaviour with respect to variability.

As with the NLMS and APA results, there is an observable correlation between SER and MOS performance metrics.

## 5.2 Modeling Summary of the Oticon Syncro V2

### 5.2.1 Audiogram “F”

Tables 5.2, 5.3, and 5.4 summarize the NLMS, APA, and QRD RLS “best” modeling performance results.

As stated earlier, for the NLMS and APA algorithms, modeling performance improves with additional analysis bands for each considered number of taps. The QRD

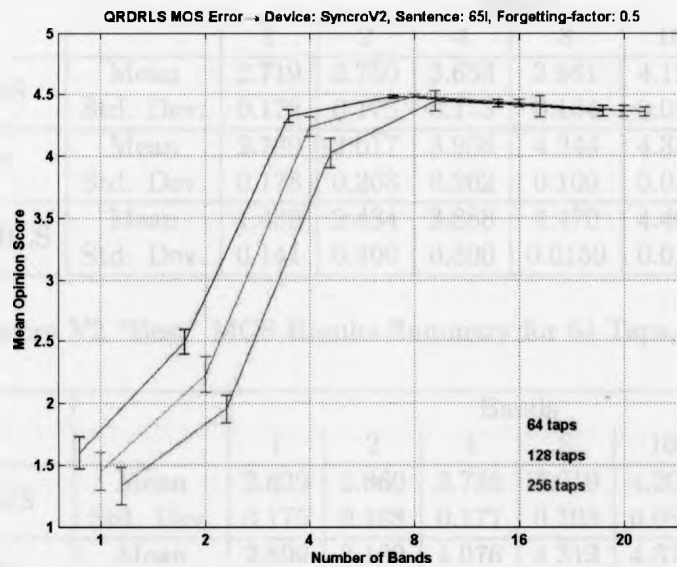


Fig. 5.18: QRD RLS MOS Mean with Error Bar, Audiogram I

RLS algorithm, on the other hand, shows, in general, an increase in MOS score from 1 to 8 bands, but then decreases with further increases to 16 and 20 bands.

For a fixed number of analysis bands, modeling performance increases with number of taps, with respect to the average MOS score, from NLMS to APA and finally the QRD RLS algorithm. For the QRD RLS algorithm this trend begins when the number of bands is 8 or greater. The QRD RLS algorithm has a lower mean MOS score than both the NLMS and APA algorithms for 1, 2, and 4 bands.

Standard deviations for 1, 2, and 4 bands, across algorithms and number of taps, are of the same order of magnitude. Standard deviations decrease with further increases in analysis bands. The QRD RLS exhibits significant decreases for larger number of bands.

		Bands					
		1	2	4	8	16	20
NLMS	Mean	2.719	2.750	3.653	3.961	4.184	4.217
	Std. Dev.	0.172	0.175	0.173	0.134	0.095	0.080
APA	Mean	2.789	3.017	3.966	4.244	4.332	4.349
	Std. Dev.	0.178	0.203	0.262	0.109	0.040	0.039
QRD RLS	Mean	1.439	2.434	3.888	4.470	4.468	4.450
	Std. Dev.	0.141	0.400	0.300	0.0159	0.011	0.010

Table 5.2: Syncro V2 “Best” MOS Results Summary for 64 Taps, Audiogram “F”

		Bands					
		1	2	4	8	16	20
NLMS	Mean	2.829	2.860	3.736	4.019	4.203	4.244
	Std. Dev.	0.175	0.188	0.177	0.103	0.084	0.075
APA	Mean	2.899	3.132	4.076	4.313	4.377	4.379
	Std. Dev.	0.195	0.189	0.251	0.075	0.028	0.021
QRD RLS	Mean	1.352	2.259	3.876	4.475	4.470	4.450
	Std. Dev.	0.093	0.398	0.313	0.014	0.012	0.009

Table 5.3: Syncro V2 “Best” MOS Results Summary for 128 Taps, Audiogram “F”

### 5.2.2 Audiogram “I”

Tables 5.5, 5.6 and 5.7 summarize the NLMS, APA, and QRD RLS “best” modeling performance results of the Syncro V2 in terms of MOS for 64, 128, and 256 taps, respectively. As stated previously, these were obtained by averaging the 10 HINT sentences.

For the NLMS algorithm, modeling performance improves with additional analysis bands for each considered number of taps. The APA algorithm demonstrates the same trend, but the average MOS value for 20 bands is smaller than the value at 16 bands. As with audiogram “F”, the QRD RLS algorithm shows, in general, an increase in MOS score from 1 to 8 bands, but then decreases with further increases to 16 and 20 bands.

For a fixed number of analysis bands, modeling performance increases with the

		Bands					
		1	2	4	8	16	20
NLMS	Mean	2.834	2.862	3.671	3.996	4.227	4.259
	Std. Dev.	0.181	0.192	0.156	0.104	0.082	0.072
APA	Mean	2.981	3.210	4.093	4.370	4.414	4.407
	Std. Dev.	0.194	0.183	0.252	0.045	0.023	0.014
QRD RLS	Mean	1.20088	2.00795	3.60266	4.45260	4.46910	4.45106
	Std. Dev.	0.121	0.430	0.393	0.025	0.012	0.009

Table 5.4: Syncro V2 “Best” MOS Results Summary for 256 Taps, Audiogram “F”

number of taps for the APA algorithm and, in general, the NLMS algorithm. For the QRD RLS algorithm, modeling performance decreases with an increase in the number of taps.

### 5.3 Fullband and Subband Model Summary

In order to compare modeling performance of the three adaptive algorithms across the five digital hearing aids, the parameters stated in Table 5.1, *Best Modeling Parameters*, are used in conjunction with results based on a 256-tap filter structure. Signal-to-error ratio (SER) and mean-opinion score (MOS) metrics are summarized for both audiogram data sets for a fullband and 20 band subband model.

		Bands					
		1	2	4	8	16	20
NLMS	Mean	3.520	3.535	3.805	3.778	4.056	4.138
	Std. Dev.	0.131	0.128	0.098	0.090	0.054	0.061
APA	Mean	3.518	3.573	4.055	4.245	4.340	4.306
	Std. Dev.	0.080	0.099	0.088	0.020	0.022	0.0372
QRD RLS	Mean	1.597	2.491	4.324	4.484	4.427	4.365
	Std. Dev.	0.130	0.101	0.050	0.013	0.0284	0.041

Table 5.5: Syncro V2 “Best” MOS Results Summary for 64 Taps, Audiogram “I”

		Bands					
		1	2	4	8	16	20
NLMS	Mean	3.698	3.705	3.876	3.882	4.017	4.104
	Std. Dev.	0.146	0.145	0.133	0.101	0.112	0.078
APA	Mean	3.669	3.743	4.129	4.3271	4.368	4.327
	Std. Dev.	0.135	0.152	0.107	0.021	0.026	0.035
QRD RLS	Mean	1.450	2.229	4.234	4.485	4.427	4.365
	Std. Dev.	0.153	0.144	0.078	0.014	0.028	0.041

Table 5.6: Syncro V2 "Best" MOS Results Summary for 128 Taps, Audiogram "I"

		Bands					
		1	2	4	8	16	20
NLMS	Mean	3.787	3.787	3.800	3.845	3.999	4.080
	Std. Dev.	0.173	0.170	0.118	0.098	0.131	0.122
APA	Mean	0.173	0.170	0.118	0.098	0.131	0.122
	Std. Dev.	0.198	0.222	0.146	0.055	0.023	0.034
QRD RLS	Mean	0.198	0.222	0.146	0.055	0.023	0.034
	Std. Dev.	0.149	0.112	0.119	0.083	0.085	0.039

Table 5.7: Syncro V2 "Best" MOS Results Summary for 256 Taps, Audiogram "I"

### 5.3.1 Subband Model

Results for audiogram "F" and audiogram "I" are presented in the next two sections.

#### 5.3.1.1 Audiogram "F"

Table 5.8 presents 20-band SER mean and standard deviation values obtained by averaging model responses for 10 HINT excitation sentences.

With respect to the adaptive algorithms, the QRD RLS algorithm had the largest SER, followed by the APA algorithm and finally the NLMS algorithm. This trend is consistent across the five hearing aids.

SER values for the Symbio 110 XT, Syncro V2, and the Perseo 311 dAZ Forte are approximately of the same order of magnitude for each respective adaptive algorithm.



SER values for the Triano S and Natura 2 SE are also of the same order of magnitude, but smaller compared to the previous three hearing aids.

Standard deviations are of the same order of magnitude across all five hearing aids and three algorithms.

		Symbio	Syncro	Perseo	Triano	Natura
NLMS	Mean	19.06	20.22	25.22	3.53	7.19
	Std. Dev.	2.08	1.87	1.68	1.41	2.80
APA	Mean	27.54	30.10	35.74	15.14	16.93
	Std. Dev.	3.43	3.21	0.87	2.60	2.68
QRD RLS	Mean	53.70	57.38	61.25	35.58	41.29
	Std. Dev.	2.94	1.98	1.58	2.86	3.60

Table 5.8: Modeling Comparison of all Instruments using 20 Band Subband Model SER Metric, Audiogram "F"

Table 5.9 presents the associated MOS mean and standard deviations for SER values presented in Table 5.8.

Similar to the SER results, the MOS value for the QRD RLS algorithm is the largest, followed by the APA and NLMS algorithms, respectively. This trend is consistent across the five hearing aids.

With respect to the adaptive algorithms, the NLMS algorithm has a larger range of MOS values across the five hearing aids. The smallest MOS value is 3.53, for the Triano S instrument, while the Perseo 311 dAZ Forte has the largest MOS value at 4.31. The range is approximately 0.73.

The range of averaged MOS values for the APA algorithm is approximately 0.15 and 0.04 for the QRD RLS algorithm.

Standard deviations are on the same order of magnitude.

#### 5.3.1.2 Audiogram "I"

Table 5.10 presents 20-band SER mean and standard deviations values.

With respect to the adaptive algorithms, the QRD RLS algorithm had the largest

		Symbio	Syncro	Perseo	Triano	Natura
NLMS	Mean	4.25	4.26	4.31	3.53	3.92
	Std. Dev.	0.10	0.07	0.03	0.27	0.13
APA	Mean	4.40	4.41	4.39	4.26	4.33
	Std. Dev.	0.02	0.01	0.02	0.11	0.03
QRD RLS	Mean	4.44	4.45	4.42	4.41	4.44
	Std. Dev.	0.02	0.01	0.03	0.01	0.02

Table 5.9: Modeling Comparison of all Instruments using 20 Band Subband Model MOS Metric, Audiogram "F"

SER, followed by the APA algorithm and finally the NLMS algorithm. This trend is consistent across the five hearing aids and identical to that found for audiogram "F".

SER values for the Symbio 110 XT, Syncro V2, and the Perseo 311 dAZ Forte are approximately of the same order of magnitude for each respective adaptive algorithm. SER values for the Triano S and Natura 2 SE are also of the same order of magnitude, but smaller compared to the previous three hearing aids.

Standard deviations are of the same order of magnitude across all five hearing aids and three algorithms.

		Symbio	Syncro	Perseo	Triano	Natura
NLMS	Mean	13.38	16.39	21.89	5.83	8.88
	Std. Dev.	1.08	1.05	2.26	1.77	1.75
APA	Mean	34.56	33.53	43.35	20.07	22.85
	Std. Dev.	1.32	1.12	1.46	1.94	0.89
QRD RLS	Mean	55.68	56.23	60.42	40.03	44.83
	Std. Dev.	2.25	4.61	4.36	2.95	1.61

Table 5.10: Modeling Comparison of all Instruments using 20 Band Subband Model SER Metric, Audiogram "I"

Table 5.11 presents the associated MOS mean and standard deviations for SER values in Table 5.10.

As with the SER results, the MOS value for the QRD RLS algorithm is the largest, followed by the APA and NLMS algorithms, respectively. This trend is consistent across the five hearing aids.

With respect to the adaptive algorithms, the NLMS algorithm has a larger range of MOS values across the five hearing aids. The smallest MOS value is 3.47, for the Triano S instrument, and the largest MOS value is 4.26, for the Perseo 311 dAZ Forte. The range is approximately 0.79.

The range of averaged MOS values for the APA algorithm is approximately 0.08 and 0.06 for the QRD RLS algorithm.

Standard deviations are of the same order of magnitude.

		Symbio	Syncro	Perseo	Triano	Natura
NLMS	Mean	3.64	4.08	4.26	3.47	3.72
	Std. Dev.	0.18	0.12	0.06	0.30	0.18
APA	Mean	4.34	4.35	4.36	4.29	4.28
	Std. Dev.	0.03	0.03	0.03	0.11	0.02
QRD RLS	Mean	4.37	4.36	4.36	4.42	4.38
	Std. Dev.	0.03	0.04	0.06	0.03	0.03

Table 5.11: Modeling Comparison of all Instruments using 20 Band Subband Model MOS Metric, Audiogram "I"

### 5.3.2 Fullband Model

Results for audiogram "F" and audiogram "I" are presented in the next two sections.

#### 5.3.2.1 Audiogram "F"

Table 5.12 presents fullband SER mean and standard deviation values obtained by averaging model responses for 10 HINT excitation sequences.

With respect to the adaptive algorithms, the APA algorithm had the largest SER values, followed by the NLMS algorithm and finally the QRD RLS algorithm. This trend is consistent across the five hearing aids.

SER values for the Symbio 110 XT and Syncro V2 are approximately of the same order of magnitude for each adaptive algorithm. SER values for the Triano S and

Natura 2 SE are of the same magnitude. The Perseo 311 dAZ Forte has the larger SER results.

Standard deviations are of the same order of magnitude across all five hearing aids for each respective algorithm.

		Symbio	Syncro	Perseo	Triano	Natura
NLMS	Mean	4.85	3.19	15.01	1.33	0.83
	Std. Dev.	3.34	2.96	1.61	0.35	1.45
APA	Mean	12.22	12.35	22.75	4.52	5.97
	Std. Dev.	5.62	4.72	1.27	2.68	2.52
QRD RLS	Mean	0.71	0.33	6.59	0.06	0.07
	Std. Dev.	0.92	0.30	1.58	0.06	0.10

Table 5.12: Modeling Comparison of all Instruments using Fullband Model SER Metric, Audiogram "F"

Table 5.13 presents the associated MOS mean and standard deviations for SER values presented in Table 5.12.

The MOS values for the Symbio XT 110, the Syncro V2, the Triano S, and the Natura 2 SE are of the same order of magnitude. The Perseo 311 dAZ Forte has the largest MOS value. These observations are present across the three algorithms.

Standard deviations are of the same order of magnitude across the five hearing aids and adaptive algorithms.

		Symbio	Syncro	Perseo	Triano	Natura
NLMS	Mean	2.88	2.83	4.06	3.60	3.66
	Std. Dev.	0.25	0.18	0.15	0.16	0.36
APA	Mean	3.11	2.98	4.25	3.30	3.58
	Std. Dev.	0.22	0.19	0.03	0.41	0.21
QRD RLS	Mean	1.33	1.20	2.32	1.18	1.63
	Std. Dev.	0.15	0.12	0.13	0.14	0.17

Table 5.13: Modeling Comparison of all Instruments using Fullband Model MOS Metric, Audiogram "F"

### 5.3.2.2 Audiogram "I"

Table 5.14 presents fullband SER mean and standard deviations values associated with audiogram "I".

As with the audiogram "F" results, the APA algorithm had the largest SER values, followed by the NLMS algorithm and finally the QRD RLS algorithm. This trend holds across the five hearing aids.

SER values are significantly different across the five hearing aids and algorithms.

Standard deviations are of the same order of magnitude across all five hearing aids and the adaptive algorithms.

		Symbio	Syncro	Perseo	Triano	Natura
NLMS	Mean	10.87	6.37	18.68	4.23	5.46
	Std. Dev.	1.14	1.21	1.32	0.86	0.54
APA	Mean	19.83	14.18	31.68	7.60	10.76
	Std. Dev.	2.49	2.00	1.89	2.67	1.34
QRD RLS	Mean	1.01	0.32	9.07	0.12	0.26
	Std. Dev.	0.58	0.18	1.84	0.11	0.10

Table 5.14: Modeling Comparison of all Instruments using Fullband Model SER Metric, Audiogram "I"

Table 5.15 presents the associated MOS mean and standard deviations for SER values presented in Table 5.14.

The MOS values are of the same order of magnitude across the five hearing aids for the NLMS and APA results. The QRD RLS MOS values are lower.

Standard deviations are of the same order of magnitude across the five hearing aids and adaptive algorithms.

## 5.4 Summary

Fullband and subband modeling results for the Oticon Syncro V2 hearing aid were presented using the NLMS, APA, and QRD RLS parameters yielding the largest

		Symbio	Syncro	Perseo	Triano	Natura
NLMS	Mean	3.32	3.79	4.05	3.50	3.58
	Std. Dev.	0.13	0.17	0.13	0.19	0.19
APA	Mean	3.60	3.68	4.28	3.38	3.82
	Std. Dev.	0.23	0.20	0.04	0.37	0.20
QRD RLS	Mean	1.26	1.33	2.15	1.18	1.81
	Std. Dev.	0.10	0.15	0.12	0.12	0.14

Table 5.15: Modeling Comparison of all Instruments using Fullband Model MOS Metric, Audiogram "I"

signal-to-error ratio (SER). Corresponding PESQ MOS scores were also presented.

Plots of SER and MOS values as a function of the number of analysis bands demonstrated linear to strong asymptotic behaviour. With poorer modeling performance, as demonstrated by the NLMS algorithm, there was a lower degree of correlation between these two trends. The APA and QRD-RLS algorithms demonstrated higher degrees of correlation. However, with larger number of analysis bands, PESQ MOS scores decreased with additional increases in the number of analysis bands for these two algorithms.

A 20-band subband model had larger SER and MOS values than a fullband model. This increase was consistent across the adaptive algorithms.

## Chapter 6

# Discussion, Conclusions, and Future Work

In this thesis, the application of a uniform subband adaptive model to characterize the compression behaviour of five digital hearing aids has been examined. The motivation for this research is to advance the work done by (24) and (30) in the application of objective measures, like the PESQ mean-opinion score (MOS), to predict subjective assessments of speech quality. It is hoped this research will lead to a timely and reliable clinical test procedure facilitating an appropriate ranking of hearing aids based on speech quality for a given sensorineural hearing loss.

### 6.1 Discussion

Results of this research confirm that a subband adaptive model is able to successfully characterize compression behaviour of a set of digital hearing aids taken from the current market. Expanding on the results found by (30), the subband model outperforms its equivalent fullband implementation.

With an appropriate level of modeling performance, it was possible to successfully apply the PESQ mean-opinion score. Preliminary results suggest this approach holds

the potential to rank hearing instruments based on the quality of speech processed by these devices.

The three adaptive algorithms examined demonstrated defined levels of performance that were commensurate with their theoretical basis. General comments of these algorithms are made.

### 6.1.1 Subband Model Versus Fullband Model

Under all of the conditions examined in this research and the five hearing aids considered, subband modeling outperformed an equivalent fullband model. To understand the underlying reason for this result, we can look at a specific modeling example and compare the error residues of a subband and fullband model.

Considering the APA algorithm with a step-size of 1.0, a projection-order of 15, and 64 taps, we can plot the time-varying spectral content for both models using a single HINT sentence. Fig. 6.1(a) illustrates the Bark spectrogram of the HINT 1-1 sentence, *"A boy fell from the window."*, which was one of the ten HINT sentences.

Fig. 6.1(b) illustrates the Bark spectrogram of the measured 2cc coupler Synchro V2 response for audiogram "F". This figure shows the gain applied to higher frequencies in addition to the noise added by the hearing aid.

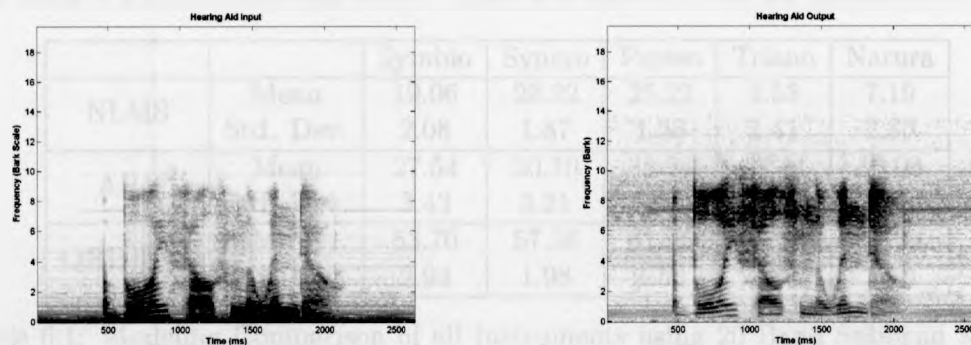
Fig. 6.1(c) illustrates the error residue of a fullband model. The fullband structure is not able to model a significant portion of the speech and noise components.

Fig. 6.1(d) illustrates the error residue of a 20-band uniform subband model. It is readily apparent that the subband model provides a better estimate of the measured hearing aid response.

### 6.1.2 Deviations on Subband Modeling Performance

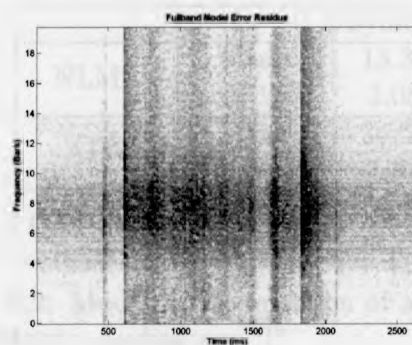
In general, characterization of compression behaviour improved with additional increases in the number of analysis bands. Linear to moderate-to-strong asymptotic



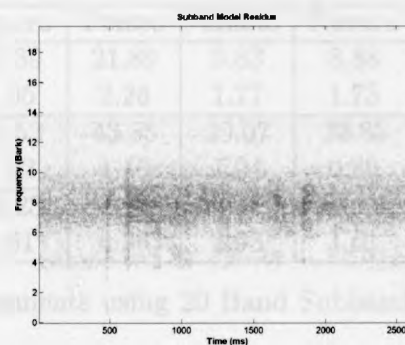


(a) Hearing Aid Input

(b) Hearing Aid Output



(c) Fullband Model Error



(d) Subband Model Error

Fig. 6.1: Bark Spectrograms

SER trends were observed (associated with NLMS, APA, and QRD RLS algorithms, respectively) for algorithm parameters considered. However, characterization of the Siemens Triano S and Sonic Innovations Natura 2 SE instruments was less effective as indicated by lower overall SER values for both audiograms, as noted in Table 6.1 and Table 6.2 for the 20-band model. These are repeated here for convenience.

		Symbio	Syncro	Perseo	Triano	Natura
NLMS	Mean	19.06	20.22	25.22	3.53	7.19
	Std. Dev.	2.08	1.87	1.68	1.41	2.80
APA	Mean	27.54	30.10	35.74	15.14	16.93
	Std. Dev.	3.43	3.21	0.87	2.60	2.68
QRD RLS	Mean	53.70	57.38	61.25	35.58	41.29
	Std. Dev.	2.94	1.98	1.58	2.86	3.60

Table 6.1: Modeling Comparison of all Instruments using 20 Band Subband Model SER Metric, Audiogram "F"

		Symbio	Syncro	Perseo	Triano	Natura
NLMS	Mean	13.38	16.39	21.89	5.83	8.88
	Std. Dev.	1.08	1.05	2.26	1.77	1.75
APA	Mean	34.56	33.53	43.35	20.07	22.85
	Std. Dev.	1.32	1.12	1.46	1.94	0.89
QRD RLS	Mean	55.68	56.23	60.42	40.03	44.83
	Std. Dev.	2.25	4.61	4.36	2.95	1.61

Table 6.2: Modeling Comparison of all Instruments using 20 Band Subband Model SER Metric, Audiogram "I"

With the range of hearing aid complexity examined and the large SER values associated with the other three devices, it is not readily known why SER results for the Triano and Natura devices are lower. It was originally thought that the application of audiograms with thresholds falling outside the manufacturer's suggested fitting region for these devices was the root of the problem. However, three devices had thresholds outside their respective fitting regions illustrated in Appendix A, *Hearing Aid Specifications*.

One possible explanation for the low SER values for the Triano and Natura devices

are the small attack and release time constants shown in Table 4.2. As shown by the tracking analysis of Chapter 2, modeling performance is not as good for small time constants due to the inability of the adaptive algorithms to track significant signal changes. Despite the overall lower SER values, the MOS scores do not appear to be influenced, suggesting this does not impact spectral cues important to the PESQ perceptual model.

Several aspects associated with hearing aid performance and methodologies were also examined in efforts to find possible explanations for this observation.

#### 6.1.2.1 ANSI S3.22 (2003) Test Results

With respect to hearing aid performance, each instrument (programmed using a “first-fit” option based on the DSL[i/o] fitting method and audiograms “F” and “I”) had a set of standard ANSI S3.22 (2003) [ANSIS3.22] tests run to verify operation. These included,

- Section 6.2, *OSPL90 Curve*, of Section 6, *Recommend Measurements, Specifications, and Tolerances*.
- Section 6.7, *Reference Test Gain*
- Section 6.11, *Harmonic Distortion*
- Section 6.12, *Equivalent Input Noise Level*
- Section 6.15.1, *Input-Output Characteristics*

Appendix B, *ANSI S3.22 (2003) Test Results*, illustrates results for all five devices. Because these results were not obtained using the manufacturer’s specific configuration, it is not possible to make a direct comparison between them and the respective data-sheet results. However, it possible to suggest each device, as programmed, was working in an expected manner. No significant anomalies were observed.

#### 6.1.2.2 Methodology

The methodology used to collect and model hearing aid recordings was standardized across all five hearing aids. Unless an inherent aspect of this process was the root of poor modeling of the Triano S and Natura 2 SE instruments, this process is likely not to be the source of the issue.

Reference and 2cc coupler recordings for all five devices were verified to ensure to potential artefacts, like clipping, were not present.

Further review is required.

#### 6.1.3 PESQ Mean Opinion Score

Based on the data collected so far, it is not possible to comment fully on the potential success of the PESQ mean-opinion score (MOS) to assess hearing aid speech quality when used in the subband model-based framework investigated in this research. Comments are made with respect to its relationship to the signal-to-error ratio (SER), its potential to differentiate between the five hearing aids based on a preliminary one-way ANOVA analysis of data, and possible limitations with its application based on the context of this work and future advances in hearing aid technology.

##### 6.1.3.1 MOS Correlation with SER

With review of the SER-MOS plots of Section 5.1, *General Modeling Performance of the Oticon Syncro V2*, and those of the other four hearing aids presented in Appendix C, *Modeling Results*, it appears a certain, consistent level of modeling performance must occur before MOS trends correlates more closely with their respective asymptotic SER trends. Inadequate or inconsistent modeling performance, as indicated by the NLMS algorithm, or over-modeling performance, as indicated by the QRD RLS algorithm, degrades the level of correlation.

## NLMS

Fig. 5.1, *NLMS Averaged SER and MOS, Audiogram F*, shows a good correlation (for a step-size of 1.0) between the SER and MOS trends for the Oticon Syncro V2. However, Fig. 5.2, *NLMS Average SER and MOS, Audiogram I*, illustrates a lower level of correlation. With the application of audiogram I, more compression is applied to the speech sequences used to excite the hearing aids. The NLMS algorithm was not able to model this behaviour as it did for the type F audiogram, even with a maximum step-size of 1.

With the use of its best modeling parameters, a step-size of 1.0, the NLMS algorithm was not able to produce well-defined asymptotic trends for both SER and MOS metrics. Other step-sizes were not able to provide adequate modeling performance as indicated by the linear to weak asymptotic SER and MOS trends.

## APA

Fig. 5.7, *APA Averaged SER and MOS, Audiogram F* and Fig. 5.8, *APA Averaged SER and MOS, Audiogram I*, show good correlation (for a projection-order of 15 and step-size of 1.0) between the SER and MOS trends for the Oticon Syncro V2. Unlike the NLMS algorithm, the APA algorithm was able to model both audiogram conditions successfully.

With the use of its best modeling parameters, a projection-order of 15 and a step-size of 1.0, the APA algorithm produced moderate to strong asymptotic trends for both SER and MOS metrics across all hearing aids for all of the conditions considered.

On a portion of the MOS trends it was observed that the average MOS values decreased with a larger number of analysis bands. Fig. 6.2 illustrates this behaviour for the Syncro V2 instrument.

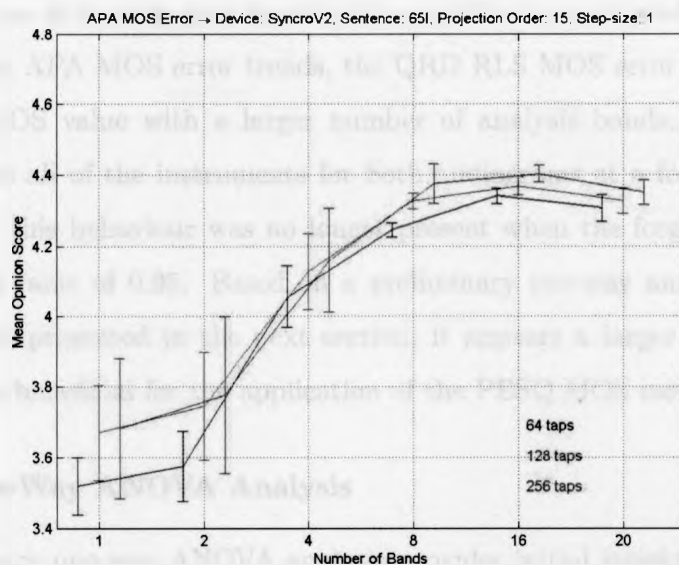


Fig. 6.2: APA MOS Mean with Error Bar, Audiogram “F”

This behaviour was not observed on a consistent basis across all of the hearing aids. It was observed for the Syncro V2, Natura 2 SE, and the Perseo 311 dAZ Forte (most pronounced), not the Triano S and Symbio 110 XT. It appears this behaviour may be associated with the band structure of the device in question.

The Natura 2 SE and the Perseo 311 dAZ Forte devices use a band structure based on critical bands. Unlike these instruments, the Triano S makes use of a uniform band structure, the Syncro V2 a non-uniform structure, while the Symbio 110 XT has no frequency-based, band structure.

## QRD RLS

Fig. 5.13, *QRD RLS Averaged SER and MOS, Audiogram F* and Fig. 5.14, *QRD RLS Averaged SER and MOS, Audiogram I*, show strong correlation (for a forgetting-factor of 0.5) between the SER and MOS trends. Like the APA algorithm, SER and MOS trends were highly correlated and demonstrate moderate to strong asymptotic

behaviour across all hearing aids for all of the conditions considered.

As with the APA MOS error trends, the QRD RLS MOS error trends decreased in averaged MOS value with a larger number of analysis bands. This behaviour occurred across all of the instruments for both audiograms at a forgetting-factor of 0.5. However, this behaviour was no longer present when the forgetting-factor was increased to a value of 0.95. Based on a preliminary one-way analysis of variance (ANOVA) test, presented in the next section, it appears a larger forgetting factor might be more beneficial for the application of the PESQ MOS metric.

#### **6.1.3.2 One-Way ANOVA Analysis**

A preliminary one-way ANOVA analysis provides initial insights to the possible benefits of this model-based assessment of speech quality. In this section results from this test will be presented for each adaptive algorithm. Best modeling parameters for both the NLMS and APA algorithms will be considered. Best modeling parameters for the QRD RLS algorithm will also be considered, but the analysis will also include the largest forgetting-factor used (0.95).

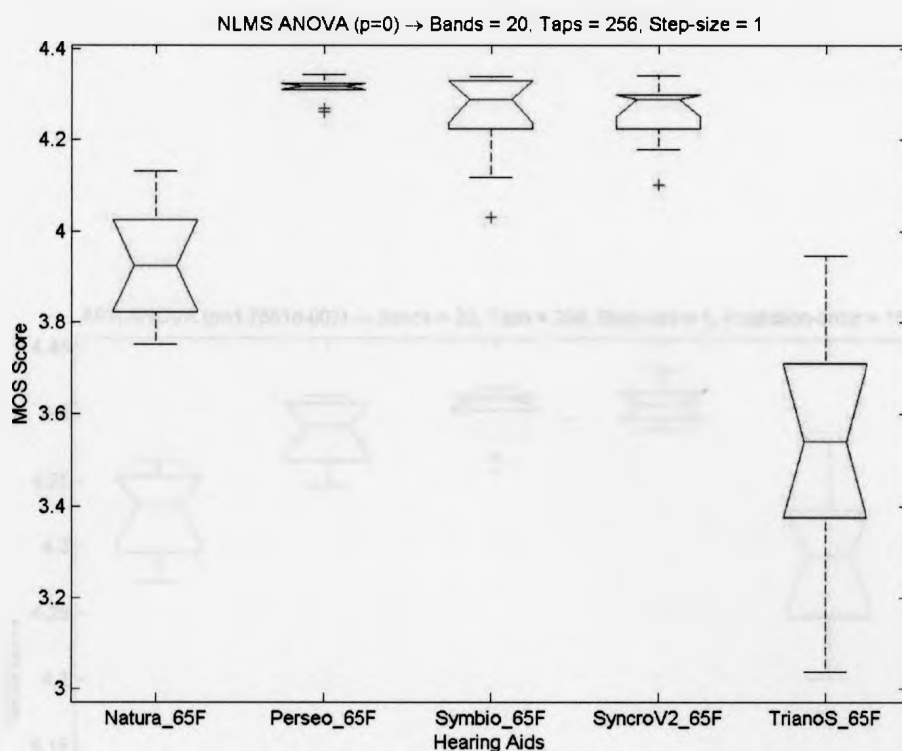


Fig. 6.3: NLMS One-Way ANOVA (20 Bands, 256 Taps, Step-size of 1.0)

Fig. 6.3 illustrates the one-way ANOVA results for the NLMS algorithm using the best modeling parameters for audiogram “F”. Fig. 6.4 illustrates the one-way ANOVA results for the APA algorithm using the best modeling parameters for audiogram “F”. Fig. 6.5 illustrate the one-way ANOVA results for the QRD RLS algorithm using the best modeling parameters for audiogram “F”.



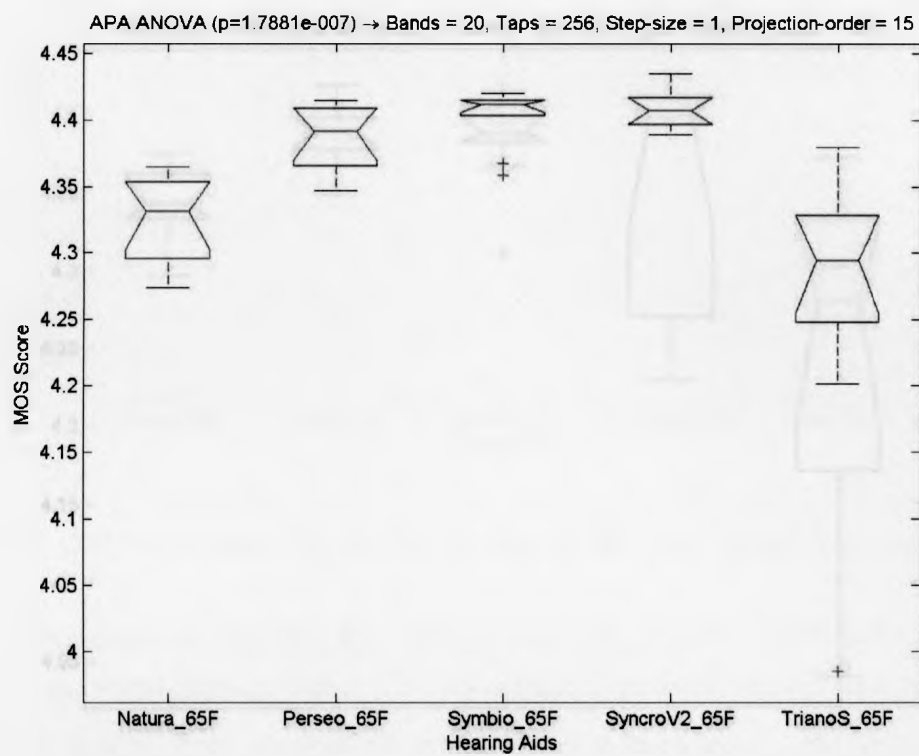


Fig. 6.4: APA One-Way ANOVA (20 Bands, 256 Taps, Step-size of 1.0, Projection-order of 15)

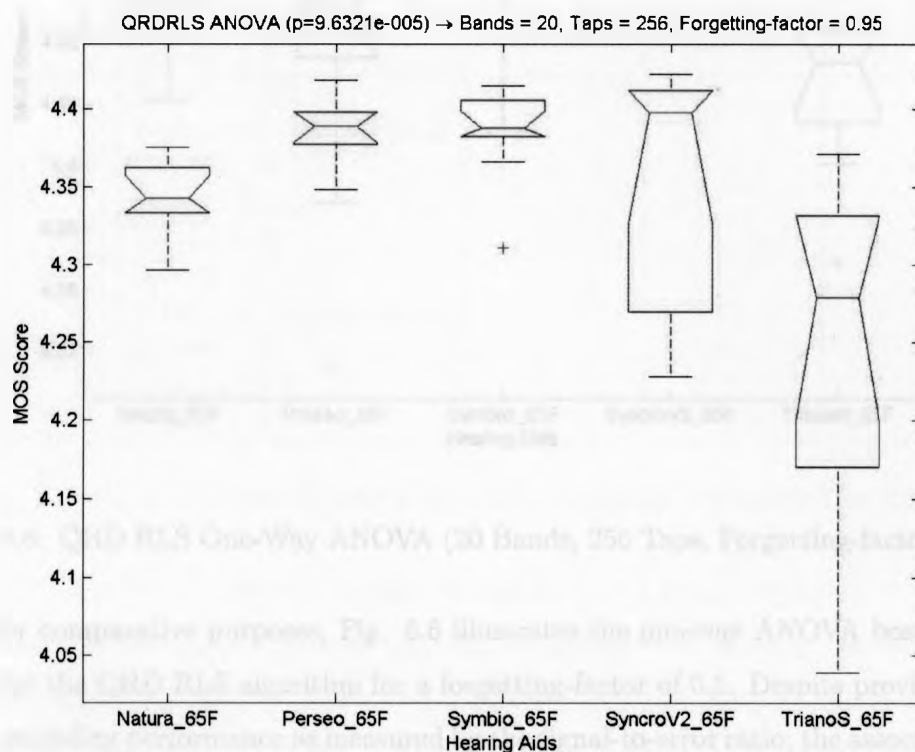


Fig. 6.5: QRD RLS One-Way ANOVA (20 Bands, 256 Taps, Forgetting-factor of 0.95)

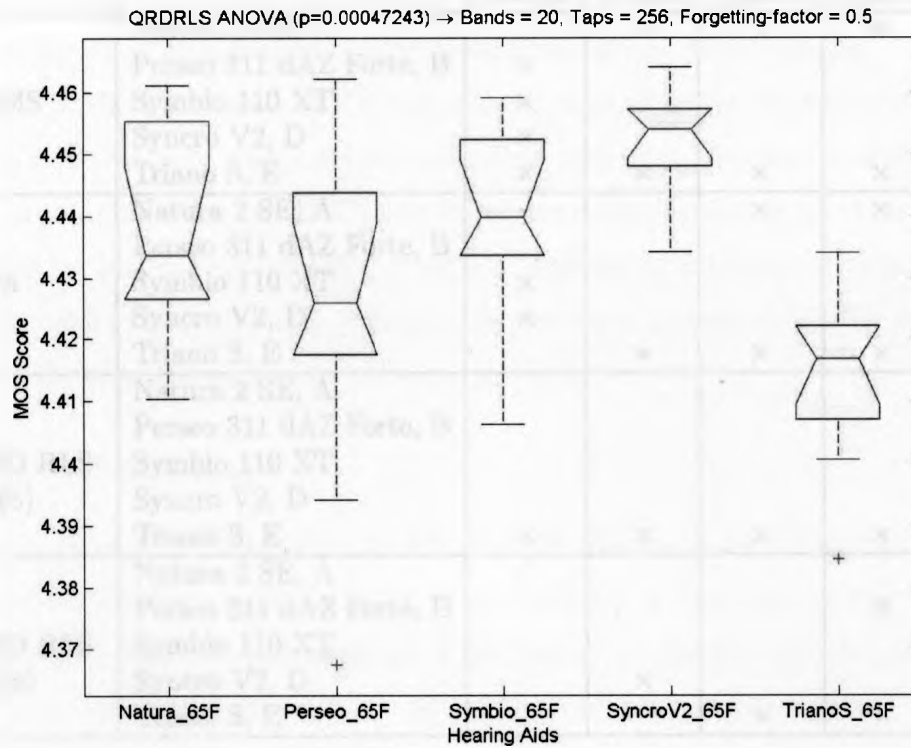


Fig. 6.6: QRD RLS One-Way ANOVA (20 Bands, 256 Taps, Forgetting-factor of 0.5)

For comparative purposes, Fig. 6.6 illustrates the one-way ANOVA box-whisker plot for the QRD RLS algorithm for a forgetting-factor of 0.5. Despite providing the best modeling performance as measured by the signal-to-error ratio, the associated decrease in mean and variability of the respective MOS scores (with additional analysis bands) appears to influence the ability to differentiate between the five instruments.

For all three algorithms the  $p$ -value was less than 0.05, indicating significant differences of the mean MOS scores across the five hearing aids. Tukey's Honestly Significant Difference criterion was applied to determine the significant differences in mean MOS score across the five hearing aids. Table 6.3 summarizes these results.

These results suggest the NLMS, APA, and QRD RLS (forgetting-factor of 0.95) algorithms might be able to differentiate between the five hearing aids.

		Natura	Perseo	Symbio	Syncro	Triano
NLMS	Natura 2 SE, A		×	×	×	×
	Perseo 311 dAZ Forte, B	×				×
	Symbio 110 XT	×				×
	Syncro V2, D	×				×
	Triano S, E	×	×	×	×	
APA	Natura 2 SE, A			×	×	
	Perseo 311 dAZ Forte, B					×
	Symbio 110 XT	×				×
	Syncro V2, D	×				×
	Triano S, E		×	×	×	
QRD RLS (0.95)	Natura 2 SE, A					×
	Perseo 311 dAZ Forte, B					×
	Symbio 110 XT					×
	Syncro V2, D					×
	Triano S, E	×	×	×	×	
QRD RLS (0.50)	Natura 2 SE, A				×	
	Perseo 311 dAZ Forte, B					×
	Symbio 110 XT					×
	Syncro V2, D		×			×
	Triano S, E			×	×	

Table 6.3: Results of Tukey's Honestly Significant Difference Criterion

The QRD RLS multiple comparison results with a forgetting-factor of 0.5 show fewer significant mean differences than the other three sets of data. Unlike the SER metric, which increased in value with a larger number of analysis bands, the MOS scores saturated near the upper 4.5 limit. This suggests that the PESQ MOS score is not able to discriminate between these modeled sequences. However, confirmation is not possible without subjective data and analysis. This idea requires further investigation.

### 6.1.3.3 Limitations

As indicated in (22), Section 8, *Preparation of Processed Speech Material*, key temporal and spectral properties of speech must be present in order to give meaningful

results. The choice of speech signals must also represent the temporal structure (including silent intervals) and phonetic structure of real speech signals.

The 10 HINT sentences used in this research meet these two conditions are limited in the fact that only a male speaker sequences were used. For proper application of the metric, (22) recommends a minimum of two male talkers and two female talkers be used for each testing condition. This is in addition to guidelines given in Clause 7 of the P.830 ITU-T standard, *Subjective Performance Assessment of Telephone-band and Wide-band Digital Codecs*" (February, 1996).

#### **6.1.3.4 Conclusions**

Preliminary results suggest the PESQ MOS objective measure applied within a subband model framework has potential to rank hearing aids based on speech quality assessment. However, consideration of the limitations noted in the last section, in addition to subjective data collection and its analysis, are required to confirm its successful application.

#### **6.1.4 General Comments on Algorithm Performance**

The basis of derivation directly impacts an adaptive algorithm's ability to perform in a given statistical environment. In this research, a complex non-stationary statistical environment is established with the application of speech sequences to excite hearing aids whose application of compression is dependent on the time varying spectral intensity of the speech signal. In light of the results presented in Chapter 4, this section makes general comments on the performance of the Normalized Least Mean-Squares, the Affine Projection, and QRD Recursive Least-Squares algorithms.

#### 6.1.4.1 Normalized Least Mean-Squares (NLMS)

As noted in Chapter 3, *Adaptive Algorithms*, updates to the tap-weights are based on a normalized corrected instantaneous estimate of the steepest descent gradient. Without the consideration of information from prior samples, the NLMS algorithm is not suitable to modeling environments with significant statistical variations with time. Results found in this research support this statement.

The following generalizations, made from NLMS modeling results presented in Appendix C, Section 1, *Normalized Least Mean Squares*, can be made. These include,

- Both the mean SER and mean MOS metric values, plotted as a function of the number of analysis bands, demonstrated linear to weak asymptotic behaviour with SER values no larger than approximately 20 dB.
- Significant variability in MOS metric value with respect to the number of analysis bands. This suggests adequate modeling was not occurring.
- In general, the degree of modeling performance was not directly associated with the number of taps or weights of the finite-impulse response transversal filter.
- Step-size had a weak to moderate impact on modeling performance.

Despite the poor modeling performance (based on SER values) and the limited number of speech sequences and audiograms applied, the one-way ANOVA results suggest it might be possible to use the NLMS algorithm in conjunction with PESQ MOS. Further work is required to confirm this point.

#### 6.1.4.2 Affine Projection Algorithm (APA)

Unlike the NLMS algorithm, the APA algorithm extracts information from a set of prior samples to obtain more accurate approximations of the autocorrelation matrix of the tap inputs,  $R_x$ , and the cross-correlation between tap inputs and the desired

sequence,  $R_{dx}$ . Because of this data re-use property, the APA algorithm demonstrated better overall modeling performance.

As with the NLMS algorithm, several generalizations based on modeling results can be made. The include,

- Both the mean SER and mean MOS metric values, plotted as a function of the number of analysis bands, demonstrated moderate to strong asymptotic behaviour.
- In general, variability of the MOS metric value decreased with increases in the number of analysis bands. This suggests adequate modeling was occurring.
- In general, the degree of modeling performance increased with the number of taps or weights of the finite-impulse response transversal filter.

APA modeling results are presented in Appendix C, Section 2, *Affine Projection Algorithm*.

#### 6.1.4.3 QR-Decomposition Recursive Least Squares (QRD RLS)

Initial application of the conventional RLS algorithm failed due to the almost immediate occurrence of an ill-conditioned state of the input covariance matrix. This condition was observed for all pairs of reference and desired sequence sets applied to the adaptive filters of the subband adaptive model.

To address this numerical instability, a more robust, numerically stable RLS implementation was applied. The QR-decomposition RLS (QRD-RLS) algorithm (46), (47), a square-root variant, was implemented.

Generalizations for this algorithm include,

- Both the mean SER and mean MOS metric values, plotted as a function of the number of analysis bands, demonstrated moderate to strong asymptotic behaviour.

- In general, variability of the SER metric, and associated MOS metric, decreased with increases in the number of analysis bands. Like the APA algorithm, this suggests adequate modeling was occurring.

QRD-RLS modeling results are presented in Appendix C, Section 3, *QR-Decomposition Recursive Least Squares*.

## 6.2 Conclusions

From the Bernafon Symbio XT 110, using time-domain processing via the Continuously Adaptive Speech Integrity process, to the Phonak Perseo 311 dAZ Forte, using frequency-domain processing in 20 bands, the applied technologies used by hearing aid manufacturer's is diverse and complex. However, despite these significant differences, a uniform subband linear adaptive model is capable of successfully characterizing complex compression behaviour.

Preliminary results suggest it may be possible to rank hearing aids using speech quality through application of objective measures of speech quality found in other research areas. These measures are well researched and have a high level of correlation to costly subjective assessments of speech quality. The PESQ mean-opinion score, applied extensively in the field of telecommunications, appears to hold promise in its ability to rank hearing aids in light of the preliminary one-way ANOVA results. However, it is not possible draw any conclusion without subject assessment and determination of any underlying correlations.

It appears a range of modeling performance must be in place for the application of an objective measure to be successful. In the context of this work, the NLMS algorithm under-modeled compression behaviour, while the QRD RLS algorithm, with smaller forgetting-factors, over-modeled it. The APA algorithm offers the most robust behaviour, confirming the work of (30; 24).



## 6.3 Future Work

By establishing a framework to support further investigation of objective measures and linear adaptive algorithms (and their non-linear counterparts) and confirmation of the work by (30), future work in this area holds promise for the realization of a clinical test to aid in the selection of hearing instruments most appropriate for a patient.

Several problems need to be solved by the next round of research. These include,

- A multi-dimensional analysis-of-variance should be conducted to investigate sources of variability for the SER and PESQ MOS scores. Dimensions should include the number of analysis bands, APA and QRD RLS algorithm parameters, and the number of taps used in the transversal filter structure.
- Assess modeling performance associated with a broadening of the speech excitation sequences. This research used only ten, male-talker HINT sentences
- Subjective assessments by impaired and healthy hearing individuals should be completed. Work is presently underway to collect and analyze data by Dr. Parsa's research group. This data will investigate possible correlations with the results provided by the experimental approach outlined in this thesis.

If the solutions to the above problems warrant continued work, several less critical questions and process refinements could be addressed and implemented, respectively. These items could include,

- Despite the increased complexity in implementation, refinements to the subband model, which might include the use poly-phase filter bank structures, would help minimize processing time. A fast and easy analysis tool would be more readily acceptable in a clinical environment.

- Research by (35; 34; 33) might improve modeling performance through the application of time-varying, non-uniform analysis filter banks. This would include the use of one-third octave bands to more closely model the critical bands of the cochlea.
- The introduction of noise to the speech sentences used to excite the hearing aids to determine the robustness of this methodology.
- Further investigation of Kates' Processing Type (27) using a swept-tone with broadband noise excitation.
- Investigate the effects of turning on other common complex hearing aid processing features like digital noise reduction, directional processing, and feedback cancelation on modeling behavior.

## References

- [1] B. Farhang-Boroujeny, *Adaptive Filters, Theory and Applications*. John Wiley & Sons, 1998.
- [2] J. Pickles, *An Introduction to the Physiology of Hearing*. Academic Press, 1998.
- [3] T. H. Venema, *Compression for Clinicians*. Singular Publishing Group Inc., 1998.
- [4] M. Killion, "The sin report: Circuits haven't solved the hearing-in-noise problem," *The Hearing Journal*, vol. 50, no. 10, pp. 28-34, 1997.
- [5] C. Berlin, "When outer hair cells fail, use correct circuitry to simulate their function," *Hearing Journal*, vol. 30, no. 4, p. 43, 1994.
- [6] H. Fletcher and W. Munson, "Loudness, its definition, measurement and calculation," *Journal of the Acoustical society of America*, vol. 5, pp. 82-108, 1933.
- [7] J. Agnew, *Hearing Aids - Standards, Options, and Limitations*, second edition ed. New York: Thieme Medical Publishers Inc., 2002, ch. Amplifiers and Circuit Algorithms for Contemporary Hearing Aids, pp. 116-130.
- [8] H. Dillon, *Compression in Hearing Aids, In: Sandlin RE, ed. Handbook of Hearing Aid Amplification*. Boston: College Hill Press, 1988, vol. Volume 1: Theoretical and Technical Considerations, pages 121-145.
- [9] M. Hansen, "Effects of multi-channel compression time constants on subjectively perceived sound quality and speech intelligibility," *Ear and Hearing*, vol. 23, no. 4, pp. 369-380, Aug. 2002.
- [10] F. K. Kuk, *Hearing Aids - Standards, Options, and Limitations*, second edition ed. New York: Thieme Medical Publishers Inc., 2002, ch. Considerations in Modern Multichannel Nonlinear Hearing Aids, pp. 178-213.

- [11] P. P. Vaidyanathan, *Multirate Systems and Filter Banks*. Englewood Cliffs, NJ: Prentice Hall, 1993.
- [12] A. Boothroyd, N. Springer, L. Smith, and J. Schulman, "Amplitude compression and profound hearing loss," *Journal of Speech and Hearing Research*, vol. 31, pp. 362-376, 1998.
- [13] M. Valente, *Hearing Aids: Standards, Options, and Limitations*, second edition ed. New York: Thieme Medical Publishers Inc., 2002, ch. Considerations in Modern Multichannel Nonlinear Hearing Aids, pp. 178-213.
- [14] M. Ruggero and N. Rich, "Furosemide alters organ of corti mechanics: evidence for feedback of outer hair cells upon the basilar membrane," *Journal of Neuroscience*, vol. 11, no. 1057-1067, 1991.
- [15] H. Dillon, "Compression? yes, but for low and high frequencies, for low or high intensities, and with what response times?" *Ear and Hearing*, vol. 17, no. 4, pp. 287-307, 1996.
- [16] G. Frye, "Understanding the ansi standard," *The Hearing Review*, vol. 12, no. 5, pp. 22-27, May 2005.
- [17] A. S3.22, *Specification of Hearing Aid Characteristics*, in ansi s3.22 ed., A. N. S. Institute, Ed. New York: ANSI, 2003.
- [18] J. M. Kates, "Cross-correlation procedures for measuring noise and distortion in age hearing aids," *Journal of Acoustical Society of America*, vol. 107, June 2000.
- [19] J. Kates, "On using coherence to measure distortion in hearing aids," *Journal of the Acoustical society of America*, vol. 91, pp. 2236-2244, 1992.
- [20] J. M. Kates and K. H. Arehart, "A metric for evaluating speech intelligibility and quality in hearing aids," *Journal of the American Acoustical Society*, vol. 116, pp. 2536-2537, 2004.

- [21] J. M. Kates and K. Archart, "Coherence and the speech intelligibility index," *Journal of the American Acoustical Society*, vol. 117, pp. 2224–2237, 2005.
- [22] *ITU-T Recommendation*. International Telecommunications Union, 2001, ch. Perceptual Evaluation of Speech Quality (PESQ), an Objective Method for End-to-end Speech Quality Assessment of Narrowband Telephone Networks and Speech CODECS, p. 862.
- [23] S. Quackenbush, T. B. III, and M. Clements, *Objective Measures of Speech Quality*. Englewood Cliffs, New Jersey: Prentice Hall, 1988.
- [24] V. Parsa and D. G. Jamieson, "Hearing aid distortion measurement using the auditory distance parameter," *Audio Engineering Society Convention Paper, 111th Convention, New York*, 2001.
- [25] *ITU-T Recommendation*. International Telecommunications Union, 1996c, ch. Objective Quality Measurement of Telephone-band (300 - 3400 Hz) Speech CODECS, p. 861.
- [26] M. R. Wirtzfeld and V. Parsa, "On subband adaptive modelling of compression hearing aids," *IEEE International Conference on Acoustics, Speech, and Signal Processing, Philadelphia, PA, March 18-23*, vol. 3, pp. 45–48, 2005.
- [27] J. M. Kates, "A test suite for hearing aid evaluation," *Journal of Rehabilitation Research and Development*, vol. 27, no. 3, pp. 255–278, 1990.
- [28] G. C. Goodwin and K. S. Sin, *Adaptive Filtering, Predication, and Control*. Englewood Cliffs, New Jersey 07632: Prentice-Hall, Inc, 1994.
- [29] M. Niedzwiecki, *Identification of Time-varying Processes*. John Wiley & Sons Ltd., 2000.

- [30] V. Parsa and D. Jamieson, "Adaptive modeling of digital hearing aids using a subband affine projection algorithm," *IEEE International Conference on Acoustics, Speech, and Signal Processing, ICASSP 2002 Proceedings*, vol. 2, pp. 1937–1940, 2002.
- [31] M. Hayes, *Statistical Digital Signal Processing and Modeling*. John Wiley & Sons Ltd., 1996.
- [32] Y. Ichikawa and T. Furukawa, "A new approach for non-uniform subband adaptive filtering," *IEEE International Symposium on Circuits and Systems, ISCAS 2005 Proceedings*, vol. 3, pp. 2271–2274, 2005.
- [33] M. McCloud and D. Etter, "A technique for nonuniform subband adaptive filtering with varying bandwidth filter banks," *IEEE International Conference on Acoustics, Speech, and Signal Processing, ICASSP 1997 Proceedings*, vol. 3, pp. 21–24, 1997.
- [34] J. Griesbach, "Non-uniform subband adaptive filters for system modeling," Ph.D. dissertation, University of Colorado, 2000.
- [35] J. Griesbach, M. Lightner, and D. Etter, "Mean square error analysis of nonuniform subband adaptive filters for system modeling," *Signal Processing, IEEE Transactions on Acoustics, Speech, and Signal Processing*, vol. 53, no. 2, pp. 550–563, Feb. 2005.
- [36] R. Crochiere and L. Rabiner, *Multirate Digital Signal Processing*. Englewood Cliffs, NJ: Prentice-Hall, 1983.
- [37] A. Croisier, D. Eseban, and C. Galand, "Perfect channel splitting by use of interpolation/decimation/tree decomposition techniques," *Proc. Int. Conf. Information Sciences and Systems*, Aug. 1976.

- [38] F. Mintzer, "Filters for distortion-free two-band multirate filter banks," *IEEE Transactions on Acoustics, Speech and Signal Processing*. Vol. ASSP-33, pp. 626–630, June 1985.
- [39] R. Koilpillai and P. Vaidyanathan, "Cosine-modulated fir filter banks satisfying perfect reconstruction," *IEEE Transactions on Signal Processing*, vol. SP-40, pp. 770–783, Apr. 1992.
- [40] C. Creusere and S. Mitra, "A simple method for designing high-quality prototype filter for m-band pseudo qmf banks," *IEEE Transactions on Signal Processing*, vol. 43, no. 4, pp. 1005–1007, 1995.
- [41] T. Ramstad, "Cosine modulated analysis-synthesis filter bank with critical sampling and perfect reconstruction," *Proceedings of the IEEE International Conference on Acoustics, Speech and Signal Processing*, pp. 1789–1792, May 1991.
- [42] H. Malvar, "Modulated qmf filter banks with perfect reconstruction," *Electronics Letters*, vol. 26, pp. 906–907, June 1990.
- [43] Y. P. Lin and P. P. Vaidyanathan, "A kaiser window approach for the design of prototype filters of cosine modulated filterbanks," *IEEE Signal Processing Letters*, vol. 5, no. 6, pp. 132–134, 1998.
- [44] J. Lee and B. Lee, "A design of nonuniform cosine modulated filter banks," *IEEE Transactions on Circuits and Systems II*, vol. 42, no. 11, pp. 732–737, 1995.
- [45] T. Petersen and S. Boll, "Critical band analysis-synthesis," *IEEE Acoustics, Speech, and Signal Processing*, vol. 31, no. 3, pp. 656–663, June 1983.
- [46] A. H. Sayed, *Fundamentals of Adaptive Filtering*. NY: John Wiley & Sons, 2003.
- [47] S. Haykin, *Adaptive Filter Theory*, third edition ed. Upper Saddle River, New Jersey 07458: Prentice-Hall, 1996.

- [48] S. Gay and S. Tavathia, "The fast affine projection algorithm," *IEEE International Conference on Acoustics, Speech, and Signal Processing, ICASSP 1995 Proceedings*, vol. 5, pp. 3023–3026, 1995.
- [49] J. Agnew, *Hearing Aids - Standards, Options, and Limitations*, second edition ed. New York: Thieme Medical Publishers Inc., 2002, ch. Amplifiers and Circuit Algorithms for Contemporary Hearing Aids, p. 168.
- [50] L. Nicolosi, E. Harryman, and J. Kresheck, *Terminology of Communication Disorders, Speech-Language-Hearing*, third edition ed. Baltimore: Williams & Wilkens, 1989.
- [51] Y. Alsaka and B. McLean, "Spectral shaping for the hearing impaired," in *South-eastcon '96. 'Bringing Together Education, Science and Technology', Proceedings of the IEEE*, 1996, pp. 103–106.
- [52] S. Barta, "Pacific soundcraft," <http://pacificsoundcraft.com/software/directx/-compressor/>, 2002.
- [53] B. W. Y. Hornsby and T. A. Ricketts, "The effects of compression ratio, signal-to-noise ratio, and level on speech recognition in normal hearing listeners," *Journal of Acoustical Society of America*, vol. 109, no. 6, 2001.
- [54] T. Schneider and D. G. Jamieson, "Electroacoustic characterization of hearing aids: A system identification approach," *IEEE International Conference on Acoustics, Speech, and Signal Processing, ICASSP 1995 Proceedings*, vol. 5, pp. 3523–3526, 1995.
- [55] V. Parsa and D. G. Jamieson, "Prediction of hearing aid performance using the multiple model least squares technique," *Canadian Conference on Electrical and Computer Engineering*, vol. 1, pp. 515–520, May 2001.
- [56] A. O'Brien, "More channels are better, right?" *Bernafon Literature*, 2002.



- [57] B. Moore, "Cochlear hearing loss," *Whurr, London*, 1998.
- [58] M. Leek and V. Summers, "Reduced frequency selectivity and the preservation of spectral contrast in noise," *Journal of the Acoustical Society of America*, vol. 100(3), pp. 1796–1806, 1996.
- [59] J. G. A. Boothroyd, B. Mulhearn and J. Ostroff, "Loudness, its definition, measurement and calculation," *Effects of Spectral Smearing on Phoneme and Word Recognition*, vol. 100(3), pp. 1807–1818, 1996.
- [60] G. Smoorenburg, "A physiological basis for hearing aid processing," *Referate des Horgerate-Akustiker-Kongresses*, 2000.
- [61] P. Switzerland, "Claro digital perception processing," *Phonak Literature*, 2002.
- [62] D. P. T. Dau and A. Kohlrausch, "A quantitative model of the effective signal processing in the auditory system. i. model structure," *Journal of the Acoustical Society of America*, vol. 99(6), pp. 3615–3622, 1996a.
- [63] D. P. T. Dau and A. Kohlrausch, "A quantitative model of the effective signal processing in the auditory system. ii. simulations and measurements," *Journal of the Acoustical Society of America*, vol. 99(6), pp. 3623–3631, 1996b.
- [64] B. G. B.C.J. Moore and D. Vickers, "Further evaluation of a model of loudness perception applied to cochlear hearing loss," *Journal of the Acoustical Society of America*, vol. 102(2), pp. 898–907, 1999.
- [65] J. Mathews and S. Douglas, *Adaptive Filters*. Upper Saddle River, New Jersey, Prentice Hall, 2000.

# Appendix A

## Hearing Aid Specifications

Section 1 - Bernafon Symbio XT 110

Section 2 - Oticon Syncro V2

Section 3 - Phonak Perseo 311 dAZ Forte


Section 4 - Siemens Triano S


Section 5 - Sonic Innovations Natura 2 SE

Data sheets are published with the permission from each manufacturer.

## A.1 Bernafon Symbio XT 110







---

[About Bernafon Canada Ltd.](#)
[About Hearing](#)
[Hearing Solutions](#)
[Professionals](#)
[News](#)
[Virtual Tour](#)
[Contact](#)

---

**Products**

SwissEar

**Symbio XT**

Channel Free™

OpenFit™

SoundMaster™

**Features**

**Instruments**

Symbio XT 100 BTE

Symbio XT 110 BTE

Symbio XT 115 BTE DM

Symbio XT 200 ITE

Symbio XT 205 ITE DM

Symbio XT 320 ITC

Symbio XT 325 ITC DM

Symbio XT 400 CIC

Symbio XT 410 MC

**Smile Plus**

Neo

Flair

Win


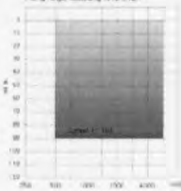
**Audioflex**

**Dahlberg Analog**

Lexia

**Products**

**Symbio XT 110 BTE**

Compact power BTE for moderate to severe hearing losses. Local M/T/O switch. Battery size 13.

**Product Features**

- ChannelFree™
- OpenFit™ to avoid occlusion
- Adaptive Feedback Canceller
- OASIS plus 3.0
- Soft Noise Management™

**Product Information**

	IEC 118-7 (2cc)	IEC 118-0 (Ears.)
Full-On Gain, Peak	62 dB	68 dB
Peak, OSPL 90	131 dB SPL	135 dB SPL
Freq. Range, ANS	100 - 5900 Hz	
Battery Type	13	
Local Controls	M/T/O switch	
Accessories	Audio shoe, FM	
Telecoil	Yes	
Direct Audio Input	Yes	

**User benefits**

- Maximal speech understanding and clear, natural sound
- Occlusion-free fitting
- Less whistling
- Unparalleled customization
- Reduced annoying low-level noise

Item

**Search**

**Bernafon worldwide**

**Download**

Product Information  
Symbio XT BTE  
(pdf, 187 KB)

## A.2 Oticon Syncro V2



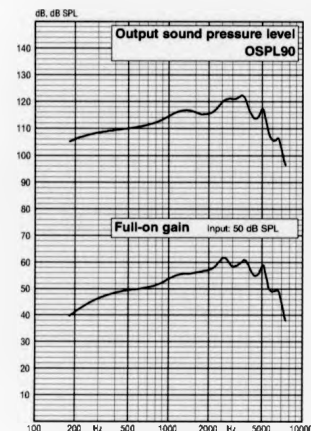
# TECHNICAL INFORMATION

## BTE

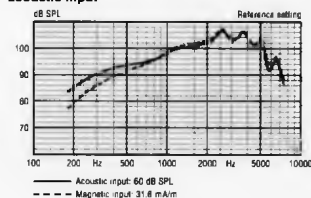
# Oticon • Syncro

### Ear simulator

Measured according to IEC publications 118-0, -1, -2, -6, -13 (incl. amendments) and 711.



### Frequency response with magnetic and acoustic input



### Data at a glance

Note: Measurement data obtained through standard pure tone measurements on advanced adaptive digital hearing aids may be misleading with regard to characteristics in normal use. For technical measurements special technical settings that disables all the adaptive features are used. Unless otherwise stated all measurements are in the Omnidirectional mode.

Ear Simulator	2cc Coupler
OSPL90	OSPL90
122	Peak
115	1000 Hz
116	1600 Hz
114	Average (DIN)
	HF Average (ANSI)
	111
Full-on gain, dB	
Input: 50 dB SPL	
62	Peak
54	1000 Hz
56	1600 Hz
54	Average (DIN)
	HF Average (ANSI)
	51
Frequency Range, Hz	
190-7300	DIN/ANSI
	130-6900

Telecoil output, dB SPL	
87	1 mA/m field, 1600 Hz
107	10 mA/m field, 1600 Hz
	SPLITS (ANSI), Right ear
	94
	SPLITS (ANSI), Left ear
	93

Total harmonic distortion, %		
Reference setting, input: 70 dB SPL		
IEC	Hz	ANSI
0.5	500, typical	0.5
0.5	800, typical	0.5
0.5	1600, typical	0.5

Equivalent input noise level (ANSI), dB SPL	
16	Typical/maximum, Omni
23	Typical/maximum, Dir

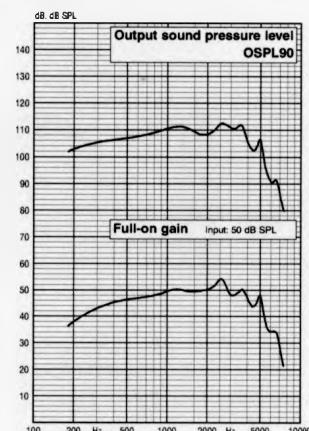
Battery consumption, mA	
1.1	Quiescent, typical/maximum
1.1	IEC
	ANSI
	1.1

Battery		
Size 13 (IEC PR48)		
Estimated life in hours	Typ	Min
1.4 V Zinc air	220	180

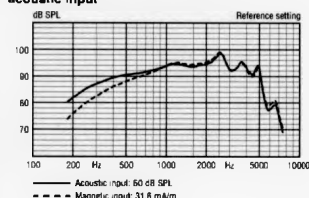
EMC Immunity (IEC 118-13)		
IRIL, dB SPL	Field strength, (V/m)	
GSM/DECT	GSM/DECT	
-48/-8	Microphone (Omni)	3/2
-39/-5	Microphone (Dir)	3/2
-33/-3	Telecoil	3/2

### 2cc coupler

Measured according to IEC publications 118-7 (incl. amendments) and 126 and to ANSI S3.22 (2003) and S3.7 (1995).



### Frequency response with magnetic and acoustic input



### A.3 Phonak Perseo 311 dAZ Forte

Phonak Perseo 311 dAZ Forte  
Hörgerät

Das Hörgerät ist ein...  
Es ist ein...  
Es ist ein...



# Perseo™ 311 dAZ Forte

with PersonalLogic

PHONAK

Highest power BTE Perseo personal, digital hearing instrument. Perseo 311 dAZ Forte combines contemporary aesthetic design with innovative environmental protection for reliability and consistent performance.

Perseo provides personally optimized clarity, comfort, convenience and control for easy listening in all hearing situations thanks to Personal System Managers, DPP<sup>2</sup> in 20 critical bands, Fine-scale Noise Canceler in 20 bands, Adaptive digital AudioZoom, with rapid, silent onset and automatic Listening Situation Manager. Personal direct and remote control options with the TacTronic Switch, WatchPilot2 and SoundPilot and optional integrated FM.

<b>Key data</b>	<b>Ear Simulator and tone hook HE4 330</b>
	Max. gain 72 dB
	Max. power output 135 dB SPL
	Frequency range <100–6000 Hz

- General features**
- BTE with battery size 13
  - Screw-on integrated hook
  - Telecoil
  - Moisture and wind noise resistant
  - TacTronic switch combining ON/OFF and program selection

- Options**
- WatchPilot2 or SoundPilot remote controls for binaural program selection and volume control
  - Confirmation beeps for program selection
  - FM Module
  - Tone hook HE4 330
  - Left/Right identification on battery cover
  - Tamperproof battery compartment

- Automatic**
- Listening Situation Manager for automatic soft switching between programs

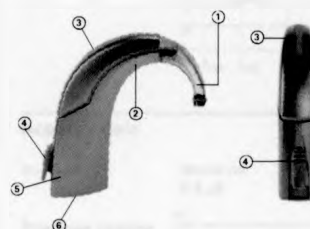
- Hearing Programs**
- Up to five hearing programs + mute mode
  - 1. QuietSituations
  - 2. NoisySituations
  - 3. SpecialSituations (choices available)
  - 4. FM or T (telecoil)
  - 5. FM + M or MT

- Processing**
- Digital Perception Processing<sup>2</sup>: Clarity Component Enhancement in 20 critical bands
  - Personal System Managers
    - Feedback Manager
    - Occlusion Manager
    - Experience Manager
  - Noise suppression technologies
    - Adaptive digital AudioZoom (dAZ)
    - Fine-scale Noise Canceler (FNC) in 20 bands
    - Soft squelch

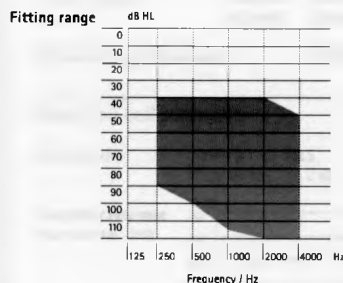
- Technical features**
- 2 Sigma/Delta AD converters, 14 bit resolution
  - Sampling rate 20 kHz, 64 x oversampling
  - 128 point FFT processor

- Software**
- PFG software version 8.1 or later, NOAH compatible

- Hardware**
- Programmable with PC (IBM compatible) and HI-PRO interface



- ① Tone hook HE4 1000 (standard)
- ② Broadband receiver
- ③ Miniature electret dual microphones (protected inputs)
- ④ TacTronic switch
- ⑤ Battery compartment (with serial number) including integrated programming socket
- ⑥ Battery cover and type identification



## WARNING TO DISPENSERS:

This hearing instrument has an output sound pressure level that can exceed 132 dB SPL. Special care should be taken when fitting this instrument as there may be a risk of impairing the residual hearing of the user.

CE  
0459



FM



Product information Perseo 311 dAZ Forte

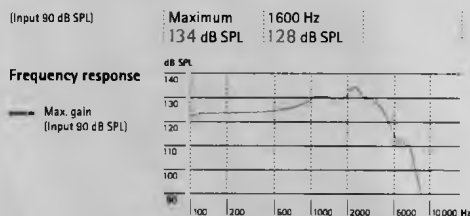
Digital Perseo



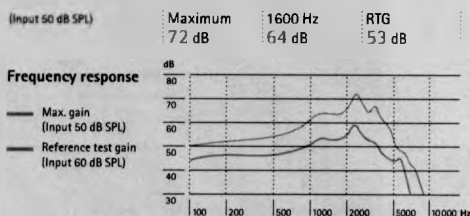
## Ear simulator data

EN / IEC 60118 and IEC 60711

### Output sound pressure level



### Acoustic gain



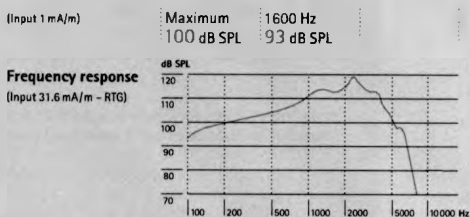
Frequency range (DIN 45605) <100–6500 Hz

Total harmonic distortion	500 Hz	800 Hz	1600 Hz
	1.0 %	0.5 %	0.5 %

Battery current	Quiescent	Working
	1.30 mA	1.30 mA

Equivalent input noise level	21 dB SPL
------------------------------	-----------

### Induction coil sensitivity



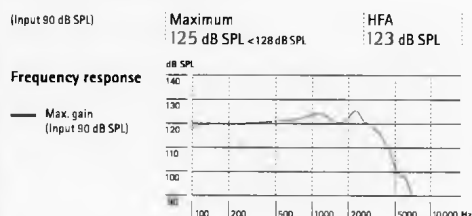
### Dynamic Data

Compression	Attack time	Recovery time
	8 ms	80 ms

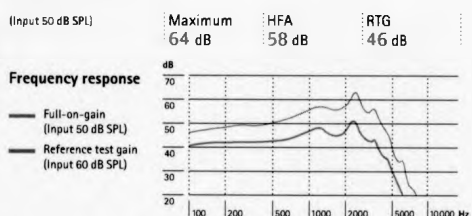
## 2 cm<sup>3</sup> coupler data

ANSI S3.22-1996

### Output sound pressure level



### Acoustic gain



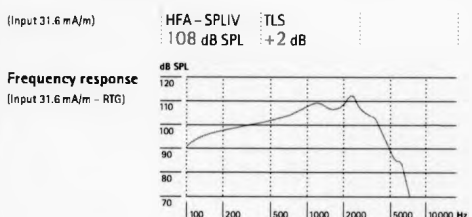
Frequency range <100–5500 Hz

Total harmonic distortion	500 Hz	800 Hz	1600 Hz
	1.0 % <4.0 %	0.5 % <3.0 %	0.5 % <3.0 %

Battery current	Quiescent	Working
	1.30 mA	1.35 mA <1.6 mA

Equivalent input noise level	20 dB SPL <23 dB SPL
------------------------------	----------------------

### Induction coil sensitivity

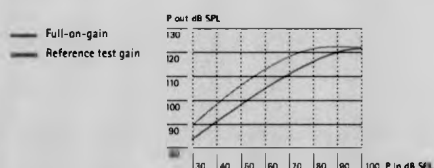


### Dynamic Data

Compression	Attack time	Recovery time
	6 ms	60 ms

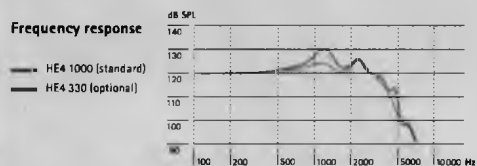
## 2 cm<sup>3</sup> coupler data

### Input/Output characteristics at 2000 Hz



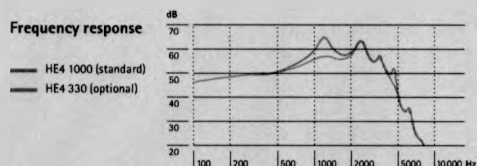
### Tone hook effects on output

(Input 90 dB SPL)



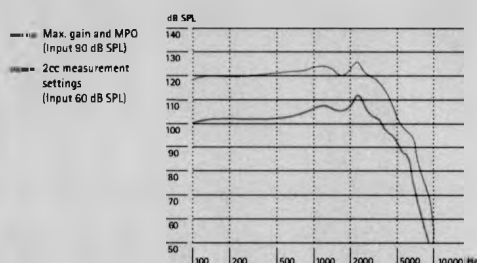
### Tone hook effects on max. gain

(Input 50 dB SPL)



### Test mode

Special program exclusively designed for coupler measurements with Perseo – access in PFG (Main menu / Hearing instruments / Measurement settings).



Unless otherwise specified, all data obtained with the ear hook type HE4 1000. Furthermore, due to the complex digital signal processing of this instrument, standard measurements as presented on this product information are only possible in a special program.

GB 0103 Data subject to change without notice.



## Application/Technical Data

## TRIANO™ S



TRIANO S

### Description

- Programmable, mini BTE instrument with fully digital, 16-channel signal processing
- Appropriate for mild to moderately-severe hearing loss
- Adaptive directional microphone system (TwinMic™)
- Automatically adapts to most listening environments using its exclusive Speech Comfort System
- 4 individual listening programs, including Telecoil (T-coil) and audio input
- Automatic feedback suppression
- Highly recommended for pediatric fitting
- Easy fitting interface using CONNEXX 32-bit programming software

### Amplifier

- Fully digital, 16-channel device with Speech Comfort System

### Options

- Standard colors are beige, tobacco, grey and granite
- Additional colors are red, green, blue and yellow
- CROS/BICROS

### Standard features

- Audio input
- Automatic detection of audio input boot
- Acoustic indicator when switching between programs
- Acoustic indicator warning of low battery
- Battery compartment door with lock and on/off switch
- Type 13 battery

### Accessories

- Audio input boot
- Audio input cord
- Red and blue type plates to indicate right and left hearing instruments

13	PROG 4	MT
		4

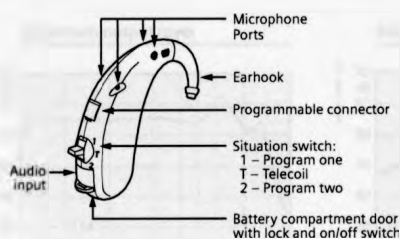
CE  
0123

## Application/Technical Data

## TRIANO<sup>®</sup> S

Standard ANSI S3.22 - 1996	2 cc coupler
Output sound pressure level	
Peak	122 dB
HF - average OSPL90	117 dB
Full-on gain (input 50 dB)	
Peak	54 dB
HF - average	48 dB
Reference test gain	40 dB
Frequency range	
Low frequency limit	<100 Hz
High frequency limit	6100 Hz
Total harmonic distortion	
500 Hz	3%
800 Hz	2%
1600 Hz	2%
Equivalent input noise	18 dB
Telecoil sensitivity	
HFA-SPLITS*	98 dB

\*SPLITS (Sound Pressure Level for Inductive Telecoil Simulator)

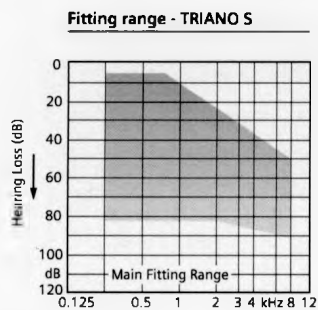


Battery	
Battery voltage	1.3 V
Battery current drain	
ANSI	1.2 mA
Battery life	
Type 13 zinc air	100-200 hrs

Compression characteristics			
Output limiter	Type	Attack	Release
	AGC-O	<0.5 ms	100 ms
Channel AGC	Syllabic compression	9 ms	90 ms
	Dual compression fast	5 ms	90 ms
	slow	900 ms	1.5 s

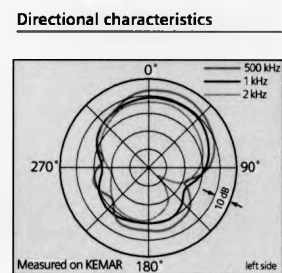
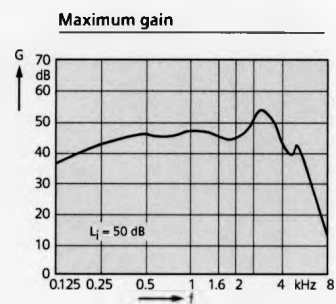
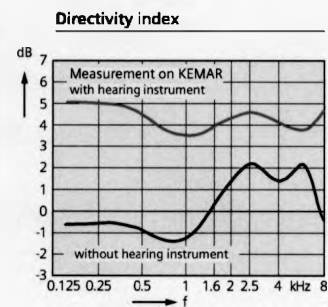
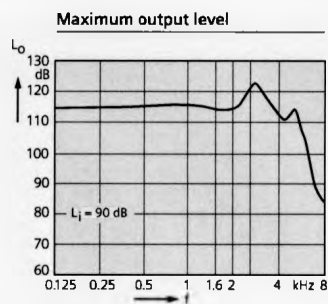
## 2 cc coupler ANSI S3.22-1996

TRIANO<sup>®</sup> S



**Directivity data - measurement on KEMAR**

AI: DI	
Articulation index (AI)	4.3 dB
Weighted directivity (DI)	
Front-side ratio (Average data at 90° and 270°)	9.8 dB
Front-rear ratio (Average data at 180°)	7.2 dB



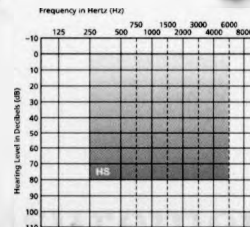
## A.5 Sonic Innovations Natura 2 SE

Sonic Innovations Natura 2 SE		
Model	Natura 2 SE	
Year	2010	
Manufacturer	Sonic Innovations	
Product Type	Portable Music Player	
Capacity	16GB	
Screen Size	2.8 inch	
Weight	110g	
Dimensions	115 x 60 x 15 mm	
Price	\$149.99	
Availability	Available	
Warranty	1 Year	
Features	Touchscreen, FM Radio, Video Playback, Photo Slideshow, Voice Recording	
Accessories	Charging Cable, Earbuds, User Manual	
Notes	This device is compatible with all major mobile operating systems.	

## Half-Shell (HS)

Ear Simulator (IEC 118-0)	2cc coupler (ANSI S3.22-1996)
Max Output (OSPL90) (P1)	123 dB SPL
Max Output (OSPL90), 1600Hz (P1)	116 dB SPL
Full-On Gain (P1)	59 dB
Full-On Gain, 1600 Hz (P1)	53 dB
Reference Test Gain (P2)	41 dB
Frequency Range (P2)	200 Hz - 5400 Hz
Total Harmonic Distortion (P2)	
..... 500 Hz	2.5%
..... 800 Hz	1.5%
..... 1600 Hz	1%
Equivalent Input Noise*	< 23 dB SPL
Telecoil Sensitivity** (P2)(31.6 mA/m at 1600 Hz)	101 dB SPL
Battery Current (P2)	1.4 mA
Attack Time (P2)	5 msec @ 2kHz
Recovery Time (P2)	11 msec @ 2kHz
EMC IRL (800 - 960 MHz Peak)	< 20 dB SPL
EMC IRL (1400 - 2000 MHz Peak)	< 40 dB SPL
Max Output (OSPL90) (P1)	113 dB SPL
HFA-OSPL90 (P1)	108 dB SPL
Peak Gain (P1)	46 dB
HFA Full-On Gain (P1)	44 dB
Reference Test Gain (P2)	31 dB
Frequency Range (P2)	200 Hz - 5400 Hz
Total Harmonic Distortion (P2)	
..... 500 Hz	2.5%
..... 800 Hz	1.5%
..... 1600 Hz	1%
Equivalent Input Noise*	< 23 dB SPL
Telecoil Sensitivity** (P2)(HFA-SPLITS)	92 dB SPL
Battery Current (P2)	1.4 mA
Attack Time (P2)	5 msec @ 2kHz
Release Time (P2)	11 msec @ 2kHz

Fitting Range



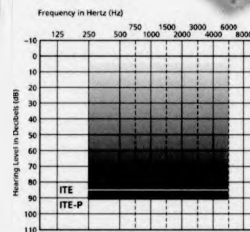
### AVAILABLE OPTIONS

- Program 1 / Program 2 Switch
- Directional / Omni Switch
- Programmable Telecoil
- On/Off Switch
- Volume Control

## In-the-Ear (ITE) & In-the-Ear-Power (ITE-P)

Ear Simulator (IEC 118-0)	2cc coupler (ANSI S3.22-1996)
Max Output (OSPL90) (P1)	126/130 dB SPL
Max Output (OSPL90), 1600Hz (P1)	118/125 dB SPL
Full-On Gain (P1)	58/63 dB
Full-On Gain, 1600 Hz (P1)	53/59 dB
Reference Test Gain (P2)	43/50 dB
Frequency Range (P2)	200 Hz - 5400 Hz
Total Harmonic Distortion (P2)	
..... 500 Hz	2.5/3%
..... 800 Hz	1.5/2%
..... 1600 Hz	1%
Equivalent Input Noise*	< 23 dB SPL
Telecoil Sensitivity** (P2)(31.6 mA/m at 1600 Hz)	101/105 dB SPL
Battery Current (P2)	1.4 mA
Attack Time (P2)	5 msec @ 2kHz
Recovery Time (P2)	11/10 msec @ 2kHz
EMC IRL (800 - 960 MHz Peak)	< 20 dB SPL
EMC IRL (1400 - 2000 MHz Peak)	< 40 dB SPL
Max Output (OSPL90) (P1)	116/118 dB SPL
HFA-OSPL90 (P1)	111/115 dB SPL
Peak Gain (P1)	47/53 dB
HFA Full-On Gain (P1)	45/49 dB
Reference Test Gain (P2)	34/38 dB
Frequency Range (P2)	200 Hz - 5400 Hz
Total Harmonic Distortion (P2)	
..... 500 Hz	2.5/3%
..... 800 Hz	1.5/2%
..... 1600 Hz	1%
Equivalent Input Noise*	< 23 dB SPL
Telecoil Sensitivity** (P2)(HFA-SPLITS)	92/96 dB SPL
Battery Current (P2)	1.4 mA
Attack Time (P2)	5 msec @ 2kHz
Release Time (P2)	11/10 msec @ 2kHz

Fitting Range



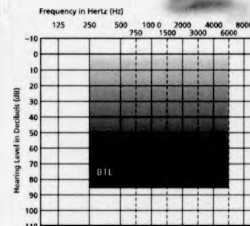
### AVAILABLE OPTIONS

- Program 1/Program 2 Switch
- Directional/Omni Switch (ITE Only)
- Directional/Telecoil/Omni (ITE only)
- Programmable Telecoil
- On/Off Switch

## Behind-the-Ear (BTE)

Ear Simulator (IEC 118-0)	2cc coupler (ANSI S3.22-1996)
Max Output (OSPL90) (P1)	129 dB SPL
Max Output (OSPL90), 1600Hz (P1)	123 dB SPL
Full-On Gain (P1)	65 dB
Full-On Gain, 1600 Hz (P1)	61 dB
Reference Test Gain (P2)	48 dB
Frequency Range (P2)	220 Hz - 5000 Hz
Total Harmonic Distortion (P2)	
..... 500 Hz	4%
..... 800 Hz	2%
..... 1600 Hz	1%
Equivalent Input Noise*	< 23 dB SPL
Telecoil Sensitivity** (P2)(31.6 mA/m at 1600 Hz)	105 dB SPL
Battery Current (P2)	1.5 mA
Attack Time (P2)	5 msec @ 2kHz
Recovery Time (P2)	10 msec @ 2kHz
EMC IRL (800 - 960 MHz Peak)	< 20 dB SPL
EMC IRL (1400 - 2000 MHz Peak)	< 40 dB SPL
Max Output (OSPL90) (P1)	119 dB SPL
HFA-OSPL90 (P1)	114 dB SPL
Peak Gain (P1)	54 dB
HFA Full-On Gain (P1)	52 dB
Reference Test Gain (P2)	37 dB
Frequency Range (P2)	220 Hz - 5000 Hz
Total Harmonic Distortion (P2)	
..... 500 Hz	4%
..... 800 Hz	2%
..... 1600 Hz	1%
Equivalent Input Noise*	< 23 dB SPL
Telecoil Sensitivity** (P2)(HFA-SPLITS)	96 dB SPL
Battery Current (P2)	1.5 mA
Attack Time (P2)	5 msec @ 2kHz
Release Time (P2)	10 msec @ 2kHz

Fitting Range



### AVAILABLE OPTIONS

- Program 1 / Program 2 Switch
- Directional / Omni / Switch
- On / Off Switch
- Programmable Telecoil
- Direct Audio Input

SONIC

5000459 Rev C



## Appendix B

### Hearing Aid ANSI Measurements

Section 1 - Bernafon Symbio XT 110

Section 2 - Oticon Syncro V2

Section 3 - Phonak Perseo 311 dAZ Forte

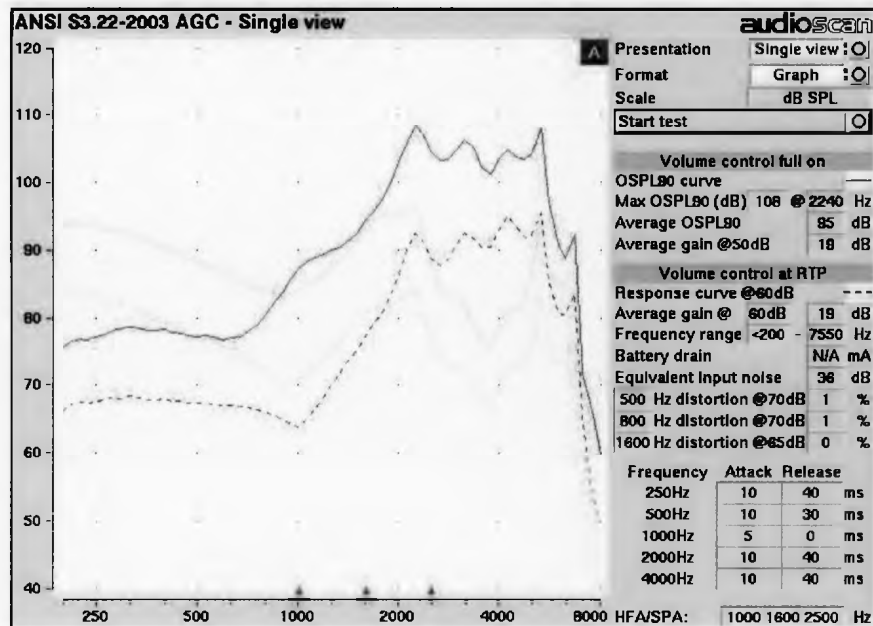
Section 4 - Siemens Triano S

Section 5 - Sonic Innovations Natura 2 SE

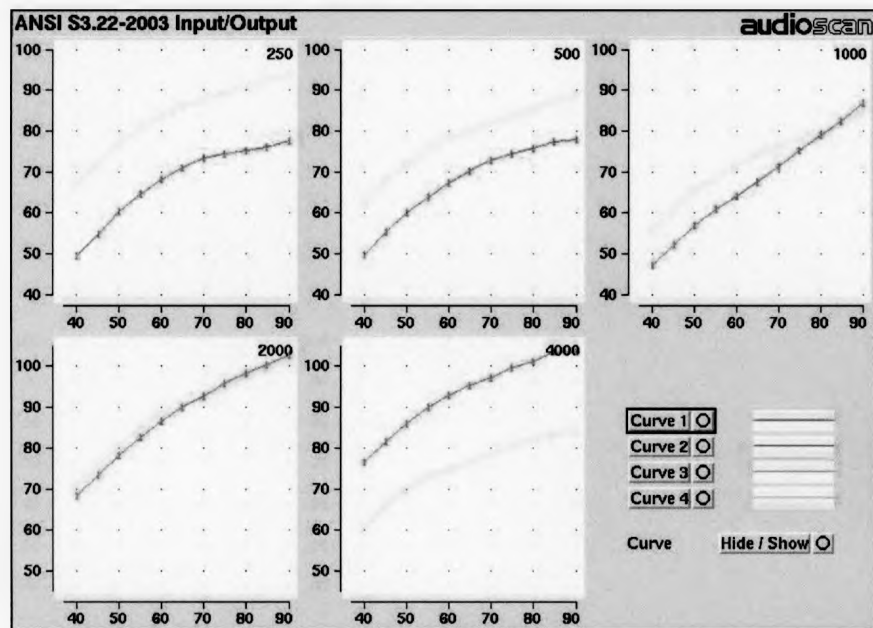
## B.1 Bernafon Symbio XT 110



FIG. B.1. Graphs of the Bernafon Symbio XT 110. The curves are: (a)  $y = 1 - e^{-x}$ , (b)  $y = e^{-x}$ , (c)  $y = 1 - e^{-x^2}$ , (d)  $y = e^{-x^2}$ .

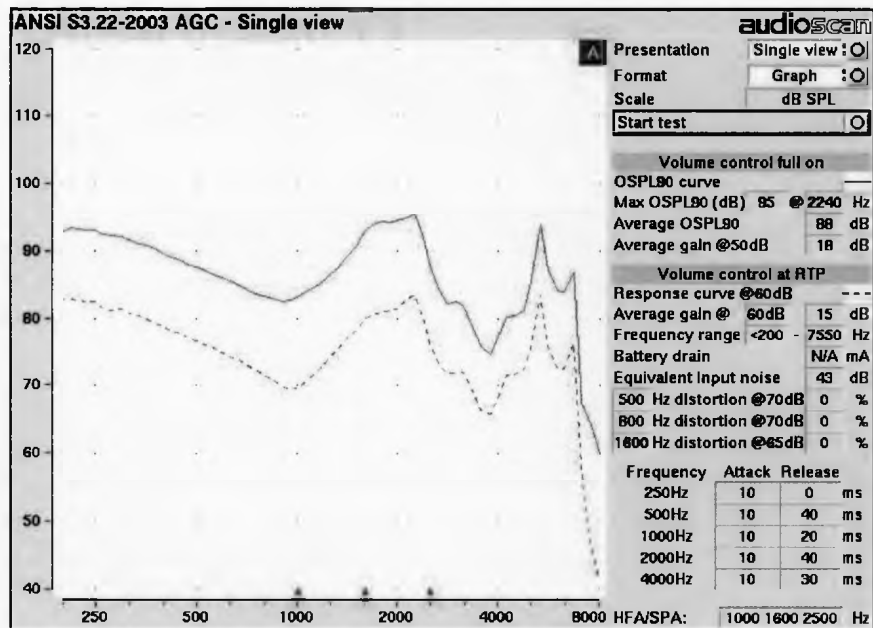


(a) Automatic Gain Control

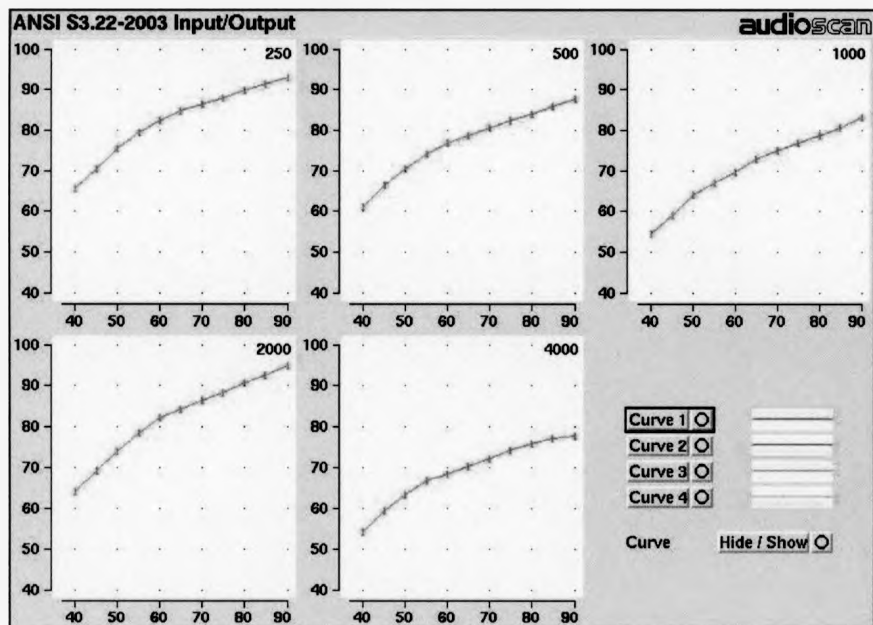


(b) Input\Output

Fig. B.1: ANSI S3.22 (2003) Test Results for Bernafon Symbio 110 XT SE (Audiogram "F")



(a) Automatic Gain Control



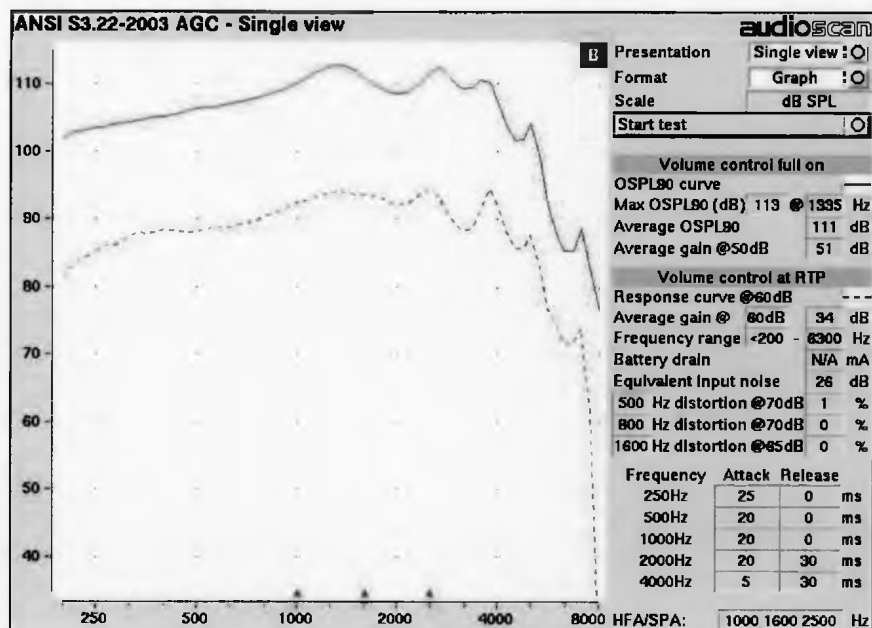
(b) Input\Output

Fig. B.2: ANSI S3.22 (2003) Test Results for Bernafon Symbio 110 XT SE (Audiogram "I")

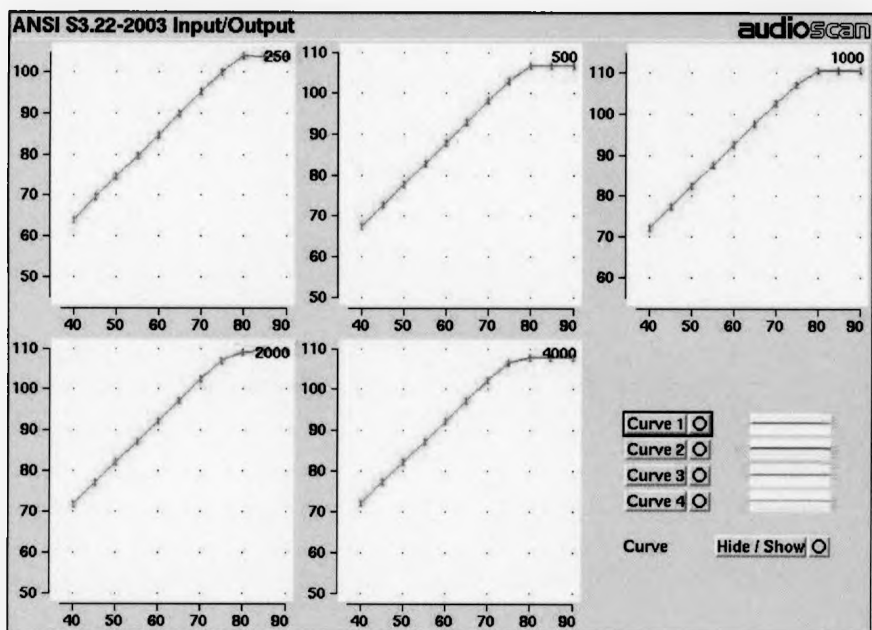
## B.2 Oticon Syncro V2



Fig. 2.12. A series of plots showing the results of a 100 Hz sine wave test for the Oticon Syncro V2.

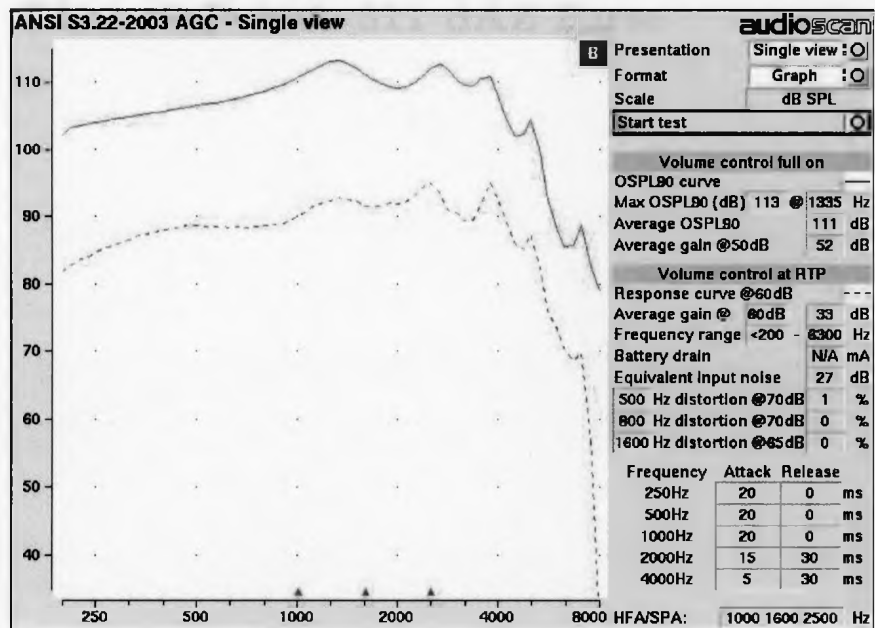


(a) Automatic Gain Control

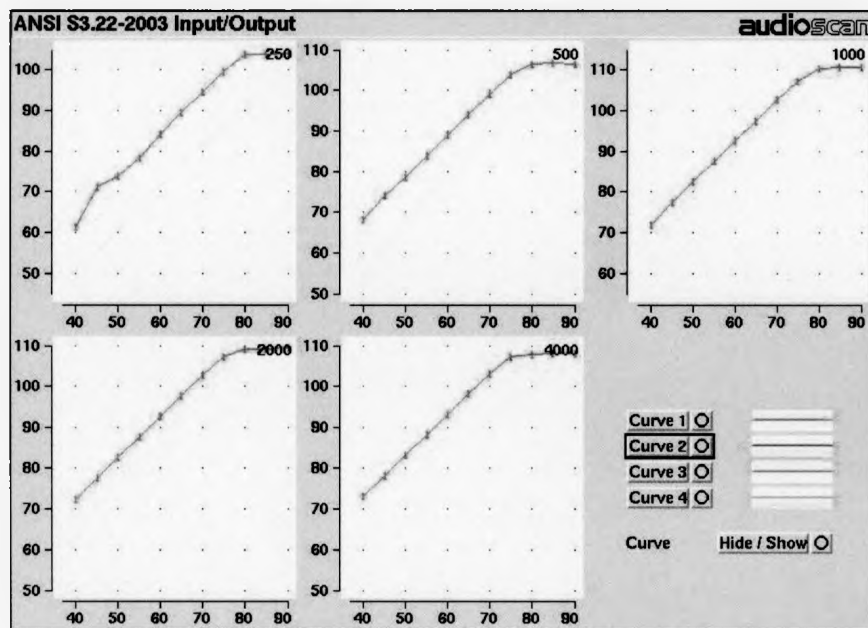


(b) Input\Output

Fig. B.3: ANSI S3.22 (2003) Test Results for Oticon Syncro V2 (Audiogram "F")



(a) Automatic Gain Control

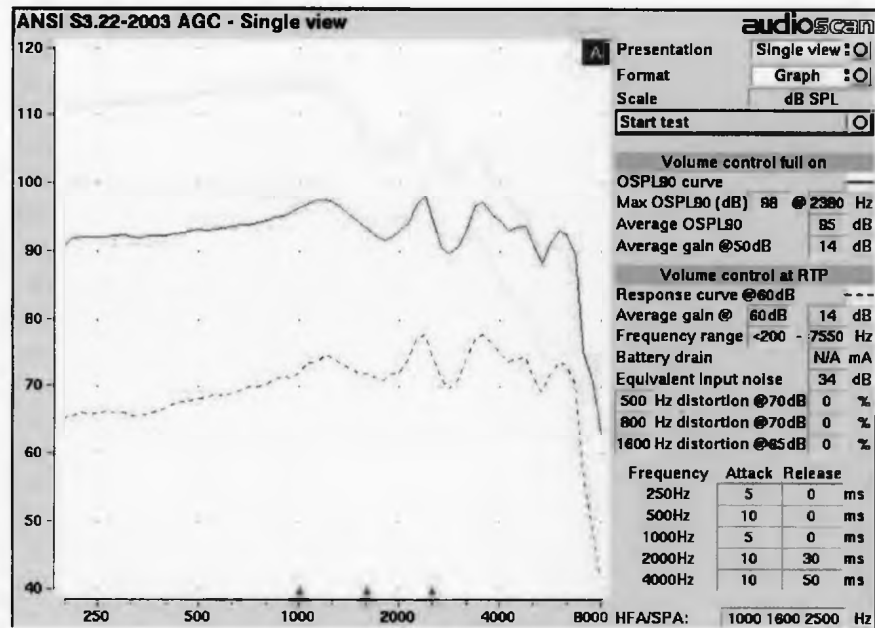


(b) Input\Output

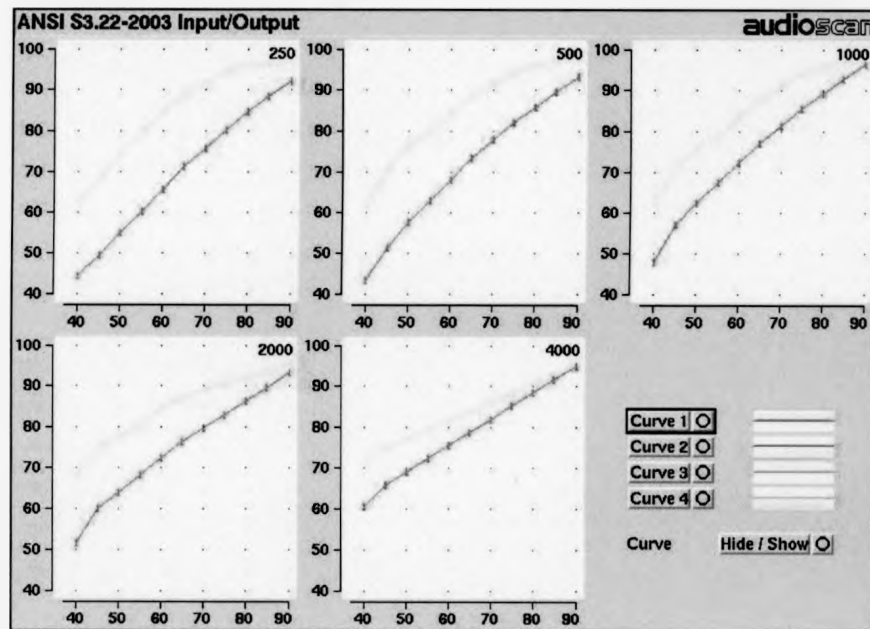
Fig. B.4: ANSI S3.22 (2003) Test Results for Oticon Syncro V2 (Audiogram "I")

# Phonak Perseo 311 dAZ Forte



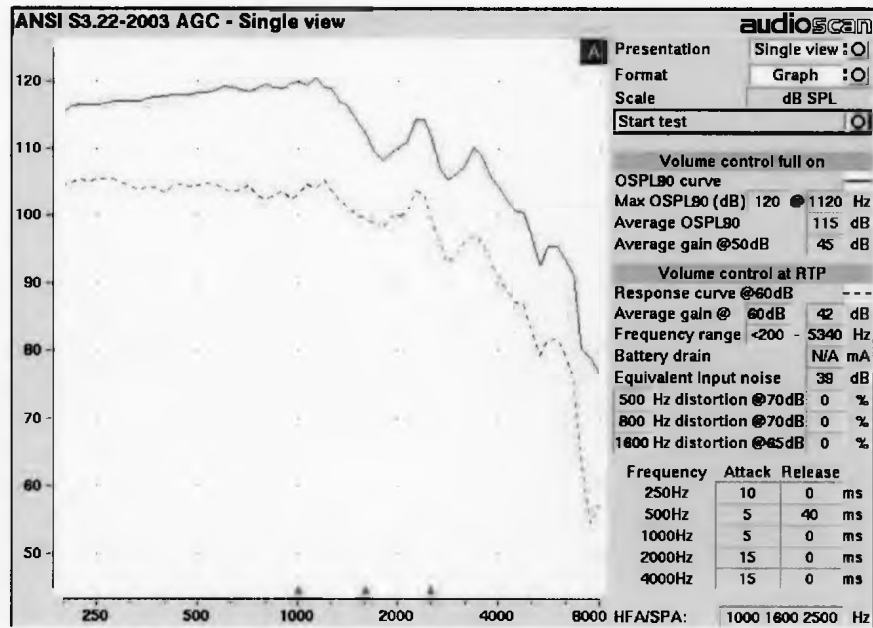


(a) Automatic Gain Control

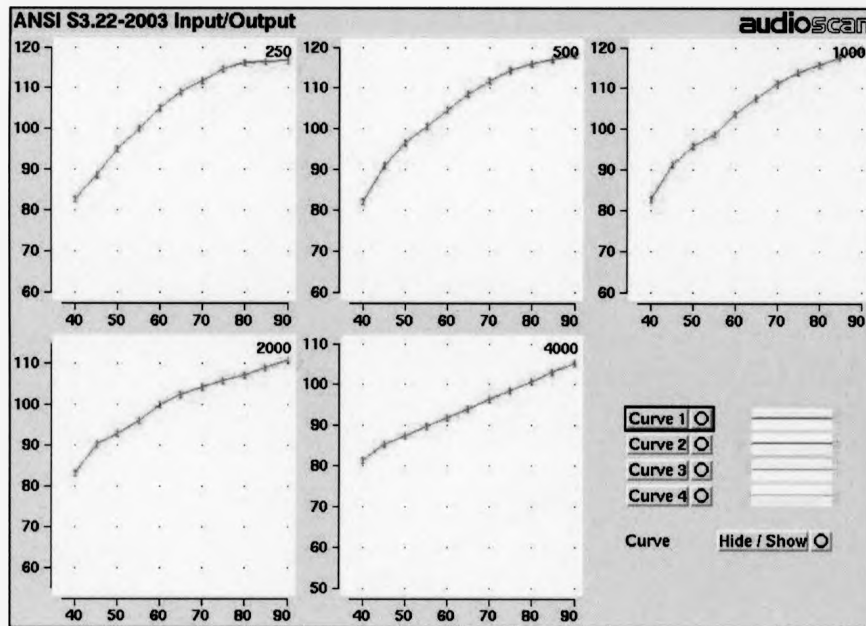


(b) Input/Output

Fig. B.5: ANSI S3.22 (2003) Test Results for Phonak Perseo 311 dAZ Forte (Audiogram "F")



(a) Automatic Gain Control



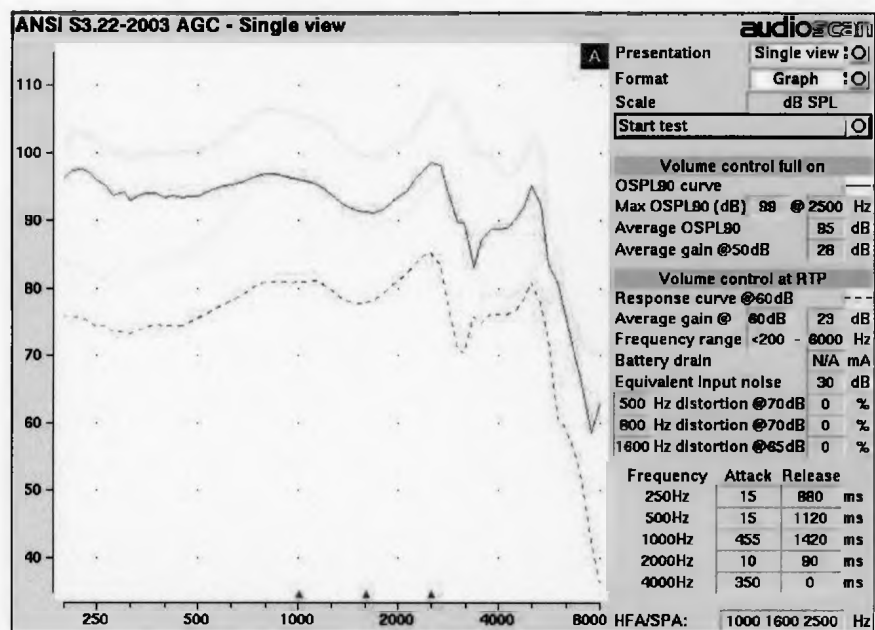
(b) Input/Output

Fig. B.6: ANSI S3.22 (2003) Test Results for Phonak Perseo 311 dAZ Forte (Audiogram "I")

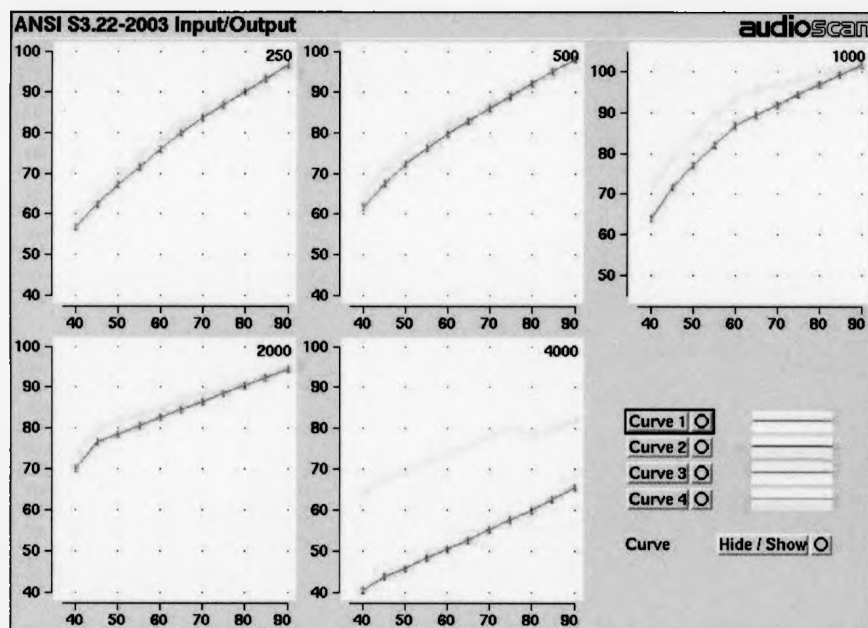
## B.4 Siemens Triano S



Fig. B.4.1. (Top) Number of iterations versus number of points. (Bottom) Number of iterations versus number of points for different values of  $\alpha$ .

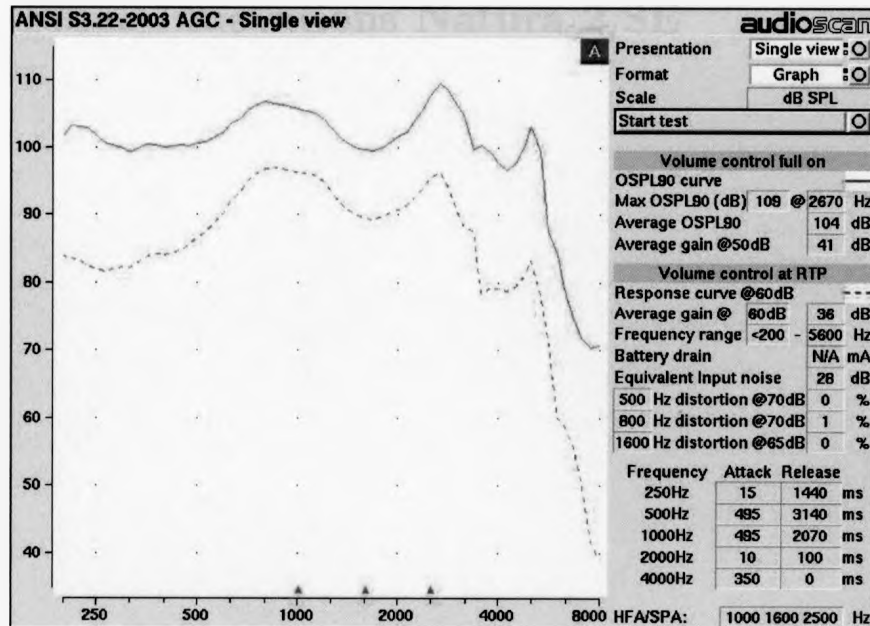


(a) Automatic Gain Control

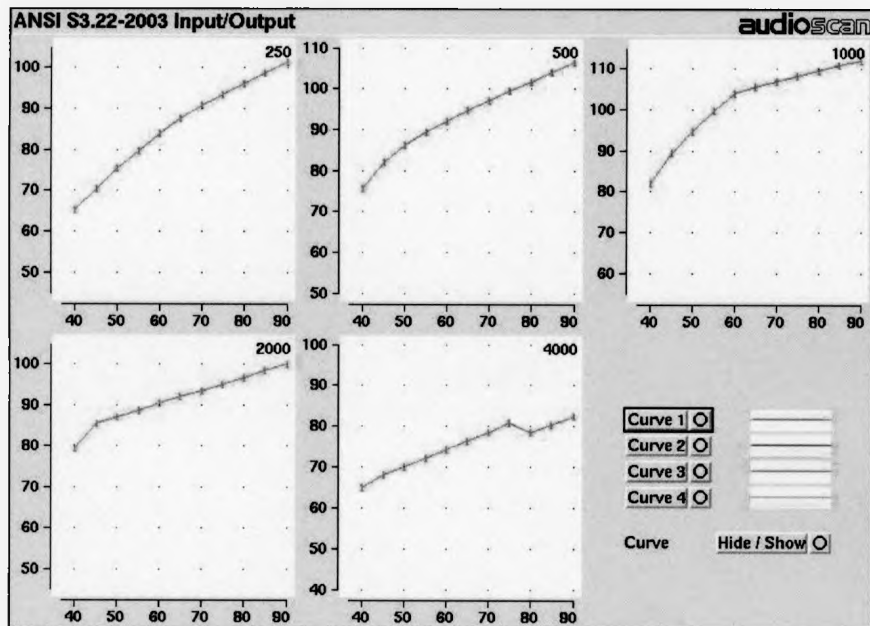


(b) Input\Output

Fig. B.7: ANSI S3.22 (2003) Test Results for Siemens Triano S (Audiogram "F")



(a) Automatic Gain Control



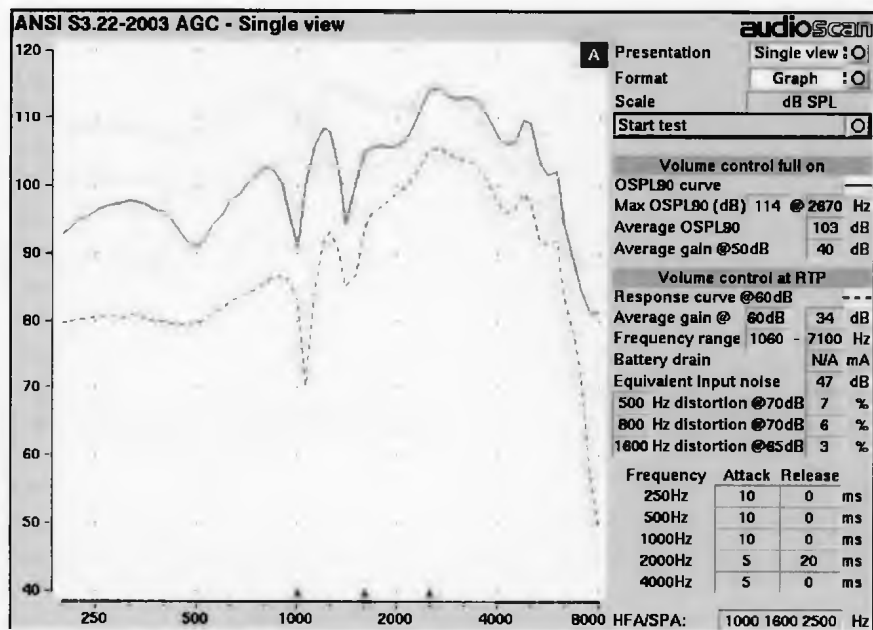
(b) Input\Output

Fig. B.8: ANSI S3.22 (2003) Test Results for Siemens Triano S (Audiogram "I")

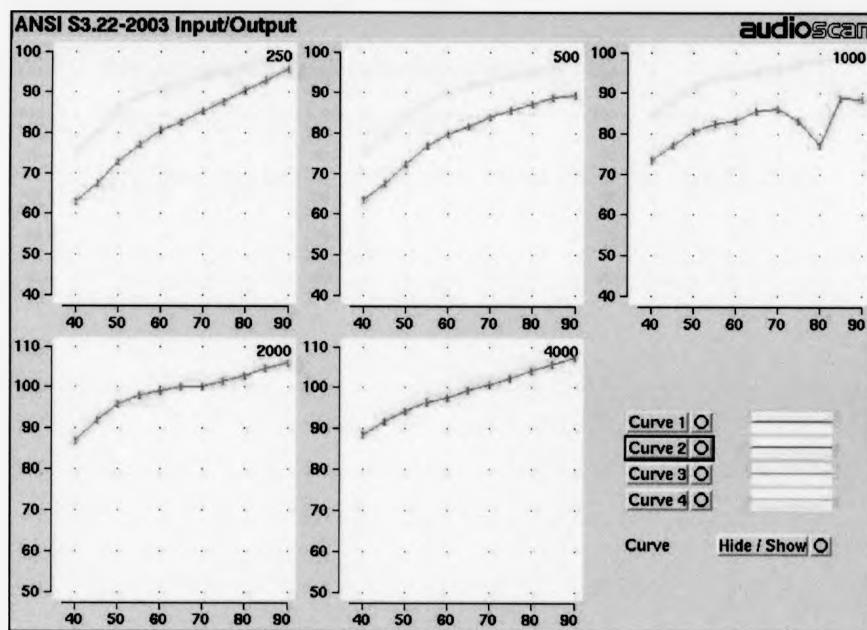
## B.5 Sonic Innovations Natura 2 SE



Fig. B.5. Sonic Innovations Natura 2 SE. The curves are for different values of the coefficient of friction.

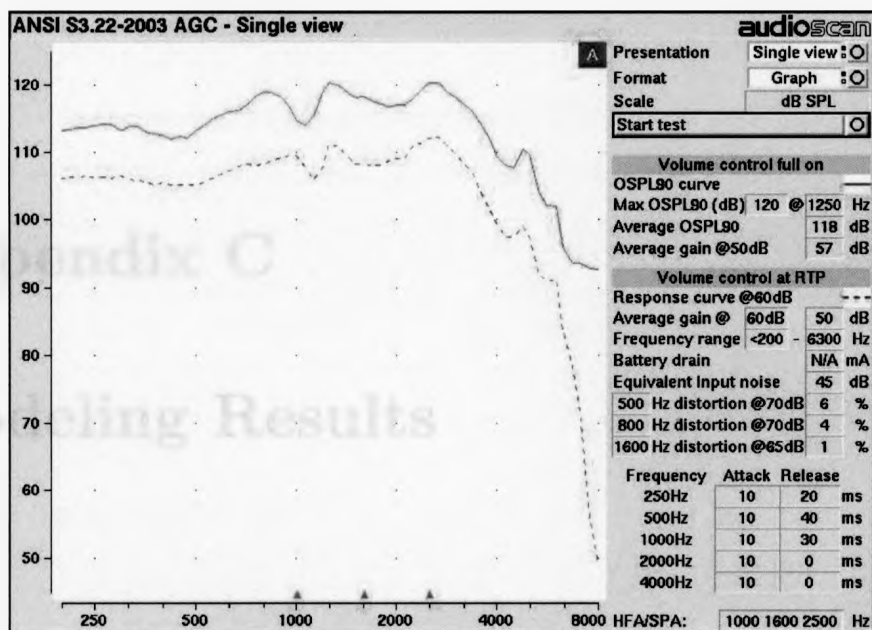


(a) Automatic Gain Control

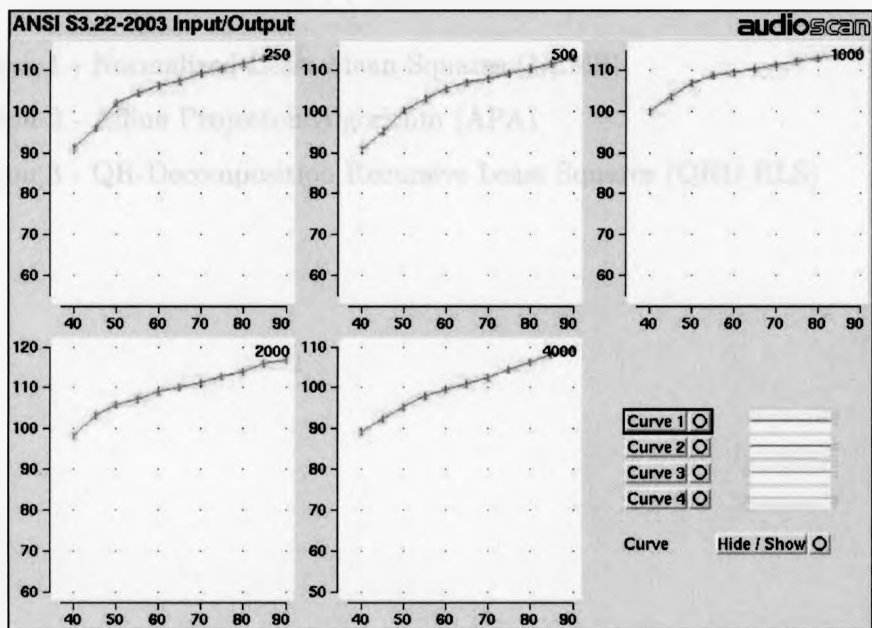


(b) Input\Output

Fig. B.9: ANSI S3.22 (2003) Test Results for Sonic Innovations Natura 2 SE (Audiogram "F")



(a) Automatic Gain Control



(b) Input\Output

Fig. B.10: ANSI S3.22 (2003) Test Results for Sonic Innovations Natura 2 SE (Audiogram "I")



## Appendix C

## Modeling Results

Section 1 - Normalized Least Mean Squares (NLMS)

Section 2 - Affine Projection Algorithm (APA)

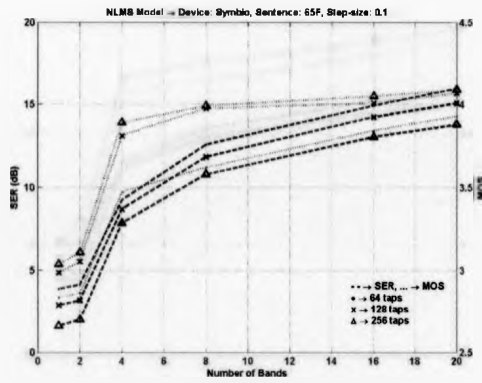
Section 3 - QR-Decomposition Recursive Least Squares (QRD RLS)

## C.1 Normalized Least Mean Squares (NLMS)

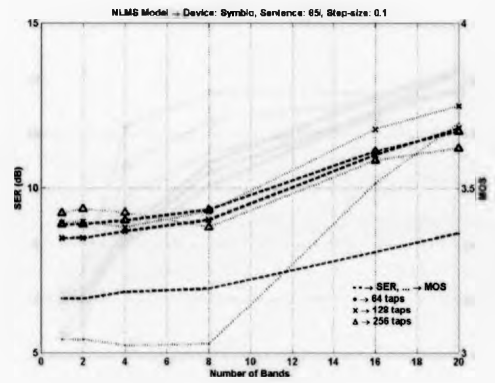
This section presents the signal-to-error ratio, PESQ mean-opinion score double-vertical axis plots for each set of NLMS modeling parameters.



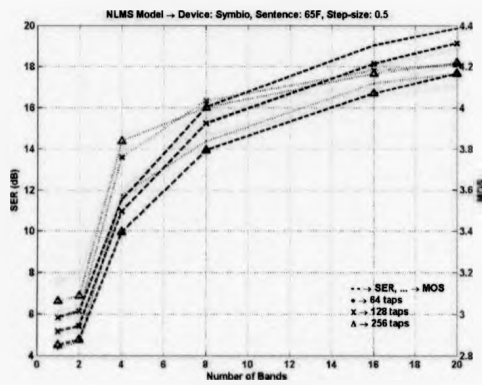
Figure C.1: Signal-to-error ratio and PESQ mean-opinion score for NLMS modeling parameters.



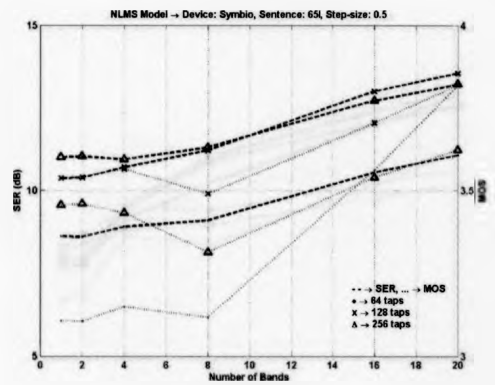
(a) Step-size 0.1, Audiogram F



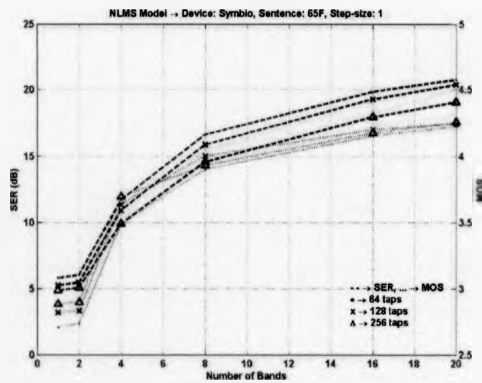
(b) Step-size 0.1, Audiogram I



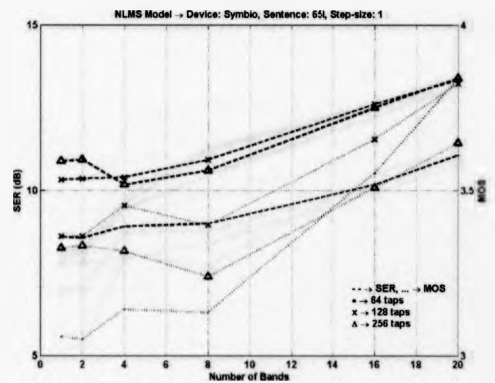
(c) Step-size 0.5, Audiogram F



(d) Step-size 0.5, Audiogram I

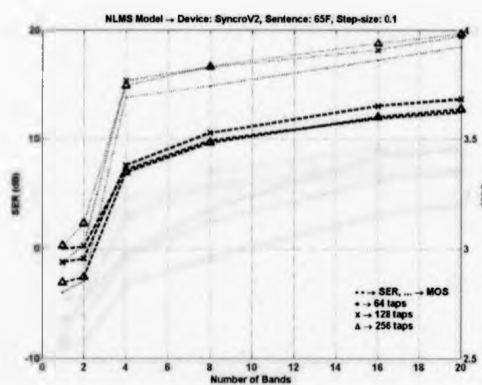


(e) Step-size 1.0, Audiogram F

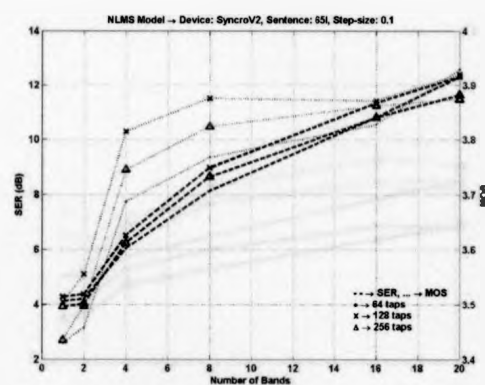


(f) Step-size 1.0, Audiogram I

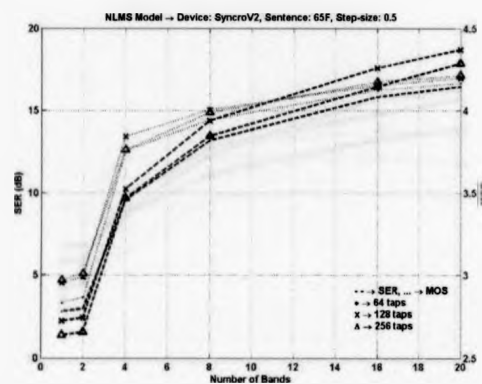
Fig. C.1: NLMS Model, SER-MOS, Bernafon Symbio 110 XT SE



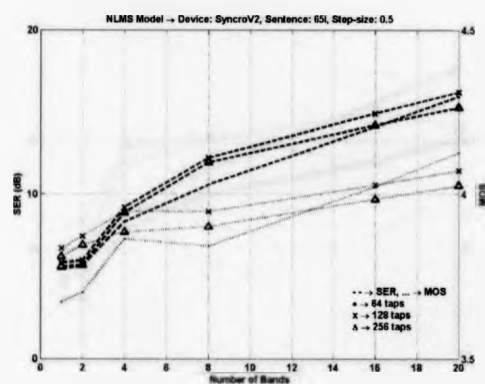
(a) Step-size 0.1, Audiogram F



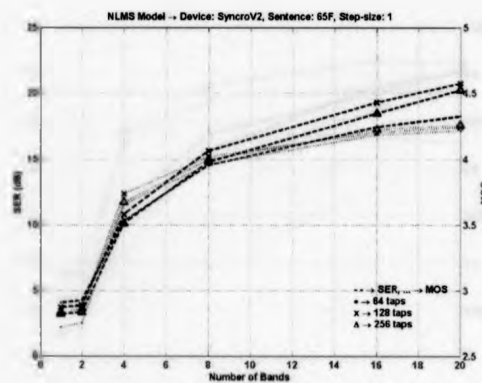
(b) Step-size 0.1, Audiogram I



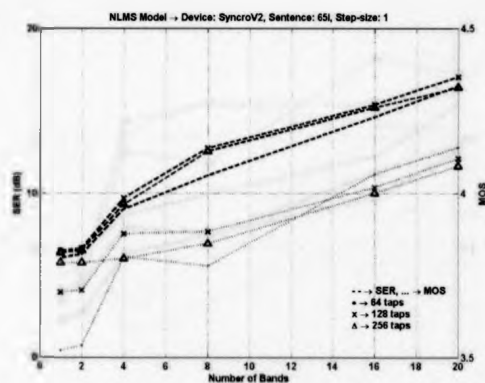
(c) Step-size 0.5, Audiogram F



(d) Step-size 0.5, Audiogram I

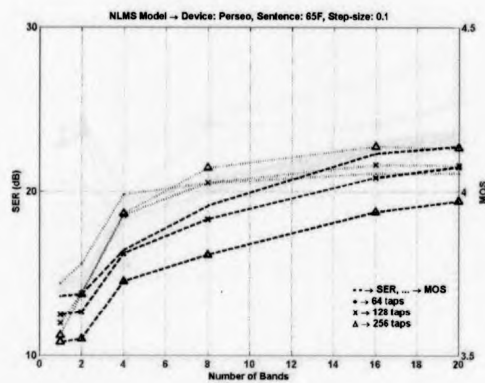


(e) Step-size 1.0, Audiogram F

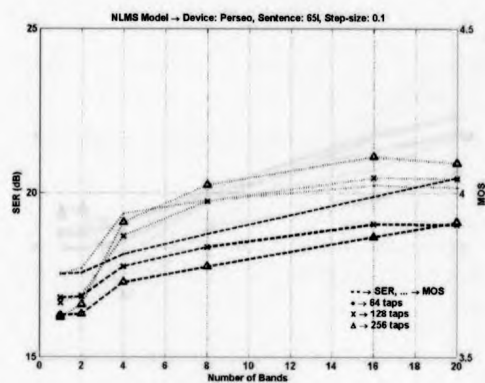


(f) Step-size 1.0, Audiogram I

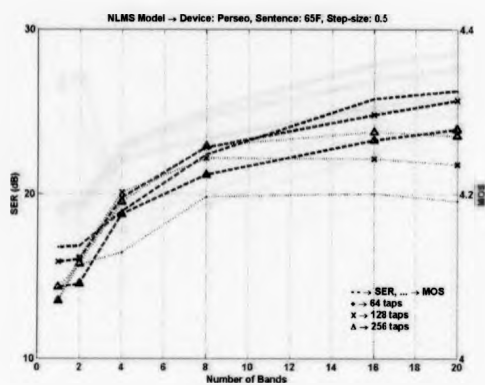
Fig. C.2: NLMS Model, SER-MOS, Oticon Syncro V2



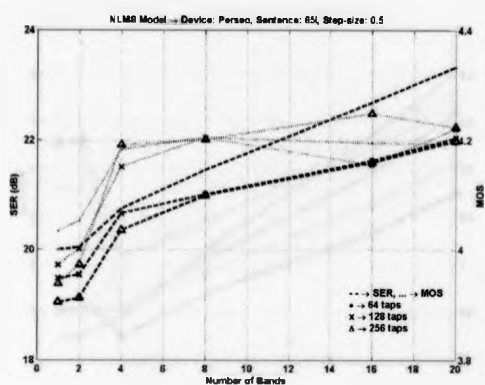
(a) Step-size 0.1, Audiogram F



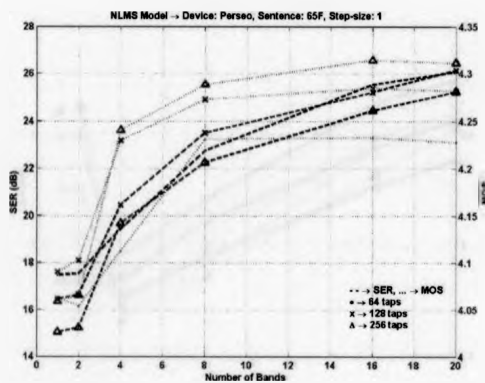
(b) Step-size 0.1, Audiogram I



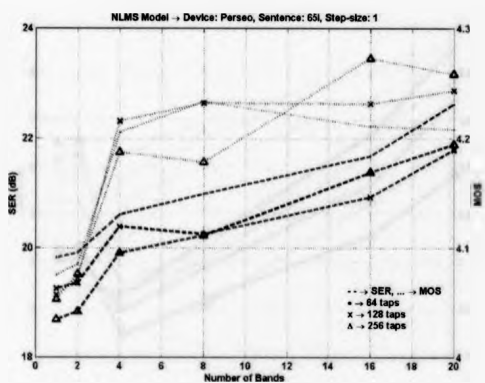
(c) Step-size 0.5, Audiogram F



(d) Step-size 0.5, Audiogram I

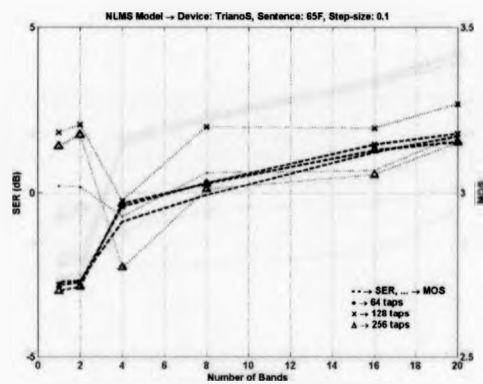


(e) Step-size 1.0, Audiogram F

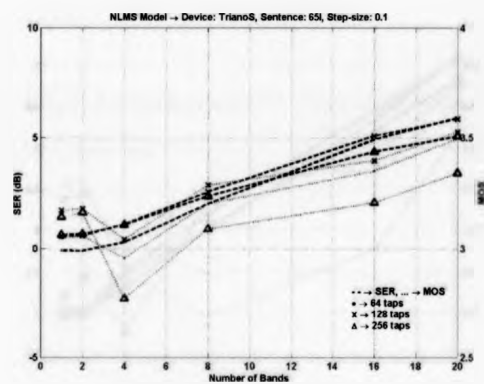


(f) Step-size 1.0, Audiogram I

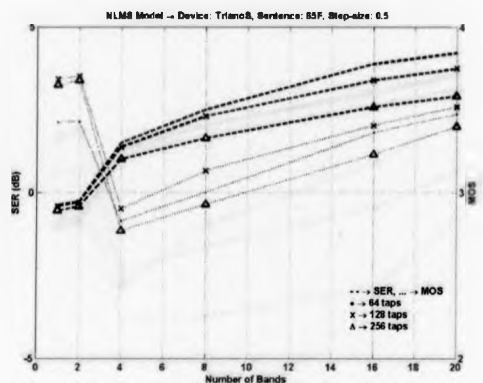
Fig. C.3: NLMS Model, SER-MOS, Phonak Perseo 311 dAZ Forte



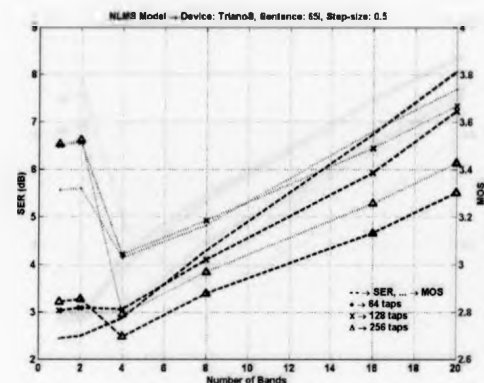
(a) Step-size 0.1, Audiogram F



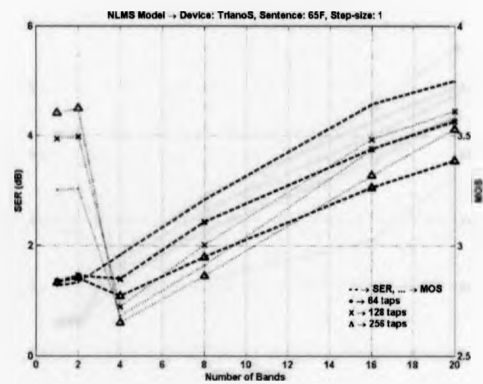
(b) Step-size 0.1, Audiogram I



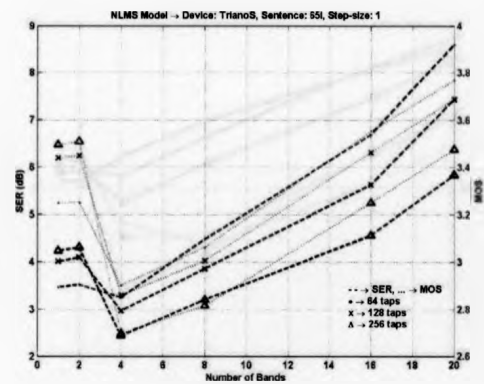
(c) Step-size 0.5, Audiogram F



(d) Step-size 0.5, Audiogram I

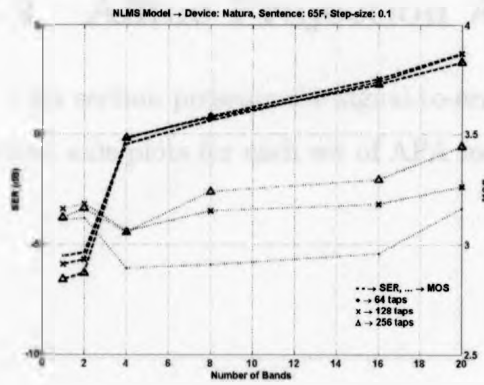


(e) Step-size 1.0, Audiogram F

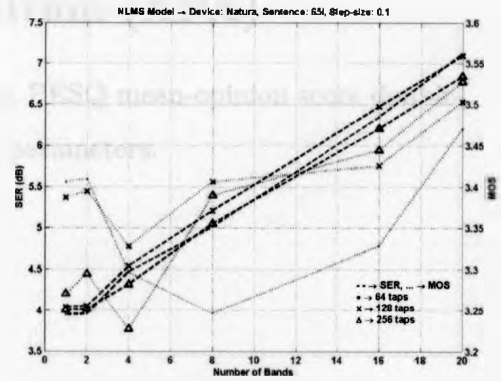


(f) Step-size 1.0, Audiogram I

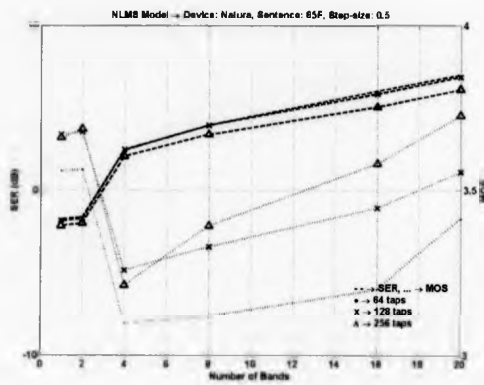
Fig. C.4: NLMS Model, SER-MOS, Siemens Triano S



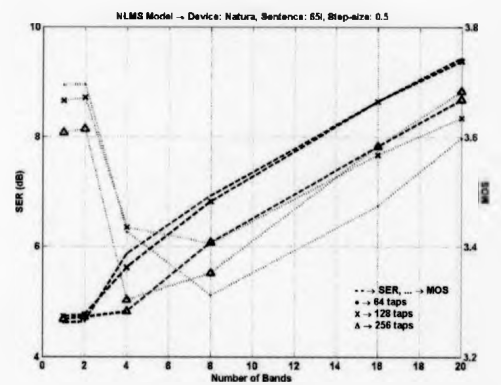
(a) Step-size 0.1, Audiogram F



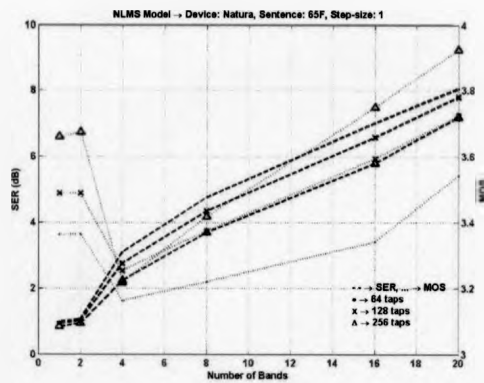
(b) Step-size 0.1, Audiogram I



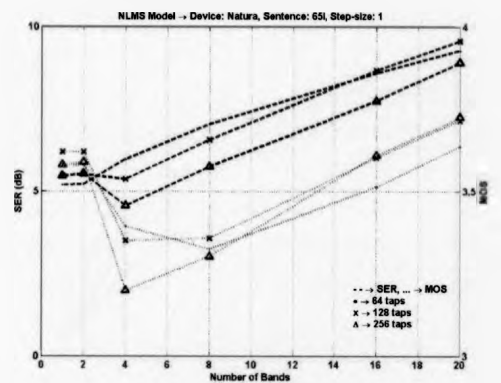
(c) Step-size 0.5, Audiogram F



(d) Step-size 0.5, Audiogram I



(e) Step-size 1.0, Audiogram F



(f) Step-size 1.0, Audiogram I

Fig. C.5: NLMS Model, SER-MOS, Sonic Innovations Natura 2 SE

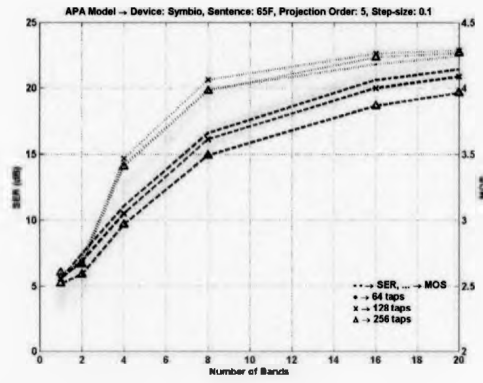
## C.2 Affine Projection Algorithm (APA)

This section presents the signal-to-error ratio, PESQ mean-opinion score double-vertical axis plots for each set of APA modeling parameters.

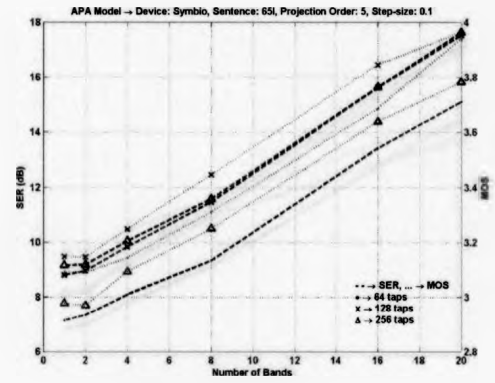


Fig. 5.10. APA modeling parameters, SER and PESQ double-vertical axis plots.

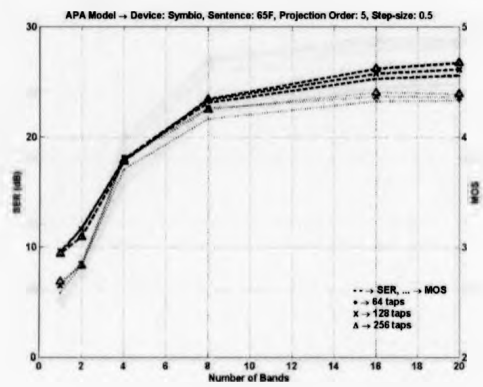




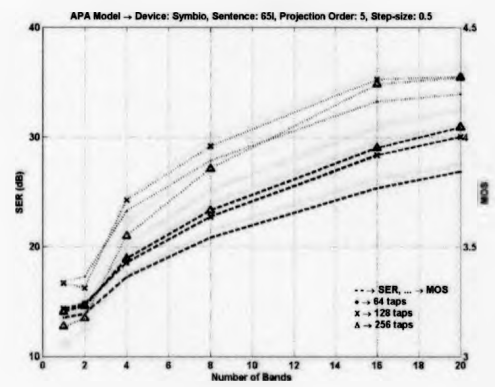
(a) Projection-order 5, Step-size 0.1, Audiogram F



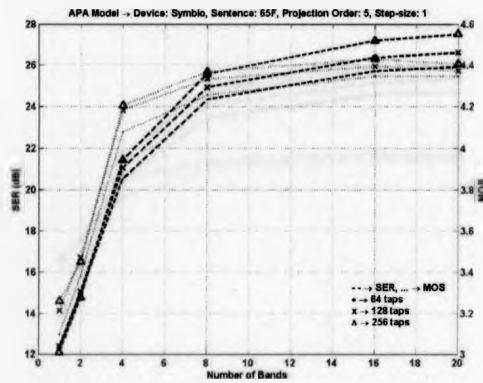
(b) Projection-order 5, Step-size 0.1, Audiogram I



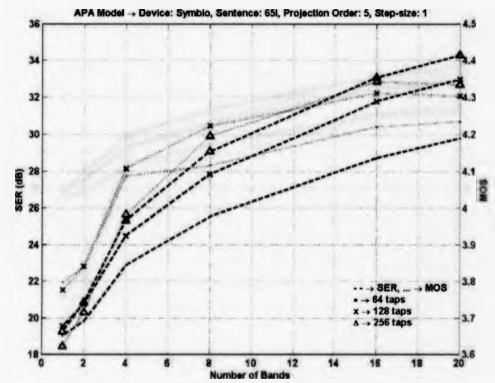
(c) Projection-order 5, Step-size 0.5, Audiogram F



(d) Projection-order 5, Step-size 0.5, Audiogram I

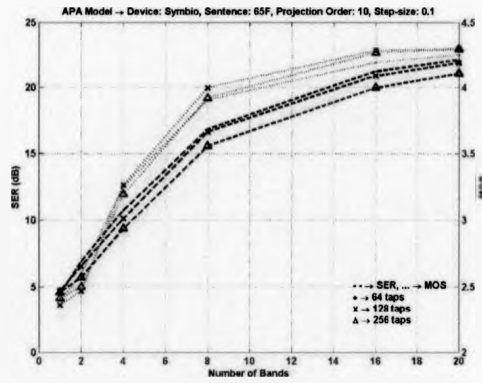


(e) Projection-order 5, Step-size 1.0, Audiogram F

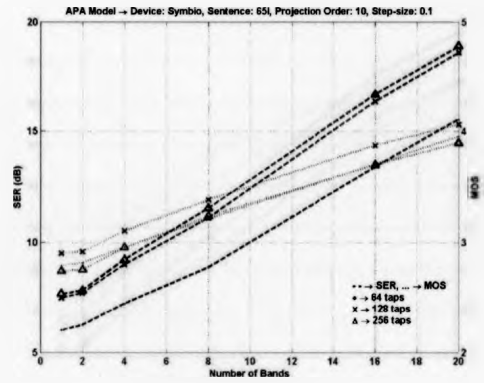


(f) Projection-order 5, Step-size 1.0, Audiogram I

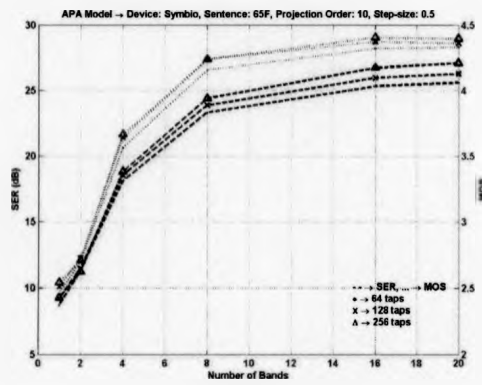
Fig. C.6: APA Model, SER-MOS, PO 5, Bernafon Symbio 110 XT SE



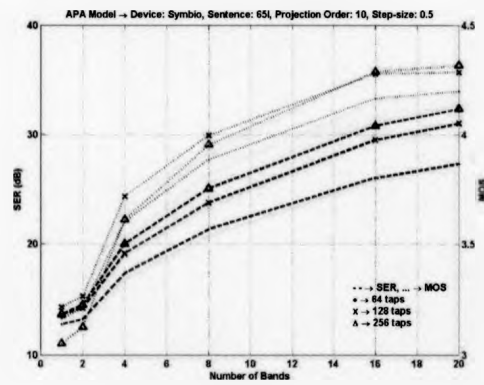
(a) Projection-order 10, Step-size 0.1, Audiogram F



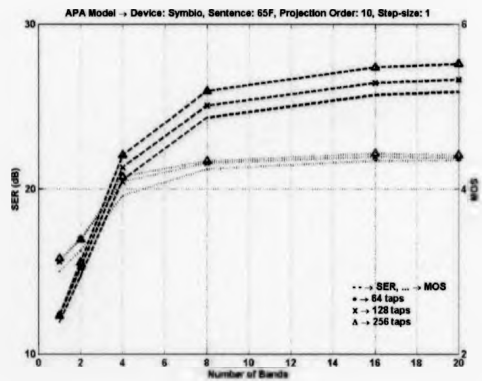
(b) Projection-order 10, Step-size 0.1, Audiogram I



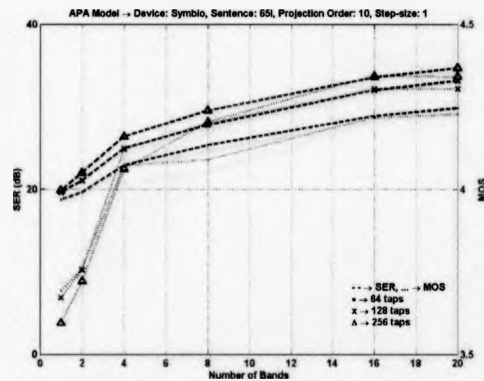
(c) Projection-order 10, Step-size 0.5, Audiogram F



(d) Projection-order 10, Step-size 0.5, Audiogram I

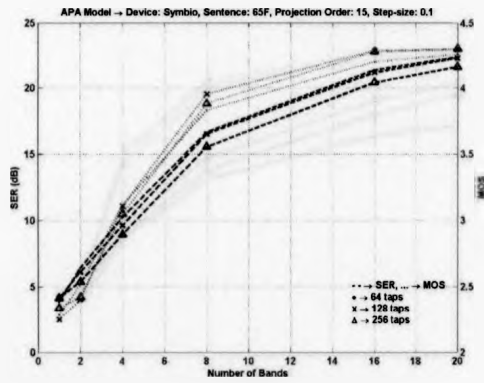


(e) Projection-order 10, Step-size 1.0, Audiogram F

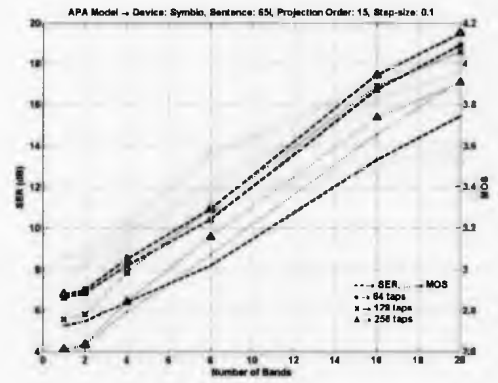


(f) Projection-order 10, Step-size 1.0, Audiogram I

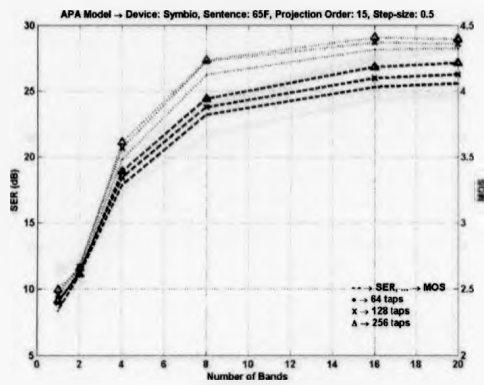
Fig. C.7: APA Model, SER-MOS, PO 10, Bernafon Symbio 110 XT SE



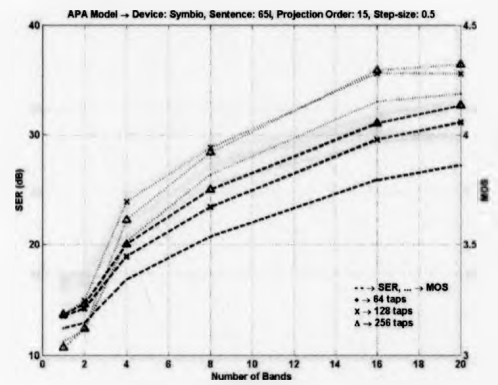
(a) Projection-order 15, Step-size 0.1, Audiogram F



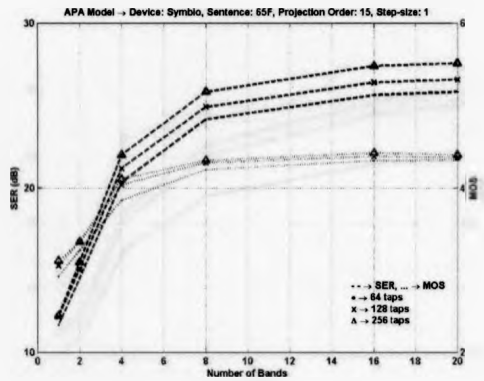
(b) Projection-order 15, Step-size 0.1, Audiogram I



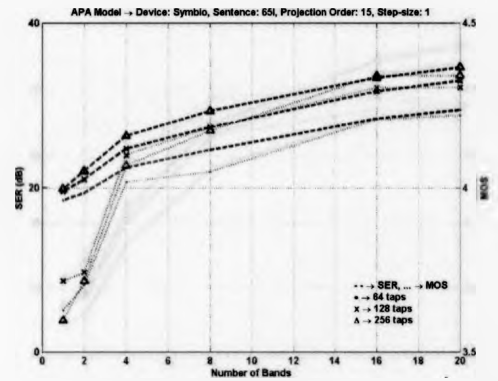
(c) Projection-order 15, Step-size 0.5, Audiogram F



(d) Projection-order 15, Step-size 0.5, Audiogram I

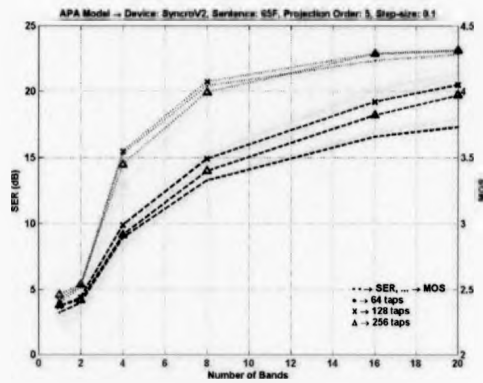


(e) Projection-order 15, Step-size 1.0, Audiogram F

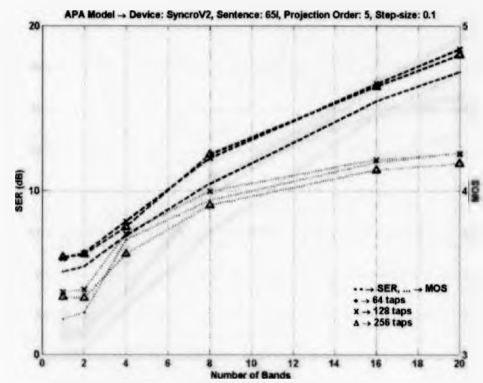


(f) Projection-order 15, Step-size 1.0, Audiogram I

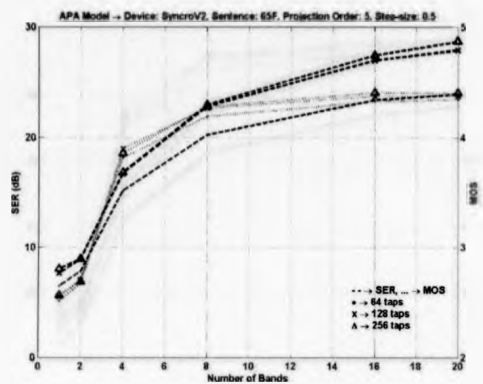
Fig. C.8: APA Model, SER-MOS, PO 15, Bernafon Symbio 110 XT SE



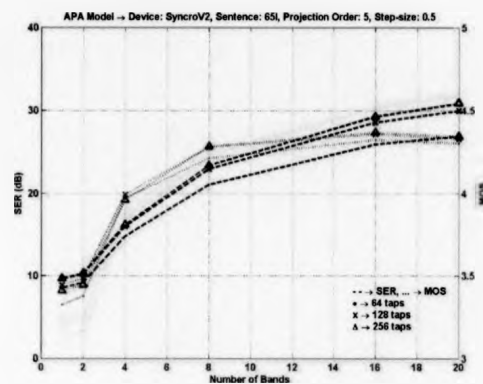
(a) Projection-order 5, Step-size 0.1, Audiogram F



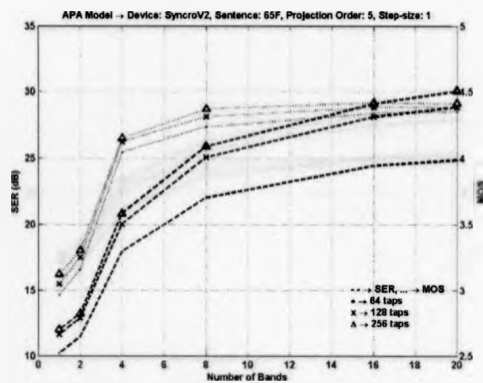
(b) Projection-order 5, Step-size 0.1, Audiogram I



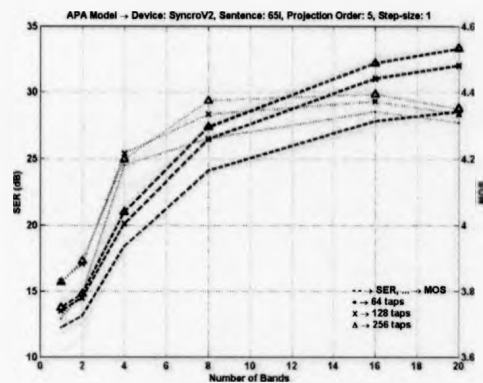
(c) Projection-order 5, Step-size 0.5, Audiogram F



(d) Projection-order 5, Step-size 0.5, Audiogram I

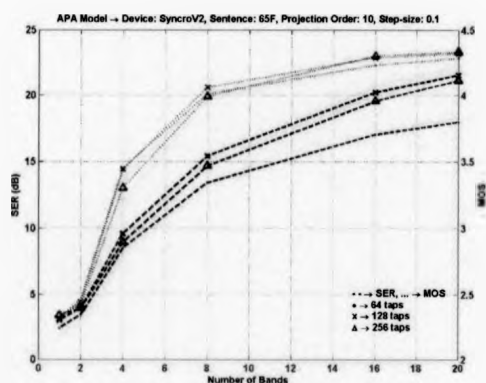


(e) Projection-order 5, Step-size 1.0, Audiogram F

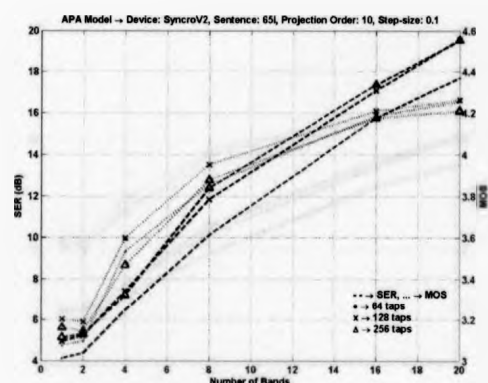


(f) Projection-order 5, Step-size 1.0, Audiogram I

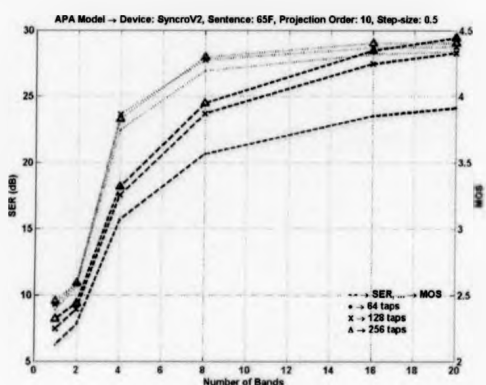
Fig. C.9: APA Model, SER-MOS, PO 5, Oticon Syncro V2



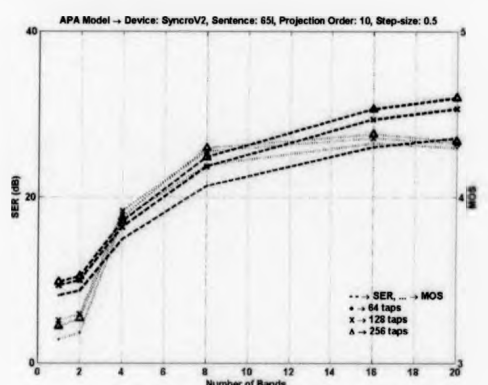
(a) Projection-order 10, Step-size 0.1, Audiogram F



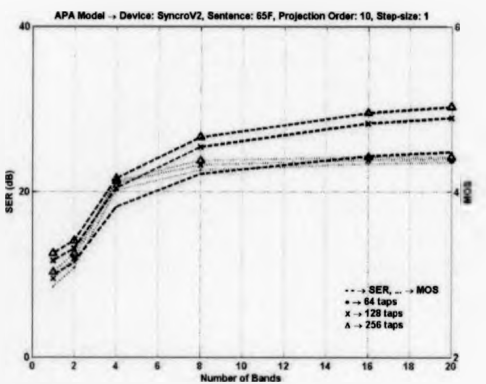
(b) Projection-order 10, Step-size 0.1, Audiogram I



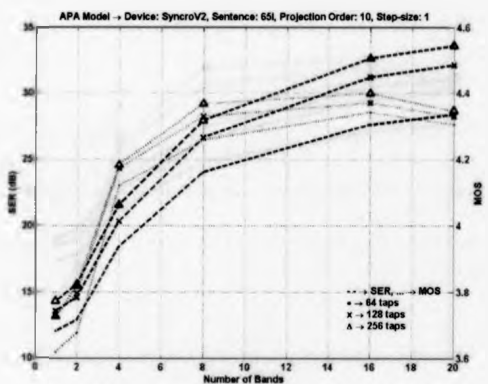
(c) Projection-order 10, Step-size 0.5, Audiogram F



(d) Projection-order 10, Step-size 0.5, Audiogram I

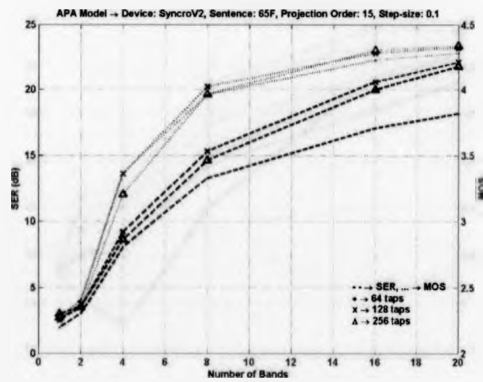


(e) Projection-order 10, Step-size 1.0, Audiogram F

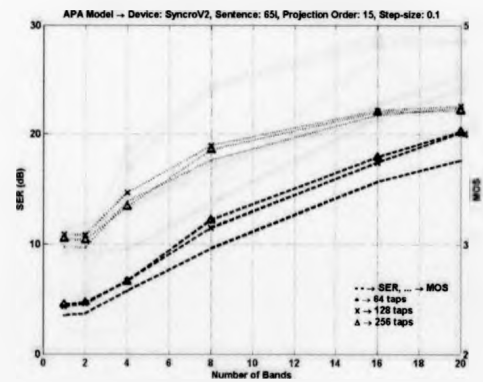


(f) Projection-order 10, Step-size 1.0, Audiogram I

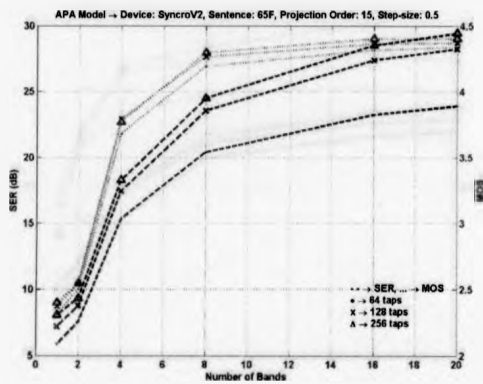
Fig. C.10: APA Model, SER-MOS, PO 10, Oticon Syncro V2



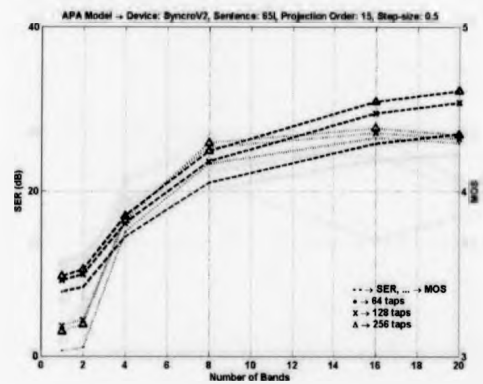
(a) Projection-order 15, Step-size 0.1, Audiogram F



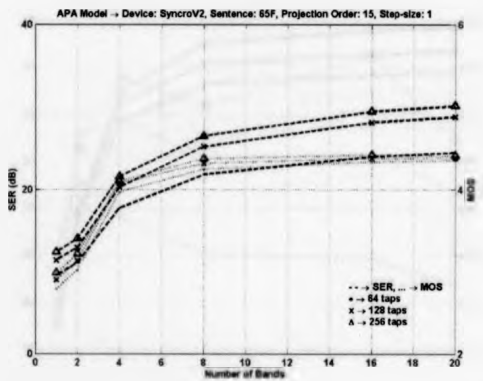
(b) Projection-order 15, Step-size 0.1, Audiogram I



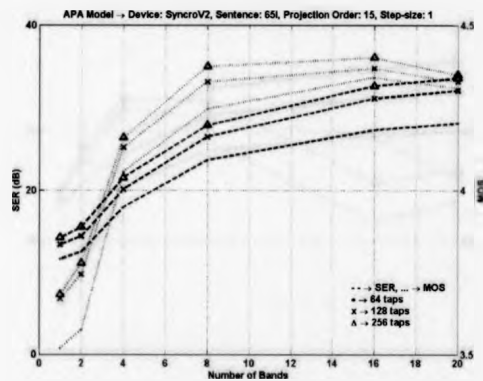
(c) Projection-order 15, Step-size 0.5, Audiogram F



(d) Projection-order 15, Step-size 0.5, Audiogram I

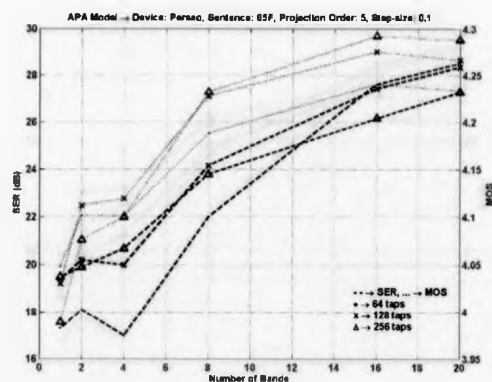


(e) Projection-order 15, Step-size 1.0, Audiogram F

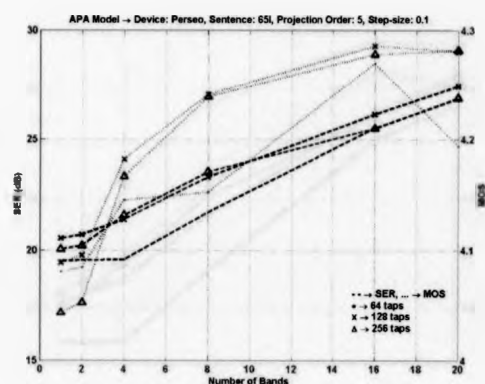


(f) Projection-order 15, Step-size 1.0, Audiogram I

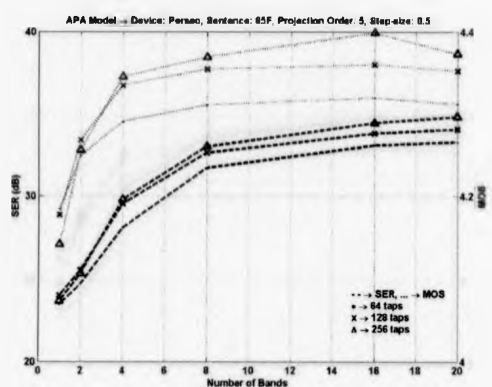
Fig. C.11: APA Model, SER-MOS, PO 15, Oticon Syncro V2



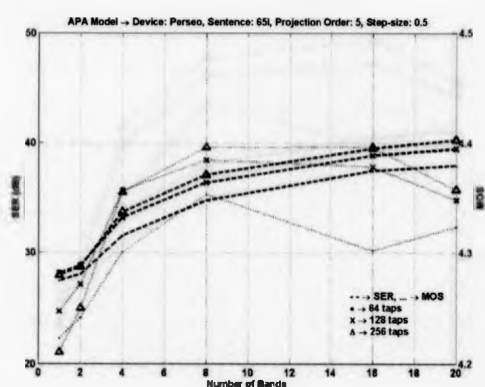
(a) Projection-order 5, Step-size 0.1, Audiogram F



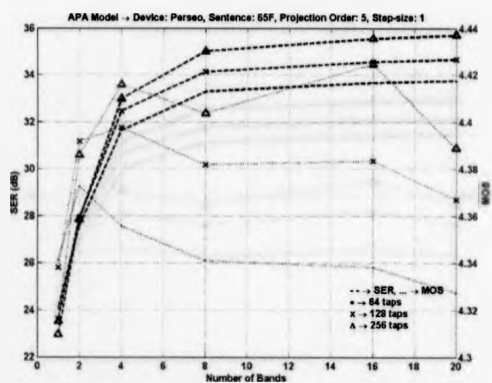
(b) Projection-order 5, Step-size 0.1, Audiogram I



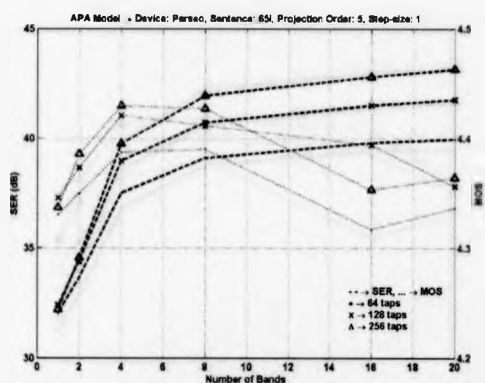
(c) Projection-order 5, Step-size 0.5, Audiogram F



(d) Projection-order 5, Step-size 0.5, Audiogram I



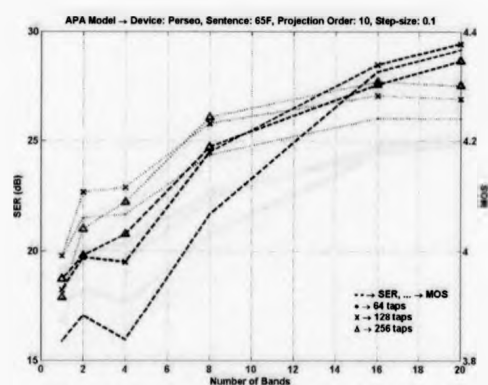
(e) Projection-order 5, Step-size 1.0, Audiogram F



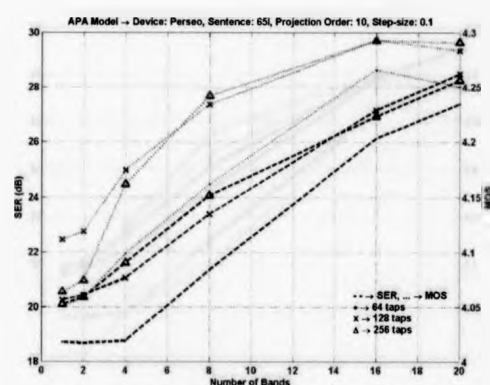
(f) Projection-order 5, Step-size 1.0, Audiogram I

Fig. C.12: APA Model, SER-MOS, PO 5, Phonak Perseo 311 dAZ Forte

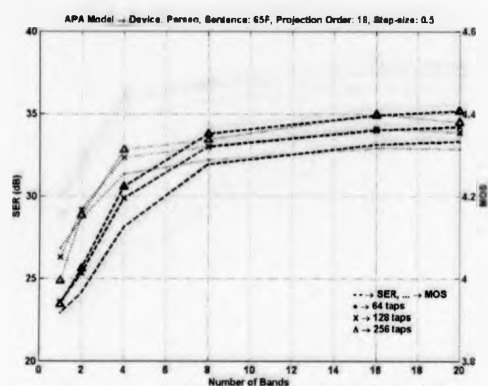




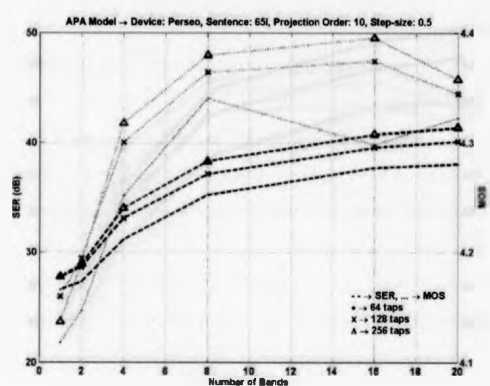
(a) Projection-order 10, Step-size 0.1, Audiogram F



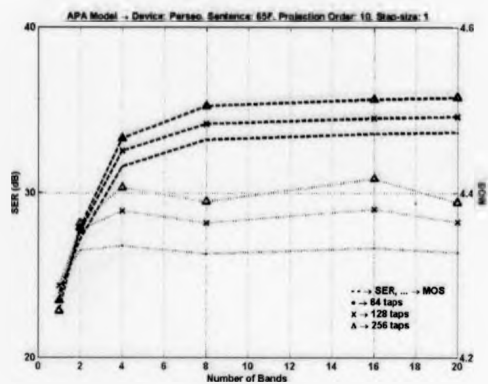
(b) Projection-order 10, Step-size 0.1, Audiogram I



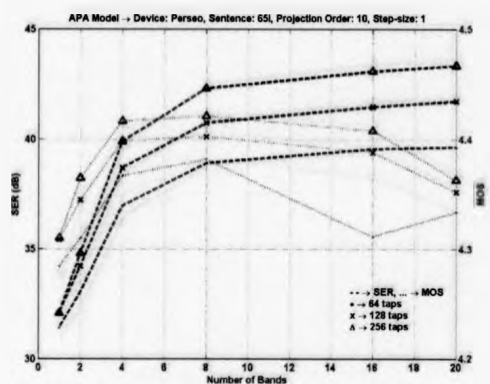
(c) Projection-order 10, Step-size 0.5, Audiogram F



(d) Projection-order 10, Step-size 0.5, Audiogram I



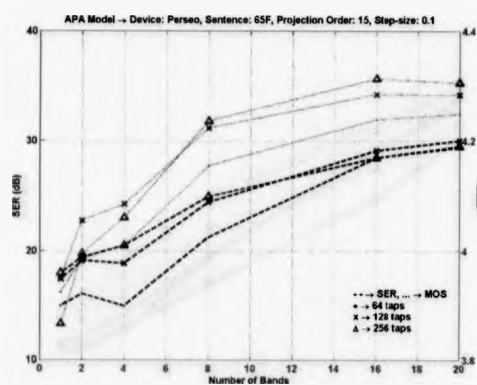
(e) Projection-order 10, Step-size 1.0, Audiogram F



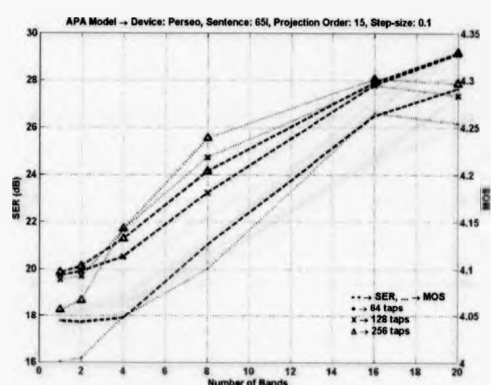
(f) Projection-order 10, Step-size 1.0, Audiogram I

Fig. C.13: APA Model, SER-MOS, PO 10, Phonak Persco 311 dAZ Forte

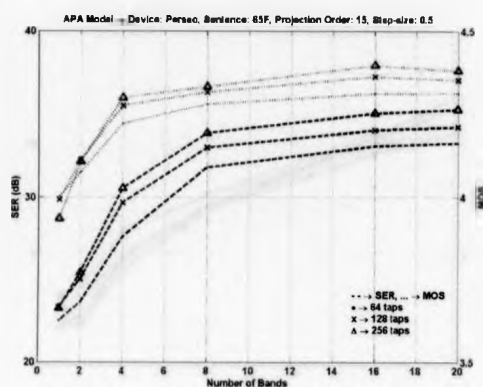




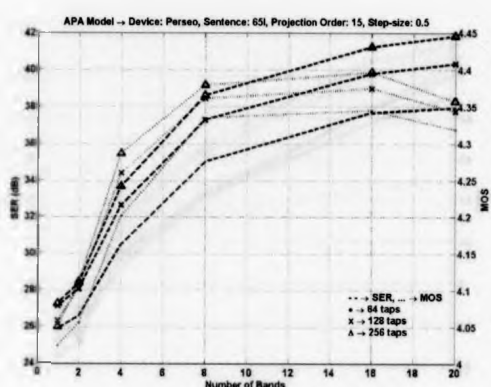
(a) Projection-order 15, Step-size 0.1, Audiogram F



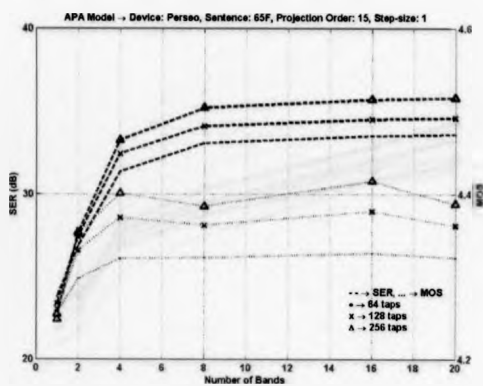
(b) Projection-order 15, Step-size 0.1, Audiogram I



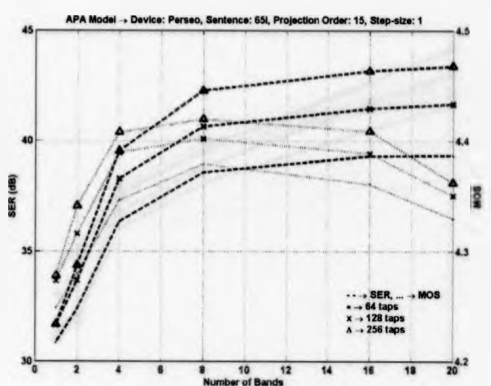
(c) Projection-order 15, Step-size 0.5, Audiogram F



(d) Projection-order 15, Step-size 0.5, Audiogram I

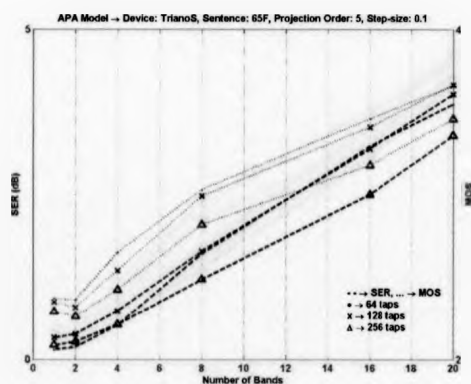


(e) Projection-order 15, Step-size 1.0, Audiogram F

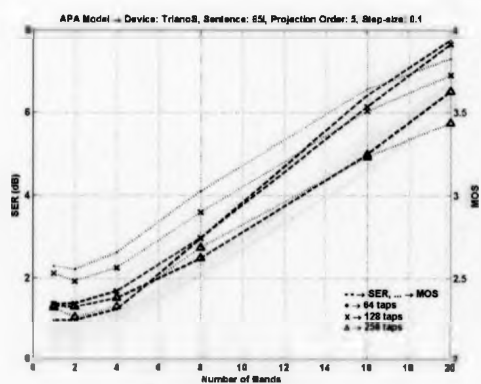


(f) Projection-order 15, Step-size 1.0, Audiogram I

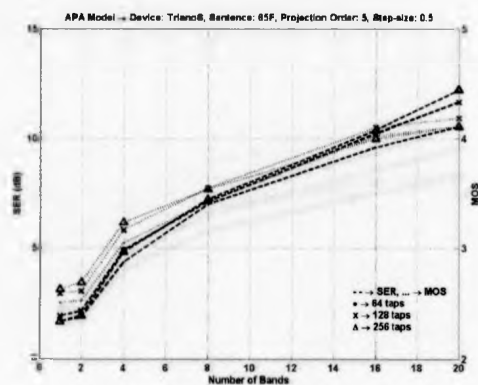
Fig. C.14: APA Model, SER-MOS, PO 15, Phonak Perseo 311 dAZ Forte



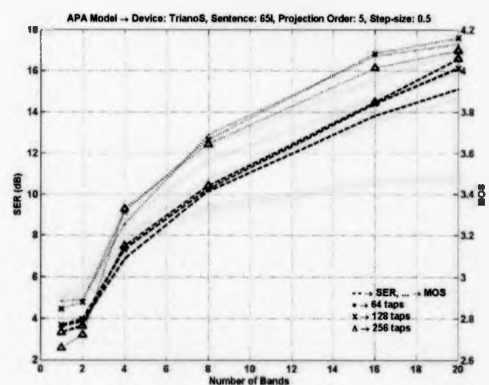
(a) Projection-order 5, Step-size 0.1, Audiogram F



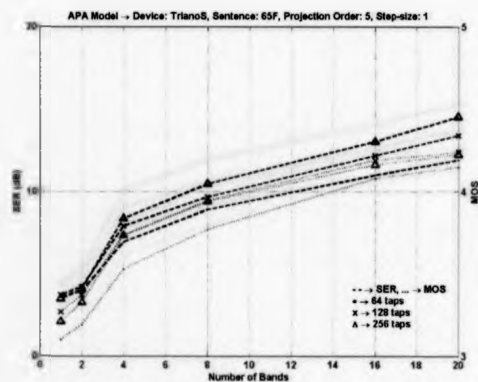
(b) Projection-order 5, Step-size 0.1, Audiogram I



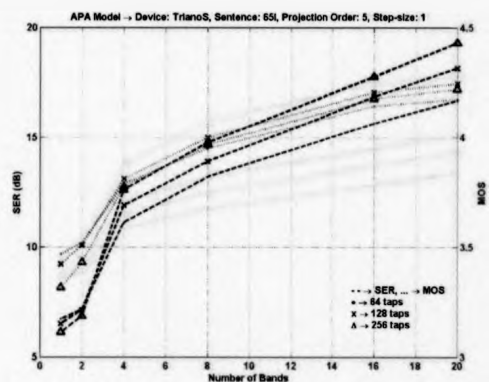
(c) Projection-order 5, Step-size 0.5, Audiogram F



(d) Projection-order 5, Step-size 0.5, Audiogram I

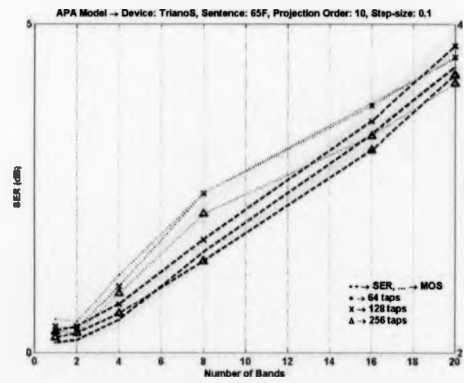


(e) Projection-order 5, Step-size 1.0, Audiogram F

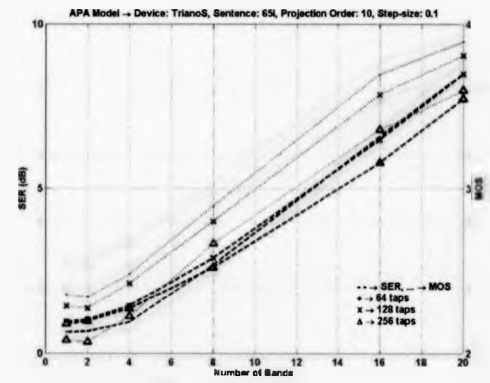


(f) Projection-order 5, Step-size 1.0, Audiogram I

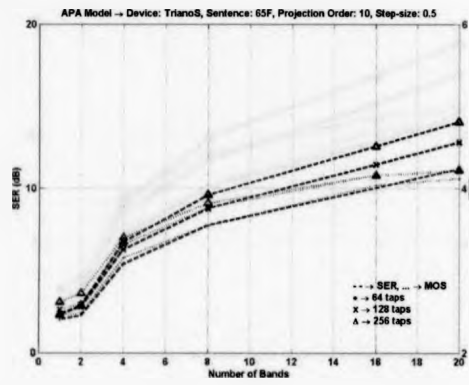
Fig. C.15: APA Model, SER-MOS, PO 5, Siemens Triano S



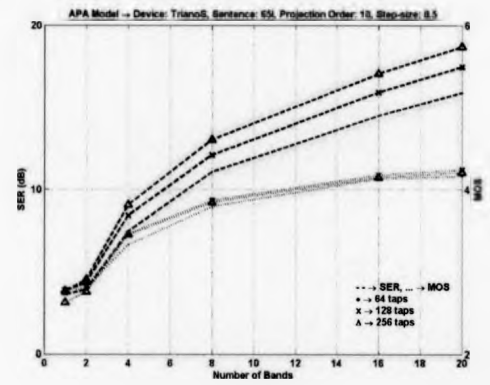
(a) Projection-order 10, Step-size 0.1, Audiogram F



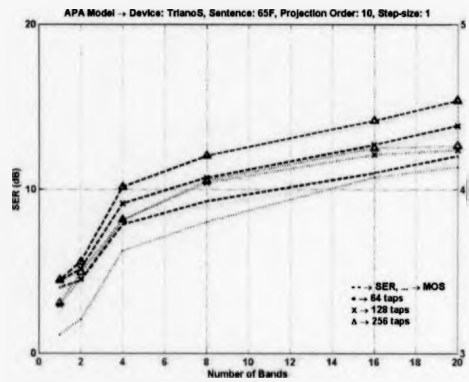
(b) Projection-order 10, Step-size 0.1, Audiogram I



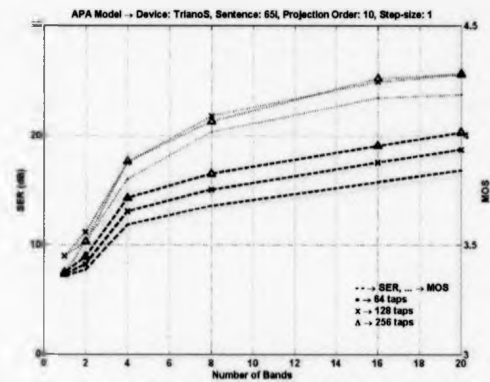
(c) Projection-order 10, Step-size 0.5, Audiogram F



(d) Projection-order 10, Step-size 0.5, Audiogram I

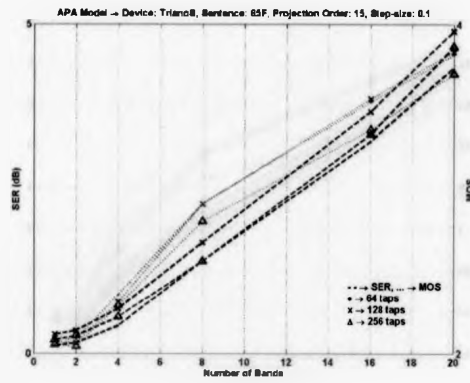


(e) Projection-order 10, Step-size 1.0, Audiogram F

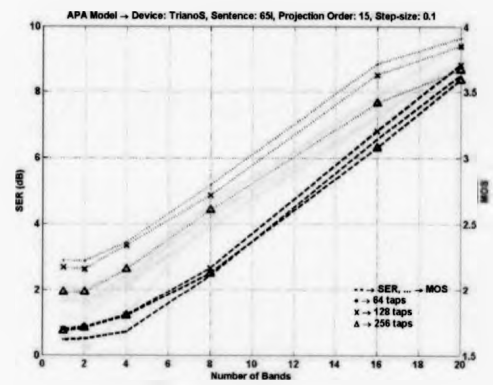


(f) Projection-order 10, Step-size 1.0, Audiogram I

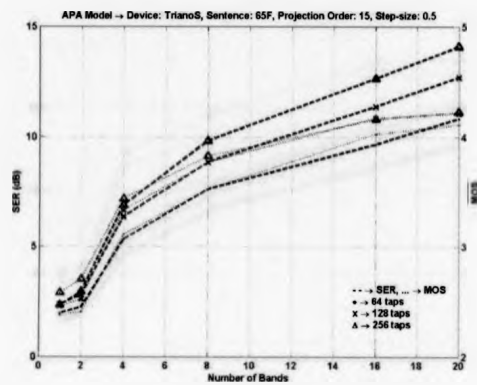
Fig. C.16: APA Model, SER-MOS, PO 10, Siemens Triano S



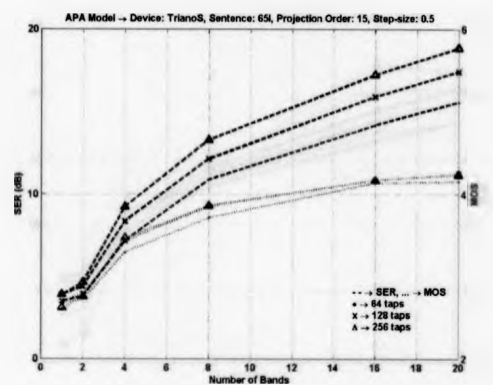
(a) Projection-order 15, Step-size 0.1, Audiogram F



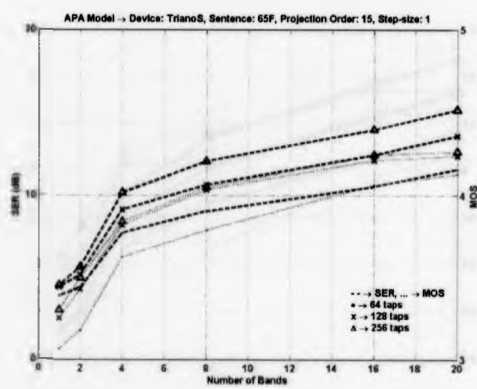
(b) Projection-order 15, Step-size 0.1, Audiogram I



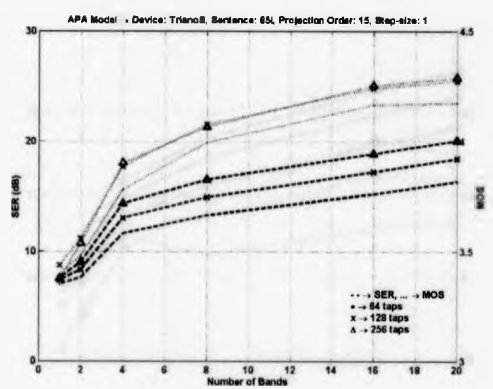
(c) Projection-order 15, Step-size 0.5, Audiogram F



(d) Projection-order 15, Step-size 0.5, Audiogram I

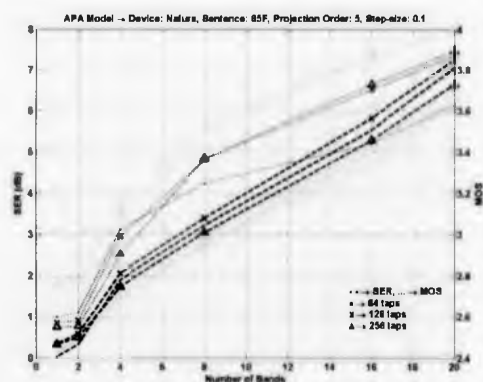


(e) Projection-order 15, Step-size 1.0, Audiogram F

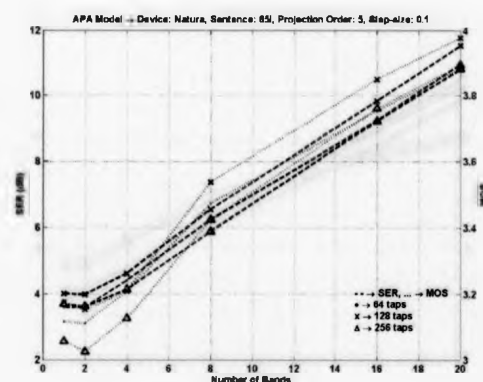


(f) Projection-order 15, Step-size 1.0, Audiogram I

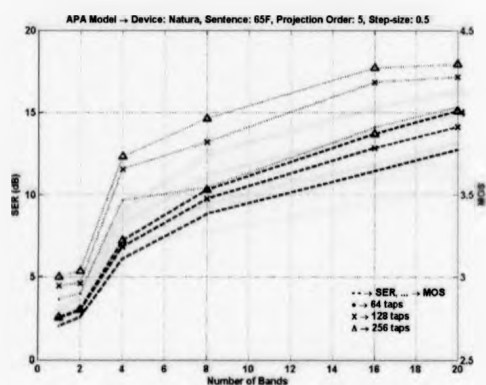
Fig. C.17: APA Model, SER-MOS, PO 15, Siemens Triano S



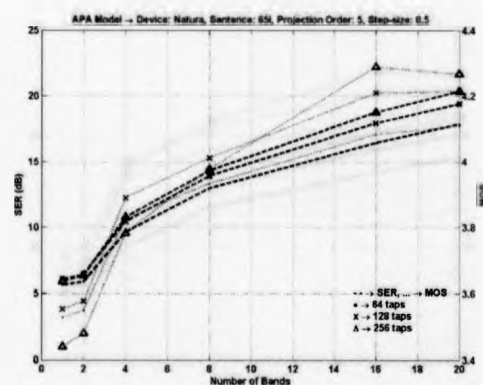
(a) Projection-order 5, Step-size 0.1, Audiogram F



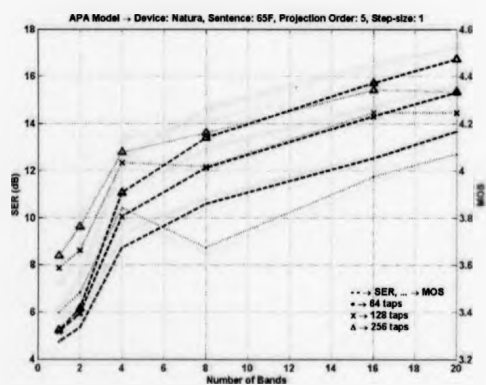
(b) Projection-order 5, Step-size 0.1, Audiogram I



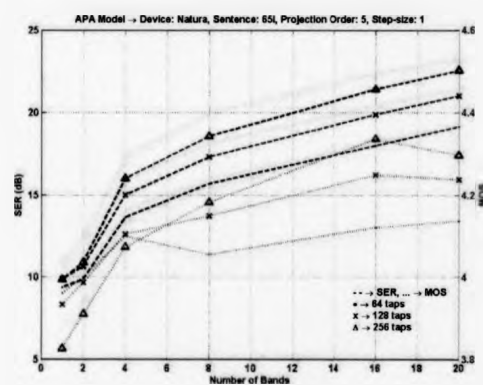
(c) Projection-order 5, Step-size 0.5, Audiogram F



(d) Projection-order 5, Step-size 0.5, Audiogram I

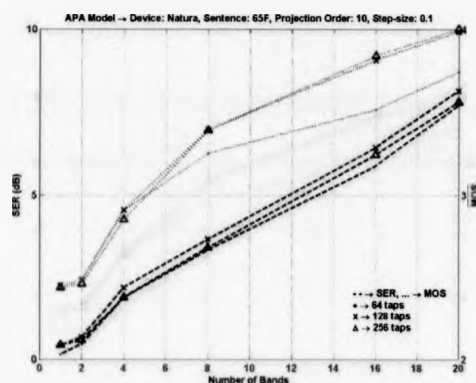


(e) Projection-order 5, Step-size 1.0, Audiogram F

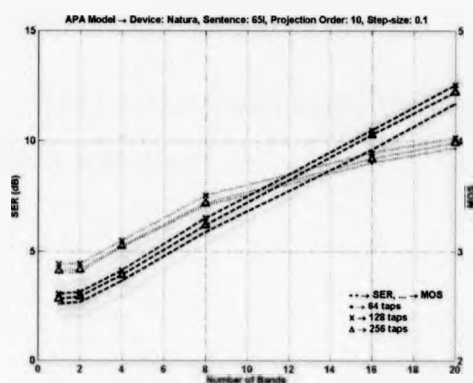


(f) Projection-order 5, Step-size 1.0, Audiogram I

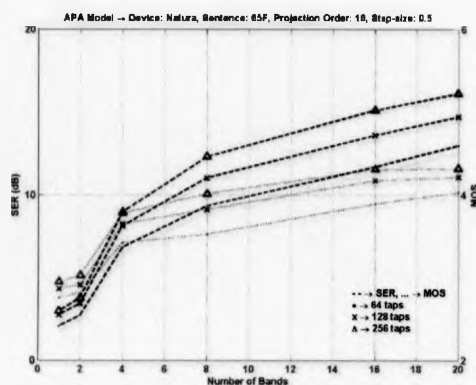
Fig. C.18: APA Model, SER-MOS, PO 5, Sonic Innovations Natura 2 SE



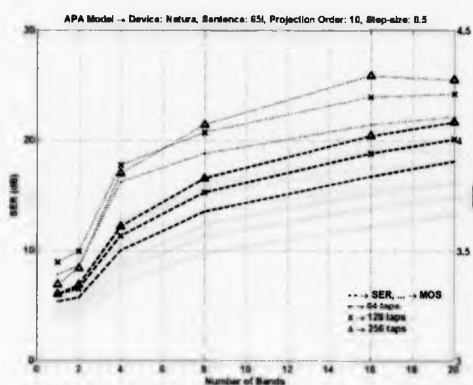
(a) Projection-order 10, Step-size 0.1, Audiogram F



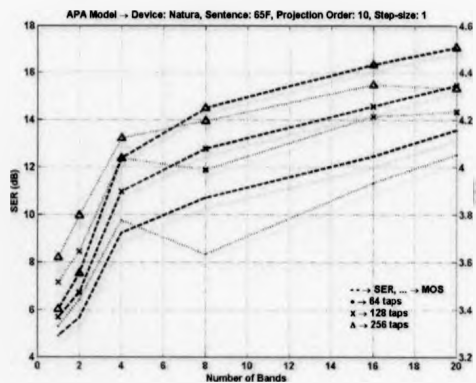
(b) Projection-order 10, Step-size 0.1, Audiogram I



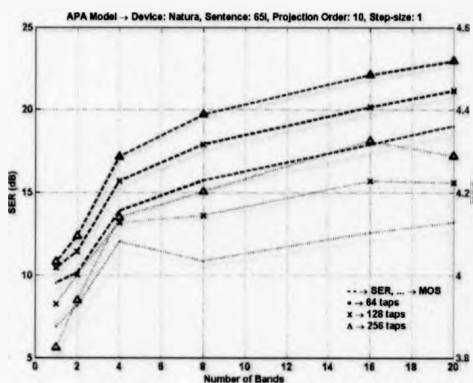
(c) Projection-order 10, Step-size 0.5, Audiogram F



(d) Projection-order 10, Step-size 0.5, Audiogram I

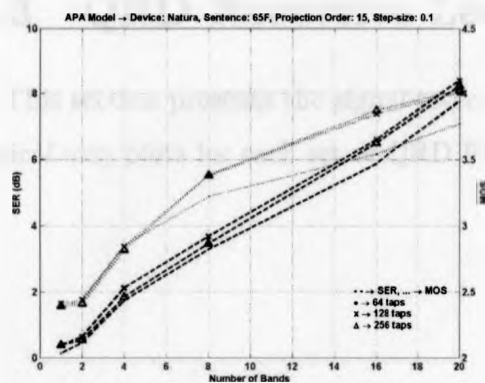


(e) Projection-order 10, Step-size 1.0, Audiogram F

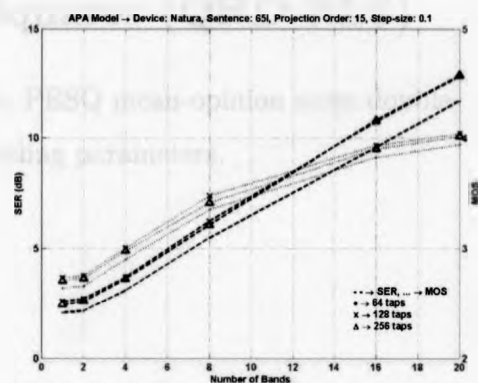


(f) Projection-order 10, Step-size 1.0, Audiogram I

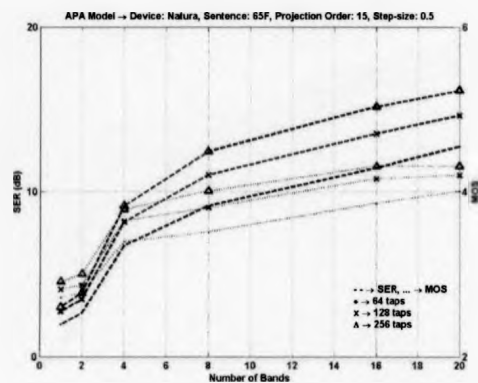
Fig. C.19: APA Model, SER-MOS, PO 10, Sonic Innovations Natura 2 SE



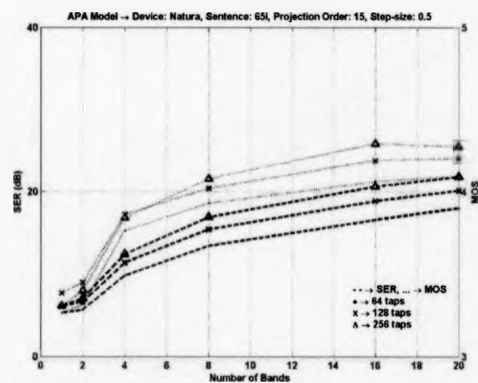
(a) Projection-order 15, Step-size 0.1, Audiogram F



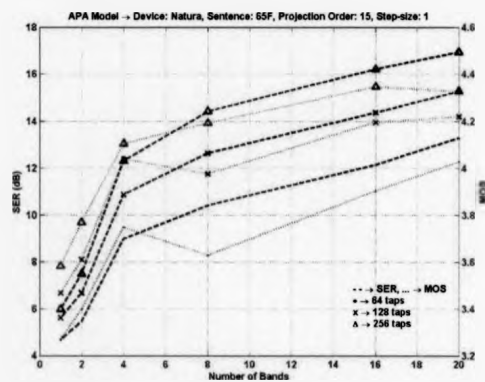
(b) Projection-order 15, Step-size 0.1, Audiogram I



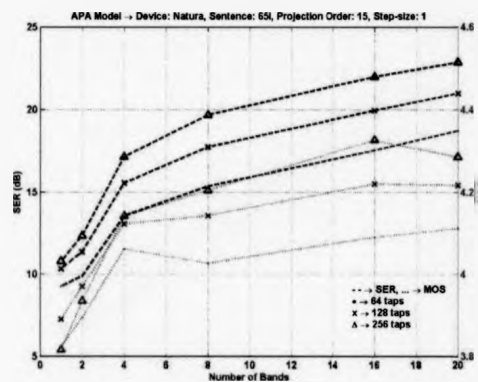
(c) Projection-order 15, Step-size 0.5, Audiogram F



(d) Projection-order 15, Step-size 0.5, Audiogram I



(e) Projection-order 15, Step-size 1.0, Audiogram F



(f) Projection-order 15, Step-size 1.0, Audiogram I

Fig. C.20: APA Model, SER-MOS, PO 15, Sonic Innovations Natura 2 SE

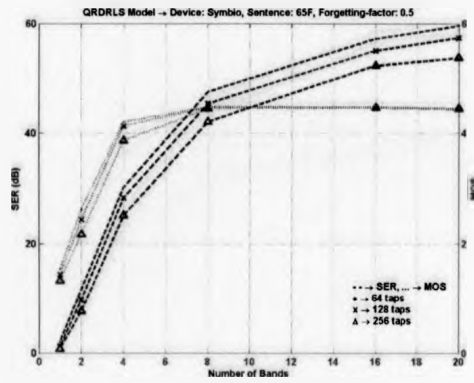


### C.3 QRD Recursive Least Squares (QRD RLS)

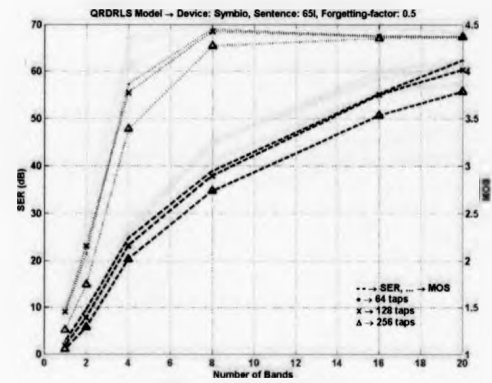
This section presents the signal-to-error ratio, PESQ mean-opinion score double-vertical axis plots for each set of QRD RLS modeling parameters.



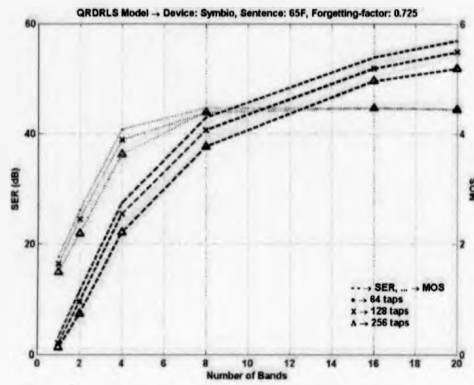




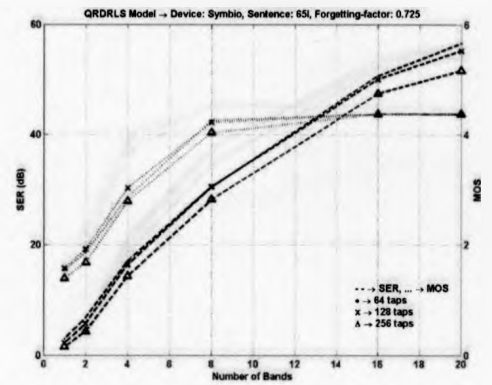
(a) Forgetting-factor 0.5, Audiogram F



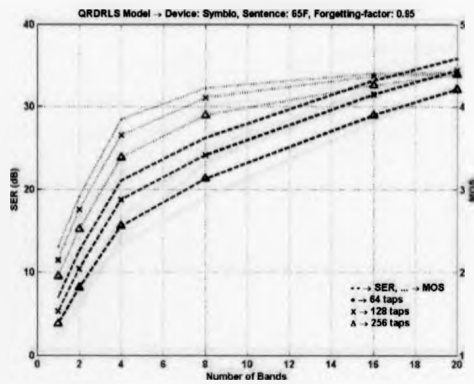
(b) Forgetting-factor 0.5, Audiogram I



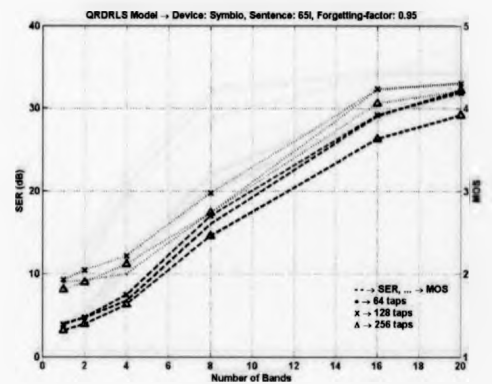
(c) Forgetting-factor 0.725, Audiogram F



(d) Forgetting-factor 0.725, Audiogram I

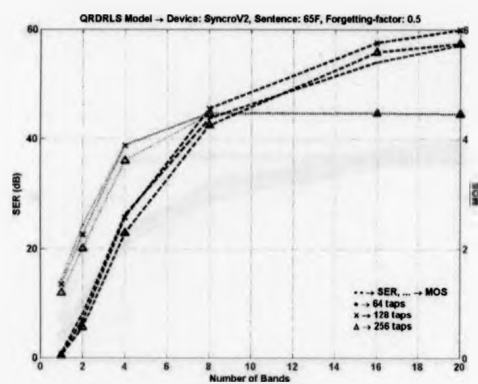


(e) Forgetting-factor 0.95, Audiogram F

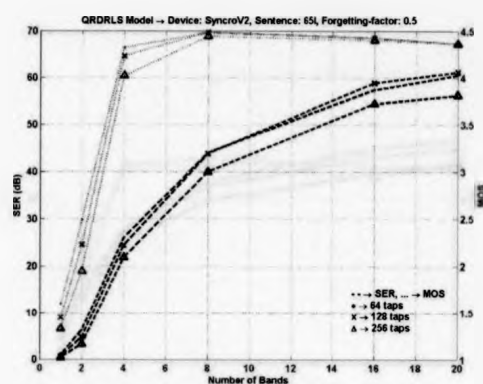


(f) Forgetting-factor 0.95, Audiogram I

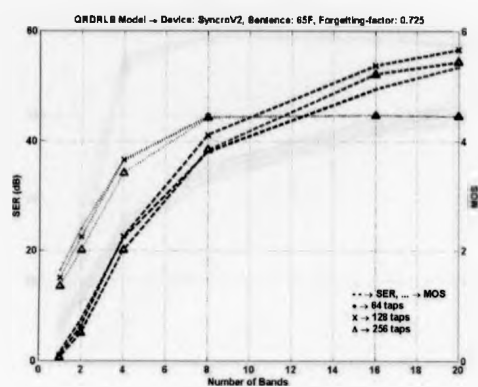
Fig. C.21: QRDRLS Model, SER-MOS, Bernafon Symbio 110 XT SE



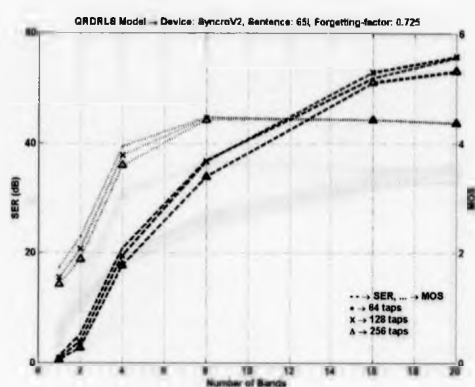
(a) Forgetting-factor 0.5, Audiogram F



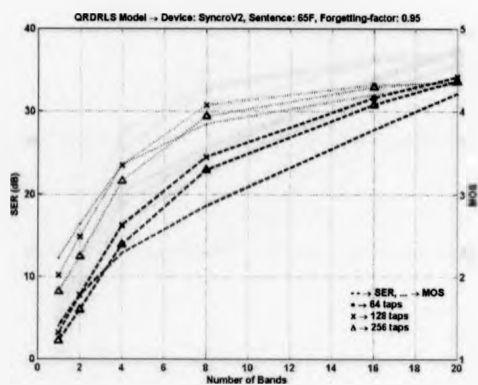
(b) Forgetting-factor 0.5, Audiogram I



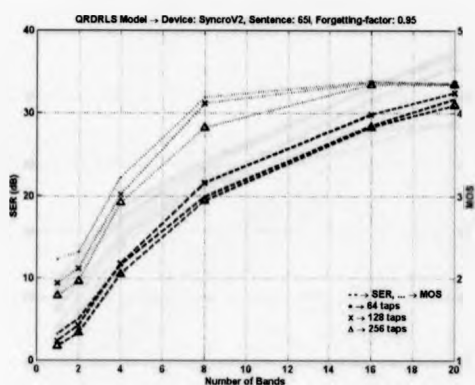
(c) Forgetting-factor 0.725, Audiogram F



(d) Forgetting-factor 0.725, Audiogram I

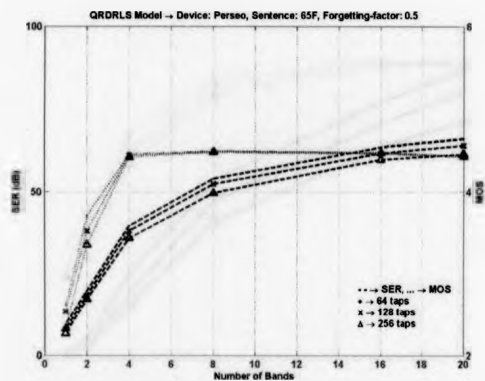


(e) Forgetting-factor 0.95, Audiogram F

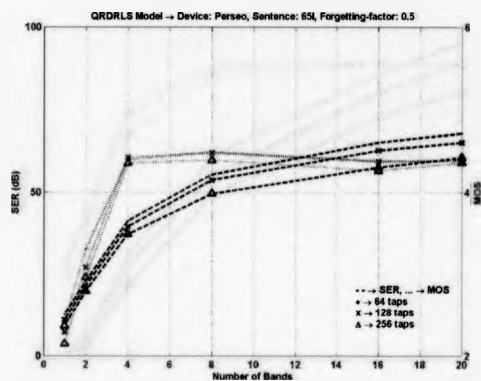


(f) Forgetting-factor 0.95, Audiogram I

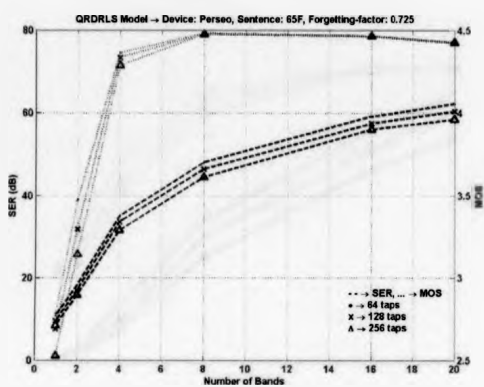
Fig. C.22: QRDRLS Model, SER-MOS, Oticon Synco V2



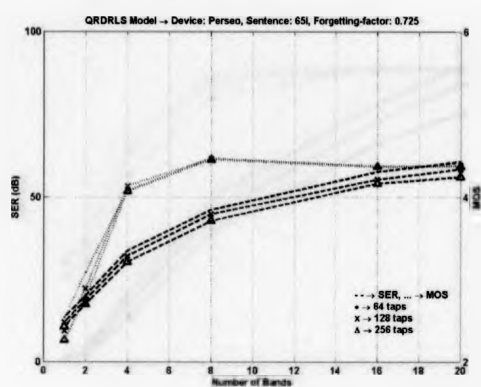
(a) Forgetting-factor 0.5, Audiogram F



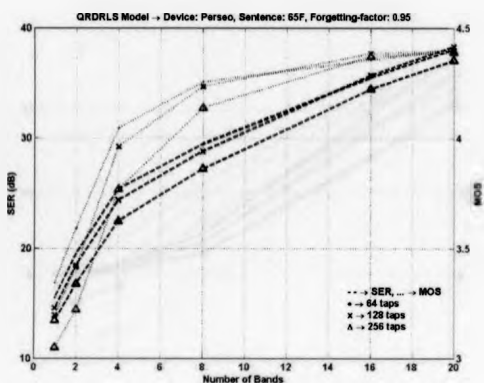
(b) Forgetting-factor 0.5, Audiogram I



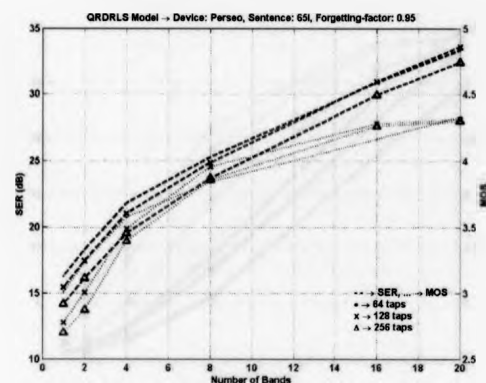
(c) Forgetting-factor 0.725, Audiogram F



(d) Forgetting-factor 0.725, Audiogram I

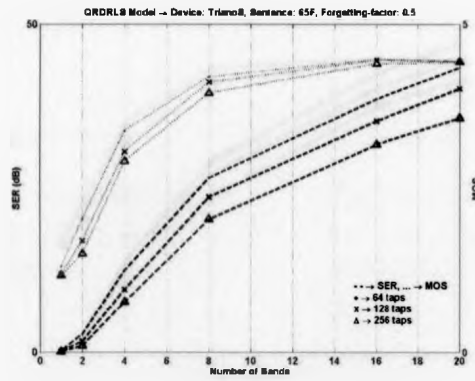


(e) Forgetting-factor 0.95, Audiogram F

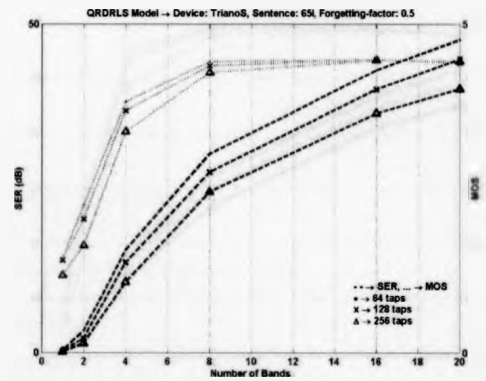


(f) Forgetting-factor 0.95, Audiogram I

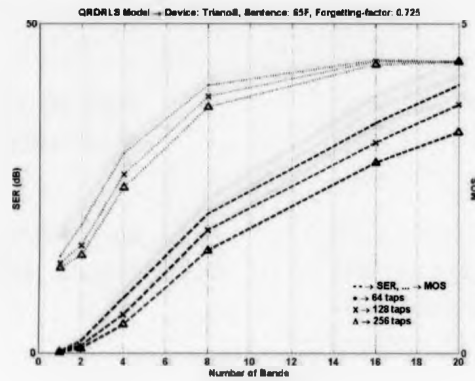
Fig. C.23: QRDRLS Model, SER-MOS, Phonak Perseo 311 dAZ Forte



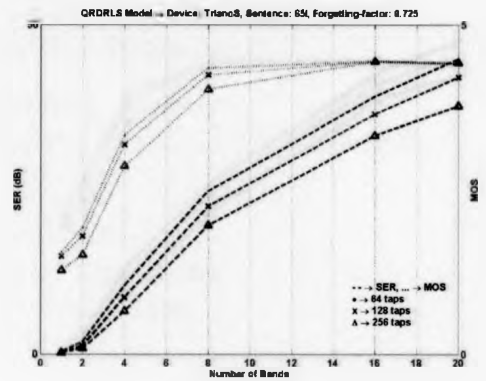
(a) Forgetting-factor 0.5, Audiogram F



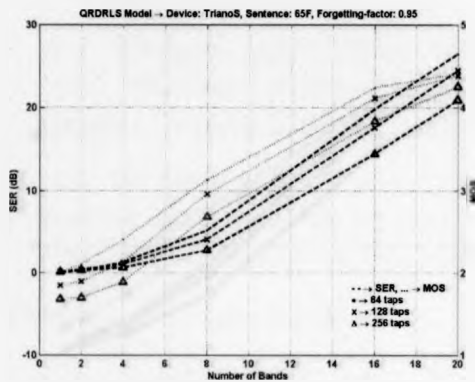
(b) Forgetting-factor 0.5, Audiogram I



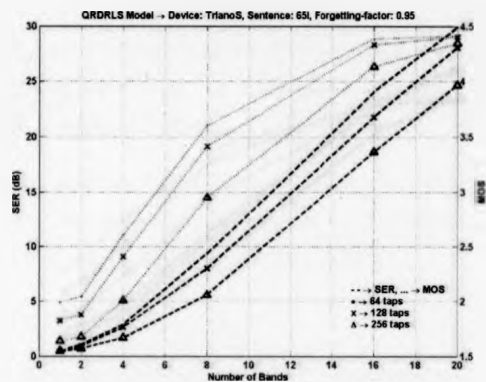
(c) Forgetting-factor 0.725, Audiogram F



(d) Forgetting-factor 0.725, Audiogram I

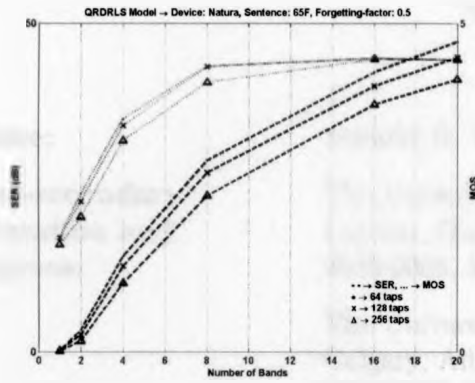


(e) Forgetting-factor 0.95, Audiogram F

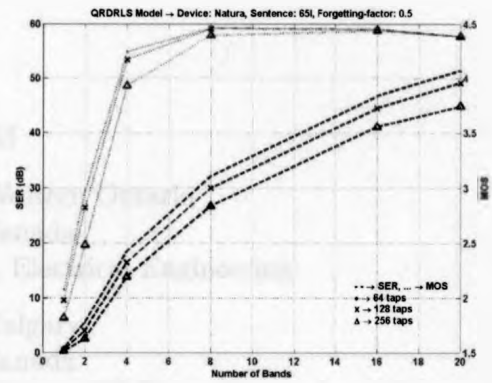


(f) Forgetting-factor 0.95, Audiogram I

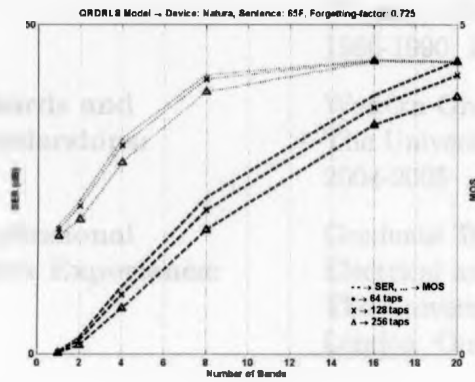
Fig. C.24: QRDRLS Model, SER-MOS, Siemens Triano S



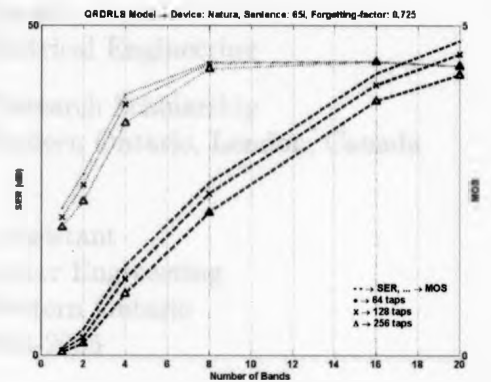
(a) Forgetting-factor 0.5, Audiogram F



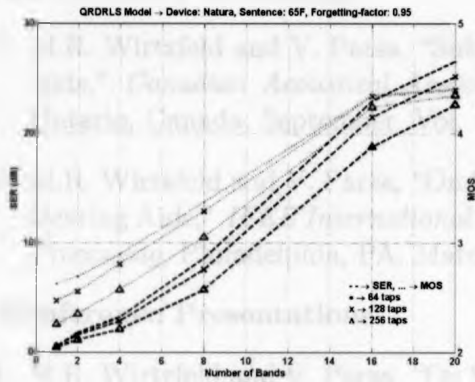
(b) Forgetting-factor 0.5, Audiogram I



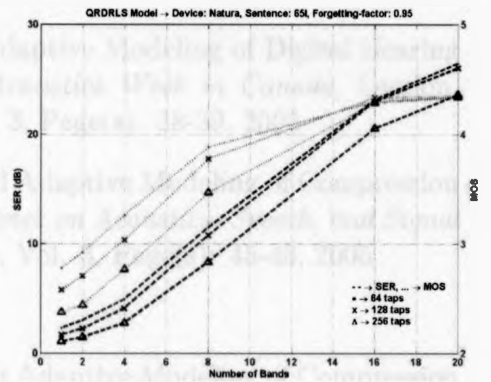
(c) Forgetting-factor 0.725, Audiogram F



(d) Forgetting-factor 0.725, Audiogram I



(e) Forgetting-factor 0.95, Audiogram F



(f) Forgetting-factor 0.95, Audiogram I

Fig. C.25: QRDRLS Model, SER-MOS, Sonic Innovations Natura 2 SE